



Design, Fabrication and Testing of Hybrid Parabolic Dish

Concentrator, Stirling Engine & PCM-Storage in Oman

PhD Thesis

Presented by

Sulaiman Salim Abdullah Al Hashmi

Submitted in accordance with the requirements for the degree of

Doctor of Philosophy

The University of Leeds

School of Chemical & Process Engineering

June 2015

ACKNOWLEDGEMENTS

It takes more than an individual to carry out and successfully complete a PhD research, and towards this end, I would like to recognize the invaluable contributions of the following people, directly or indirectly during the last three years, towards this goal.

Firstly, I would like to thank the Almighty God for having given me the strength and guidance during this challenging period, and to have seen me through it. Without Him, none of this would be possible.

Secondly, I would like to thank my supervisors Prof. Peter J. Heggs and Dr. Darron Dixon-Hardy for their wisdom, support and guidance throughout the journey to successful completion of my research.

Also, I would specifically like to thank my family; my parents, my beautiful wife, and my adorable son for their encouragement and moral support always and more so during the period of my research. I will forever appreciate this.

I would like to thank colleagues and friends in the Energy Research Institute who have, in one way or another, been instrumental towards the successful completion of this research.

In summary, I would like to thank everyone for putting up with me for the last three years. I believe that this dissertation has made real contribution to the field of solar thermal technology. I hope that everyone who reads this dissertation finds it useful in their work it has been a hard and challenging journey so far, even in developed processes. But I look forward to catching up with everyone and having good times after all this hard work.

“This copy has been supplied on the understanding that it is copyright material and that no quotation from the thesis may be published without proper acknowledgement.”

© 2015, The University of Leeds and Sulaiman Salim Abdullah Al Hashmi

ABSTRACT

This work outlines the conceptualization, design, fabrication and parameters that influence the operation of direct hybridisation of solar parabolic dishes with the thermal energy storage in phase change material (PCM) and hybrid Stirling engine. This mathematical method consists of two different sizes of parabolic dishes, PCM-storage and hybrid Stirling engine. The hybrid Stirling engine was used reflective heat to electrical energy in direct and indirect ways. The direct way involved using the sunrays directly from the parabolic dishes into the engine to generate energy. This was done simultaneously while charging the PCM-storage system for later use. For the indirect way, stored heat energy in the PCM-storage was used to supply heat energy to the Stirling engine for applications at night.

Tests were carried out to ensure the system performs optimally based on the design. Each part of prototype model was first tested alone and then later on as part of the complete system of the prototype model. This was carried out continuously over a period of 24 hours over a number of days.

The result from the experiments showed the system was designed to work for 24h, which depends on efficiency of parabolic concentrator, Stirling engine, heat transfer, and storage. The system combines the solar parabolic concentrator and solar energy storage connected in one system. The design, fabrication and testing of each part as well as the complete system were presented. Result presented hybrid Stirling engine proved promising, it was working, as it showed the ability to increase energy production from morning until midday and decreases as the sunset approaches. Also, PCM-storage system proved was working, as it showed the ability to store heat production from morning until sunset approaches and the ability to supply hybrid Stirling engine at night.

This project has shown positive steps towards the future of solar thermal technology; one major finding and benefit from this design is that energy generated during the day can be stored for applications during the night when there is no solar radiation. The design also offers the flexibility of adjusting storage area for more space. Moreover, the entire system is affordable, less cumbersome, and with greater ease of movement.

LIST OF PUBLICATIONS

“The candidate confirms that the work submitted is his own, except where work which has formed part of jointly authored publications has been included. The contribution of the candidate and the other authors to this work has been explicitly indicated below. The candidate confirms that appropriate credit has been given within the thesis where reference has been made to the work of others.”

The following lists of publications capture some of the work in the design, manufacture and testing of hybrid parabolic dish concentrator Stirling engine & PCM-storage (gamma type) in Oman. The prototype was presented at the Omani Open Day 21-1-2015 in London and received the best PhD research topic award for an Omani student in 2014 – 2015. The prototype also attracted a lot of interest from Omani officials and potential investors who were keen to understand its potential applications and implementations.

1. Sulaiman Al Hashmi, Heggs P.J, Dixon-Hardy D.W. “Design, Fabrication and Testing of a Parabolic Dish Concentrator Stirling Engine & PCM-Storage Hybrid in Oman”. Poster published in: Omani Open Day Conference, January 20 - 22, 2015, London.
2. Sulaiman Al Hashmi, Heggs P.J, Dixon-Hardy D.W. “Design, Fabrication and Testing of a Parabolic Dish Concentrator Stirling Engine & PCM-Storage Hybrid in Oman”. Full article published in: Omani Open Day Conference, January 20 - 22, 2015, London.

TABLE OF CONTENTS

ACKNOWLEDGEMENTS.....	ii
ABSTRACT	iii
LIST OF PUBLICATIONS.....	iv
TABLE OF CONTENTS.....	v
LIST OF TABLES	x
LIST OF FIGURES	xi
CHAPTER (1):- Introduction	1
1.1- Introduction	1
1.2- Objective, Aims and Scope of this Research	2
CHAPTER (2):- Literature Review	7
2.1- Introduction	7
2.2- Energy Resources Review	7
2.3- Solar Engine Technology Review	8
2.3.1- Solar Engine History.....	9
2.3.2- Solar Thermal Technologies.....	14
2.4- Cost of Solar Thermal Technologies.....	18
2.5- Technology Area.....	20
2.6- Solar Thermal Energy Storage System:	20
2.6.1- Sensible Heat Storage.....	21
2.6.2- Latent Heat Storage.....	22
2.7- Summary	23
CHAPTER (3):- Design and Fabrication Solar Parabolic Dish with Stirling Engine	25
3.1- Introduction	25
3.2- Solar Position.....	27

3.2.1- Solar Insolation	27
3.3- Factors Affecting Solar Collector Design	28
3.3.1- Intercept Factor	28
3.3.2- Beam Spread Factor	29
3.3.3- Collector Rim Angle (Ψ_{rim}) and Concentration Ratio	29
3.3.4- Parabolic Collector System Imperfections	31
3.3.5- Non - parallel Sun Rays	32
3.4- Energy Intercepted by Receiver	33
3.5- Design Parabolic Dish Concentrator (PDC)	35
3.5.1- Construction Stages of Dishes used in the System	36
3.6- Solar Thermal Receiver Review	39
3.6.1- Heat Losses in Receiver of Parabolic Dish Concentrator	42
3.6.2- Receiver Design Criteria.....	42
3.6.3- Heat Transfer and Power Analysis in Thermal Receiver	43
3.7- Thermodynamic Cycle Solar Parabolic Dish with Engine	50
3.7.1- Theory of Heat Useful and Power Generator analysis in Stirling engine	51
3.7.2- Time of Each Possess in Operation Stirling Engine working	55
3.8 - Design hybrid Stirling Engine Criteria	57
3.8.1- Design and Fabrication <i>a Hybrid Stirling Engine Design Process in system</i>	58
3.8.2- Technical Problems in Fabrication of Stirling Engine:.....	67
3.9- Fabrication of Thermal Receiver in Research System	69
3.9.1- Receiver Size and Focus Point.....	69
3.9.2- Heat Exchanger Receiver Connecting Direct with Stirling Engine.....	69
3.9.3 Cavity Receiver	71
3.10- Conclusion	72
CHAPTER (4):- Design and Fabrication of PCM - Storage in Research System.....	73
4.1-Introduction	73
4.2- Importance of Energy Storage in Solar Technologies	74
4.3. The Methods of Solar Thermal Storage.....	76
4.3.1-The Sensible Heat Storage (SHS).....	77
4.3.2-The Thermal-Chemical Storage (TCS).....	78
4.3.3- The Latent Heat Storage (LHS)	78
4.4- Comparison between Sensible heat & Latent heat Storage in Solar Energy	80
4.5- Phase Change Materials used in Thermal Solar Storage System	81

4.6-Storage Capacity of a LHS System	81
4.7- Characteristics of PCMS used in solar thermal technology	85
4.7.1-Thermal Properties of PCM	85
4.7.2- Physical Properties of PCM	86
4.7.3- Kinetic Properties of PCM	87
4.7.4- Chemical Properties of PCM	87
4.7.5- Economics Specifications of PCM	87
4.8- Basic Review of Latent Heat in Solar PCM-Storage	91
4.9- Design and Fabrication suitable PCM Storage.....	92
4.9.1- Design of PCM storage	93
4.9.2- Measurement of the Storage Volume in Model.....	93
4.10- Conclusion	104
CHAPTER (5):- Design and Construction of External Devices current apparatus	105
5.1- Introduction	105
5.2- Base Stand for the Parabolic Dishes.....	105
5.3- Design Base Stand Suitable apparatus	106
5.4- External Devices	108
5.4.1- Air Compressor	109
5.4.2- Stainless Steel Flexible Pipe	111
5.4.3- The Properties of Stainless Steel Flexible Pipe:-	112
5.4.4- Thermal Valves (Y- Pattern Gas Ball Valves).....	113
5.5- Choice of other Materials for the mathematical model	115
5.5.1- Solar Reflector (98 % reflective flexible mirror sheeting)	115
5.5.2- PCM Molten Salt Composition ($\text{NaNO}_3 + \text{KNO}_3$)	117
5.5.3- Working Fluid (Helium).....	119
5.6- Conclusion	123
CHAPTER (6):- Construction of a Solar Tracking System in Research System	125
6.1- Introduction	125
6.2- Solar Tracking System	125
6.3- Review of solar tracking system.....	126
6.4- Solar Angles	127
6.4.1- The hour angle (h_s)	128
6.4.2- The latitude	129
6.4.3- The declination angle	129

6.4.4- Fundamental Angles	131
6.5- Solar Tracker Types	131
6.5.1- Single Axis Trackers	132
6.5.2- Dual Axis Trackers.....	134
6.6- Solar Tracking Dish Systems	135
6.7- Design and Construction of Solar Tracking System	136
6.7.1- Design of Solar Tracking System using Solidworks	136
6.7.2- Fabrication of Solar Tracking System for Prototype	138
6.7.3- How the Tracking System operates.....	139
6.7.4- Installation of All Parts of the Final Prototype	139
6.7.5- The principle work of the system.....	142
6.8- Conclusion	145
CHAPTER (7):- Testing and Comparing Main Parts of equipment with Experiments	147
7.1- Introduction	147
7.2- Some Basic Information of the Location of Experimental Testing	147
7.3- Test Reflective Materials	148
7.3.1- Result of Parabolic Dish Concentrators.....	150
7.3.2- Comparing between Different Parabolic Dishes Sizes and Materials	153
7.4- Testing of Hybrid Stirling Engine	155
7.4.1.1-Test 1.....	157
7.4.1.2-Test 2.....	158
7.4.1.3-Test 3.....	158
7.4.2- Calculations Hybrid Stirling Engine Efficiency.....	158
7.5- Parabolic Dish Flexible Reflective (4.2 m ²) with and Without Hybrid Stirling Engine.....	159
7.5.1- Analysis of Temperature Profiles without Hybrid Stirling Engine	161
7.5.2- Analysis of Temperature Profiles with Hybrid Stirling Engine	162
7.6- Discussion and Summary	164
7.7- Parabolic dish flexible reflective (3 m ²) with Hybrid Cavity Receiver and PCM-Storage	165
7.7.1- Parabolic Dish Flexible Reflective (3 m ²) with Hybrid Cavity Receiver	166
7.7.2- Parabolic Dish Flexible Reflective (3 m ²) with Hybrid Cavity Receiver and PCM-Storage	168
7.8- Conclusion	171
CHAPTER (8):- Experiment Results & Discussion	173
8.1- Introduction	173

8.2- Working of the Prototype Model During Day and Night	173
8.3- Heat Transfer from PCM - Storage System in Current System	176
8.3.1- Results of System Working at Night (only).....	178
8.3.2- Results of System Working for 24 h without Control System	180
8.3.3- Thermodynamics of the 24 h Working System	183
8.3.4- Result of System is working for 24 h with Thermal Control System	186
8.4- Comparison for System working for 24 h with and without Thermal Control System	189
8.5- Conclusion	192
CHAPTER (9):- Conclusions and Recommendations for Future Work	193
9.1- Introduction	193
9.2- Conclusions	194
9.2.1- Summary of Design and Fabrication	194
9.2.2- Summary of Experimental Results	195
9.3- Recommendations for Future Work	196
9.4- Concluding Remarks for this Thesis	197
References	199
Appendices Section.....	205

LIST OF TABLES

Table 2. 1 (SG3-400m ² and SG4-500m ²) two types of parabolic dish mirror in Australia 1994-2008 [12].....	13
Table 2. 2 The comparison between solar power technologies and cost [20].	20
Table 3.1 Concentrator system specifics for several manufacturers SBP, SES& WGA (Mod 2) [20].	31
Table 3.2 Typical error values for a Stirling dish collector system [3, 9].	32
Table 3.3 Heat losses in Stirling dish system (conduction, convection, radiation) in SES and WGA models [19].	42
Table 3.4 The wind cut-out velocity and how it affects the parabolic concentrator [19].	45
Table 4. 1 Comparison between various heat storage mediums (Stored thermal energy=5000Kj, ΔT= 25 °C) [10].....	80
Table 4. 2 Advantages and disadvantages of organic and inorganic PCM materials [7].....	89

Table 4. 3 time of day in Oman at summer and winter	94
Table 4. 4 Thermo physical properties of solid – liquid PCM.....	98
Table 5. 1 The characteristics of the two parabolic dish systems in mathematical model.	106
Table 5.2 The properties of helium gas with different pressures.	121
Table 6.1 Solar tracking system used in solar thermal technologies [1]	126
Table 6. 2 The principle working of the system	144
Table 7. 1 The parameters of hybrid Stirling engine.....	157
Table 8. 1 Compare Results of System is working for 24H with and without Thermal Control	191

LIST OF FIGURES

Figure 1. 1 Diagram shows the proposed design for the possibility of power generation, storage and consumption throughout the day time in Oman.....	4
Figure 1. 2 The proposed design for the possibility of power generation after stored it in PCM and consumption throughout the night time in Oman.....	5
Figure 2. 1 (a) is first Stirling engine in 1815 by Robert Stirling and (b) is Stirling’s brother developed with pressurised cycle engine in 1845[8].....	10
Figure 2. 2 The first solar engine with parabolic mirror was built in 1870 by John Ericsson [8]......	11
Figure 2. 3 Beta-Stirling engines with rhombic drive mechanism [10].	12
Figure 2. 4 The large parabolic dish mirror was built by a large American corporation, in 1985[11].	13
Figure 2. 5 the southern California solar station produces 0.90 GW [12].....	14
Figure 2. 6 A and B solar technologies system power tower and parabolic trough [13.14].	15
Figure 2. 7 The Solar furnace powers in France in1970 [16].....	17

Figure 3.1 The process of gas cycles during day and night in the complete system	26
Figure 3.2 The relationship between intercept factor in parabolic dish (A) and aperture size of solar parabolic dish technology (B) [33].....	29
Figure 3.3 The relationship between f/d ratio and rim angle in parabolic dish system (A) and (B), different rim angles (20°, 30°, 40°) [30].....	30
Figure 3.4 Beam spread in the plane perpendicular to the centreline of the reflected light [40]	33
Figure 3.5 Parabolic curve is in three dimensions x, y and z with rim angle designed using solidworks	35
Figure 3.6 Two satellite dishes (3 m ² and 4m ²) with reflective flexible sheets .. Error! Bookmark not defined.	
Figure 3.7 4 m ² parabolic dish with installed long iron base stand.....	38
Figure 3.8 Both parabolic dishes installed at both ends of long iron base (5 m)	39
Figure 3.9 Two different types of receivers are used in solar parabolic dish technology	41
Figure 3.10 The geometry of thermal receiver with Aaput and Arec areas	43
Figure 3.11 The processes of heat losses in terms of convection, radiation, heat storage and heat useful ...	44
Figure 3.12 Helium gas and flow through copper pipe in the system	46
Figure 3.13 Schematic diagram of the cavity receiver [37]	49
Figure 3.14 Thermodynamic power generations in hybrid Stirling engine by parabolic dish system in cycle (2).....	50
Figure 3.15 Regenerator and working fluid temperatures through Stirling engine cycle [36]	54
Figure 3.16 Stirling engine designs using the Solidworks Software.....	59
Figure 3.17 The Final Sterling Engine Design for processes of Fabrications.	60
Figure 3.18 The base plate of the engine machined from a piece of 30 mm thick board	62
Figure 3.19 The main body of the cylinder heat sink made from the 52 mm pipe cut to 100 mm	63
Figure 3.20 The displacer guide bush.....	63
Figure 3.21 The displacer made from a piece of light wood turned on a lathe machine to diameter of 30 mm and length of 80 mm	64
Figure 3.22 The power cylinder made purely of cast iron	64
Figure 3.23 The fly wheel cut from a 4.5 mm thick steel plate	65
Figure 3.24 The connecting rod	66
Figure 3.25 Fly wheel and Shaft assembly	66
Figure 3.26 Completed hybrid Stirling engine and testing in the workshop	67

Figure 3.27 Hybrid Stirling engine within AC generator	68
Figure 3.28 hybrid Stirling engine installed into cavity receiver	69
Figure 3. 29 Steps of hybrid Stirling engine been installed into cavity receiver.....	70
Figure 3.30 The thermal receiver installed into the system	71
Figure 4.1 Methods of thermal storages system with the latent heat storage (LHS), the sensible heat storage (SHS) and the thermo-chemical storage (TCS).....	77
Figure 4.2 Capsule shells of PCM of heat charging and discharging from Solid to liquid	84
Figure 4.3 The diagram of the stages of transformation of material from solid to a liquid state and vice versa when heat is added gain or loss	86
Figure 4.4 Classifications of PCM-Storage [47].....	87
Figure 4.5 Different types of PCM use for thermal storage and melting temperatures [41].....	90
Figure 4.6 Design of thermal storage using Solidworks	102
Figure 4.7 The final form of thermal storage which fabrication	103
Figure 5.1 The solid-work design of long base stand made from iron	107
Figure 5.2 The final design of mathematical model by use solidworks software which (A) basic stand, (B) long iron stand, (C) Two long iron stands in system and (D) two parabolic dishes in system with stand	108
Figure 5.3 A gas compressor which uses in system.....	109
Figure 5.4 The air compressor connecting the thermal control system as well as helium supplying system.....	110
Figure 5.5 The high quality flexible stainless steel-pipes used in the mathematical model.	112
Figure 5.6 Thermal valves (Y- Pattern Gas Ball Valve)	114
Figure 5.7 Both dishes are cover by 98 % reflective flexible sheet.....	116
Figure 5.8 The plotting obtained results on phase diagram of KNO_3 - NaNO_3 [61].	117
Figure 5.9 Phase Change Materials KNO_3 - NaNO_3 (60/40) % suitable storage through (out and in) iron balls	119
Figure 5.10 Processes of Helium in Current Model	120
Figure 6. 1 Solar anlages; altitude angle (α) and azimuth angle (α_s) in solar system [21].	128
Figure6. 2 The latitude angle (L) [23]	129
Figure6. 4 Solar declination angle [22].....	130

Figure 6. 4 The fundamental angles with respect to vector S along the solar beam direction [2].....	130
Figure 6. 5 Types of Solar trackers which used in solar concentrators.....	132
Figure 6. 6 Single axis trackers (A) Horizontal single axis, (B) Vertical single axis tracker and (C) Tilted single axis tracker [13].....	133
Figure 6. 7 Tilted Single Axis Tracker in summer, winter, spring and fall [14].....	134
Figure 6.8 Solar parabolic dish system, different azimuth angle and altitude angle [13].....	135
Figure 6.9 Current design showing direction of movement and gas struts.	137
Figure 6. 10 Solar hour's sensor	138
Figure 6.11 Novel model with tracking system	141
Figure 6.12 The principle and working of the system.	142
Figure 7.1 The parabolic dish concentrators with different reflective materials and different area sizes; A cover by normal mirror with (3 m ²), 'B' also normal mirror but (4.2 m ²), 'C' cover by flexible reflective sheet (3 m ²) and 'D' also cover by flexible reflective sheet.....	149
Figure 7.2 Thermal receiver used during the experiment and thermocouples used to measure temperatures	150
Figure 7.3 Result of Parabolic Dish Concentrators, focal temperature, in solar radiation and ambient temperature	151
Figure 7.4 Results of parabolic dish Mirror with different sizes (3 m ² & 4.2 m ²).....	153
Figure 7.5 The results of parabolic dish with the flexible reflective at size (4 m ²)	154
Figure 7.6 The processes of testing of hybrid Stirling engine	156
Figure 7.7 The experiment step of hybrid Stirling engine and measurement system.....	160
Figure 7.8 Results of testing (4m ²) parabolic dish as well as operation temperature, hot engine space temperature, cold engine temperature and solar radiation	161
Figure 7.9 Results of testing (4 m ²) parabolic dish with hybrid Stirling engine; operation temperature, hot engine space temperature, cold engine temperature, power generator and solar radiation	163
Figure 7.10 Testing parabolic dish (3 m ²) flexible reflective sheets with thermal receiver in current system.....	165
Figure 7.11 The experiment step of cavity receiver and measurement system	166
Figure 7.12 Results of parabolic dish flexible reflective (3 m ²) and hybrid cavity receiver	167
Figure 7.13 The experiment step of PCM - Storage and measurement system	169

Figure 7.14 Results of heat store in PCM- Storage during day	170
Figure 8. 1 The principle work of current model processes during day and night.	175
Figure 8.2 The current model under operation in 24 h in workshop (Oman).	177
Figure 8.3 the results of system working at night (only)	179
Figure 8. 4 Results of system at operation for 24 h (24-7-2014).	182
Figure 8. 5 The Discussion results how system work in thermodynamic.	184
Figure 8.6 The result of system working for 24h with thermal control system (25-7-2014)	188
Figure 8. 7 Compare between Results of System is working for 24 h with and without Thermal Control in model.	190

CHAPTER (1):- Introduction

1.1- Introduction

The constant demand for energy is increasing day after day, which led to the energy crisis that the world is facing today. It is expected that this crisis could increase if a radical solution is not taken to address the growing influence of fossil fuel, and this fossil fuels may not last forever while the world is still experiencing growing hunger for energy. With the change in the cost of fossil fuels daily and the current greenhouse effect, it is becoming more apparent to look at renewable energy sources as possible solutions to the problem. There are many types of renewable energy resources in world, but there is the need to give a closer look at the more natural and sustained source as the answer. Many researchers and experts in energy believed that solar energy can play a vital role in meeting the world's energy demand. There is a simple barrier standing between the solar production and implementation into power grid this barrier is the difference in price to performance ratio in the station.

To date, the cost effectiveness of the application of solar energy is still largely expensive as compared to fossil fuels. This may be due to the availability of the fossil fuel and cheap enough to supply us with the majority of our energy needs at the moment. With the latest rise in fuel prices and other problems associated with fossil fuels, this creates more uncertainty on the reality of sustaining the use of the fossil fuel for our energy demand. Hence the urgent need to consider renewable energy sources, with the use of solar energy as an option as this will be able to compete with other types of renewable energy in commercial market.

Arab Gulf countries are now making future plans to reduce the demand of fossil fuel for energy and focus on solar energy as the future energy resource because of its privileged position with high solar radiation within the region. Oman is one of these countries, with an energy future plan called "the future of clean energy in 2050", and this plan intends to maximise the benefits from solar energy in power generation [1, 2,5]. In view of this, the country supported scientific projects in this area with

scholarships to indigenes in order to attract scientific expertise in the development of this field, and this project is funded by this plan.

1.2-Objective,Aims and Scope of this Research

The objective of this research was to design a novel solar thermal technology and solar thermal storage for continuous power generation throughout a given day.

The main aim of this thesis is to explore the possibility of continuous power generation, storage, and consumption, irrespective of the time of the day, using the proposed designs for solar thermal prototypes, as described in figures 1.1 and 1.2.

Parabolic dish solar concentrator (PDSC) will be designed, fabricated and improved through the addition of thermal phase change material storage. These additions will improve its performance and allow for more periods of work for the Stirling engine and increase efficiency as much as possible. To validate the efficiency in energy storage of the prototype model, its structural and thermal properties will be compared with others based on different application scenarios.

The design of the solar thermal prototype model was achieved using a series of steady state thermodynamic equations, gas transfer temperature dependent equations, and heat stored in PCM and power generation by Stirling engine. The method of working of the system consisted of three basic operations; two operations at day and one at night to keep system working all-day. In terms of the main processes of heat absorb, heat transfer (flux), heat storage, heat supply the engine. In this respect, helium gas was used as the working fluid based on its good thermal absorption and heat transfer properties.

During the day, the red line as shown in Figure 1.1 shows the helium gas which transfer heat during movement through the Stirling engine in the system (1) as well as from thermal receiver to PCM - storage in system (2).

The PCM-storage system was manufactured after studying many of the previous solar thermal models. In this system, potassium nitrate and sodium nitrate (KNO_3 - NaNO_3) was used as phase change storage material because it has high ability to store solar heat. This prototype model was designed at Leeds University from

September 2011 to June 2013; it was fabricated in June 2012 and tested in Oman from 01 July 2013 to 30 July 2013.

During the night, the red line as shown in Figure 1.2 shows the helium gas movement in the system from the hot storage to the heat exchanger located in front of Stirling engine. In the stored heat energy in the PCM - storage was used to heat the system; as long as the oil in the heat exchanger was shown to still retain heat, the control valve was left closed until the required amount of heat was achieved. In view of this, the system was shown to function 24 h a day thereby justifying the application of PCM-storage to extend the hours of power generation through the night as intended and as shown in Figure 1.2.

The use of the control valve to regulate the inflow of the heat energy to the storage and also to the Stirling engine at night was shown to be beneficial in extending the number of hours the system works as compared to free flow without control. Hence, the application of valve to regulate the amount of heat required is considered to enhance the efficiency and recommended to be applied to other parts of the system in the future.

During the initial design, Solidworks software was used to design each part of the prototype since it enables ease of design, modifications, control sizes, and also gives a good image of the final prototype.

Novel solar thermal prototype testing in Oman July 2014 (System prepared to generate over 24 h – 52 weeks of the year), 5-50 w.

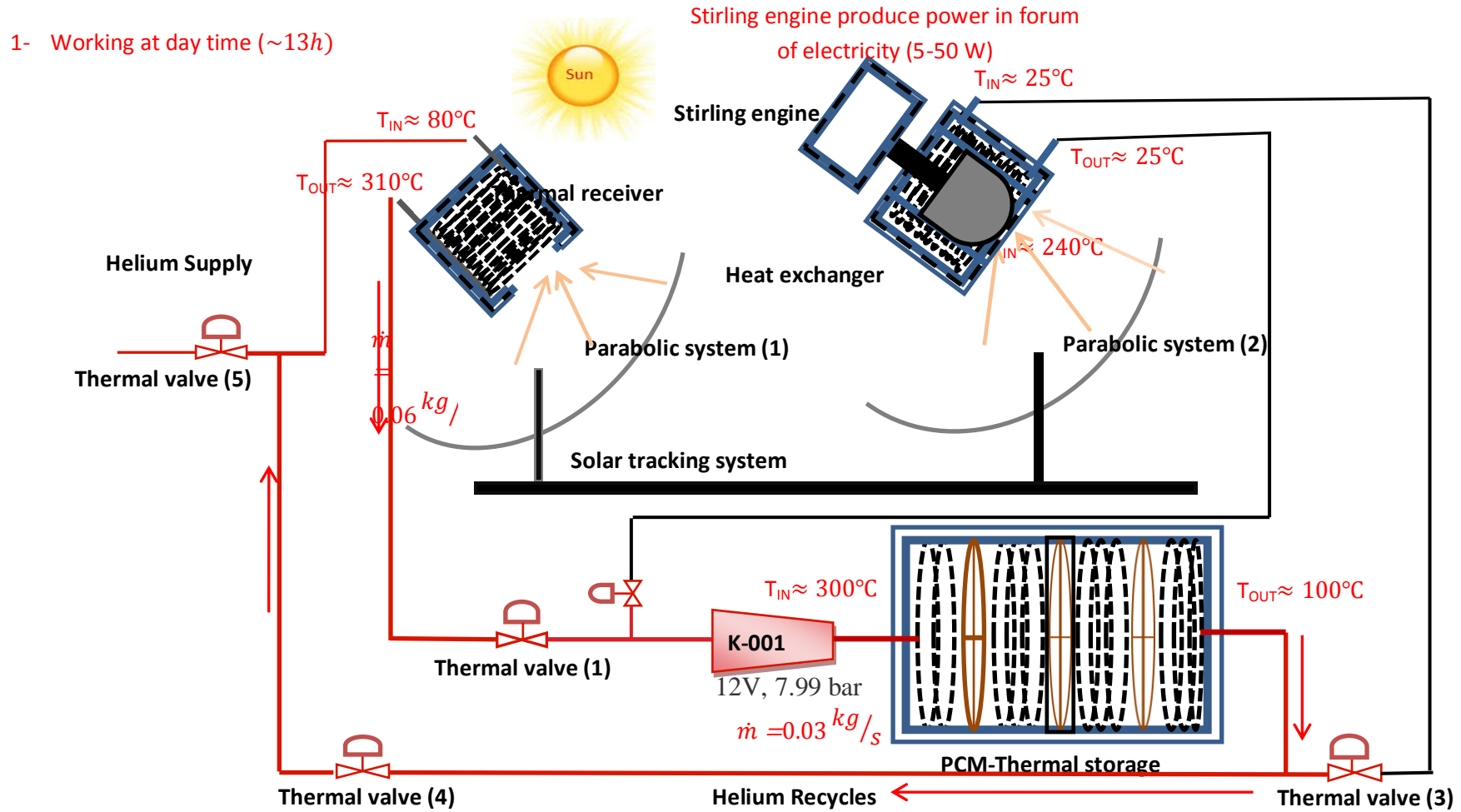


Figure 1.1 Diagram shows the proposed design for the possibility of power generation, storage and consumption throughout the day time in Oman.

2- Working at night time (~11h) in

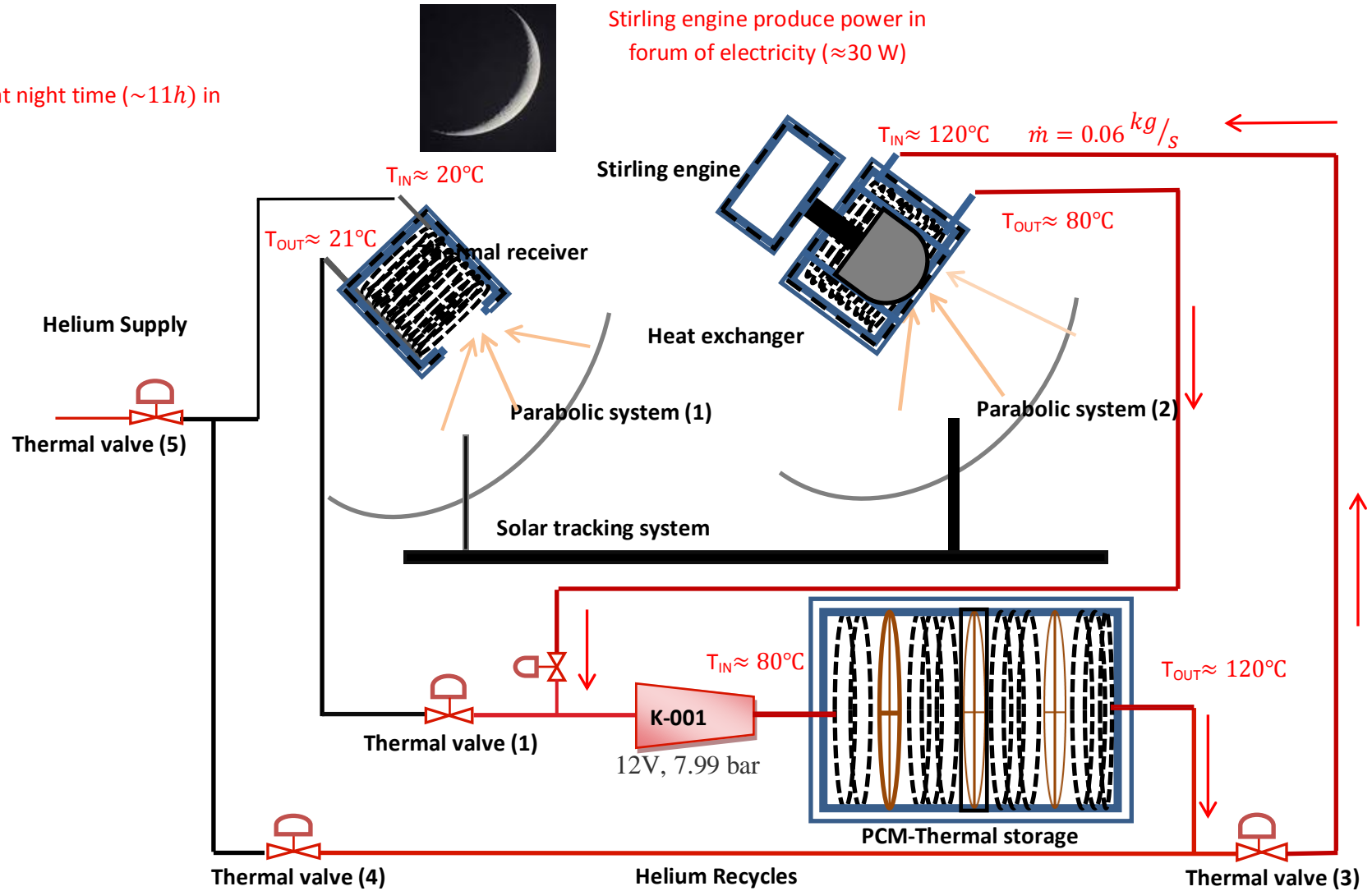


Figure 1.2 The proposed design for the possibility of power generation after stored it in PCM and consumption throughout the night time in Oman.

Chapter two presents a brief history of energy sources and solar thermal technologies in order to give basic background, discuss previous experiments of similar systems and review existing literature on solar thermal technologies such as solar power tower, solar parabolic trough, solar furnace power and parabolic dish mirror.

Chapter three, focus on discussing the design and fabrication of the parabolic dish, Stirling engine and cavity receiver. It is divided into three sub-sections including the design of two different parabolic dishes, hybrid Stirling engine and two thermal receivers.

Chapter four aim to give detailed description of the design and fabrication of second part of the final prototype. It is divided into two sections, the first focuses on the solar thermal storage background and review. Second section was conceding in processes of design and fabrication suitable PCM-storage

The **fifth chapter** intends to review and describe external devices which were used for heat charging and discharging of the thermal storage as well as heat space of the engine. All these devices must have certain specifications of high thermal quality for heat transfer at high pressure, high conductivity and high melting temperature.

The main objective of **chapter six** is to discuss the solar tracking system, installation of different parts of the system and detail description of how the system works. The design of the tracking system is to compliment the external and internal parts of the current prototype.

Chapter seven will test the flexible reflective material 98%, running hybrid Stirling engine, cylindrical receiver, compressor and PMC-storage. The practical experiments will be conducted in Oman (Muscat) from certain dates during summer season. In **chapter eight**, further discussions of some other areas of the experiments will be carried out.

Furthermore, more detailed discussions and comparison with result of the previous sections will be highlighted, and also the working of the system during the day and night. Conclusions and possible future work to come from this prototype is summarized in the final section, **chapter nine**.

CHAPTER (2):- Literature Review

2.1-Introduction

The objective of this review is to provide a brief history of energy sources and solar thermal technologies in order to give basic background, discuss previous experiments of similar systems and review existing literature on solar thermal technologies such as solar power tower, solar parabolic trough, solar furnace power and parabolic dish mirror. The history of solar energy shows that Stirling engines were used in the design of parabolic dish mirror technology like generators. In addition, the review intends to focus on the parabolic dish mirror and Stirling engine, showing advantages, and disadvantages of these systems to help in the design of a new prototype. Furthermore, the comparison between solar technologies and their cost will be studied, and finally solar thermal energy storage will also be discussed [6, 7, 17].

2.2- Energy Resources Review

There are two possible ways of electrical power generation; this can be achieved by the use of non-renewable and renewable resources. Non-renewable energy is a common energy source for most countries including Oman, the U.K, U.S.A and other countries that rely on fossil fuel for energy generation. This type of energy source will run out in coming decades or may diminish within 50 years from now [6]. The use of Non-renewable energy has already brought an impact into the global climate by emission of greenhouse gases from fossil fuel combustion [6, 7]. Currently, the world cannot afford to continue to accommodate emissions resulting from non-renewable energy (oil - gas- nuclear) after combustion of CO₂, as this poses serious and increasingly threat to the future of life on Earth. It is obvious that the world looks to alternative energy, such as solar energy which is environmentally friendly and does not increase the temperature of the Earth surface. This is because solar technologies do not release heat to atmosphere but convert heat to electricity (direct or indirect).

The combustion of fossil fuel increases air pollution, acid rain, and the depletion of natural resource and the dangers of nuclear radiation. These are the major causes of

climatechange as a result of the emission of greenhouse gases from fossil fuel combustion [6].In the last few years, many countries in the world have focused on solar thermal technology as alternative sources of energy to reduce emissions resulting from the combustion of non-renewable fuel. For example the United States, Germany, Spain, Australia, most South American countries, France, India, and China have adopted the technology [2, 6]. The quest to use of solar energy has gradually increased with many other countries employing the technology as compared to the last decade. Non-renewables have been in existence for more than hundred years with common sources such as natural gas, petrol oil and nuclear power. In non-renewable energy, the materials of combustion producing higher thermal energy than renewable energy that helps to sustain its application, usage and popularity.

Renewable energy is mainly natural resources such as wind turbine, geothermal, biomass and solar thermal. These resources can be grouped into two different types and these are solar or non-solar. Non-solar resources are not dependent on the sun light directly, this includes geothermal (internal earth thermal) and tidal (gravitational force between earth and moon) [8.9]. Solar energy resources are mainly, free energy and depend on solar radiation such as solar thermal, photovoltaic and wind energy. Solar energy is also divided into two types; the first type is solar energy indirectly used like hydropower and wave power. The Second type is solar thermal directly used like solar thermal and photovoltaic. Solar thermal resources are widely known though their use depends on geographical location and the strength of the sun and are divided into four solar thermal technologies for example, solar power tower, solar parabolic trough, solar parabolic dish mirror and solar furnace.

2.3- Solar Engine Technology Review

Solar technology uses two names for the same generating engine namely the solar engine or Stirling engine. The principle work of a solar engine converts heat coming from the sun to mechanical movement to generate electrical power. Robert Stirling invented the first design of Stirling engine in 1815. After 54 years work from the first design, Mr John Ericsson was able to build a first solar power engine in 1870 which was a global event at that time. Different variations of solar engines were developed

from time to time, and presently there are four configurations including the alpha engine, beta engine, gamma engine and free pistons engine [7].

Solar energy can supply all energy needs for the following applications:-

- ❖ Electric power generation:
 - Solar-Thermal Power concentrator
 - Photovoltaic Cells
- ❖ Space heating and cooling (Air Conditioning)
- ❖ Industrial process heating
- ❖ Desalination and water heating (Flat plate Solar Collectors)
- ❖ Transportation fuel

2.3.1- Solar Engine History

The history of solar engine evolution started from the steam engine in the 18th century when the engine was widely employed as a prime actuator for all sorts of industrial applications such as pumping, lifting heavy loads and driving rotating machinery. The efficiency of steam engine had developed from 2% to reach approximately 10% in the early 19th century but still had too low efficiency and so technical engineers resulted to using coal which was cheaper at that time. In the early 19th century, some engineers, inventors, researchers, and entrepreneurs were thinking of a robust engine to work with hot air in which a hot air source could be used for expanding the gas pressures in the engine when heated and contracted when cooled [8.10].

Robert Stirling's original engine of 1816 (British patent No.4081) was a simple engine and along with his brother James (an engineer in thermodynamic and mechanics) were responsible for developing the engine design which at that time was associated with this engine named as the Stirling engine. There were two separate inventions in the Stirling engine at that time, the first was the economiser (regenerator) and other parts in the patent was the actual engine and more description about engine is given in the section below.

Robert Stirling's brother was responsible for developing the first five working versions of the Stirling engine for about 30 years until 1845. The first version was very similar to the current gamma design (γ) which consists of two separated

cylinders with open fire heating and air cooling. The second version Beta (β) type engine had the displacer and power piston in the same cylinder [11,12].

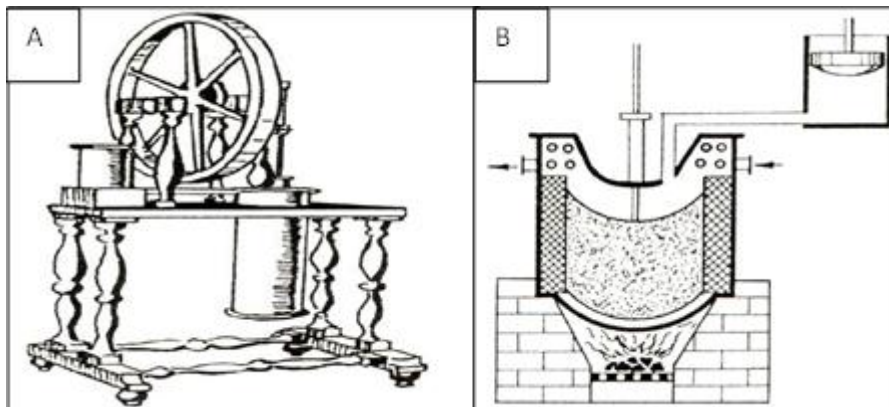


Figure 2.1(A) is first Stirling engine in 1815 by Robert Stirling and (B) is Stirling's brother developed with pressurised cycle engine in 1845 [8,18].

This design was not working until 1827 because Stirling's brother developed the description of the regenerator or economiser for space filled with successive layers of plates by using the thinnest iron, pierced with holes and increased distances. This regenerator had a temporary heat storage element that consisted of hot and cold gas which the piston passed back and forth through the regenerator. This helped to reduce the amount of heat needed to be transferred by the heat exchangers and dramatically increased the overall efficiency of the engine. The third engine design as shown in Figure 2.1-B was built in 1845 which used a separate pump to fill the engine housing with compressed air, produced around 1.8 kW and powered all the machinery at a foundry in Dundee, Scotland for many months until it was superseded by a larger version of the same engine [8]. Afterwards, Johan Ericsson built the first solar model for generating power by Stirling engine in 1870. This design was an open cycle engine, one horse power demand, fresh cool air, and area 10 square feet and used a manual handle to get the sun rays as shown in figure 2.2.

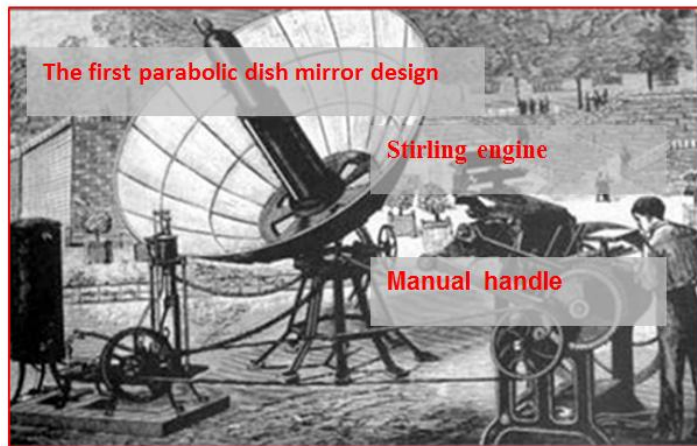


Figure 2.2 The first solar engine with parabolic mirror was built in 1870 by John Ericsson [8]

During the end of the '19th' and early '20th' century, the Rider Engine Company built the fourth type of engine recorded as the 'Alfa-type' of Stirling engine. The steam engine still dominated industry which was rapidly shifting towards the internal combustion engine. During this period, the Stirling engine was still a small engine used to pump water and small power domestics but not used to produce electricity and the possibilities at that time marked its evolution difficult. After that, Philips developed a number of engine designs that produced power between 6W to 1HP [10]. Philips did many experiments in order to increase the performance of the Stirling engine and released his type '10th' engine in 1941. The performance of prototype '10th' was to run as a heat pump by driving the shaft of the engine with an electric motor. The initial motivation was to find a possible alternative to the Freon compression-evaporation cooling systems which were found in refrigerators and air conditioners. However with this model, it was found out that the Stirling cycle cools at temperatures around 100°C and worked with even with minimal insulation around the cylinder head and after three years of further development it reached 200°C with only minor changes to the engine [8, 9, 11].

During the mid of '20th' century Philips developed his 19th type engines. This engine was called the Philips 19th prototype engine with its compact size and high power output. After few years, Philips designed a type 20 engine, a 4-cylinder double-acting engine, a swept volume of 2.9 litres and 50HP power output. This design was fast, smooth-running, had a good torque capability, and had a respectable efficiency of

15% [10]. In 1953 Philips tried to solve the problem of balancing a small displacer type engine, as well as better piston sealing through lack of side loading forces. In addition he invented the rhombic drive mechanism which is effectively a small Beta type as shown in figure 2.3. Furthermore, the properties of this engine had the crankcase working without pressure, a significant weight and cost reduction, fewer vibrations, higher possible working pressures and a compact design.

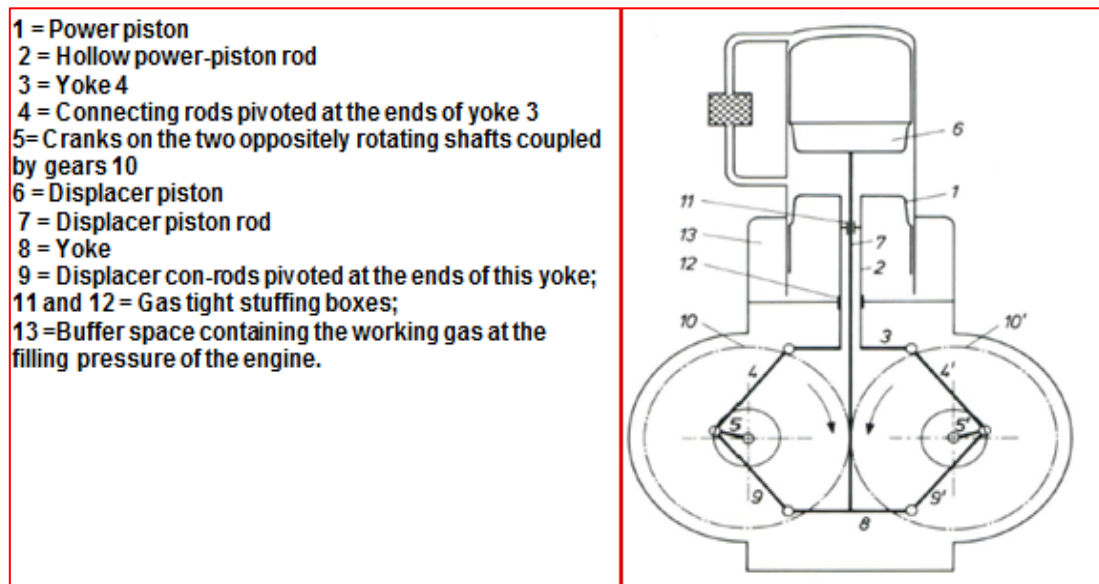


Figure 2.3 Beta-Stirling engines with rhombic drive mechanism [10].

Engines companies devised and built several engine generators over the next few years but cost was an issue. Philips companies started from his '19th' prototype engine to produce types of refrigerator's engine and stopped producing other types.

After several years later and many experiments, Mc Donnell Douglas in 1985 designed a large parabolic dish mirror system (PDM) with big Stirling engine (STM4-120) as shown in Figure 2.4 [8, 9, and 11]. This design tracked the solar radiation beam by a large reflected mirror, converged on the centre of Stirling engine at a temperature of around 1430°C to produce 25 kW of electricity with respectable thermal efficiency of about 31% [11]. In addition more ability to use the design gradually increased as compared to other engines because of its properties and efficiency.



Figure 2.4 The large parabolic dish mirror was built by a large American corporation, in 1985[11]

This large design was accepted in many countries and the use of a parabolic dish mirror system to generate electricity became more common. At that time, countries such as Australia in 1994-2008 and Southern California in 2005-2010 applied this technology. Australia was one of the countries that were concerned about using the high technology of parabolic dish mirror. Table 2.1 shows the two experiments applied in Australia between 1994 and 2008. The first experiment used SG3 (Stirling generator type 3), area of 400m² parabolic dish mirror, collected approximate 600°C heat temperature, 86% mirror reflectivity and produced 50kW of electrical power. Other experiments used a larger area of roughly 500m² with SG4 (Stirling generator type 4), focal temperature at 1200°C, 93.3% mirror reflectivity and produced between 60 - 100 kW of electrical power [12].

Table 2.1 (SG3-400m² and SG4-500m²) two types of parabolic dish mirror in Australia 1994-2008 [12]

Comparing points	Parabolic Dish Mirror Solar System in Australia (1994,2008)	
	1994	2008
Parabolic Dish Mirror Area (m ²)	400	500
Efficiency of Reflectivity Mirror (%)	86	93.30
Engine Type	SG3	SG4
Focus Temperature (°C)	400-600	1200
Generator Efficiency (%)	18.60	20
Power Generator (kW)	50	60-100
Thermal Efficiency (%)	80-90	90

This amount of power produced by solar parabolic systems was not enough for use in cities with high population, such systems needed to produce more power in MW or GW quantities. Such systems are called solar stations and consist of hundreds or thousands of units of solar dishes each one capable of generating a kW of electrical power and eventually generating MW or GW of energy. A Southern California solar station applied this technology in 2005 by using 20000 solar Stirling dishes, with each dish having 100m² areas and produced 25kW of power. This station produced a total of 0.5GW capacities. However in 2010, the dishes increased to 34000 and generating capacity also increased to 0.9GW as shown in Figure 2.5 [16].



Figure 2.5 the southern California solar station produces 0.90 GW [12]

Today's modern Stirling engines have two types, the kinematic and free piston. Kinematic have three configurations such as Alpha, Beta, Gamma. Each of the configurations has different facilities such as design, properties, components and uses in high and low temperature. Many countries tried to benefit from using solar technology but Southern California in the USA was the first that built several kinds of solar technologies to cover around 40% of California energy consumption [20, 21, 22]. The solar technology systems have mainly two issues for example area and cost which made some countries unable to use this technology at the present time.

2.3.2- Solar Thermal Technologies

Solar thermal technologies are a type of direct solar energy sources which concentrate solar heat in a thermal receiver as shown in figure 2.5. The technologies can be divided into four sections depending on the receiver design such as solar power tower, solar parabolic trough, solar furnace power, and parabolic dish mirror. All sections have similar characteristics such as using a reflected mirror, high

conductivity materials, heat exchanger system, working fluid and engines. However, the main differences are in thermal receiver design which are either an in line tube receiver shape or cylinder receiver shape on the top of tower, or directly inside the engine. In addition, some of those technologies have thermal storage, which have working fluid used and different engine (steam and gas). In the past few years the use of solar thermal systems have developed and gained acceptance around the world because of the Non-renewable resources forcing investment in free energy.

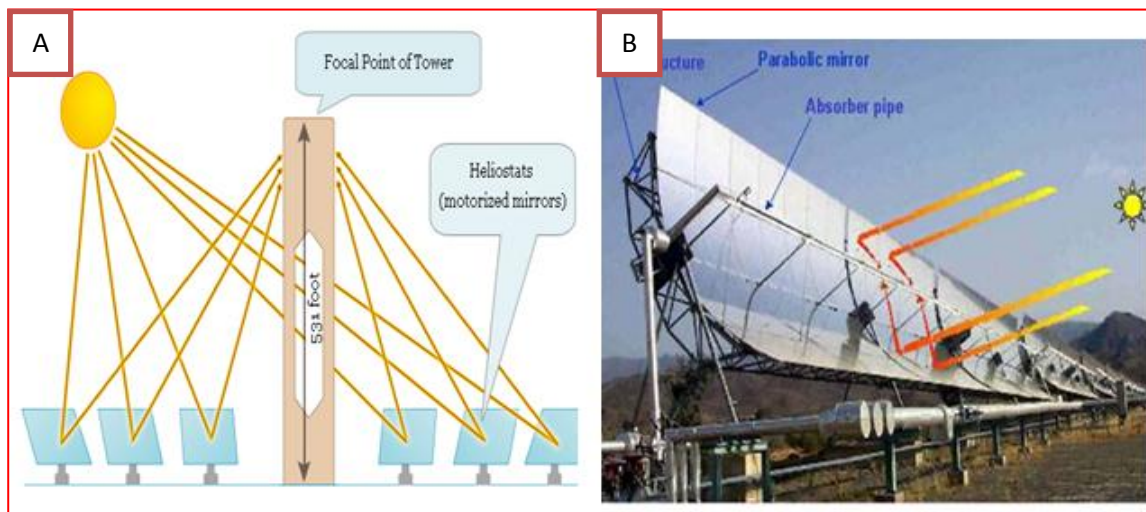


Figure 2.6A and B solar technologies system power tower and parabolic trough [13,14].

2.3.2.1- Solar Power Tower (SPT)

Energy researchers and design engineers built a high solar power tower at 20m height and around it there were array of heliostats in form of circular or semi-circular. There are central receivers at the head of tower as shown in Figure 2.6-A. This system used a head of tower to absorb the solar radiation by reflecting from motorized mirrors (heliostats) with a removable system. Afterwards it convertsthe sun's energy into thermal energy by molten salts, steam /water, liquid sodium or air to superheated steam to generate power in a steam turbine. The Power tower system uses two-axis, horizontal axis are heliostats areas and long tower in vertical axis. This system is used in many countries such as Spain in 2007 which built a solar power tower (PS10) to generate 11MW at a cost of around €35million [17]. Also, California in 2001 built a 96m²long tower with 2,493 heliostats for more than 1000°C operating temperature to produce 10 GW and the ability of molten salt storage

around 600kWh. Moreover, solar power tower is the first solar technology that used thermal storage system to keep some of heat energy in molten salt storage technology during the day and use it like a second resource at the night. The characteristics of this system produced MW power depending on number of heliostats, working 24 h by using thermal storage, less services, neglecting any problem occurring in the plant mirrors and using a Stirling engine or steam engine to generate power [13.14].

2.3.2.2- Solar Parabolic Trough (SPT)

Solar parabolic trough systems are considered the most economic and mature system in the application of solar technologies today. Solar parabolic trough is used with an in-line parabolic mirror to concentrate high temperature into thermal receiver tubes or in-line with a focal trough. The thermal transfer fluid used inside in the tube is typically synthetic oil that is heated to 400°C by the parabolic mirror. However, the heating oil is paired with heat exchanger to power a superheated steam turbine to generate electricity [15]. This system is using thermal storage to transfer heat in a hot phase fluid allowing it to produce electricity into several hours at night as shown in Figure 2.6-B. In 2010, also Southern California created a big solar parabolic trough station with high efficiencies approximate 30%-40% to generate more than 80MW within large 6.5km² area. This station used synthetic oil filled in central tube heat exchangers to produce a working fluid temperature of around 400°C and cost \$250million. The total price of this station is reasonable when compared with other solar energy technology. This technique has gained acceptance in recent times in many countries around the world such as Spain, China, Australian, the USA and Germany.

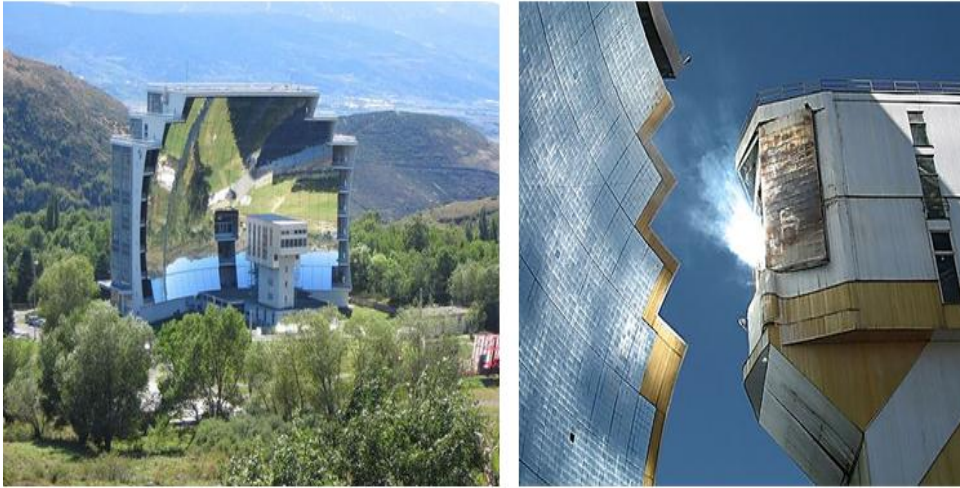


Figure 2.7 The Solar furnace powers in France in 1970 [16]

2.3.2.3- Solar Furnace Power (SFP)

A solar furnace is one of the modern solar thermal technologies with wider applications that have developed in the last few years. The design technology is a combination between solar tower and parabolic dish technology which collects a huge amount of heat energy compared to other solar technologies. A solar furnace power system uses parabolic plate mirrors to cover a building wall and heliostats in front of it in a semi-circular form. The system is easily capable of melting steel materials as the mirrors concentrate very high temperature with over 3000°C in the centre of the receiver. The receiver must therefore be made from high quality materials resistant to high temperatures. The most famous application of solar furnace technology was located in France called 'Odeillo' that was built in 1970 as shown in figure 2.7. However this station produced around 1MW output electricity power and concentrates more than 3500°C thermal heat with the total area used 2000m^2 by 63 heliostats. Each heliostat has dimension of 4.5m height and 2.5m length, and had a total manufactured cost of about €200million. The high temperature in Solar furnace can be used to melt steel, make hydrogen fuel or nano-materials. This system is a less common application in solar technologies because of high cost and technical difficulty [17].

2.3.2.4- Solar Parabolic Dish Mirror (PDM)

Solar Parabolic dish mirror is the oldest technology used in the solar field. This system has a parabolic shape covered by mirror-like surface (each one dish is called

a unit) usually aluminium, silver or polymer films which reflects solar radiation to the solar engine directly. It has been extensively reported in the literature as operating for many years. The characteristic of this system uses two-axis, short distance between mirror and receiver, and dish structure must track fully the sun to reflect sun light onto the engine. Usually, the receiver connects with the Stirling engine by hydrogen or other gas inside the tube. In addition, the temperature gathered in the receiver engine is around 1000°C [18]. This system is more popularly used in solar technologies because of easy service and isn't complicated, has a high concentration ratio around 600-200 and high efficiency at 30%[19]. Australia, California, and Spain were countries that applied this technology while each unit can generate power at 25kW in a direct way without using thermal storage.

2.3.2.5- Disadvantage of Solar Thermal Technologies (STT)

Unfortunately, all Solar Thermal Technologies have some disadvantages. The weaknesses include the technology location, high cost, consume large area, vulnerability to external contamination, and requires continues sun rays to work. Furthermore, all the weaknesses listed can be eliminated except large area and cost which needs more effort and time. Nevertheless, productive capacity of the solar energy is weak compared to oil, nuclear or natural gas but there are some improvements expected in the future.

2.4-Cost of Solar Thermal Technologies

Several researchers in energy sources showed that Solar Thermal Technology (STT) has a high cost compared with non-solar energy and non-renewable energy. The Sandia laboratory in USA has published papers on solar power technologies with high cost as shown in Table 2.2, which it gives an overview of the future cost studied and the results show that solar stations can construct in any place in the world but need billions of dollars according to the previous studies. For example, California in 2008 constructed a station and spent \$5.4 billion to produce 2000MW and the capacity later increased but this technology worked without fuels and low services [17].

There are a variety of reasons that makes the cost of producing energy using solar thermal technology very high:

- The materials are of high specifications, require a high ability to absorb thermal heat, have high heat conductivity and a long life period.
- Solar tracking system is expensive. This system is required to move the reflecting mirror in two directions –axial vertical and horizontal always within the sun direction.
- Reflective mirrors with high specifications and high price.
- Designing technology needs specialists in this technique.

Table 2.2 shows the comparison between four solar thermal technologies and the cost. Solar parabolic trough produces energy around 320MW, low peak efficiency 20%, uses limited thermal storage but the cost is still high about (270 to 630) $\$/m^2$ and (2.7 to 4) $\$/W$. Solar parabolic dish mirror technology produces low energy (each dish unit) between 5kW to 25kW, high efficiency 25%, without thermal storage, high operation temperature at 750°C and also high cost, around (320 to 3100) $\$/m^2$ and (1.3 to 12.6) $\$/W$ [18]. Solar power tower is more applicable than the others because it produces around 200 MW power with high operation temperature at 565°C, high efficiency at 20% and high cost also (200 to 475) $\$/m^2$ and (2.5 to 4.4) $\$/W$. Moreover, solar furnace technology has a large capability of power production, high capacity factor, high efficiency, and available thermal storage as compared to the others as shown in Table 2.2 On the other hand, the cost of producing one kilowatt of energy is very high, there is often a problem with the short life span of materials used and it needs to be renewed with the passage of time.

Table 2.2 The comparison between solar power technologies and cost [20]

	Parabolic Trough	Power Tower	Parabolic Dish Mirror	furnace power
Power	30-320 MW	10-200 MW	5-25 kW	10-500 MW
Operating Temperature °C	390	565	750	1000-3500
Annual Capacity Factor	23-50%	20-77%	25%	26%
Peak Efficiency	20%	23%	29.40%	22%
Net Annual Efficiency	11-16%	7-20%	12-25%	11-20%
Storage Available	Limited	Yes	Battery	Yes
Cost				
\$/m²	630-275	475-200	3100-320	450-300
\$/W	4.0-2.7	4.4-2.5	12.6-1.3	3.9-3

2.5- Technology Area

A solar thermal technology always requires the use of enormous area for the system. The total area used in solar tower station in California in 2001 was about 28 km² for parabolic dish mirror and 6.5km² for solar parabolic trough. The principle of this work is requiring more power providing more electricity which involves massive reflected area. As a result some cities have a space issue which means this technology is difficult to use. In addition it is very expensive and there is global need to have good technology at lower cost [18, 23].

2.6-Solar Thermal Energy Storage System:

There is solar energy in abundance but of course it is only available when the sun is shining and there are additional limitations that prevent its use including storage of heat and the intermittent characteristics of this energy source. These phenomena are dependent on the weather variation on a daily or seasonal basis, also during day and night. All solar energy technologies used for generating power require sun to be available and if the sun is not available or at night the system will not work. Above mentioned reasons necessitate the need for thermal energy storage in order to

satisfy the energy demand of solar energy systems. There are many different ways the system can store energy collected from a parabolic dish [18, 19]. Thermal energy storage refers to storage within well insulated liquid or solid materials, and it includes three techniques:

- Sensible heat; exploiting the thermal capacity of the storage media. Heat is accumulated to the storage media, causing an increase in media temperature.
- Latent heat; exploiting the phase change of the storage media, heat is absorbed by the storage media, through the isothermal change phase of this media.
- Quasi-latent heat or chemical energy; based upon irreversible endothermic chemical reactions. The quasi-latent heat storage, is based on the principle of irreversible chemical reactions, i.e. the heat is stored to the product of such an end thermal reaction.

2.6.1-Sensible Heat Storage

Sensible heat storage is based on the thermal capacity property of materials. Typical materials used for this purpose are liquids, solids or a mixture of these two phases. The temperature of the storage media increases during charging and decreases during discharging, on a reversible process, that can be repeated many times. Actually, this process is the most common technique for heat storage, especially for low temperatures, where liquid media are used. The quantity of energy that may be charged to a storage media, when its energy increases from T_1 to T_2 can be calculated using equation 2.1.

$$Q = m \int_{T_1}^{T_2} C_p \cdot dT = V \int_{T_1}^{T_2} \rho \cdot C_p \cdot dT = m \cdot C_p (T_2 - T_1) \quad (2.1)$$

where 'm' is the mass of used material (kg), 'V' is the volume (m^3), ' ρ ' the density of the material (kg/m^3), ' C_p ' is heat capacity (J/kg·K) and the change between temperatures T_1 to T_2 ($^{\circ}k$).

The sensible heat storage technologies in solar thermal system have a simple principle of heat storage, even though there are some phenomena that require further research and improvement. These phenomena like the exploitation of stratification and the influence of geographical and climatic conditions to improve the capacity of sensible storage system.

Water is the best liquid storage media, for low temperature applications at less than 100°C, presenting the highest thermal capacity (4.2 MJ) and the best thermo-physical properties. Other media used are thermal oils and organic substances. Storage of liquids is preferable to be implemented in underground stores, presenting low thermal losses [35]. There exist two basic techniques for underground heat storage:

- The use of a tank, installed at a low depth, near the ground surface
- The use of a physical cavity consisting of non-porous rock or the store in physical/technical saving banks.

Most usual materials of tanks are steel, cement, glass-wool and wood (with plastic coat). It must be noted though that when using water, special care must be taken into consideration to avoid corrosion.

The optimum design of an energy storage system, focusing at the size of the storage tank, is dependent on the following factors:

1. The operational characteristics of the solar system
2. The load of the system, referring to the temperature demand and the duration that this demand lasts
3. The total surface of the collectors
4. The local climatic data.

2.6.2-Latent Heat Storage

As mentioned earlier in the introduction, an option to store thermal energy is the latent heat storage. This method is based on the utilization of Phase Change Materials (PCM). These materials store heat when they go from solid to liquid, from liquid to gas or from solid to solid (change of one crystalline form into another without a physical phase change). Then they release energy when they have the reverse phase change. It must be mentioned that until now, the PCM studies and applications have been mainly focused on the solid-liquid phase change. The

storage capacity of a LHS system in the concrete case of solid-liquid transformation is given in equation 2.2.

$$Q_{storage,PCM} = \int_{T_{initial}}^{T_M} m_{PCM} C_{p,solid} dT + m_{PCM} \cdot a_{PCM} \Delta h_{PCM} \quad (2.2).$$

$$+ \int_{T_{PCM}}^{T_{final}} m_{PCM} C_{p,liquid} dT$$

Where, 'T_{initial}' is the initial temperature, 'T_M' is the melting temperature, 'T_{final}' is the final temperature 'm_{PCM}' is the mass of heat storage medium, 'C_{p,solid}' is the specific heat of solid, 'C_{p,liquid}' is the specific heat of liquid, 'a_{PCM}' is the fraction melted, 'Δh_{PCM}' is the heat of fusion per unit mass (J/kg).

The heat of fusion or the heat of evaporation is much greater than the specific heat. The latent storage materials have a larger volumetric energy storage capacity than the sensible storage materials. Another advantage is the fact that the absorption and release of the energy stored takes place at a constant temperature which makes it easier for the choice of the material to use in the different applications. The different materials which have the properties mentioned before are classified in different groups. There are three main groups: organic materials, inorganic materials and eutectics. It must be mentioned that generally the materials do not respect all the properties listed in the previous section and it has to be compensated with the system design and different enhancement methods such as the use of fins or composite materials in the form of matrixes [36].

2.7- Conclusion

In summary of SPDT reviews had discussed three main topics; the history of solar thermal technologies and constantly evolving development of it was initially discussed. The second section was more specific on solar thermal technologies such as solar power tower, solar furnace power, solar parabolic dish mirror and solar parabolic trough. Also this review mentioned some of the countries where this technology were applied. The last section discussed the advantages and disadvantages of the application of solar thermal technology in those countries.

In addition, the review showed two main issues when solar technology was applied; firstly it has high cost and secondly used large area. Some solar technologies were used to generate power directly from the sun, such as parabolic dish and solar furnace but do not use thermal storage. However this could reduce its working time or use other resources at night. The best way to exploit the use of the technology without hindrance is to use the roof or walls of buildings.

A variety of solar collectors have been discussed, including non-concentrating types and concentrating types. Among non-concentrating collectors, the solar thermal technologies show the best overall performance. Sun-tracking concentrating solar collectors have also been examined, in terms of optical optimisation, heat loss reduction, heat recuperation enhancement, different sun-tracking mechanisms. Three different types of concentrating solar collectors have been described and compared: heliostat field collectors, parabolic dish collectors and parabolic trough collectors [37].

The materials used for high-temperature thermal energy storage systems have been compared, and a comparison between different categories of thermal storage systems has been presented. Molten salts with excellent properties are considered to be the ideal materials for high-temperature thermal storage applications. Heat transfer enhancement is also essential to overcome the poor heat transfer in these applications. For this purpose, graphite composites and metal foams are found to be the ideal materials. Lastly, the current status of existing solar power stations has been reviewed.

CHAPTER (3):- Design and Fabrication Solar Parabolic Dish with Stirling Engine

3.1-Introduction

The previous chapter discussed in details the literature survey on various aspect of the energy generation as it affects the current project including renewable energy, non-renewable energy, solar thermal technologies, solar thermal applications and solar thermal storage. In view of this, this section of the thesis will focus on discussing the design and fabrication of the parabolic dish, Stirling engine and cavity receiver. It is divided into three sub-sections including the design of two different parabolic dishes, hybrid (gamma) Stirling engine and two thermal receivers. Furthermore, there are three gas circuits within the system, with two of the circuits working during the day and one working at night, with schematic diagram of the circuits as shown in Figure 3.1.

The Parabolic Dish Technology (PDT) is key aspect of the current project, as it redirects solar radiation into the aperture of a specially designed receiver. As part of the PDT, the receiver concentrates heat on the absorber, and so it must be designed to be large enough to enable a significant fraction of reflected radiation. However, there is a drawback when the receiver is too large as the absorber temperature may then be too high. In general, increasing the size of the receiver will increase the amount of solar radiation intercepted by the receiver. This also increases the heat losses owing to convection and radiation out of the receiver aperture. This aspect of the prototype model will be discussed in more detailed subsequently.

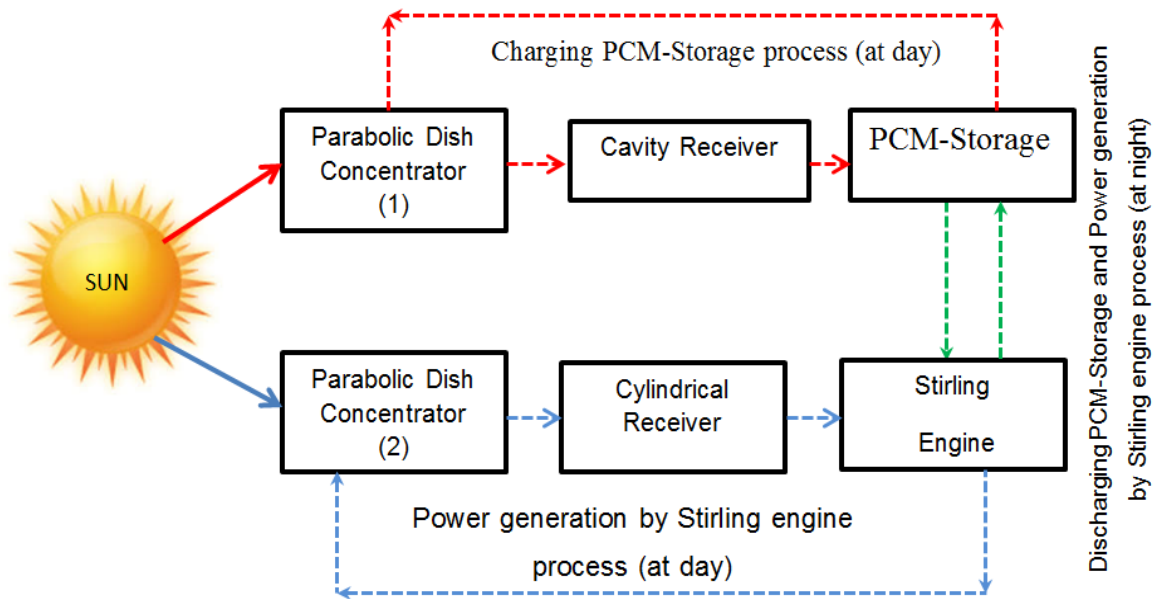


Figure 3.1 The process of gas cycles during day and night in the complete system

Figure 3.1 shows the working principle of the complete system including the gas movement when the system operates based on the three operational circuits. The need to understand the individual parts of the system will assist the successful design of the new prototype model. Also, it is important to note hot gases flow through the closed cycles; each of these cycles has different thermal devices as mentioned earlier such as the parabolic dish concentrator, cavity and cylindrical receivers, PCM-Storage and the Stirling engine. Each of the devices has complicated thermodynamic processes that add to the complexity of the design.

The three main processes in the cycle (two during day and one at night) are given as following:

1. **Charging PCM-Storage:** In the first process, the helium (He) gas in the copper pipe absorbs heat which and collected in the cavity of receiver and transfers that heat to PCM- Storage during the day.
2. **Power generation by Stirling engine:** In the second process, helium gas in the system through the second cycle absorbs heat from the receiver and supplies that heat to the Stirling engine directly to generate power during the day.

3. **Discharging PCM-Storage and Power generation:** For the third process, the gas transfers heat from the PCM-Storage to the Stirling engine and this process occurs at night or periods when solar radiation is not available.

The design of different part of the new prototype model was carried out using the Solid-work software, the software is user friendly and allow for easy modification and simulation of the prototype model as additional advantage. Hence, this chapter intends to discuss the design of two parabolic dishes, hybrid Stirling engine and two thermal receivers.

3.2-Solar Position

In generation of energy using the solar technology, the amount of energy generated depends highly on the amount of sun rays, with the solar position as a factor [37, 38].Furthermore, geometric position changes from hour to hour, day to day and month to month, the position of the sun in relation to angle of the panel receiver influences the amount of solar heat obtained.Hence, at any given instance the sun's position can be fixed by two different angles:

1. Altitude is the angle between the sun and the horizon.
 - When the sun is on the horizon during sunrise and sunset, this angle is zero.
 - Solar altitude is at the maximum in the noon.
 - The complement of solar attitude angle or the angle of sun from a vertical line directly overhead is called the zenith angle.
2. Azimuth is the angle between a north – south on the earth surface and the horizontal projection of the sun's rays, it is measured from true south. By convention, solar azimuth is negative before noon and positive after noon.

3.2.1- Solar Insolation

Solar insolation ' I ' is the amount of radiation ' P ' arriving from the sun onto a flat surface with surface area ' A ' [2 and 3].

$$I = \frac{P}{A} \quad (3.1)$$

Equation 3.1 shows that the power generated by sun depends on solar radiation (W/m^2) and collector area ' A ' (m^2).The solar radiation has other natural factors which vary with geographical position on the earth, orientation of dish concentrator,

meteorological conditions and intensity of sun rays at different times of the day (sun time). Furthermore, solar radiation can be assumed to be constant when applied in one location and for one material with sun tracking system (moving with sun) [32 and 33]. Equation 3.1 can be corrected for the actual power collected on the focal point by using reflective efficiency ' η ' as given in equation 3.2.

$$P = A \times I \times \eta \quad (3.2)$$

3.3- Factors Affecting Solar Collector Design

3.3.1- Intercept Factor

The intercept factor is the fraction of solar radiation reflected from the parabolic collector that enters the aperture as shown in Figures 3.2 and 3.3-B. It is influenced by the size of the aperture, errors in the parabolic dish system, the collector rim angle and other factors with nonparallel sunlight [35 and 36]. However, increasing the intercept factor will:

- Increase the small amount of the energy entering the receiver (although this may not always be beneficial).
- Reduce errors in the parabolic reflecting collector surface, and then increase in the intercept factor in order to improve the system performance.
- Increasing the size of the aperture that requires further analysis so as to determine if the increase in energy intercepted by the receiver will be greater than the energy lost owing to thermal losses.

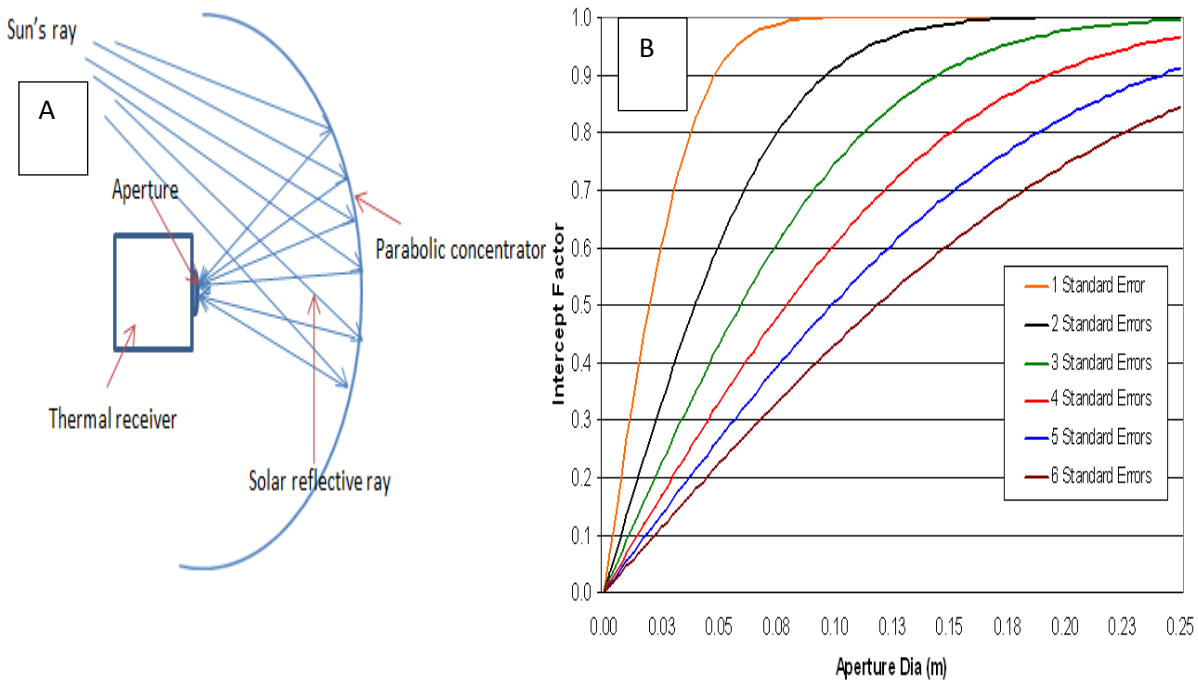


Figure 3.2 The relationship between intercept factor in parabolic dish (A) and aperture size of solar parabolic dish technology (B) [33]

3.3.2- Beam Spread Factor

The beam spread is the distance light spreads perpendicular to the direction of propagation after the reflection on the collector surface on the parabolic dish. Decreasing the spread of the beam between the point where it reflects from the collector and to where it enters the focal plane of the receiver will allow for the aperture to be designed, as increasing the size will lead to an increase in system performance. For this purpose, solar tracking system was used to determine how far the beam of sunlight will spread. The beam spread can be controlled by adjusting the collector rim angle, nonparallel rays, collector errors, and focal length [16].

3.3.3-Collector Rim Angle (Ψ_{rim}) and Concentration Ratio

The rim angle is an indicator of the arc for the parabolic receiver. A parabolic dish with a larger rim angle has a steeper slope. This angle can be determined by equation 3.3 when the focal length and parabolic dish diameter.

$$A_{REC} = 4\pi f^2 \cdot \sin^2 \frac{\Psi_{rim}}{[1 + \cos(\Psi_{rim})]^2} \quad (3.3)$$

$$\Psi_{\text{rim}} = \tan^{-1} \left[\frac{(f/d)}{2} \times \left(\frac{f}{d} \right)^2 - 1/8 \right] \quad (3.4)$$

Where 'A_{REC}' aperture receiver area (m²), 'f' is the focal length of the collector (m), 'd' is the diameter of the collector (m) and 'Ψ_{rim}' is the rim angle (°).

These equations 3.3 and 3.4 show the relationship between aperture area 'A_{REC}' with rim angle 'Ψ_{rim}' and the rim angle depends on the diameter 'd' and the focal length 'f' as shown in Figure 3.3. Furthermore, if the rim angle was determined before sizing the aperture, then it will have an impact on the maximum concentration ratio, the intercept factor, collector slope error, and heat losses due to convection and radiation [10]. But the best solutions are to use the known available dimensions for several collectors to determine this angle.

Equation 3.4 was applied to find the rim angle for three different common systems in solar thermal applications. Summary of the rim angle for specific systems are shown in Table 3.1, and the depiction of the rim angle is given in Figure 3.3 with the curved lines representing the outline of the parabolic dish collector.

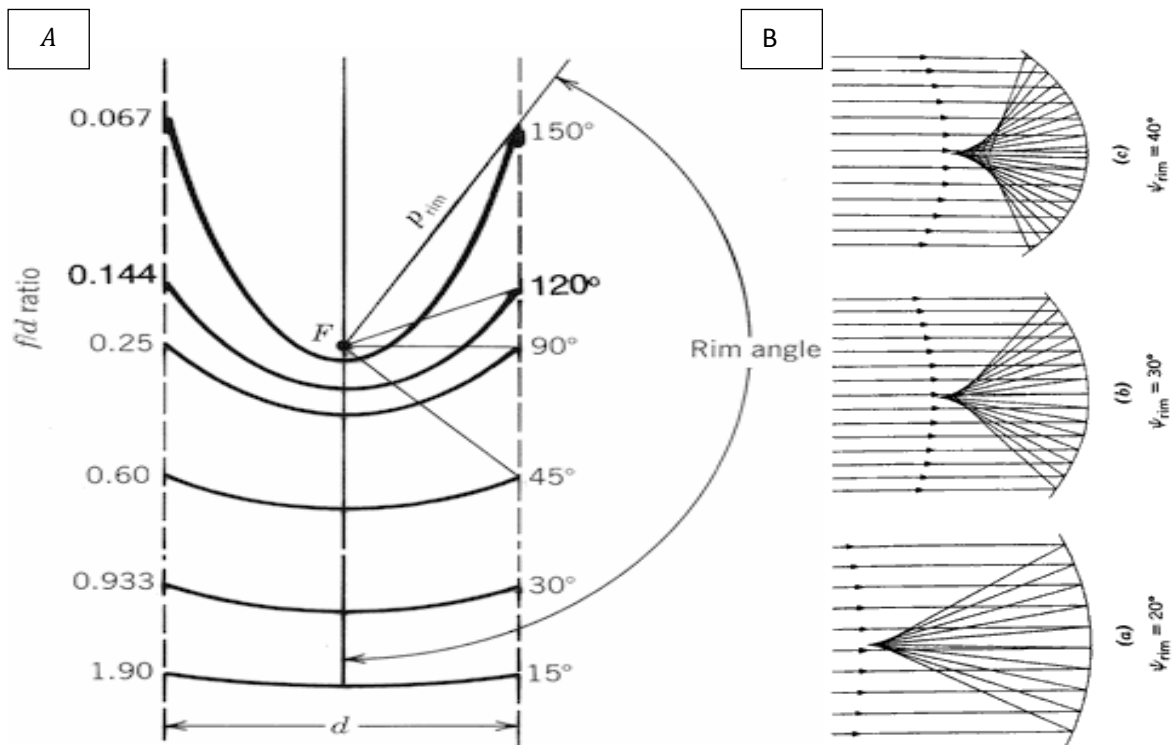


Figure 3.3 The relationship between f/d ratio and rim angle in parabolic dish system (A) and (B), different rim angles (20°, 30°, 40°) [30]

On the other hand, the ratio of the area of aperture collector 'A_{apr}(m²)' to the surface area of receiver 'A_{rec}(m²)' is called the concentration ratio 'CR' given as;

$$CR = \frac{A_{apr}}{A_{rec}} \quad (3.5)$$

It is important to get high concentration ratio in the parabolic dish system; this is to improve the efficiency of the whole system. The smaller the area of the receiver will result in reduced thermal losses and the intercept factor will be larger for a specified aperture diameter. For example, the Table 3.1 showed the three different famous solar manufacturers with the peak concentration ratio at constant solar radiation of 1000 W/m².

However, there is a relationship between the rim angle and concentration ratio within the same system, from which the largest concentration ratio of 45,000 was shown to be obtained at a rim angle of (45°) (theoretical maximum). In view of this, manufacturers designed most of their systems with rim angle of approximately 45°.

Table 3.1 The concentrator system specifics for several manufacturers SBP, SES & WGA (Mod 2) [20].

Manufacturer	Rim angle [degrees]	Peak CR (suns)	Reflectivity %	Focal Length(m)	Glass area(m ²)	Projected area(m ²)
SBP	12730	52	94	4.5	60	56.7
SES	7500	40	91	7.45	91	87.7
WGA(MOD2)	>13000	37	94	5.45	42.9	41.2

3.3.4- Parabolic Collector System Imperfections

The literature has shown that the spread of beam on the parabolic dish systems are affected by intercept factors and this in turn results in several imperfections on the collector system. The summary of these errors are given below and typical error values shown in Table 3.2:

1. Slope of the parabolic mirror created during manufacturing.
2. Receiver alignment discrepancies.
3. Variations in the mirror specular reflectance.
4. Tracking error from the tracking sensors.

5. Tracking drives not being in a uniform position.

All previous errors have a significant impact to decrease the intercept factor and must be considered during prototype model operations.

Table 3.2 Typical error values for a Stirling dish collector system [33, 29].

Error type		One standard deviation of error (1 σ)
Structure-Slope (mrad)	σ_s	2.5 x 2
Tracking-Sensor(mrad)	σ_t	2
Tracking-Drive(mrad)	σ_d	2
Receiver Alignment(mrad)	σ_r	2
Specular Reflectance(mrad)	σ_p	0.25 x 2
Sun's Width(mrad)	σ_w	2.8

The total error in solar parabolic dish technology can be given by equation 3.6.

$$\Sigma\sigma_T = \sqrt{[(2.\sigma_s)^2 + \sigma_s^2 + \sigma_d^2 + (2.\sigma_r)^2 + \sigma_w^2]} \quad (3.6)$$

The values in Table 3.2 are placed in equation 3.6 to calculate the total collector system error ' σ_T ' which is 6.7 mille-radians.

3.3.5- Non-parallel Sun Rays

Non-parallel sun rays contribute significantly to solar radiation diffusion after reflection from the parabolic mirror that contributes to a lower fraction of intercepted solar energy in the aperture of receiver. Equation 3.7 was used to determine the beam spread resulting from non-parallel rays as show in Figure 3.4.

$$\Delta r = 2p \times \tan\left(\frac{\varepsilon}{2}\right) \quad (3.7)$$

where ' ε ' is the angular size of the sun ($^\circ$), 'p' is the distance from the concentrator surface to the focal point of the aperture (m), ' Δr ' is the total beam spread in the plane perpendicular to the centreline of the reflected light as shown in Figure 3.4.

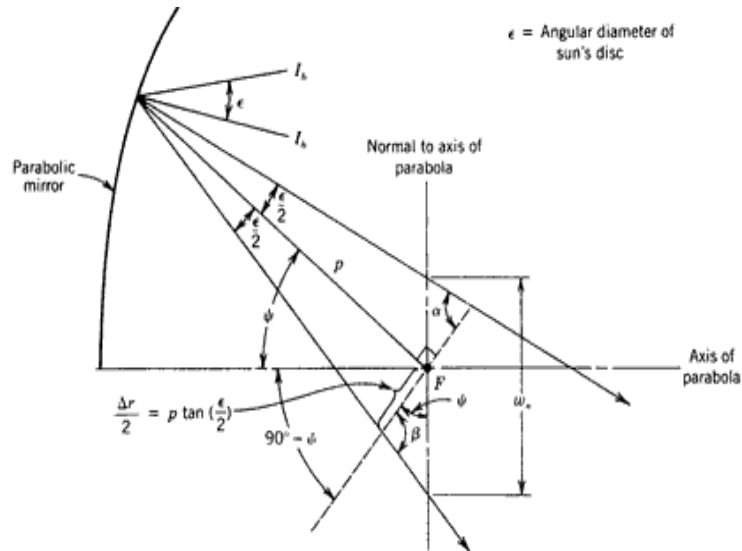


Figure 3.4 Beam spread in the plane perpendicular to the centreline of the reflected light [40]

$$p = \frac{2f}{[1 + \cos\phi]} \quad (3.8)$$

where 'p' is the focus of the aperture (m), 'f' is the focal length of the collector (m) and 'φ' is the angle between the line between the collector and focus (°). Equation 3.8 and Figure 3.4 are used to determine the distance from the collector surface to the focus of the aperture, the focal length of the collector, the angle between the line and the collector, and the location of interest on the collector.

3.4-Energy Intercepted by Receiver

Measuring the focus temperature 'T_{focus}' required in the parabolic concentrator design can be achieved using Equation 3.9.

$$T_{\text{focus}} = T_{\text{am}} [(1 - \eta) \times \frac{\eta_{\text{opt}}}{\epsilon_{\text{opt}}} \times CR \times \sin\theta^2]^{\frac{1}{4}} \quad (3.9)$$

where 'T_{am}' is ambient temperature of system (°C), 'η' is efficiency of transferring heat to working gas, 'η_{opt}' is optical efficiency of concentrator system, 'ε_{opt}' is emissivity of absorber, 'CR' is concentrator ratio and 'θ' is the angle between the line between the collector and focus (°). The temperature of focal point is related to the instantaneous rate of thermal energy coming from the receiver, this energy known as useful energy (heat actually being used for power generation) can be obtained using equation 3.10.

$$Q_{useful} = Q_{in} - Q_{out} \quad (3.10)$$

From the thermodynamic law cycle, useful energy in any system is equal to the energy coming 'Q_{in}' into the system after excluding the heat loss 'Q_{out}'. The energy coming from parabolic dish concentrator can be given as;

$$Q_{in} = I_b A_a E (\cos\phi) \rho \phi \tau \alpha \quad (3.11)$$

Also output energy can be written using equation 3.12;

$$Q_{out} = A_{rev} [U (T_{rev} - T_{amb}) + \sigma f (T_{rev}^4 - T_{amb}^4)] \quad (3.12)$$

Placing equations 3.11 and 3.12 in equation 3.10 will form a complex equation 3.13 given as;

$$Q_{useful} = I_b A_a E (\cos\phi) \rho \phi \tau \alpha - A_{rev} [U (T_{rev} - T_{amb}) + \sigma f (T_{rev}^4 - T_{amb}^4)] \quad (3.13)$$

where 'Q_{useful}' is instantaneous rate of thermal energy coming from the receiver (W), 'A_a' is area of the concentrator aperture (m²), 'A_{rev}' of receiver aperture (m²), 'E' is function of concentric aperture area not shaded by receiver structure, 'f' is equivalent radioactive conductance (m), 'I_b' is beam normal solar radiation (W/m²), 'σ' is Stefan-Boltzmann constant (5.6696 × 10⁻⁸ W/m² K⁴) for energy transfer, 'T_{rev}' operating temperature receiver (°k), 'T_{amb}' is ambient temperature (°k), 'U' is convection-conduction heat loss coefficient for air currents within the receiver cavity and conduction through receiver walls, 'ρ' is concentrator surface reflectance, 'τ' is transmittance of anything between the reflector and absorber, 'φ' is the angle of incidence or angle between the sun's ray and a line perpendicular to concentrator aperture and 'ϕ' is capture function or intercept.

Equation 3.13 has many factors depending on heat energy to be used in the receiver design such as solar radiation, reflected area, Stefan-Boltzmann constant for energy transfer and reflecting efficiency.

High temperature in the receiver requires a large concentrator area which has a positive relationship between parabolic dish area and focal temperature. While increasing the parabolic dish area increases the operation temperature and this affects the input temperature of Stirling engine. However when the operating temperature of this engine is increased, more power is generated as shown in Table

3.3. For example, if temperature of approximately 200°C has to be achieved, about 4 m² of reflective mirror or more is required. High temperature at the thermal receiver increases the power generation because the engines are more efficient with high temperatures [34].

3.5-Design Parabolic Dish Concentrator (PDC)

A parabolic dish concentrator (PDC) is a curve generated by the intersection of a right circular cone and the plane parallel to an element of the curve which is given as $y=ax^2$ as given in Figure 3.5. The area of the parabolic dish concentrator depends on the intercept thermal energy.

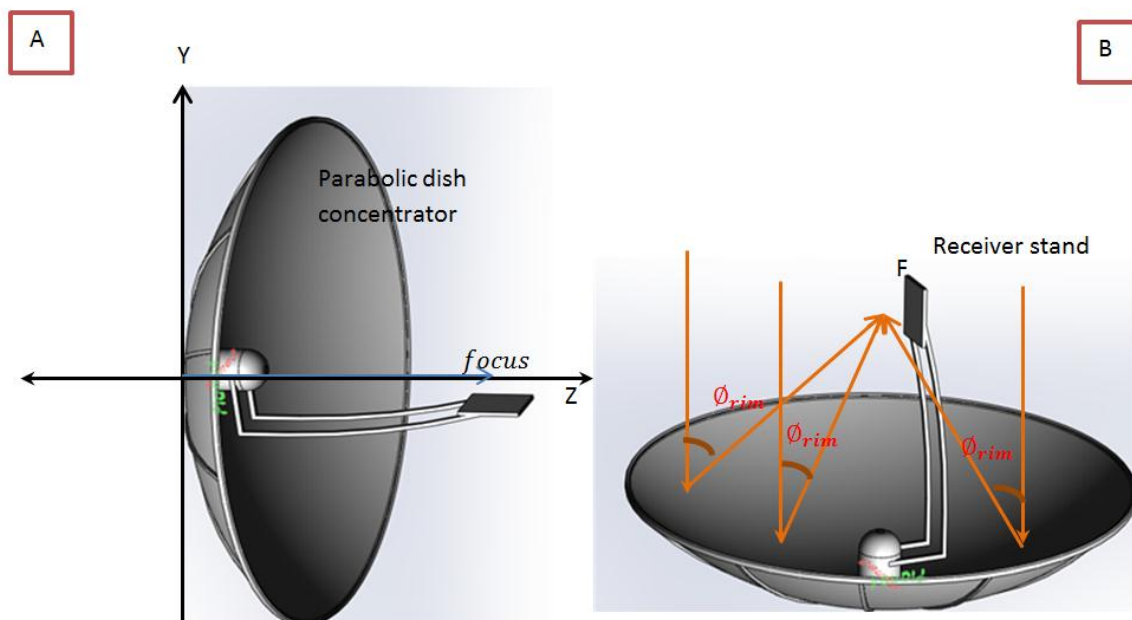


Figure 3.5 Parabolic curve is in three dimensions x, y and z with rim angle designed using solidworks

Figure 3.5 describes a parabolic curve symmetrical to x, y and z-axis, and this is related to the point at the centre of parabolic dish called the focal point. Solar energy is collected at this point which is reflected by parabolic curves and this point can be obtained using equation 3.14.

$$F = \frac{1}{4a} \quad (3.14)$$

Solidworks was used to design the parabolic curve which and later constructed as shown in Figure 3.2. The tracking system on the parabolic dish was displayed on focal point and this point depends on the rim angle which is defined as the incident angle of solar radiation with the outer rim of the concentrator as shown in Figure 3.5. Further discussions on the design and fabrication of the two parabolic dishes used in the current work are given in the subsequent sections.

3.5.1- Construction Stages of Dishes used in the System

The construction stages in order to make the appropriate parabolic dishes were not simple. It was initially designed using parabolic concentrator models in the solidworks software and then were developed using existing satellite dishes as show in Figure 3.6. The constructions of the dish concentrators were divided into fifth stages as follows:

- Proper selection of satellite dishes
 - A workshop in Oman was chosen for the work, and concentrators were constructed from satellite dishes after buying from a local market.
 - Installation of the two satellite dishes (3m^2 and 4m^2) is as shown in Figures 3.6 and 3.7.
 - A normal satellite of 4m^2 was first used to save time and money, and later 3m^2 was made.
- Sheet covering for the satellite dishes
 - Both satellite dishes were covered by flexible reflective mirror sheet with thickness of $610\text{mm} \times 610\text{mm}$ and efficiency of 98%.



Concentrator dish (4m²) with reflective flexible sheet

Concentrator dish (3m²) with reflective flexible sheet

Figure3.6 Two satellite dishes (2 m² and 4m²) with reflective flexible sheets

- Installation of focal arm into the central position of both dishes
- To install the long iron base from the central position of the parabolic dish to the focus point at the base of thermal receiver or Stirling engine was carried out as follows:
 - In front of the first parabolic curve the receiver hybrid Stirling engine was installed using a 1.4 m length of iron rod from the centre of the dish.
 - Also installed were two long iron pieces from the centre of curve to be a base of engine and generator. The thermal heat exchanger was later added in front of hot space of engine.
 - In front of second parabolic dish 3 m² is cylinder thermal receiver using iron rod of length 1.2 m and section 3.6 gives more information.
- Install a long iron base stand at the back of central of central position of both dishes:

- From the back of parabolic dishes, a long iron base 1.5 m was installed to keep the dish in the same place, for easy movement to different directions during operation as shown in Figure 3.7.



Figure 3.7 4m² parabolic dish with installed long iron base stand

- Install both dishes using long iron base stand:

Both parabolic dishes were installed at both ends of a long iron base of 7 m length. This is to keep the dishes firm and allow easy movement with solar track system to all directions when operated during day as shown Figure 3.8.

On the completion of the design construction and installation of both parabolic dishes (3m² and 4m²), there was need to look into other aspects of the complete system. Hence, detailed discussions of suitable thermal receivers for both dishes were considered in the next section.



Figure3.8 Both parabolic dishes installed at both ends of long iron base (5 m)

3.6-Solar Thermal Receiver Review

In the design of this model, each parabolic dish has a different thermal receiver depending on the function of the receiver. Thermal receivers in solar thermal technology have two main functions; firstly it absorbs thermal energy using heat transfer fluid, and secondly it transfers the absorbed energy to the heat transfer fluid within the system. Liquid or gases are normally used as working fluid in solar thermal receiver applications.

Solar receiver consists of body of the receiver, an aperture in focus point, coil copper pipe, and working fluid. The aperture is placed at the focal point of the solar parabolic dish to reduce radiation and convection losses.

Furthermore, aperture has some properties such as high concentration ratios of over 13000, and has smaller diameters ranging from 0.14m to 0.20m, to ensure an appropriate fraction of the concentrated solar energy is intercepted by it. The ratio between energy from the collector that enters the aperture which is not blocked by

the receiver housing is known as intercept factor, and often between 94% and 99%. The receiver attached to the Stirling engine absorbs solar radiation and transfers the thermal energy into hot space of Stirling engine. The flux intensity in the receiver ranges from 100 - 110 W/cm² (CR of ~1,000), and both prevents absorber material degradation and allow the working fluid to effectively absorb the energy.

In the parabolic dish receivers, two different heat transfer methods are commonly used including Direct-illumination receivers (DIR) and indirect receiver (liquid-metal, heat-pipe solar receivers). These methods are explained as follows:

- The first method uses the heater tubes of the Stirling engine to absorb solar radiation. It is capable of absorbing high level of solar flux. This type of receiver is normally used in several PSDT systems such as EURO-dish, Sun-catcher and Sun-dish.
- Indirect-illumination receivers (IDIR) (Liquid-metal, heat-pipe solar receivers), uses a liquid-metal intermediate heat-transfer fluid, the liquid sodium metal is vaporized on the absorber surface of the receiver and condenses on the Stirling engine heater tubes, which ensures uniform temperature on the heater tubes [38,32,36].

Figure 3.9 and appendices (B) shows that the direct-illumination receiver uses pipes to directly heat the working fluid in the Stirling engine by using the heat that is absorbed on the external surface of the tubes. The working fluid is either (hydrogen or helium) which can absorb solar radiation of about 75 W/cm² due to the high heat transfer capabilities of these gases at high velocities and pressures up to 20 MPa [37].

Disadvantages of the direct illumination receivers:

- ❖ Difficulty in balancing thermal input between the Stirling cylinders.
- ❖ The heater tubes will incur more thermal hot spots as compared to heat pipe absorbers.
- ❖ The flux can be more uniformly distributed across the direct illumination receiver tubes by increasing the reflectivity of the receiver cavity walls

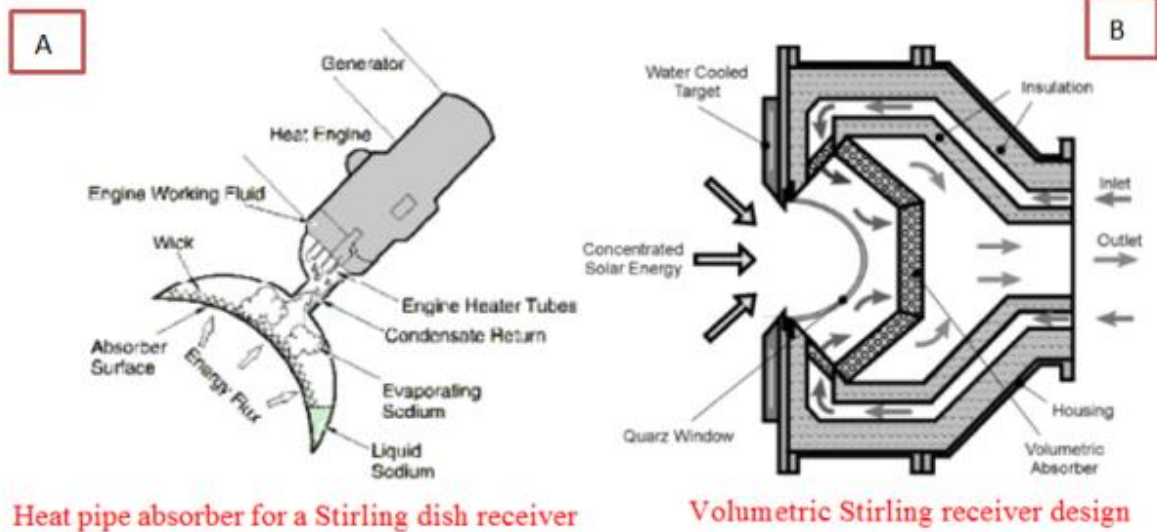


Figure 3.9 Two different types of receivers are used in solar parabolic dish technology

Comparing Figure 3.9-A and B which are both direct receivers, the volumetric receiver have the potential to be more cost effective and reliable than the heat pipe absorbers.

Disadvantages of the direct illumination receivers:

- It has the potential to operate at a higher temperature.
- It has larger heat transfer areas.
- Reduce engine dead volumes.
- Reduce the amount of expensive high temperature alloys in current Stirling engines.
- Reduce heat losses.

For above reasons, volumetric receiver is a better choice for connecting hybrid Stirling engine with the parabolic dish with the helium gas. Hence, the current prototype model considers the volumetric model more appropriate and compatible to achieve the objective of the work. Key problems associated with the receivers in general are heat losses. There is the need to consider heat losses (convection and radiation) from the receiver, and how to reduce net effect of reduction of heat radiation entering the receiver to the minimum.

3.6.1- Heat Losses in Receiver of Parabolic Dish Concentrator

The heat waste during heat transfer to the centre of receiver is called heat losses in parabolic concentrator system. There are three ways of losing heatfocal point of the thermal receiver; by conduction, convection and radiation.

The receiver is responsible for most of the thermal losses that occur before the energy was converted into electrical in the Stirling engine. Table 3.3 gives the breakdown of percentage heat losses in two different parabolic dishes with Stirling engine receivers including Stirling Engine System (SES) and Wilkinson Goldberg and Associates, Inc. (WGA).

Table3.3 Heat losses in Stirling dish system (conduction, convection, radiation) in SES and WGA models [39].

MODEL(Stirling Engine)	SES	WGA
Collector Heat Losses	37 %	24 %
Receiver Intercept Losses	12%	2%
Receiver Thermal Losses	51%	76%

The table above also shows collected heat losses owing to the mirror reflectivity comprising of 37 % and 24 % of the thermal losses for the SES and WGA collectors respectively. Secondly, receiver intercept losses represent 12 % and 2% of the total thermal losses for the SES and WGA systems. Lastly, receiver thermal losses (conduction, convection, radiation) consist of 51 % and 76 % of the total thermal losses for the SES and WGA.

3.6.2- Receiver Design Criteria

In general, the parabolic dish concentrator reflects direct solar radiation into the aperture of the receiver, which is the most important part of the overall system. For this reason, aperture must be designed to be as large enough as possible to collect a significant fraction of reflected radiation as shown in Figure 3.10.

There are several important points in the design of receiver and this can be summed upas follows:

- Increasing the aperture area will:
 - Increase the amount of intercepted solar radiation by the receiver.
 - Increase heat losses of receiver body.

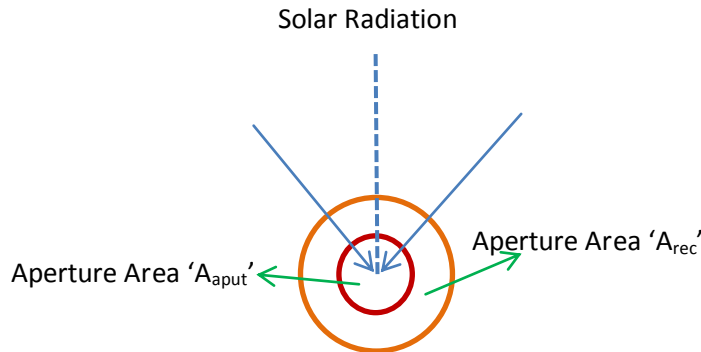


Figure 3.10 The geometry of thermal receiver with A_{aput} and A_{rec} areas

- Decrease the factors of convection and radiation of the effective radiative energy absorbed in the receiver.
- Decreasing the aperture area will:
 - Decreases the solar radiation and amount intercepted by the receiver.
 - Decreases the heat losses of receiver body by convection and radiation out of the aperture.
 - Increases the factors of convection and radiation, and the effective radiative energy absorbed in the receiver.
 - Decreases absorbing area (There is no space for absorbing materials).

Before carrying out the design of any thermal receiver, it was necessary to determine the impact of receiver loss mechanisms resulting from errors in the collector system, aperture diameter and the temperature of the absorber. Absorber temperature is used to move pistons of the engine; hence it is important to study the theoretical part before the actual design.

3.6.3- Heat Transfer and Power Analysis in Thermal Receiver

The cavity receiver is the part of the system that converts solar radiation to heat energy and transferring to the working gas (helium). The cavity receiver consists of an aperture, copper pipe and good thermal insulation. The absorber is the collecting surface for reflecting solar radiation to aperture. Radiation is absorbed into the absorber material as heat and transfers the energy to a working gas by pipe that carries the energy out of the receiver as shown in Figure 3.11.

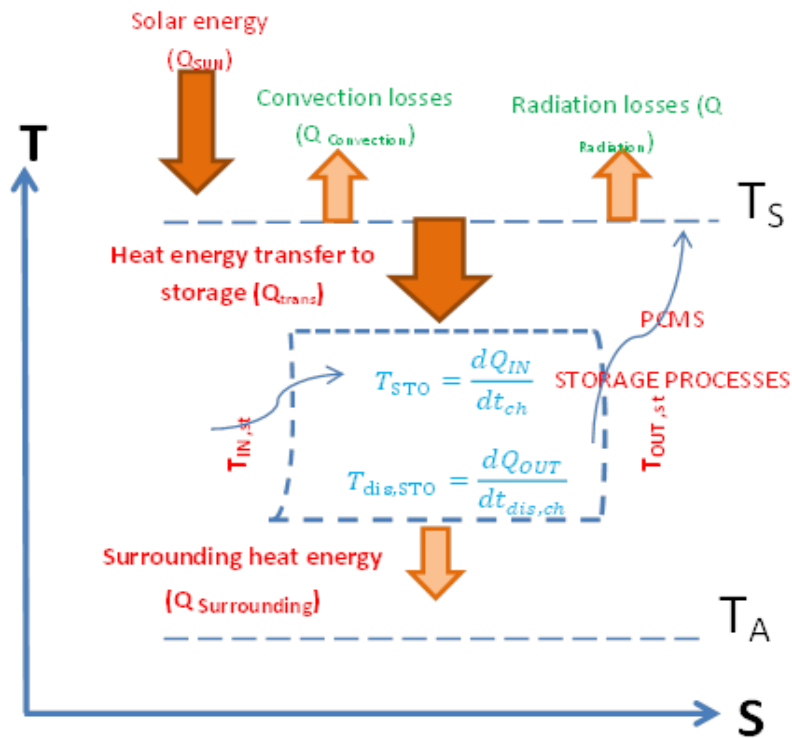


Figure 3.11 The processes of heat losses in terms of convection, radiation, heat storage and heat useful

Figure 3.11 shows the processes of heat collection, absorption and transferring to phase change materials by helium gas in the cavity receiver. It also shows the heat losses in cavity receiver by convection and radiation losses.

The parabolic dish concentrator design predicts intercepted solar power ' Q_{REF} ' by the cavity receiver as given in equation 3.15.

$$Q_{REF} = I_{DNI} \times A_{DISH} \times \rho_{REF} \times \phi_{WID} \times \phi_{INF,FAC} \times \phi_{SHADE} \quad (3.15).$$

Where ' Q_{REF} ' intercepted solar power (W), ' I_{DNI} ' is solar radiation (W/m^2), ' A_{DISH} ' is parabolic dish area mirror (m^2), ' ρ_{REF} ' is mirror reflectivity (%), ' ϕ_{WID} ' is wind factor

cut-out velocity intercept factor (%) , $\phi_{INF,FAC}$ is intercept factor and ' ϕ_{SHADE} ' is shading factor (%).The wind cut-out velocity is a value indicating the wind speed which the parabolic concentrator sends into the aperture position to prevent wind damage as shown in Table 3.4. When the wind speed factor is equal to 1, then the amount of wind speed will be neglected.

Table3.4The wind cut-out velocity and how it affects the parabolic concentrator [39]

Wind position	Wind factor	Case
Wind speed \leq wind _{cut} ,out	$\phi_{WID} = 1$	Can be neglected
Wind speed $>$ wind _{cut} ,out	$\phi_{WID} = 0$	damage

Furthermore, the effect of shading factor is determined using the theory from the work of Osborn [16]. This theory is a function of the number of parabolic dishes used in the project, the collector diameter, and the North-South and East-West collector separation distance. However it is possible to use two parabolic dishes in parallel, same direction and large interval distance between dishes ($\phi_{WID}=1$).Hence, heat transfer from the receiver ' $Q_{TRANSFER}$ ' to helium is given in terms of heat absorbed ' Q_{ABSORB} 'and heat losses ' Q_{LOSS} ' as given in equation 3.16.

$$Q_{TRANSFER} = Q_{ABSORB} - Q_{LOSS} \quad (3.16)$$

3.6.3.1- Heat Absorbing in Receiver(Q_{ABSORB})

The amount of heat absorbed in the receiver depends on absorption materials used in thermal receiver. This material must have good thermal properties such as high transmittance and thermal absorbance as given by equation 3.17.

$$Q_{ABSORB} = Q_{REF} \times \tau \times \alpha \quad (3.17)$$

- **Transmittance(τ).**

Transmittance is simple fraction of heat energy which gets through the cover of receiver and the value of transmittance clean fused quartz is about 0.9.

- **Absorbance(α).**

Absorbance is another fraction of heat energy which is absorbed on material cover of the receiver body. Metals used as absorbers are mostly dark materials with less reflection, high heat transfer property and attain relatively high absorbance level when exposed to the atmosphere at high operating temperature of parabolic dish. Covering the surface receiver with such material with high absorbance value for radiation enhances receiver performance. From compensation equation 3.15 to 3.16, the amount of energy absorbed is given in equation 3.18.

$$Q_{\text{ABSORB}} = (I_{\text{DNI}} \times A_{\text{DISH}} \times \rho_{\text{REF}} \times \varphi_{\text{WID}} \times \varphi_{\text{INF,FAC}} \times \varphi_{\text{SHADE}}) \times \tau \times \alpha \quad (3.18)$$

An energy balance indicates that at any interface, absorbance plus reflectance and transmittance must be equal to unity

$$\rho_{\text{REF}} + \tau + \alpha = 1 \quad (3.19)$$

From second law of thermodynamics, heat transfer to helium can be obtained using equation 3.20.

$$Q_{\text{ABS,H}_2} = \dot{M}C_p\Delta T_{\text{in,out,rec}} \quad (3.20)$$

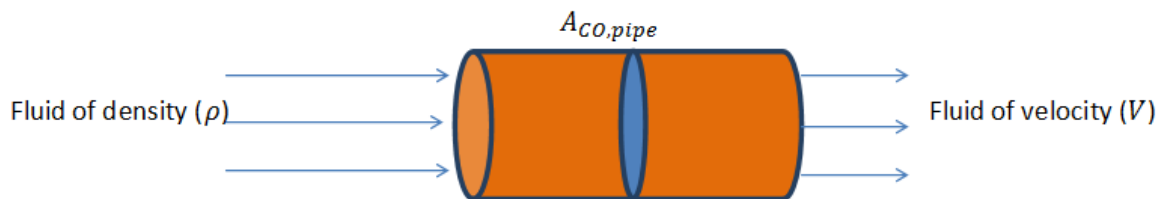


Figure3.12 Helium gas and flow through copper pipe in the system

$$\dot{M} = \rho \times V \times A_{CO,pipe} \quad (3.21)$$

The diagram in Figure 3.12 shows the fluid dynamics by examining the simplest case of fluid flow; laminar flow with constant velocity in a uniform pipe which consists of fluid with density ' ρ ' through a uniform copper pipe of area ' $A_{CO,pipe}$ ' with velocity ' V '.

3.6.3.2 - Heat losses in Cavity Receiver:-

Considering thermodynamics nature of different materials, there are three ways of heat losses in cavity receiver system as mentioned in section 3.6.1. Each of these heat losses have different fractions which effects the main heat transfer system equation and efficiency of system as given in equation 3.27 and 3.28.

I. Conduction losses ($Q_{\text{Conduction}}$) in Receiver

The heat losses due to conduction through the receiver housing are also dependent on the convective heat transfer on the exterior of the receiver housing. So series of resistance model can be used to obtain the total conductive losses.

The total losses resulting from conduction is given by equation:

$$Q_{\text{Convection}} = \frac{T_{\text{WALL}} - T_{\text{AMB}}}{R_{\text{Convection}} + R_{\text{Conduction}}} \quad (3.22)$$

where ' T_{WALL} ' is interior wall temperature of the receiver ($^{\circ}\text{C}$), ' T_{AMB} ' is ambient temperature around project ($^{\circ}\text{C}$) the convection and conduction resistances respectively ' $R_{\text{Conduction}}$ ' can be written in two specific equations 3.22a and b.

$$R_{\text{Conduction}} = (1/h \cdot A_{\text{Convection}}) + \left(\frac{L}{k} \cdot A_{\text{Conduction}} \right) \quad (3.22a)$$

$$R_{\text{Conduction}} = \left(\frac{L}{k} \cdot A_{\text{Conduction}} \right) \quad (3.22b)$$

The total heat loss due to conduction is given by:

$$Q_{\text{Convection}} = \frac{T_{\text{WALL}} - T_{\text{AMB}}}{(1/h \cdot A_{\text{Convection}}) + \left(\frac{L}{k} \cdot A_{\text{Conduction}} \right)} \quad (3.23)$$

where ' L ' is the width of the receiver insulation which is used around the receiver body, h is the convective heat transfer coefficient of the exterior of the receiver housing and ' $A_{\text{Conduction}}$ ' and ' $A_{\text{Convection}}$ ' are the areas associated with conduction and convection respectively.

II. Convection Losses ($Q_{\text{Convection}}$) in receiver

The heat loss is due to convection transfers energy that is from the absorber surface directly to the air in contact with it. When the air is fixed (not moving) it is known as natural convection but when it is moving (not fixed) it is forced convection.

However, convective heat losses in the receiver represent a significant fraction of the total losses in the receiver system. From the newton's law (cooling case) it can be given as the convection loss due to natural convection as in equation 3.24 [16]:

$$Q_{\text{Convection}} = \bar{h} \cdot A_{\text{Convection}} \cdot (T_{\text{Sur}} - T_{\text{amb}}) \quad (3.24)$$

where \bar{h} is the average heat transfer coefficient, cavity receiver area ' $A_{\text{Convection}}$ ', temperature of receiver surface ' T_{Sur} ', ambient temperature ' T_{amb} '. The amount of heat convection loss in equation 3.24 depends on the average heat transfer coefficient, cavity receiver area, temperature of receiver surface and ambient temperature. There is more detailed information on the average heat transfer coefficient fraction in the literature [14].

III. Radiation losses ($Q_{\text{Radiation}}$) in receiver

The radiation losses in the cavity receiver contribute to a significant fraction of the total losses in the receiver and other parts of the system as discussed in section 3.6.1. There are a lot of research effort focusing on the study of the effect of parabolic concentrator system such as SES and WGA.

$$Q_{\text{Radiation}} = \epsilon_{\text{cav}} \cdot \delta \cdot A_{\text{ser}} \cdot (T_{\text{cav}}^4 - T_{\text{amb}}^4) \quad (3.25)$$

where ' ϵ_{cav} ' is the effective emissivity of the cavity aperture, ' δ ' is Stefan Boltzmann's constant which equal ($\delta = 5.67 \times 10^{-8} \text{ W/m}^2 \text{ k}^4$), ' A_{ser} ' is the surface area emitting radiation (simplified to be the aperture area), ' T_{cav} ' is the temperature of the surface losing net energy due to radiation (cavity interior), ' T_{amb} ' is the temperature of the surface that is receiving net energy (ambient conditions).

It is important to note that the cavity walls are always at a higher temperature than that of the absorber, while the thermal energy used for generating power is not coming from the wall but from the absorber fluid. Hence, the average internal temperature of receiver must be used for T_{cav} . A view factor analysis was also performed and compared, which gave similar results. The view factor ' F_{2-1} ' and ' F_{1-2} '

was determined by applying the reciprocity relation to surfaces (1 and 2) as shown in Figure 3.13 as shown by most researchers [37 and 38].

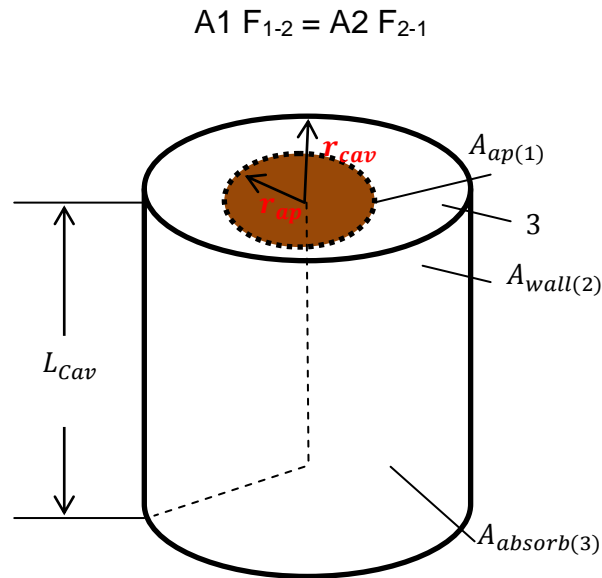


Figure 3.13 Schematic diagram of the cavity receiver [37]

Figure 3.13 shows the body of the cavity thermal receiver, where L_{cav} is the depth of the cavity, r_{ap} is the radius of the receiver aperture, and r_{cav} is the radius of the internal cavity walls. The same factors also affect the cylinder side wall to the aperture and from the absorber surface to the aperture as shown in figure 3.13. The total thermal losses using the view factor is given by equation 3.26.

$$Q_{\text{Radiation}} = \epsilon_{cav} \cdot F_{2-1} \cdot \delta \cdot A_{\text{wall}} \cdot (T_{\text{wall}}^4 - T_{\text{mirror}}^4) + \epsilon_{cav} \cdot F_{4-1} \cdot \delta \cdot A_{\text{absorber}} \cdot (T_{\text{asorber}}^4 - T_{\text{mirror}}^4) \quad (3.26)$$

The total heat transfer in the system by the working fluid is given by equation 3.27.

$$Q_{\text{Tr,st}} = [I_{\text{DNI}} \times A_{\text{DISH}} \times \rho_{\text{REF}} \times \phi_{\text{WID}} \times \phi_{\text{INF,FAC}} \times \phi_{\text{SHADE}} \times \tau \times \alpha] - [\bar{h} \cdot A_{\text{Convection}} \cdot (T_{\text{Sur}} - T_{\text{amb}}) + \epsilon_{cav} \cdot \delta \cdot A_{\text{ser}} \cdot (T_{\text{cav}}^4 - T_{\text{amb}}^4)] \quad (3.27)$$

And the efficiency of heat transfer in system is as given in equation (3.28).

$$\eta_{\text{rec}} = \tau \times \alpha - \frac{\bar{h} \cdot A_{\text{Convection}} \cdot (T_{\text{cav}} - T_{\text{amb}}) + \epsilon_{cav} \cdot \delta \cdot A_{\text{ser}} \cdot (T_{\text{cav}}^4 - T_{\text{amb}}^4)}{\eta_{\text{rec}} \times \text{CR} \times I_{\text{DNI}}} \quad (3.28)$$

Hence, the efficiency of heat transfer in system depends on losses (convection, radiation and radiation), transmittance, absorbance, reflective efficiency, solar radiation and concentrator ratio of system. This heat energy is usually transferred by the indirect way to PCM-Storage in the operating of cycle (1) as discussed in section (3.1). Next section discusses the thermodynamics of power generation in Stirling engine mainly in the second cycle (cycle 2).

3.7- Thermodynamic Cycle Solar Parabolic Dish with Engine

It is important to understand the theory related to the thermodynamics of power generation in hybrid Stirling engine by parabolic dish system in cycle (2). This cycle consists of parabolic concentrator and receiver of the absorber which transfers heat to the Stirling engine. The parabolic dish was connected to an expansion chamber of the heat engine. This engine was directly heated, and the heat was released to the ambient by radiation and natural convection as the surface temperature of the collector increases.

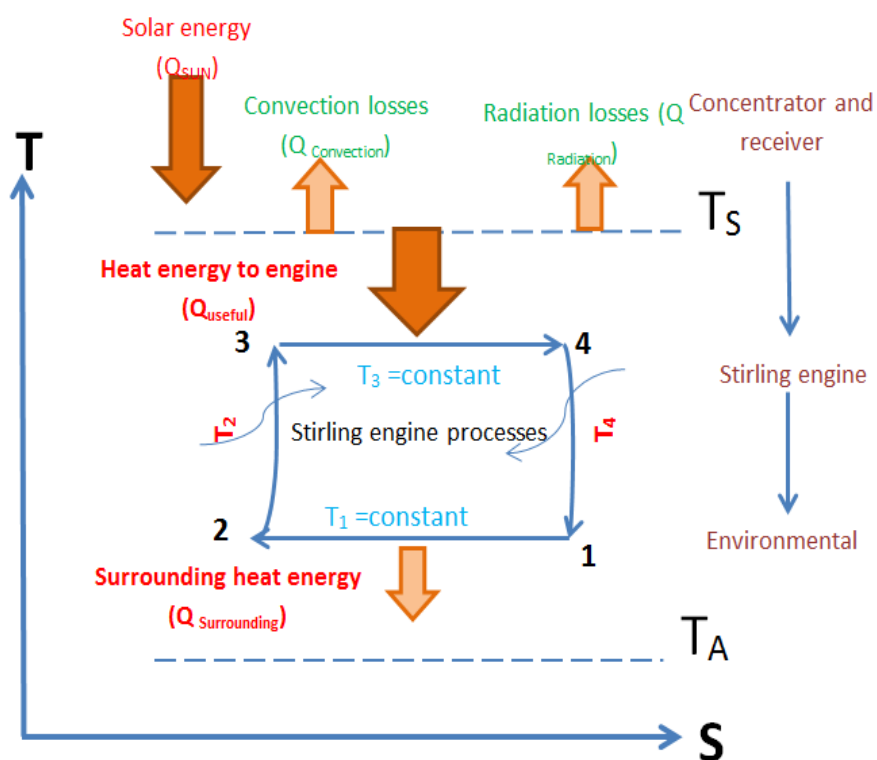


Figure 3.14 Thermodynamic power generations in hybrid Stirling engine by parabolic dish system in cycle (2)

Figure 3.14 shows the energy demand Stirling engine in processes of power production in system. The theories of heat transfer and power analysis in parabolic dish mirror system are discussed in this section. It is important to note that the Stirling engine is working to generate power during both cycles (1) and (2).

3.7.1-Theory of Heat Useful and Power Generator analysis in Stirling engine

Solar energy 'Q_{sun}' reflected by area of concentrator mirror area (m²), solar radiation I_{SUN} (W/m²) with mirror efficiency η_{CO} this represents energy accumulated at the aperture of receiver as show in Figure 3.14 and also given in equation 3.29.

$$Q_{\text{sun}} = A_{\text{CO}} \times \eta_{\text{CO}} \times I_{\text{SUN}} \quad (3.29).$$

The heat loss in concentrator can be expressed by the efficiency of concentrator 'η_{CO}' given by equation 3.30.

$$\eta_{\text{CO}} = \frac{Q_{\text{IN}}}{I_{\text{SUN}} \times A_{\text{CO}}} \quad (3.30).$$

In the receiver, there are two ways it contributes to radiation heat loss; in the first instance heat is emitted from the aperture owing to the large temperature difference between cavity walls and parabolic mirror.

Secondly, the solar radiation reflected off the cavity walls and back through the aperture. But there are some energy losses by concentrator and receiver materials for instance convection losses and radiation cannot be neglected. The heat loss 'Q_R' in the receiver that contributes to significant fraction of the total losses in the receiver of parabolic dish system is given by equation 3.30.

$$Q_{\text{R}} = \varepsilon \delta A_{\text{RE}} (T_{\text{W}}^4 - T_{\text{A}}^4) \quad (3.31).$$

Where 'ε' is the surface radiation emission rate, 'δ' is Boltzmann constant, 'A_{RE}' is receiver area m², T_W⁴ is receiver wall temperature (K), T_A⁴ and is aperture temperature (K). In general, as the temperature of absorber and receiver walls increase, the heat conduction loss through receiver surface to ambient air occurs at a more rapid rate. The Conduction loss 'Q_C' represents a small fraction of receiver thermal loss in the receiver system as defined in equation 3.32.

$$Q_C = h_n A_{RE} (T_W - T_A) \quad (3.32)$$

where h_n is the coefficient of natural convection and the total energy useful in parabolic dish system is ' Q_{USF} ' as given in equation 3.33.

$$Q_{USF} = A_{CO} \times \eta_{CO} \times I_{SUN} - A_{RE} [h_n (T_W - T_A) + \varepsilon \delta (T_W^4 - T_A^4)] \quad (3.33)$$

“This amount of heat energy will be transferred to Stirling engine processes”.

In this system, heat is transferred to the expansion chamber where a high conductive coefficient and extremely thin surface of the collector is applied such that the temperature on the interior surface of the expansion chamber is almost equal to that of the collector. The working fluid is considered as the ideal gas and the heat transfer process follows Newton's law of linear heat transfer.

$$Q_{stirling,in} = \alpha_n (T_W - T_3) t_{3,4} = h_n A_{RE} (T_W - T_3) t_{3,4} \quad (3.34)$$

In each cycle, ' $Q_{stirling,in}$ ' is the heat absorbed by the working fluid, and ' $Q_{stirling,out}$ ' is the heat released to the ambient. The temperature of the parabolic dish is denoted as T_W and the ambient temperature is denoted as T_S . The heat from the collector to the Stirling engine satisfies equation 3.35. This is also heat released out of Stirling engine to surrounding.

$$Q_{stirling,out} = \alpha_m (T_1 - T_{sur}) t_{1,2} \quad (3.35)$$

where $t_{3,4}$ and $t_{1,2}$ are the time of each process in the entropy equation in terms of isothermal and endothermic process, which is also given by equation 3.36.

$$T dS = T \left[\frac{dP}{dT} \right]_V dV \quad (3.36)$$

Based on the ideal gas law of equation 3.37, the compensation (P/T) when integrated gives process stages 3-4 using equation 3.38.

$$PV = nRT, \quad \frac{P}{T} = \frac{nR}{V} \quad (3.37)$$

$$\int_3^4 T dS = \int_3^4 \frac{nRT}{V} dV \quad (3.38)$$

Substituting entropy equation ($S \cong \frac{\partial Q}{T}$) in the internal part of Stirling engine receiver, gives.

$$Q_{3,4} = nRT_3 \ln \frac{V_4}{V_3} \quad (3.39)$$

During the cycle of working fluid in Stirling engine process the entropy is incremental as given below. Furthermore, if both sides of equation 3.40 are integrated, then the entropy behaves analogously to heat, and total change of entropy during (initial – final) cycle states which is zero as shown in Figure 3.14.

$$\Delta S = \oint \frac{\partial Q}{T} + S_G = \frac{Q_{in}}{T_3} - \frac{Q_{out}}{T_1} + S_G = 0 \quad (3.40)$$

$$(3.41)$$

$$\text{Now let, } \frac{Q_{in}}{T_3} = \frac{Q_{out}}{\alpha T_1}, \text{ when } \alpha \geq 1$$

The irreversible property of Stirling engine is always greater than or equal to one, this includes the heat loss, thermal friction, and thermal resistance. The irreversible property is related to the thermodynamic second law, known as the irreversible factors. This factors cannot be ignored because it increases entropy in each process. The amount of heat transfer Q_{in} and amount heat engine Q_{out} are identical, and the reversible heat engines Q_{out}^{rev} at $\alpha > 1$, and given by:

$$\frac{Q_{in}}{T_3} - \frac{Q_{out}^{rev}}{\alpha T_1} = 0 \quad (3.42)$$

$$Q_{out} = \alpha Q_{out}^{rev} \quad (3.43)$$

In engine, heat is released to storage in the cold chamber in a reversible isothermal process which is given by:

$$Q_{3,4} = nRT_3 \ln \frac{V_4}{V_3} \quad (3.44)$$

Compensation equations 3.43 and 3.44 when combined give equation 3.45.

$$Q_{\text{stirling,out}} = \alpha nRT_1 \ln \frac{V_1}{V_2} \quad (3.45)$$

From the thermodynamic second law, the total volume of gas is constant during engine circle; this is called compressive ratio r_v and is defined by:

$$\frac{V_4}{V_3} - \frac{V_1}{V_2} = 0 \rightarrow \frac{V_4}{V_3} = \frac{V_1}{V_2} = r_v \quad (3.46)$$

The endothermic time ' $t_{3,4}$ ' of heat engine happens as part of second law of the thermal process 3 to 4 in the 'T/S' diagram (Figure 3.14), which is given equation 3.47.

$$h_n A_{RE} (T_W - T_3) t_{3,4} = nRT_1 \ln r_v \rightarrow t_{3,4} = \frac{nRT_3 \ln r_v}{h_n A_{RE} (T_W - T_3)} \quad (3.47)$$

The exothermic time ' $t_{1,2}$ ' of heat engine from process 1 to 2 in 'T/S' diagram is given in equation 3.48, and this is also shown in Figure 3.15.

$$\beta (T_1 - T_s) t_{1,2} = \alpha nRT_1 \ln r_v \rightarrow t_{1,2} = \frac{\alpha nRT_1 \ln r_v}{\beta (T_1 - T_s)} \quad (3.48)$$

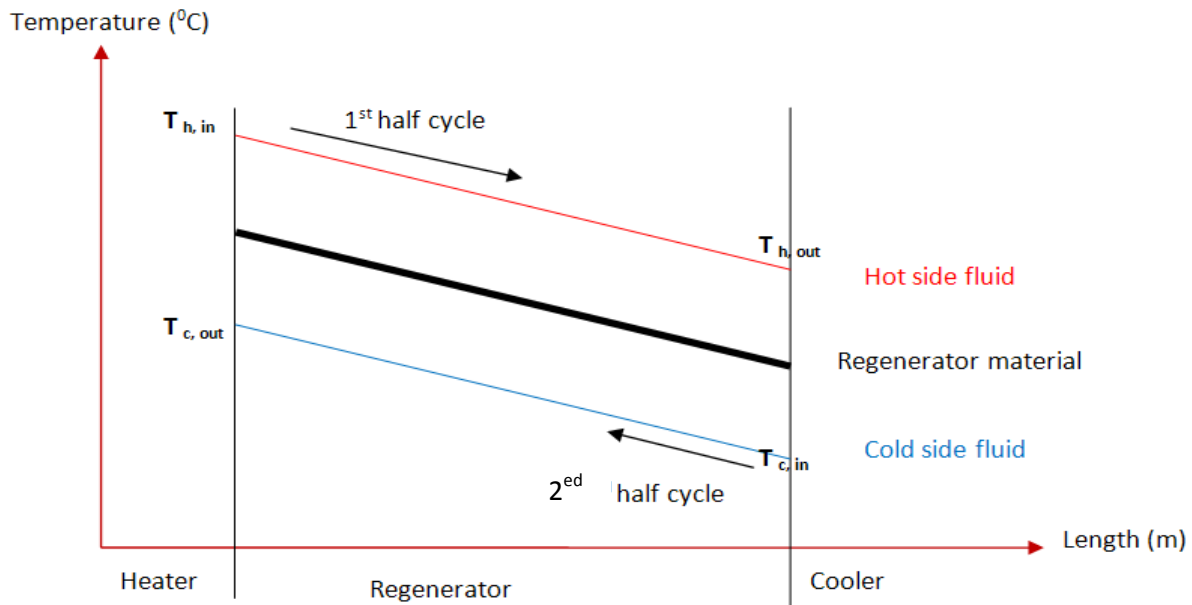


Figure 3.15 Regenerator and working fluid temperatures through Stirling engine cycle [36]

In the regenerator process, the working fluid temperature 'T_f' changes at time dt and is given constant value:

$$\frac{dT_f}{dt} = \pm C \quad (3.49).$$

At C>0 is the average rate of temperature change during each process and this rate is reliant on heat generator material because it is responsible for transfer of heat inside the engine. The regenerative time coefficient (dt) may be a positive or negative sign shows that the temperature increases or decreases with time respectively as shown Figure 3.15.

3.7.2-Time of Each Process in Operation Stirling Engine working

For the regenerative time coefficient(dt), a positive sign shows increase in temperature while negative sign shows decrease in temperature with time as shown Figure 3.15. Time of heat regenerative process from (2 → 3) is given by:

$$t_{2,3} = \frac{(T_3 - T_2)}{C_1} \quad (3.50)$$

Time of heat regenerative process (4 → 1) are given by:

$$t_{4,1} = \frac{(T_4 - T_1)}{C_1} \quad (3.51)$$

The total time for four process of Stirling engine from (1→4) is given by:

$$t_{\text{total}} = t_{1,2} + t_{2,3} + t_{3,4} + t_{4,1} \quad (3.52)$$

Compensation for values of time (t_{1, 2}, t_{2, 3}, t_{3, 4} and t_{4, 1}) in equation 3.51 is given by the total time in equation 3.53.

$$t_{\text{total}} = \frac{\alpha n R T_1 \ln r_V}{\beta (T_1 - T_S)} + \frac{(T_3 - T_2)}{C_1} + \frac{n R T_3 \ln r_V}{h_n A_{RE} (T_W - T_3)} + \frac{(T_4 - T_1)}{C_1} \quad (3.53)$$

However, the effectiveness of energy 'Q_{in}' coming into Stirling engine is given by:

$$Q_{\text{St,in}} = q_{\text{in}} \times t_{\text{total}} \quad (3.54)$$

The total amount of heat applied to Stirling engine is given by equation 3.55:

$$Q_{St,in} = \frac{h_f}{\frac{1}{A_C(T_W - T_3)} + \frac{\alpha T_1 h_f}{\beta T_1 h_f (T_1 - T_S)} + \frac{2h_f(T_3 - T_1)}{nRT_3 \ln r_V C}} \quad (3.55)$$

Normally, the thermal efficiency of Stirling engine is given by:

$$\eta_{Sti} \equiv \frac{P_{Sti}}{Q_{St,in}} = 1 - \frac{T_1}{T_3} \alpha \quad (3.56)$$

$$Q_{St,in} = \frac{h_f}{\frac{1}{A_C(T_W - T_3)} + \frac{\delta^2(1-\eta_{Sti})}{\left[\frac{(1-\eta_{Sti})T_3}{\alpha} - T_S\right]} + \frac{\omega}{\ln r_V} \left[1 - \frac{(1-\eta_{Sti})}{\alpha}\right]} \quad (3.57)$$

However, heat transfer to the surrounding of Stirling engine is given by:

$$q_{out} = \frac{Q_{Sti,out}}{t_{total}} = \frac{h_f(1 - \eta_{Sti})}{\frac{1}{A_C(T_W - T_3)} + \frac{\delta^2(1-\eta_{Sti})}{\left[\frac{(1-\eta_{Sti})T_3}{\alpha} - T_S\right]} + \frac{\omega}{\ln r_V} \left[1 - \frac{(1-\eta_{Sti})}{\alpha}\right]} \quad (3.58)$$

The power produced by Stirling engine is as shown in equation 3.59:

$$P_{Sti} = Q_{St,in} \times \eta_{Sti} \quad (3.59)$$

From focal temperature, thermal efficiency and equation 3.28, the amount of applied heat to the collector can be determined. Equation 3.59 can be used to solve for the endothermic temperature of Stirling engine which is expressed in equation:

$$q_{in} = \frac{h_f}{\frac{1}{A_C(T_W - T_{3,opt})} + \frac{\delta^2(1-\eta_{Sti})}{\left[\frac{(1-\eta_{Sti})T_{3,opt}}{\alpha} - T_S\right]} + \frac{\omega}{\ln r_V} \left[1 - \frac{(1-\eta_{Sti})}{\alpha}\right]} \quad (3.60)$$

Equation 3.60 is complex and shows the amount of power to be produced by Stirling engine. This is part of the theoretical approach with the next section discussing the design of the hybrid Stirling engine compatible with the final model.

3.8-Design Hybrid Stirling Engine Criteria

The choice of the appropriate Stirling engine for the prototype model requires consideration of several factors. It is difficult to modify most model of Stirling engine suit the objective of the current research. However, the gamma type of Stirling engine is easy to modify in order to have proper connection of the heat exchanger within the system. This section describes the mechanism of different parts and materials of the modified gamma-Stirling engine (hybrid Stirling engine) used in the present work. This engine consists of hot space, cooling space, crankshaft and other parts which will be discussed in more detailed later. Before discussing the main design of the Stirling engine, other areas related to the design will be analysed as follows:

1. The Schmidt theory [39] was used for calculations based on the following assumptions:

- There is no pressure loss in the heat exchangers of engine and also there are no internal pressure differences.
- The expansion and the compression process changes are isothermal.
- Conditions of the working gas are considered as an ideal gas.
- The heat exchanger or regenerator is perfect.
- The expansion dead space maintains the expansion gas temperature ' T_E ', the compression dead space maintains the compression gas temperature T_C during the cycle.
- The regenerator gas temperature is the average of the expansion gas temperature ' T_E ' and the compression gas temperature ' T_C '.
- The expansion space ' V_E ' and the compression space ' V_C ' changes according sine curves.

2. Secondly, analysis using mathematical model of a French scientist called Serge Klutchenko [30]. The mathematical model had some advantages which were not found in the analysis above:

- Takes into account the calculations of dead volumes.
- Takes into account the effectiveness of the regenerator.

- Mathematical model by input available conditions (hot chamber temperature from parabolic dish concentrator has a diameter of 120mm)-with available cold chamber temperature using different cooling systems such as air fans and water cooling system.
- The capacity of engine to generate between 10 to 50 Joules of energy using gamma type Stirling engine from the outputs of the mathematical model (swept volume, dead volumes and displaced volume).

3.8.1- Design and Fabrication a Hybrid Stirling Engine Design Process in System

The Gamma configuration was used in the design with a separate chamber for the displacer to ease fabrication. The heating chamber was given a special design to facilitate heating using both open flame as well as solar heat. The solar concentrator was then designed to be detachable, used together with the hybrid Stirling engine and the designed cylindrical receiver in the system. All the parts used for the fabrication was obtained bearing in mind the overall cost, it was ensured that the final model was as cost effective as possible.

3.8.1.1- Initial design

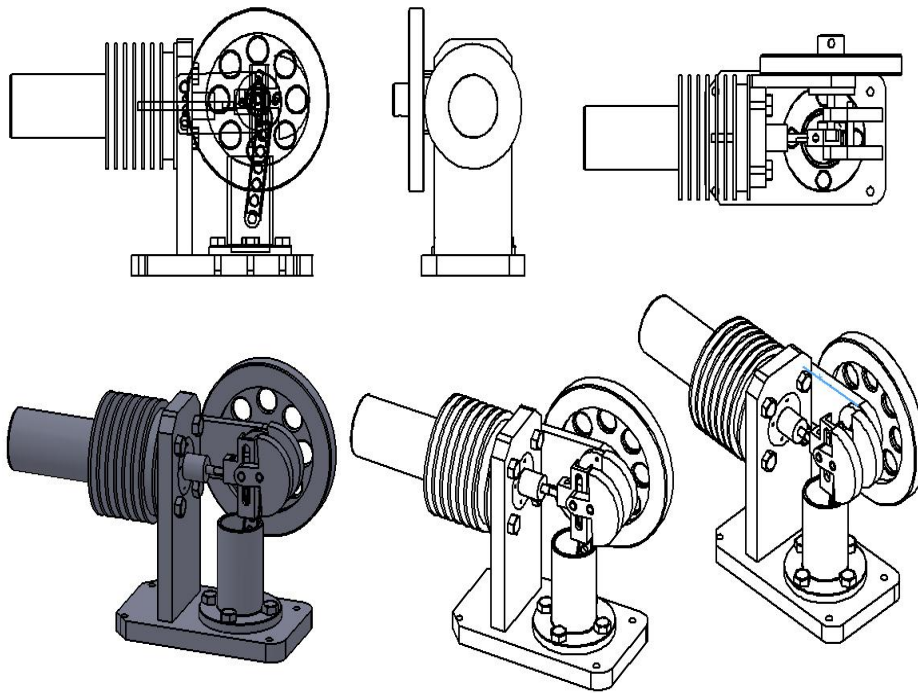


Figure 3.16 Stirling engine designs using the Solidworks Software

The design process started off with simple hand sketches that were drawn using solid-works software. The first set of sketches shown in Figure 3.16 was drawn using the Solidworks Software. These preliminary sketches were too simple and machine dynamics was not taken into account. These sketches, however, were the first step towards project actualization.

3.8.1.2-First revised design

The revised designs were drawn on the Autodesk Inventor software, better in kinematics and gave the best simulation on the computer. This design as shown in Figure 3.15 was the closest to getting to the Stirling engine final design. It was noted here that this first revision of the design was not used because the connectors used in the design would be too hard to fabricate. Furthermore, the heating portion had to be changed in the design to counter overheating of the system.

After certain adjustments, the final design is as shown in figure 3.17 and this was drawn using Autodesk Inventor. The revisions made included a new heating chamber that made it easy to heat using an open flame.

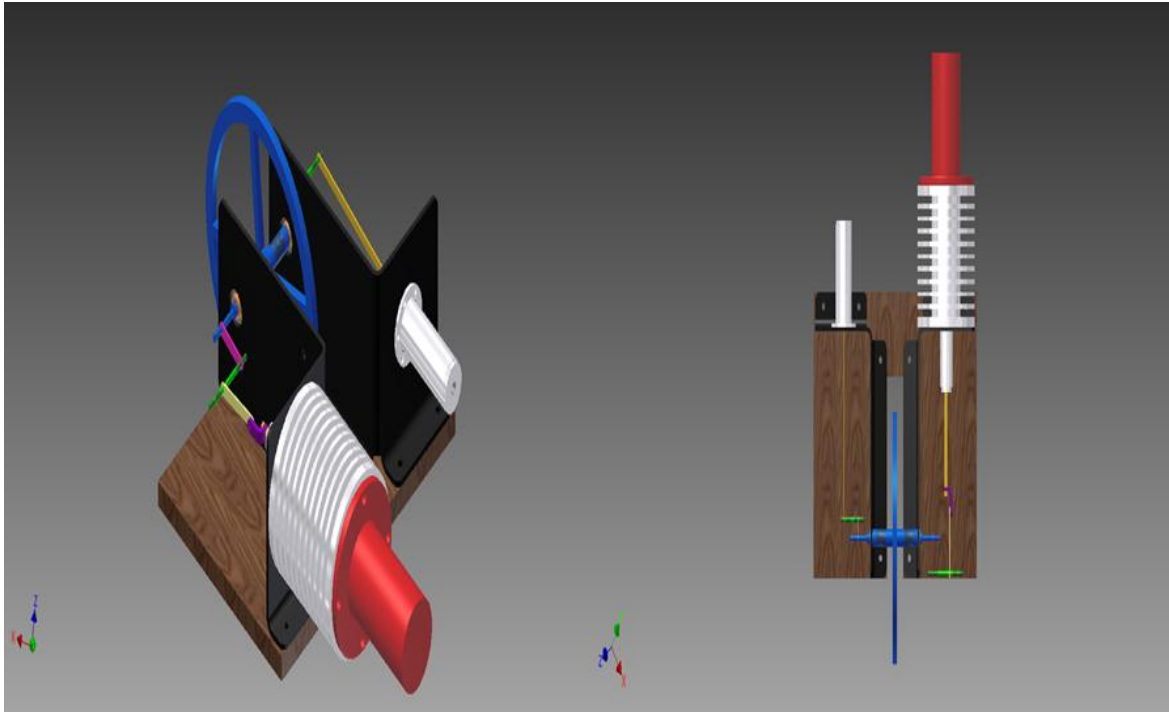


Figure 3.17 The Final Stirling Engine Design for processes of Fabrications.

3.8.1.2- Engine Mechanism Parts

Getting all the different parts of the Stirling engine into one piece in order to achieve the desired objective was a difficult task, as it takes much time, energy and resources. This engine works by expansion and compression of the working gas located in the hot and cooling space of the engine. It normally uses air, hydrogen or helium as the working gas. The actual fabrication was carried out in the workshop located in Oman. It was however noted that some high precision parts such as the piston cylinder couldn't be machined in the workshop. This was because the machines available were old and the work pieces were prone to vibrations during machining which is not ideal for high precision parts especially owing to finishing.

There were five stages involved in the fabrication of the engine:

- I. The first stage was to carry out research on the engine as part of the entire project. The research included gathering information as discussed in section

3.8 about Stirling engines, their history and theory and also made investigations on its application to solar energy.

- II. The 2nd stage of the project began after the research of the project was completed. This stage included reviewing of old designs and making preliminary sketches. From this review, it was decided that the gamma configuration was best suited for design & to test the viability of the solar energy. In addition, it was simple to fabricate and its design could easily accommodate the solar concentrator proposed.
- III. The 3rd stage of the project involved deciding what materials to use from what was readily available. During this period, the designs were taken for approval and requests for funding made.
- IV. The 4th stage involved fabrication and assembly which took time to complete.
- V. In the 5th stage, testing started immediately after the fabrication of the parts was completed. From the testing, minor adjustments continually took place and more tests were carried out for a certain period.

The following are the parts before and after assembly:

3.8.1.2.1- Base plate:

The base of the engine was machined from a piece of 30mm thick board. The board was cut using the CNC cutting machine, because it was faster and more accurate. The engraving on the board was made using a CNC laser cutter. The bearing plate was cut from a 3.5 mm mild plastic plate, this was the strongest plate available for use as it would be rigid enough to support the fly wheel and crank web.



Figure 3.18 The base plate of the engine machined from a piece of 30mm thick board

3.8.1.2.2- The Cylinder heater

The cylinder heater was made from a 52mm diameter pipe of length 100mm. The end of the pipe was sealed off by brazing a 3 mm plate onto one end. The same end had the flanges which were made from a 3.5mm plate that had been shaped from a 4.5mm plate and welded onto the pipe cut-off.

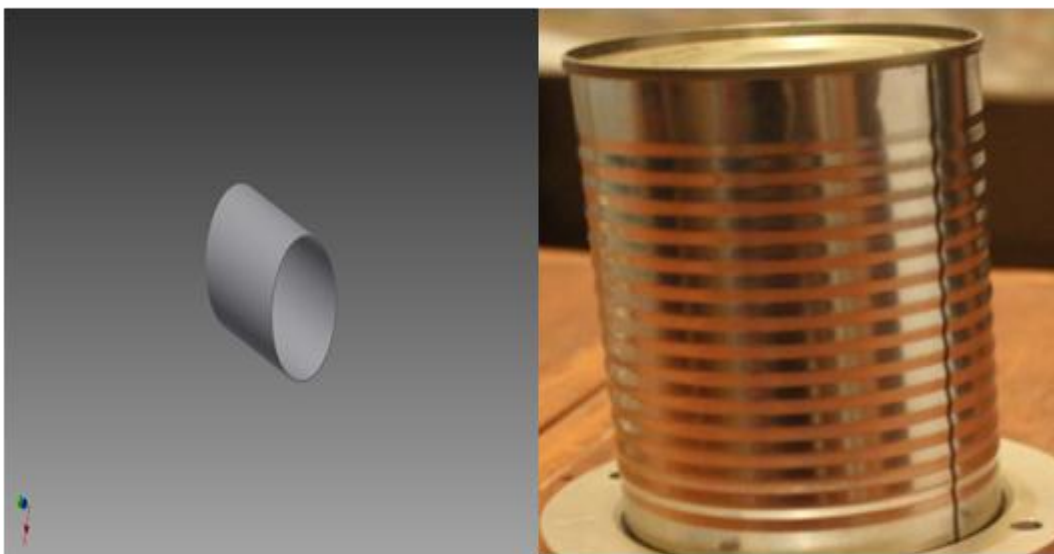


Figure 3.19 The cylinder heater was made from a 52 mm diameter pipe of length 100 mm.

3.8.1.2.3- The cylinder heat sink



Figure 3.19 The main body of the cylinder heat sink made from the 52 mm pipe cut to 100 mm

The main body of the cylinder heat sink was also made from the 52 mm pipe, cut to 100mm. The cooling fins were cut from a 3mm thick sheet metal using a lathe and were brazed onto the pipe. The flanges were made from a 3.5mm mild steel plate and arc welded to each end. A piece of 8mm drill was used to make holes for bolting.

3.8.1.2.4- The Displacer Guide Bush

The guide bush was made by turning a one inch mild steel rod on a lathe machine with diameters (24 & 12) mm and length of 62mm. The finishing was done using an emery cloth.



Figure 3.20 The displacer guide bush

3.8.1.2.5-The Displacer

The displacer was made from a piece of light wood that was turned on a lathe machine to a diameter of 30mm and a length of 80mm. It would then be threaded to accommodate the displacer rod.

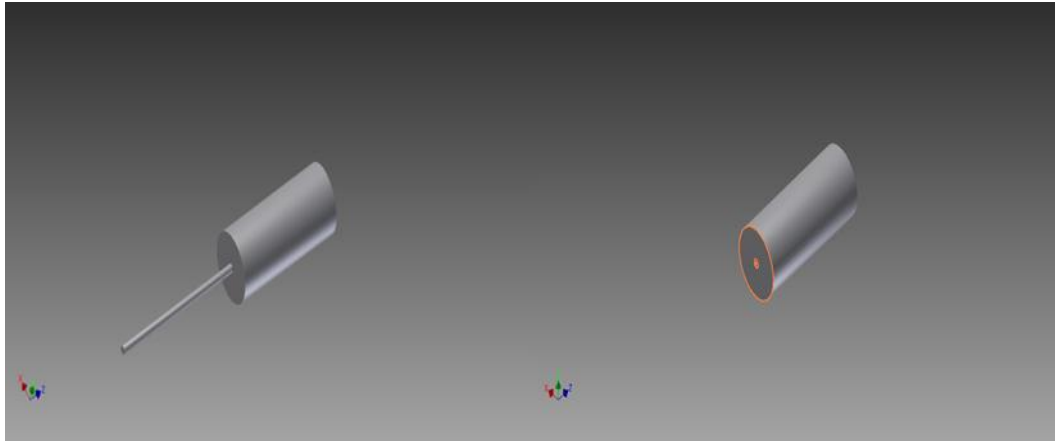


Figure 3.21 The displacer made from a piece of light wood turned on a lathe machine to diameter of 30 mm and length of 80 mm

3.8.1.2.6-The power cylinder

The power cylinder was made purely of cast iron. This was a high precision part and could not be machined on the workshops using lathe machines because of vibrations. Outsourcing this piece was the best option. The initial dimensions of the sleeve were 20mm internal diameter and 180mm length. The sleeve was machined to 40mm internal diameter and horned on the inside to accommodate the power piston.

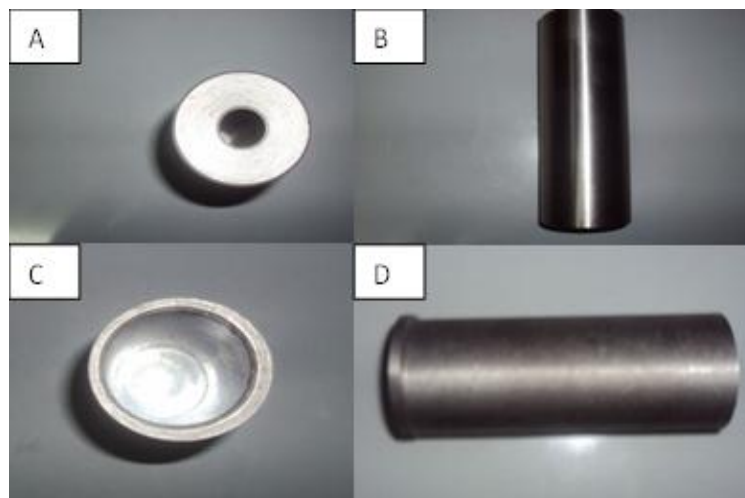


Figure 3.22 The power cylinder made purely of cast iron

3.8.1.2.7-The power piston

The power piston was a high precision part and therefore machining would be difficult. Buying a piston of a 50cc motorcycle piston complete with its oil rings seemed to be a better option. The piston was of 40mm diameter.

➤ The fly wheel:

The fly wheel was cut from a 4.5mm thick steel plate. To make fitting onto the bearing easier, the power pin was forced fitted onto the fly wheel.



Figure 3.23 The fly wheel cut from a 4.5mm thick steel plate

For the purpose of rotating mechanical device that was used to store rotational energy, the flywheels have a significant moment of inertia and thus resist changes in rotational speed. The amount of energy stored in a flywheel is proportional to the square of its rotational speed. Energy is transferred to a flywheel by applying torque to it, thereby increasing its rotational speed, and hence its stored energy. Conversely, a flywheel releases stored energy by applying torque to a mechanical load, thereby decreasing its rotational speed.

➤ The connecting rod

The connecting rod was machined from a one inch rod to a diameter of 6mm and a length of 150mm. The flat edge was machined on an end miller and a hole of diameter 6mm made on the face so as to accommodate the pin.



Figure 3.24 The connecting rod

- The bearing plate assembly:

The fly wheel, crank web and bearing plate were connected using 12mm pin. On the fly wheel, a steel rod was machined to support its upright position on the bearing plate.



Figure 3.25 Fly wheel and Shaft assembly

3.8.1.2.8-The Complete Engine Assembly

The cylinder heater, cylinder heat sink and power cylinder were fastened to the cylinder plate by M8 bolts. To seal off the joint, gaskets were cut and silicon applied onto the surfaces before the fasteners were tightly put. The lever con rods and other small levers were riveted onto each other and the bearing plate with ample clearance to facilitate movement between joints. Finishing of most of these parts was done by using different grades of emery cloth. To support the base, rubber stands were fitted onto the base.

3.8.1.3- Assembled Hybrid Stirling Engine

The individual parts of the Stirling engine fabricated above were assembled together into the hybrid Stirling engine. This was followed by testing of the engine before it was connected to the focal point of the parabolic dish and AC generator to measure the power it produces. During the testing processes, helium gas was used as the working fluid in the Stirling engine with initial pressure of 1.6 bar. However, when the gas pressure was increased the fly wheel and shaft moved faster, which also means increase in power generated. At 1.6 bar the expansion to compression of engine worked very well. Afterwards the fly wheel was connected to AC current generator to measure how much power engine can be produced.



Figure 3.26 Completed hybrid Stirling engine and testing in the workshop

3.8.2- Technical Problems in Fabrication of Stirling Engine:

There are two main problems to be discussed in this section:

➤ Heat receiver problem :

In order to maximize heat transfer rate through the hot chamber, an efficient Stirling engine runs with high speed and makes quick positive and negative pressure pulses by expansion and contraction of the working gas. To achieve this, the heat loss must be minimised by using materials with high thermal conductivity in order to minimize the thickness which are usual problems in welding.

➤ Mechanical seal problem:

To make efficient mechanical seal, it requires relatively high friction which decreases the efficiency of the Stirling engine and may cause it to fail.



Figure 3.27 Hybrid Stirling engine within AC generator

The figure below shows the gamma- Stirling engine with generator with mass 15 kg which was fixed at the base of the engine. The generator was connected to software to measure how much energy it could produce as shown in Figure 3.30.

After fixing two different satellite dishes as concentrator parabolic dishes and fabricated gamma sterling engine generator in the centre of the large dish. The next step was to add thermal technology to absorb heat and the heat transfer to the other part of the system in close circuit. This system is called thermal receiver as mentioned earlier. One of the receiver heat exchanger was attached to cover the hot space of the engine and the other was located at the centre of the small parabolic dish.

3.9-Fabrication of Thermal Receiver in Research System

The Receiver is part of the energy generation system that transfers solar radiation in form of heat energy into the working fluid [33]. This is an important part of the system, and it consists of the absorbing surface, heat exchanger, heat storage made from iron, aluminium or copper [33]. The heat energy absorbed in the surface of receiver through the engine (Q_{engine}) is equal to heat energy absorbed (Q_{in}) from solar radiation with the heat energy loss (Q_{loss}).

3.9.1- Receiver Size and Focus Point

It is important to understand the effect of the relationship between the heat accumulated in the receiver and the receiver size. However, the receiver area is always in a cylindrical form which depends on the steady axis with symmetric configuration. The focal temperature depends on a single coordinate (R_1 , R_2 and R_3 is the radius of aperture) and the radius of the central part of the receivers. When R is increased, the receiver area also increases, and the generated power in the system decreases because it requires more energy to heat the large gas volume.

3.9.2- Heat Exchanger Receiver Connecting Direct with Stirling Engine

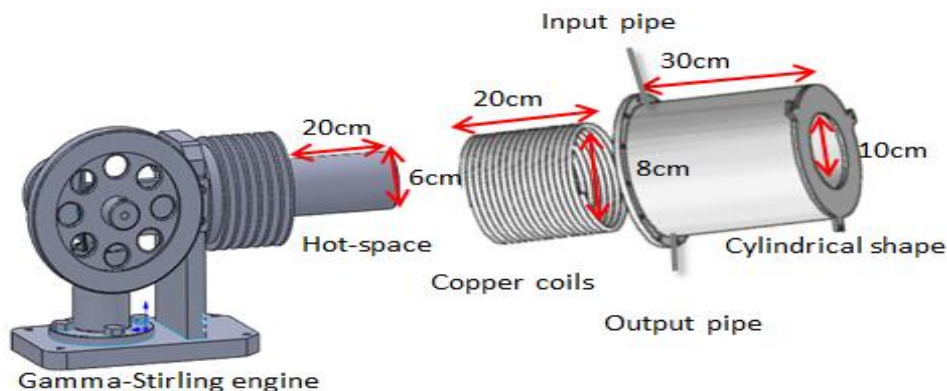


Figure 3.28 hybrid Stirling engine installed into cavity receiver

In Figure 3.28, solid works was used to design the heat exchanger receiver located around the hot engine space. This heat exchanger consists of:

- Cylindrical shape carved from the inside to enter the hot space of engine which is shown in Figure 3.31.

- Copper coils (20 Coils) inside the cylindrical shape which is connecting the PCM-storage and hot space in the Stirling engine by solar flexible stainless steel pipe (50cm length, 5mm diameter, 15 coils), Gamma Stirling engine ($T_{MAX}=450^{\circ}C$, $T_{MIN}=50^{\circ}C$), and external copper cover (3mm width, 5cm diameter).
- The cylindrical walls of the receiver were made of 0.16 cm thick stainless steel.
- The tubing was topped by a flange that is 0.64 cm thick with an outer diameter of 31.8 cm. There was a 10cm radius aperture in front of the receiver which was also insulated by 5cm wall.
- R100-Sentinel oil is high conductive thermal oil inside the cylindrical shape and copper coils which absorbs, transfers and control heat.

Heat exchangers which were modelled had two input pipes; one for high thermal conductivity oil and second for copper coils. On the other hand, its size must be considered with respect to the focus sun ray.



Figure 3.29 Steps of hybrid Stirling engine been installed into cavity receiver

This heat exchanger receiver works as follows:

1. At night:
 - I. To provide heat to engine.
 - II. To control heat within the engine.
 - III. To transfer heat from gas pipe to hot engine space.
2. During the day:
 - I. To store some heat in oil and its body.
 - II. To control heat provided to the engine during sunset.
 - III. During sunshine, to absorb focus heat and raise the temperature at centre to become suitable for the engine to work. This process needs more time (minimum 30 minutes) where the performance of power generator is usually weak.

3.9.3 Cavity Receiver

The centre of small parabolic dish accommodates the cavity receiver which was fixed using three large iron bases. Thermal receiver consists of copper coils and two cylindrical shapes open from -front with a good insulation between each cylinder as shown in Figure 3.30. The copper pipe (in-and output) comes through the back wall

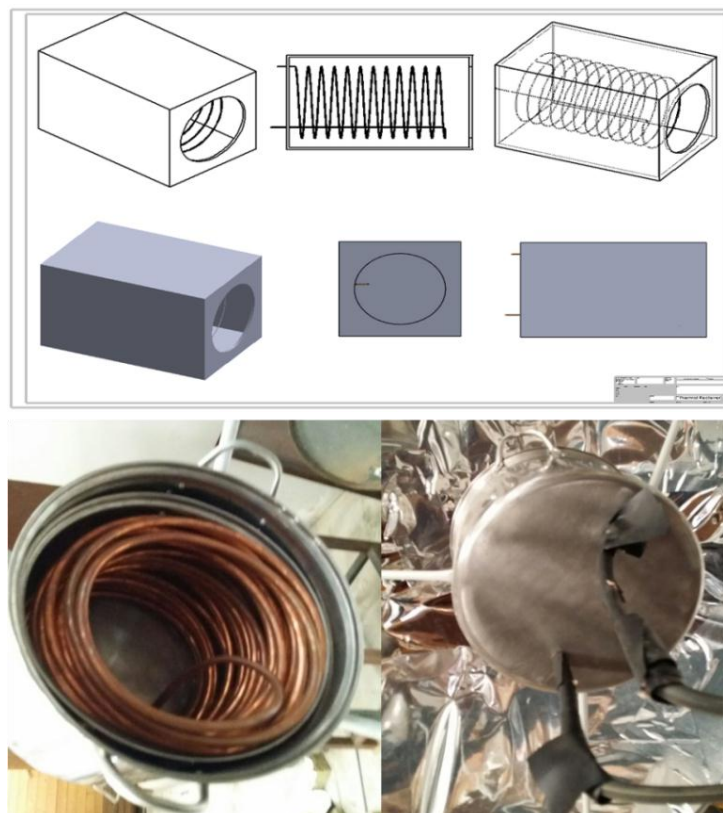


Figure 3.30 The thermal receiver installed into the system

of the receiver. Also, thermo cables (flexible pipes) were installed to connect the copper pipes from the closed end of the receiver. The copper pipe 0.95cm (in-out) was used to connect to the same size of thermal fixable pipe which have the ability to transfer heat to PCM-Storage. This cavity receiver works as follows:

- I. At night is mostly closed.
- II. During the day it is open and absorbs heat from focal point and transfer the heat from receiver to PCM-Storage through the thermal pipe.
- III. At sunset it does not work.
- IV. During sunrise usually open and commences operation.

3.10- Conclusion

This chapter is an important part of the thesis, and focus was discussing the theory of parabolic dish system as well as design and fabrication of hybrid Stirling engine and two thermal receivers. It was divided into several sections including the study of solar position, factors affecting solar collector design, and energy intercepted in the receiver. And also, the design of the parabolic dish concentrator, solar thermal receiver review, thermodynamic cycle solar parabolic dish with Stirling engine, design of the hybrid Stirling engine criteria and fabrication thermal receiver were all discussed.

There are three processes as part of the working principle, with two during the day and one at night. For the first process gas in copper pipe absorbs heat which was collected in the cavity of receiver and transferred to the PCM-Storage, and done during the day. In the second process, the gas in the other system absorbs heat and the heat directly supplied to the Stirling engine which also happens during the day. And third process involves direct transfer of heat from the PCM-Storage to the Stirling engine, this process occurs at night time. In the concluding aspect of the chapter, two different thermal receivers were shown to be fabricated and installed into the main parabolic dishes. Both parabolic dishes installed on both ends of long iron base (length 5m). This is to ensure it is firm and easier to move with solar track system in any directions during day. It also gives the flexibility to ensure maximum heat energy obtained for use on the hybrid Stirling engine during the day or transferred to the PCM-Storage system which is the focus of the next chapter.

CHAPTER(4):- Design and Fabrication of PCM-Storage in ResearchSystem

4.1-Introduction

The previous chapter discussed the theory of the parabolic dish concentrator and Stirling engine. It also presented the steps to make the parabolic dishes and hybrid Stirling engine. This chapter aims to give a detailed description of the design and fabrication of second part of the final experimental model. It is divided into two sections, the first focuses on the other solar thermal storage background and review. Secondly, it will also discuss in more detail the design and fabrication of phase change material (PCM-storage), as storage of solar energy is important for the future success of solar energy utilization.

The size of storage in the model is reliant on thermal energy stored and materials used. The energy storage during the day was made available and associated with the parabolic dish area as well as the total amount of heat going into the engine to work at night or when the sun is not available.

The major problem with the storage was the selection of materials with suitable thermo-physical characteristics in which solar energy in the form of heat can be stored [53].

The materials can be divided into two broad types as shown in Figure 4.1. Those that store energy in the form of sensible heat and those that undergo a change of state or physical-chemical change at some temperature within the practical range of temperature provided by the parabolic dish concentrator at possibly 50°C to 420°C [54].

The thermal heat storage to be made will depend on how much heat to be collected by parabolic dish systems and storage material; this includes liquid such as oil and hot water or solid such as rocks and salts. The heat storage materials considered need to increase the temperature level without undergoing a change in its phase or

changes in state from latent heat of fusion in suitable chemical compounds such as paraffin waxes and inorganic salts sodium or potassium .

In this case, the latent material absorbs the heat supplied from the system and goes through a phase transition from the solid to the liquid state at a constant melting temperature. Even within the operating temperature increase as the system works, this is called the principle works of PCM [5].

The objective of this chapter is to design and fabricate the thermal storage with phase change material (PCM) based on a heat exchanger which can act as a thermal energy storage device, hence can be incorporated into the solar parabolic dishes. The PCM will be active during day time as energy storage device. Solid-works software was used for the initial design and fabrication in the workshop in Oman.

This chapter is split into two sections; first is to discuss the thermal storage review and second is the design and fabrication of PCM. The latent heat storage provides a solution to correct the mismatch between the supply and the demand for energy. High capacity storage applications can be done with Phase Change Materials (PCM). The advantage of using a PCM is that energy can be stored without temperature increase when the material is changing from solid to liquid form and other phase change.

4.2- Importance of Energy Storage in Solar Technologies

In discussing the importance of solar energy storage, there is the need to understand the difference between solar thermal energy and solar thermal storage. Both systems derive energy from the solar resources, but the main difference is that solar thermal energy can only provide intermittent energy supply directly from the sun and this is called direct solar way. The energy provided in this case changes with the change in solar radiation during the day. For the later, the solar thermal storage system stores energy received from the solar sources during the day for later use. Hence, this is a fixed energy supply, considered as second source of energy to the system for indirect use (when solar radiation is not available). This fundamental difference makes it complementary to each other during operation and these differences are the principle adopted in the final model.

The solar thermal storage system has an important role in conserving the energy storage and improves the reliability and performance of the systems. Is it possible to have solar concentrator system to work without energy storage? “What happens when sun light is not available or when the weather is cloudy or at night”? The system stops working. Hence, the storage system keeps the entire system functional in these circumstances.

The important roles of energy storage system are summarised as follows:-

1. Energy storage is important where sun is not available or cloudy weather.
2. Energy storage is more important where the energy source is intermittent in parabolic dish concentrator.
3. Energy storage can increase production time of system.
4. Energy storage can increase total production capacity of system.
5. Energy storage can reduce the time or mismatch between energy supply and demand, thereby playing a vital role in energy conservation.
6. The magnitude and importance of solar energy as a renewable energy source is obvious.
7. If solar energy is to become an important energy source, efficient, more economical and reliable solar thermal energy storage devices or methods or techniques will have to be developed [1].

The literature has shown that there are limited efforts or few projects tailored towards improving the capacity of parabolic concentrator system. When parabolic concentrator technology are used for power generation, connecting the system with thermal storage in one unit tend to improve the operation capacity of the whole system. Spain has two pioneer projects introducing thermal storage in area of Andosol (I) and (II). It has a nominal power of 50kW each and a solar field that uses molten-salt thermal storage system to extend plant full-load operation 4.7 h beyond daylight hours [50, 51].

Energy storage is employed in solar thermal energy systems to shift excess energy produced during times of high solar availability to times of low solar availability. Two situations exist in solar energy system design where energy storage may be needed; for the situation in which some of the solar thermal energy produced during the day

is stored for use later during the night, and to provide energy during events such as cloudy days [52].

4.3. The Methods of Solar Thermal Storage

The methods required for thermal energy storage depends on the changes in internal energy of material used, schematic of major techniques for the storage of solar thermal energy is shown in Figure 4.1. Three methods are considered for heat storage in order to store thermal energy, this include the sensible heat storage (SHS), the latent heat storage (LHS) and the thermo-chemical storage (TCS). In the present work, the last two techniques (LHS and TCS) will be presented in the subsequent sections, focusing on the high temperature storage exceeding 100°C. All these techniques were used in solar thermal storage applications, with ARMENA using the LHS, while Spain applied both LHS and TCS techniques in their solar technologies (Solar through and tower) [6].

However, solar parabolic dish concentrators with Stirling engine application using thermal storage technology in direct or indirect ways are not common, as this technology is mostly at the research stage. In view this; there is an urgent need to use thermal storage in solar energy generation due to increase in demand of solar energy.

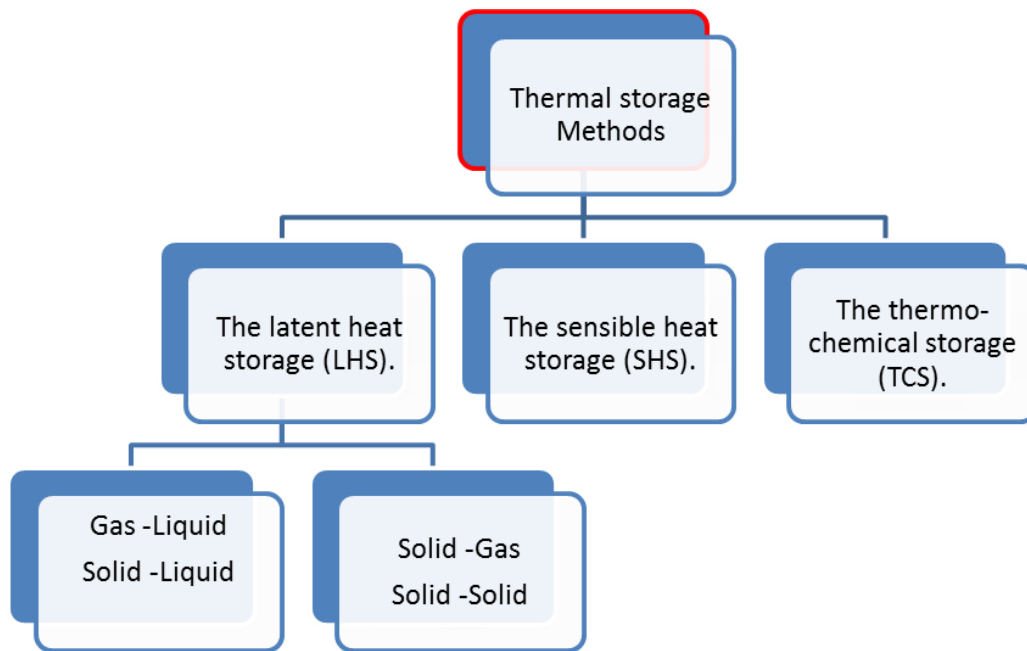


Figure 4.1 Methods of thermal storages system with the latent heat storage (LHS), the sensible heat storage (SHS) and the thermo-chemical storage (TCS).

4.3.1-The Sensible Heat Storage (SHS)

The first technique used in storing heat in solar storage application is the SHS. This technique of sensible heat storage (SHS) was based on the temperature increase or rise in temperature of a solid or liquid material to store heat is known as heat charging. And also the process of discharging the stored heat was the reverse process of charging, by decreasing the temperature of the material when the stored heat was used. The volume of the energy in demand determines the amount of heat storage using this method. This implies that for large energy requirement, extremely large amount of heat as well storage material was required to meet this demand, in any model.

Sensible technique depends on the mass of the material used, its heat capacity and the temperature rise. So it can only store relatively small quantity of thermal energy with larger volume requirements of materials (disadvantage). Another setback of this method is that at high temperature, there is no difference in heat transfer material between the process of charging and discharging energy of the working material. This is because these materials do not change phase or state, as the heat discharges

simultaneously with the charging process. Hence, it is not possible to use this technique for the current model due to insufficient storage when compared to other techniques [47, 50,54].

4.3.2-The Thermal-Chemical Storage (TCS)

This method of storage is commonly used in solar tower and solar trough as described in the literature review. The thermal chemical storage is the second technique studied to store heat in solar technology applications. This technique is based on using reversible thermo-chemical reactions, and chemical compounds store energy by endothermic reaction. The stored energy is then released in the recombination of the compounds by an exothermic reaction [55].

The advantages of this technique can be summed up as follows:

- The enthalpy of reaction is considerably larger than the specific heat or the heat of fusion.
- It has better storage density as compared to other techniques.
- With this technique thermal insulation is not required thereby reducing cost.

The main disadvantage of this technique is that the chemical compounds must be heated and cooled using special system, and this special system is expensive to acquire, adding to the overall cost. This thermal chemical storage technique is still underdevelopment at an early stage, although thermo-chemical heat storage can store high amounts of thermal energy, there are a lot of concerns in its application. For these reasons, it is also not possible to adopt this technique in the current model due to insufficient storage when compared to other techniques [52, 53].

4.3.3- The Latent Heat Storage (LHS)

The principle work of latent heat storage is based on the absorption or release of heat when material changes from solid phase to liquid or liquid to gas phase, and vice versa. The heat storage capacity when latent technique was used in the PCM is given in equation 4.1. This is a reliable technique for heat storage suitable for solar concentrator power generation as mentioned in section 2.6.2. The application of LHS has been of common use for some time, and solid to liquid PCM-Storage is the most

popular, which works like normal storage materials using temperature increase to absorb heat.

Latent heat storage uses phase change materials which transfers thermal energy when materials change from to phase the other; this is called change in state or phase. The materials suitable for LHS technique have the following three phase changes:

- Solid - Liquid transition PCM.
- Liquid - Gas transition PCM.
- Solid - Gas transition PCM.

Latent heat storage starts thermal energy storage at nearly isothermal level at the initial stage, and PCM later changes from Solid to Liquid thereby storing heat. Also, the latent heat of vaporization occurs during the liquid to vapour transition [43]. The PCM has ability of a higher storage energy density as compared to sensible heat materials. The utilization of heat of fusion energy near isothermal operation results in very small charge and discharge of stream temperature differences and lower heat losses.

Furthermore, at solid–liquid transition operations with latent heat flow has attracted research interest in recent time [14]. PCM-Storage can also adopt the conservative two tank storage system in solar power plants. This increases the volume of the storage capacity, but this will increase the cost of production as compared to the single tank storage.

The main advantages of PCM-storage as potential storage system for solar power systems are [14-16]:

- ❖ A30% reduction in heat transfer fluid volume.
- ❖ A60% reduction in container size.
- ❖ It improves the overall system efficiency by 2-3%.
- ❖ Flexibility to operate with different steam cycles.
- ❖ Flexibility to store energy when collected temperature is less than the desired high temperature.
- ❖ Prospective to reduce the level of cost of energy by 6 – 9%.

Normally, stored energy discharges heat when there is a reverse phase change. It must be mentioned that many researches and applications have focused mainly on the PCM solid to liquid phase change in solar thermal technologies, up till date. Hence, the use of LHS PCM as storage material is viable for the current model, as it is a recent technology.

Table 4.1 Comparison between various heat storage mediums (Stored thermal energy=5000Kj, $\Delta T= 25^{\circ}\text{C}$) [50]

Heat storage material / properties	Paraffin wax	Water	Cast iron	Rock
Latent heat of fusion (kJ/kg)	190	N/A	N/A	N/A
Specific heat (kJ/kg K)	2.15	4.19	0.54	0.88
Storage mass (kg)	20.513	47.72	370.3	227.3
Density (kg/m ³)	790	1000	7200	1600
Storage mass (kg)	0.02597	0.04773	0.0514	0.142

Table 4.1 shows heat storage materials commonly used sensible, latent and thermo-chemical storage techniques. This comparison for different materials was based a maximum storage energy capacity of 5kW with initial temperature of 25°C. It is important to note that water, cast iron and rocks do not have latent heat of fusion and cannot be used for sensible heat storage. However, paraffin wax is a good material for LHS with 190 kJ/kg latent heat of fusion and specific heat of 2.15(kJ/kg K), and it is commonly used for solar hot water storage applications [56]. Heat of fusion can be defined as the amount of energy one kilojoule of heat stored in one kilogram of material and this depends on the properties of each material.

4.4-Comparison between Sensible heat & Latent heat Storage in Solar Energy

This section of the thesis will focus on more detailed discussions on both sensible and latent heat of fusion. The following are two main differences between sensible and latent thermal energy storage:

1. The most interesting advantage of this technique is that the latent thermal energy storage requires less volume than sensible thermal energy storage.
2. Latent thermal energy storage can store large amount of thermal energy with a small change in temperature than sensible thermal energy storage. This temperature known as the melting temperature of the material is required to change from solid to liquid, which is an important property of the material.

Furthermore, latent thermal energy storage have disadvantages are still facing many problems concerning than sensible thermal energy storage is better than it. For example, the materials used to perform the storage process have high cost, low thermal conductivity and stability of thermo physical properties after working processes. In view of the above, the next section will focus on the choice of materials to suit current model and also carry out theoretical study on how energy is stored in the PCM.

4.5-Phase Change Materials used in Thermal Solar Storage System

A phase change material (PCM) is a one with high heat of fusion which melts and solidifies at a fixed temperature. It is capable of storing (heat charging) and releasing (heat discharging) large amount of energy during operation. The storage system absorbs heat or releases heat when the material is changing from solid to liquid and the reverse process happens when it is discharging. These materials are classified in group of latent heat of storage unit which has three types of phase changes, and this can happen at constant temperature of a material including solid to liquid, solid to gas, and liquid to gas.

Furthermore, change from solid to liquid phase is the most favoured mode of latent heat storage. The capacity of PCM-storage depends on physical, kinetic, chemical and thermal properties of materials used. The thermal-physical properties are connected to the melting temperature, mass of material, volume of storage, and energy supplied from parabolic dish during the day.

4.6-Storage Capacity of a LHS System

The thermal capacity of a LHS system in terms of changes from solid to liquid transformation is represented in equation 4.1.

$$Q_{\text{storage,PCM}} = \int_{T_{\text{initial}}}^{T_M} m_{\text{PCM}} C_{p,\text{solid}} dT + m_{\text{PCM}} \cdot a_{\text{PCM}} \Delta h_{\text{PCM}} \quad (4.1).$$

$$+ \int_{T_M}^{T_{\text{final}}} m_{\text{PCM}} C_{p,\text{liquid}} dT, (\Delta h_{\text{PCM}} \gg C_p)$$

where, ' T_{initial} ' is the initial temperature($^{\circ}\text{C}$), ' T_M ' is the melting temperature, ' T_{final} ' is the final temperature ($^{\circ}\text{C}$), ' m_{PCM} ' is the mass of heat storage material (kg), ' $C_{p,\text{solid}}$ ' is the specific heat of solid(J/kg), ' $C_{p,\text{liquid}}$ ' is the specific heat of liquid(J/kg), ' a_{PCM} ' is the fraction melted, ' Δh_{PCM} ' is the heat of fusion per mass unit (J/kg). Equation 4.1 is one of the complex equations in thermal storage systems with different available factors. These factors include specific heat of solid, fraction melted, the heat of fusion per unit mass, melting temperature, specific heat of liquid and mass of heat storage material. In phase change materials the heat of fusion (heat of evaporation) is much more than the specific heat for this reason, the latent storage materials have got a larger volumetric energy storage capacity than sensible storage materials. This equation of heat energy storage has three storage parts:

1. Heat stored in material in the solid state $\left(\int_{T_{\text{initial}}}^{T_M} m_{\text{PCM}} C_{p,\text{solid}} dT \right)$.
2. Heat store in material in the transmutation state $(a_{\text{PCM}} \Delta h_{\text{PCM}})$, where a_{PCM} in must be in range of $0 \leq a_{\text{PCM}} \leq 1$.
3. The heat of fusion of this materials ' Δh_{PCM} ' is much greater than the specific heat.
4. Heat store in material in the liquid state $\left(\int_{T_M}^{T_{\text{final}}} m_{\text{PCM}} C_{p,\text{liquid}} dT \right)$.

This equation can be used during the charging operation of storage system as well as discharging operation of material or vice versa.

The melting temperature of the PCM must be between the initial temperature and the final temperature even storage process occurs in these conditions $T_M > T_{\text{initial}}$ and $T_{\text{final}} > T_M$ used during the charging operation. There are two important cases must be understood from equation 4.1:-

- When the $T_M < T_{\text{initial}}$ the heat storage system is not working because there is no heat energy supplying the system.
- When the $T_{\text{final}} > T_M$ the heat storage system release heating.

From second case, PCM do not solidify immediately upon cooling below the melting temperature, but start crystallization only after a temperature well below the melting temperature is reached, it called subcooling or supercooling. During the supply of heat, there is no difference whether a PCM shows subcooling or not.

During extraction of heat however, the latent heat is not released when the melting temperature is reached due to subcooling. The effect of subcooling makes it necessary to reduce the temperature well below the phase change temperature to start crystallization and to release the latent heat stored in the material. If nucleation does not happen at all, the latent heat is not released at all and the material.

Furthermore, the important benefit of operating PCM is the charging (absorption) and discharging (release) of the energy stored which takes place at a constant temperature as shown in Figure 4.2. This benefit makes it easier to choose the suitable material to be used in the current model, which is also dependent on the melting temperature.

The disadvantages of PCMs are:

- It has high cost when compared with the sensible heat storage.
- Corrosiveness.
- Low density change.
- Low thermal conductivity.
- Low phase separation.
- Incongruent melting and super cooling.

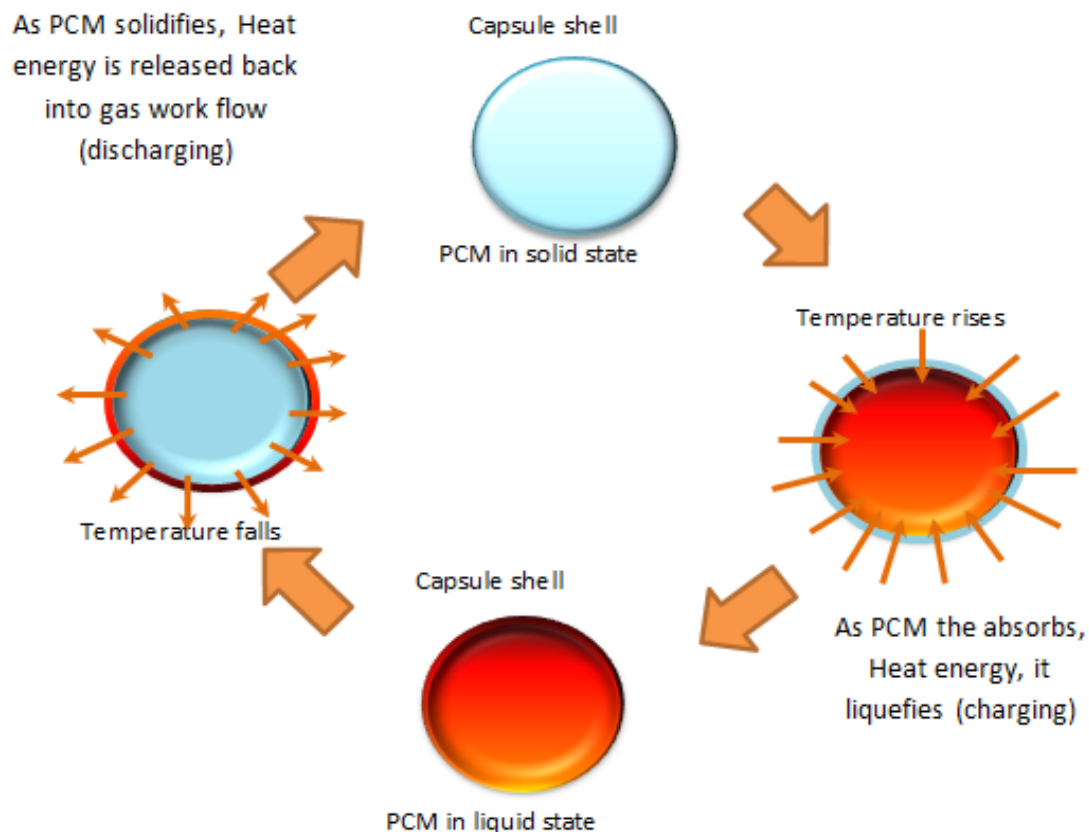


Figure 4.2 Capsule shells of PCM of heat charging and discharging from Solid to liquid

Figure 4.2 gives the schematic representation of the phase change material during the charging and discharging process of the storage system. It was shown in the capsule shell of PCM and how the charging and discharging process is completed within the circle from different phases (solid and liquid).

The four different operations can be summarised as follows:

- PCM when in the solid state at initial temperature.
- PCM absorbs heat energy and transfer it to liquid (charging), between the initial and melting temperature.
- PCM in liquid state.
- PCM released heat energy and transfer to solidify (discharging).

Furthermore, encapsulation or leak proof containment of the PCM is necessary to avoid leakage during solid to liquid transitions. In spite of the current research interest, the concept of encapsulation itself is not new; the literature [4] explored the

pros and cons of potential encapsulation materials, their geometries, and potential PCM compatibilities over two decades ago. It was recommended that the containment mechanisms should [4]:

- ❖ Meet the requirements of strength and flexibility.
- ❖ Act as a barrier to protect the PCM from harmful interactions with the process environment.
- ❖ Provide adequate heat transfer, structural stability and easy handling.

4.7-Characteristics of PCMS used in solar thermal technology

PCM-Storage was applied in solar thermal technology especially in the storage of heat from the sun using hot water as fluid and solar concentrator [6]. Furthermore, there has been an ongoing research to investigate the properties of PCM for applications in solar thermal storage systems [46]. The main focus of this section is to select a good material with heat of fusion and melting temperature within the desired operating temperature between 50°C to 350°C systems (1) of the current model. The materials considered must have the required properties for possible use in the system as good PCM-Storage material [41, 42, and 43]. Prior to the discussions on the design of the thermal storage and making the appropriate choice of the PCM to be used in storage system experiments, it was necessary to study the properties of phase change materials as shown in Figure 4.3.

4.7.1-Thermal Properties of PCM

The properties of PCM are divided into five main classes or groups and this will be discussed in more detail subsequently. Thermal properties are related to the phase transition temperature and thermal conductivity of the materials. Furthermore, PCM must have high thermal level properties with a suitable melting temperature for the specific solar application. And also it must have high latent heat of transition in order to occupy the minimum possible volume, high thermal conductivity in order to provide the minimum temperature gradients, and facilitate the charging and discharging of heat during operation [6].

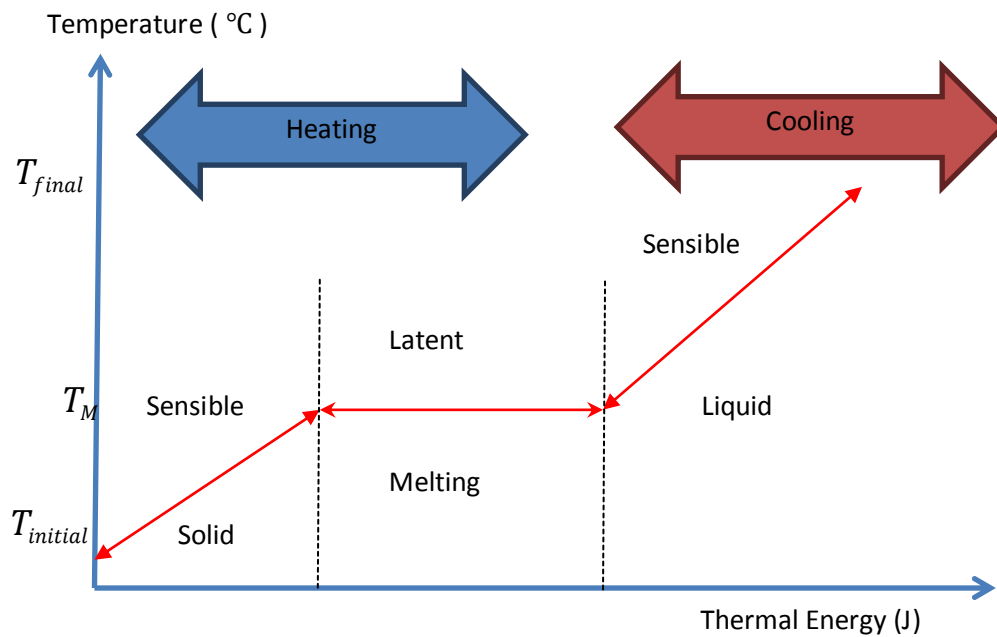


Figure 4.3 The diagram of the stages of transformation of material from solid to a liquid state and vice versa when heat is added gain or loss

Figure 4.3 shows the change in phase which happens within the PCM, and increasing the absorbed heat energy also increases the operating temperature. The diagram in Figure 4.3 gives the summary of activities within the Capsule shells of PCM at different operating conditions as shown in Figure 4.2. The latent heat storage starts at melting temperature in the solid phase and maintains this temperature before changing to liquid. This happens during the charging period of the PCM, while the reverse process happens during discharging or release of energy.

4.7.2-Physical Properties of PCM

The second properties of PCM are physical, and the materials to be considered must have good physical properties. These properties include high density to occupy the minimum possible volume, favourable phase equilibrium to facilitate the heat storage, small volume change to facilitate the construction of the different needed containers and heat exchangers. It should also have low vapour pressure in order to avoid stress, problems with the containers and heat exchangers needed [47].

4.7.3-Kinetic Properties of PCM

The third properties of PCM has to do with it kinetic nature, as the materials must have sufficient crystallization rate in order to avoid super-cooling. No super-cooling as it makes it difficult to control the heat transfer and the true melting temperature that is given in principle [7,33].

4.7.4-Chemical Properties of PCM

The chemical properties are important aspect of the PCM as it changes state based on the constant chemical properties. These materials must have constant chemical properties as these properties are required and responsible for the various changes of phases and the verse versa during operation. Other properties are compatibility with materials of construction and other safety issues including toxicity, fire hazard and explosive nature of the materials which are vital [66].

4.7.5-Economics Specifications of PCM

These materials have high level of economics specifications, which must be abundant, good recyclability and cost effective to help into the feasibility of the use of the storage system.

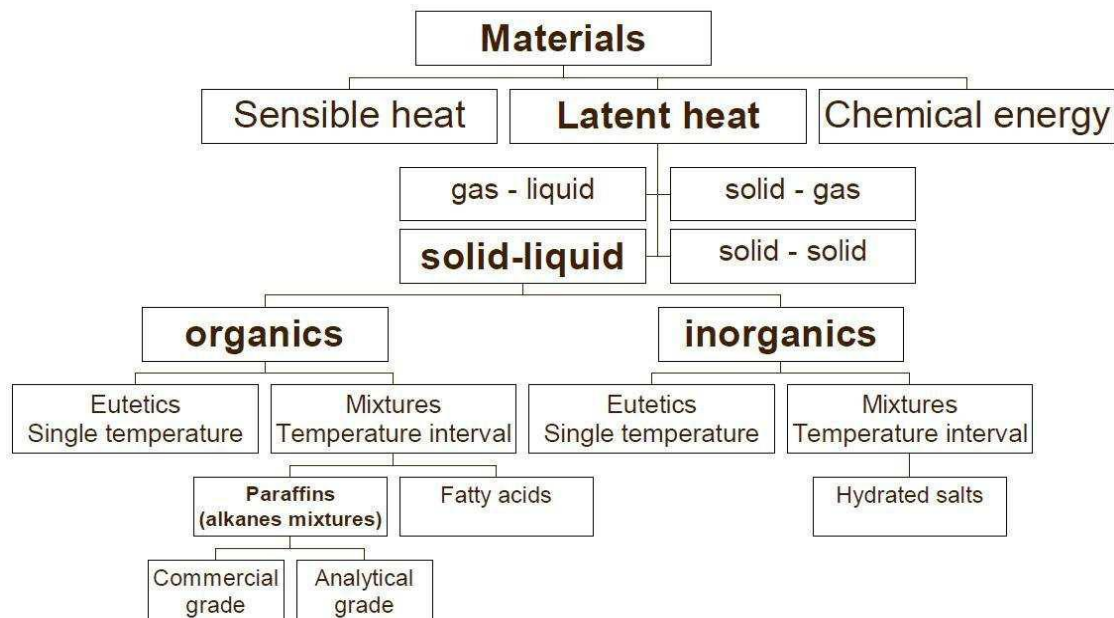


Figure 4.4 Classifications of PCM-Storage [47]

4.7.5.1-Organic Materials

The organic materials are not mostly used for solar thermal storage at low temperature of less than 100°C. It usually do not suffer segregation and sub-cooling (refers to a liquid existing at a temperature below its normal saturation temperature) problems during thermal cycling, which can be a severe problem for some salt hydrates [46]. Organic materials include paraffin waxes (C_nH_{2n+2}), fatty acids, and sugar alcohols [8] have been used in many developmental researches recently in solar thermal storage. Paraffin wax is the most popular PCM used for active forced hot air systems. It consists of a combination of different hydrocarbons obtained from petroleum distillation. The properties of the different paraffin compounds are quite similar and make it easy to study [4.5 and 9]. There was the need to consider the organic properties of the phase change materials in this study. It has poor heat transfer properties such as lower density and also more expensive when compared with inorganic salts in general.

4.7.5.2- Inorganic Materials

Inorganic materials also called non-paraffin covers all type of esters, fatty acids, alcohols and glycols. These materials have several properties and are divided into two different groups with more details given in the literature.

4.7.5.2.1- Salt hydrate

Salt hydrates which are the first of the two groups of inorganic materials are alloys of inorganic salts and water forming a typical crystalline solid of general formula ($AB \cdot nH_2O$). Salt hydrates are phase change materials that have been studied including $CaCl_2 \cdot 6H_2O$, $MgCl_2 \cdot 6H_2O$, $Na_2SO_4 \cdot 10H_2O$... etc. They offer a range of operating temperatures, melting points within the range of 20°C to 317 °C. [52].The thermal properties of salt hydrates include high latent heats of fusion, good heat transfer properties as compared to organic materials, and relatively cheap. But there are two setbacks as it suffers from segregation and sub-cooling.

4.7.5.2.2- Metallic

The metallic types of inorganic materials include low melting metals and metal eutectics. These materials have large weight and for this reason are not considered to be good PCM.

On the other hand, there are some exciting points to say:-

- It has got high thermal conductivity.
- Low vapour pressure (relatively).
- High heat of fusion per unit volume.

Table 4.2 Advantages and disadvantages of organic and inorganic PCM materials [45]

Classifications PCM	Advantages	Disadvantages
Organic	Not corrosive Low or no sub-cooling Chemical and thermal stability	Lower phase change enthalpy Low thermal conductivity Flammability
Inorganic	Lower phase change enthalpy Low thermal conductivity Flammability	Sub-cooling due to super-saturation Corrosion Phase separation Lack of thermal stability
Techniques for improvement		
Organic	High aliphatic hydrocarbon, acid/esters or salts, alcohols, aromatic hydrocarbons, category, polymers	Crystalline hydrate, molten salt, metal or alloy
Inorganic	High thermal conductivity additives, fire-retardant additives	Mixed with nucleating and thickening agents, thin layer arranged horizontally, mechanical stir

4.7.5.3- Eutectic

Eutectic is a type of minimum-melting component group as shown in Figure 4.6 which eutectic is a mixed minimum melting composition of two or more constituents. Each of these constituents is melts and freezes similarly forming a mixture of the component crystals during crystallization [48]. Table 4.2 shows the comparison between organic and inorganic materials with different techniques adopted to improve both types. More information on different types of materials, there advantages and disadvantages, melting temperature and heat of fusion can be obtained from the literature [81, 82, 83, and 85].

This collection can be divided into three different groups as shown in Figure 4.6:

- ❖ Organic – Organic PCM.
- ❖ Inorganic – Inorganic PCM.
- ❖ Inorganic – Organic PCM.

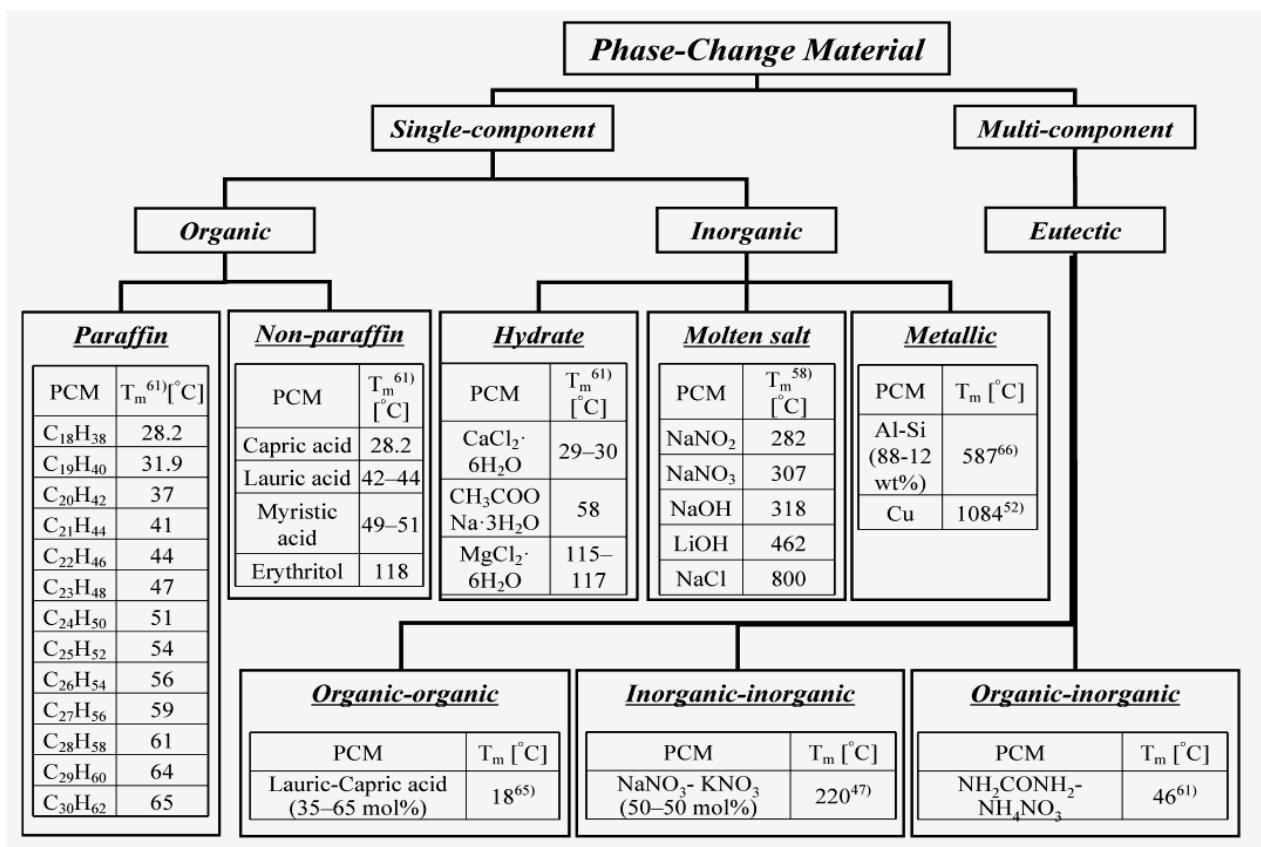


Figure 4.5 Different types of PCM use for thermal storage and melting temperatures [41]

Figure 4.5 displays the different types of PCM used in thermal storage and their melting temperatures. There are a number of recent researches on double and triple eutectics particularly the ones with fluorides and chlorides origin. These fluorides and chlorides containing basic hydroxides, nitrates, carbonates and extra salts are of considerable interest. Furthermore, it was also shown that the eutectics obtained on the basis of fluorides or chlorides have more prospects [95]. Other researchers focused on inorganic salts with melting temperature within the range of 250°C to 1480°C, and a heat of fusion between 0.068–1041 J/g [96].

Moreover, the materials used for PCM-Storage in the current research are certain type of eutectic inorganic salts which is mixture of potassium and sodium nitrate. The mixture of the two compounds is suitable and adopted in the current model, and has a temperature range of 100°C-300°C. These mixtures of eutectic inorganic salts as PCM have their respective melting temperatures, heat of fusions as shown in Figure 4.5. These salts mixtures compositions also have different thermo-physical properties which are different, depending on the original of the salt such as melting

point, heat of fusion, different thermal capacity, thermal conductivity and thermal diffusivity.

The main focus of the present work as mentioned in chapter 2 is to discuss high temperature storage systems within the range of 100°C to 400°C. Furthermore, only inorganic salts and their eutectic mixtures are considered to be adopted as PCM materials, with possible metallic materials as will be discussed in more detail in the next section.

4.8- Basic Review of Latent Heat in Solar PCM-Storage

It has been established in the literature that the use of latent heat storage system as phase change materials (PCMs) is an effective way of storing thermal energy and has the advantages of high-energy storage density and the isothermal nature of the storage process [6]. The storage of thermal energy in the form of sensible and latent heat has become an important aspect of energy management with the emphasis on efficient use and conservation of the waste heat and solar energy in industries and buildings.

Other studies on thermal energy storage system consider the shell and tube type heat exchanger during charging and discharging. An experimental and numerical investigation was carried out of transient forced convective heat transfer between the heat transfer fluid (HTF) with moderate 'Prandtl' numbers and the tube wall. It was shown that heat conduction through the wall and solid-liquid phase change of the phase change material (PCM) was reliable, based on the enthalpy formulation. A fully implicit two-dimensional control volume FORTRAN computer code, with algorithm for non-isothermal phase transition was developed for the solution of the corresponding mathematical model. The comparison between numerical predictions and experimental data shows good agreement for both paraffin non-isothermal melting and isothermal solidification [97].

The use of different paraffin types with different properties were considered as PCM in recent study. This was based on the consistency of the liquid material shown to possess for a typical phase change material after a close study and analysis on the ability of the material to meet certain laid down characteristic of a standard PCM ideal material [8]. Water had also been used previously as heat transfer fluid

(HTF). Certain properties of the materials determined were shown to be affected by the Reynolds and Stefan number. The observation from the study shows positive ability of a good PCM based on the storage system considered in the research [9].

Brian and Paul [10] carried out the study to determine the market value of PCM for possible use in commercial buildings, with the aim of assessing the potential demand as well as how much energy can be saved from the use of this technology. A number of factors were considered in this study, this includes discussion with the manufacturers in order to have knowledge of the demand for PCM and how efficient is this energy source. Furthermore, comparison of PCM with other existing materials, climatic or natural conditions that could affect installation, properties of typical PCM and variation of day and night that could affect phase changes [81,90].

In view of the above, the following conclusions were made:

- ❖ Use of phase change material is an effective way of storing thermal energy and has advantages of high storage density and isothermal nature of energy storage.
- ❖ Use of phase change material is an important aspect of energy management, by utilisation of excess available energy.
- ❖ A vertical tube in shell type storage system is a simple and effective way of storing thermal energy using phase change material.
- ❖ The geometry of tube in shell type storage system can be made consistent with melting and solidification characteristics.
- ❖ $\text{KNO}_3\text{-NaNO}_3$ for 100 (kJ/kg) was a good choice of phase change material storage for solar parabolic dish concentrator due to its ease of workability, melting temperature and availability.
- ❖ Phase change material is an important part of energy efficient future.

4.9- Design and Fabrication suitable PCM Storage

The previous section introduced the importance of thermal energy storage, the method of storage systems, and PCM properties for LHS materials. Subsequent sections will discuss the design of the storage system used in the final model.

4.9.1-Design of PCM storage

The design of the storage system was carried out bearing in mind the cost of the final model and the heat it can store. Other factors considered in the design include the storage volume, total energy storage, amount of energy produced at night and type of storage materials.

It is important to note that the storage was located under parabolic dish concentrator in the final model, and it was connected to the parabolic dish mirror by copper pipe and air compressor mentioned in section 5.2.2. The storage design consists of three layers, and does not allow transfer of heat outside the layers (thermally insulated) and stored within the material. Small balls of $\text{KNO}_3\text{-NaNO}_3$ were used as phase change material inside the storage system; obtain energy in the form of heat and gets energy from heat which was transferred through copper pipe.

4.9.2- Measurement of the Storage Volume in Model

To determine the storage volume in the current model, some important aspects must be investigated including the engine capacity, total heat capacity of storage, charge and discharge time, dimensions of storage, physical and chemical properties of materials. The storage capacity of sensible heat storage with a solid or liquid storage medium is given by the following.

4.9.2.1-Engine Working Time

The model consists of two parabolic systems including system (1) and system (2) as explained in section 3.1. The first system was connected to the hybrid Stirling engine, while the second was connected to the PCM- storage. The size of storage in second system is related to the energy supplied by the parabolic dish to the system during operation. The operating capacity of the system depends on time of the day, which varies depending on the season within the year (from summer to winter) as shown in Table 4.3. In Oman where the fabrication of the system was carried out, January 21st was known to have the least daylight hours each year and the hours of day light was used to measure the capacity of storage. However, the capacity of energy storage depends on four factors including density of material, specific heat of material, temperature difference between maximum and minimum temperature of medium and storage volume as given in equation 4.2 and Table 4.3.

The energy stored in PCM–Storage approximately equal the energy used to generate power during night by hybrid engine" $Q_{STO,STI}$ " .

$$Q_{storage,PCM} \times t_{CH,DAY} = Q_{STO,STI} \times t_{night}$$

$$Q_{STO,STI} \times t_{night} = 50 \text{ W} \times t_{night} \quad (4.2).$$

$$= \int_{T_{initial}}^{T_M} m_{PCM} C_{p,solid} dT + m_{PCM} \cdot a_{PCM} \Delta h_{PCM} + \int_{T_M}^{T_{final}} m_{PCM} C_{p,liquid} dT$$

$$\times t_{CH,DAY}$$

where, the power generated by Stirling engine controlling at 50W, t_{night} is engine working time during night, $t_{CH,DAY}$ charging time of PCM during day , 'm' is mass of material (kg), 'c_p' is specific heat capacity (J/kg K) and 'ΔT' is temperature change between input and output system (K).

Table 4.3 The time of day in Oman at summer and winter [49]

Seasons(Oman)	Sunrise	Sunset	Day (Hours)	References
Summer (21-07-2013)	5:31am	6:53pm	13	Oman's weather centre
Winter (21-01-2013)	6:50am	5:45pm	11	Oman's weather centre

To know how much storage volume is required, this can easily be calculated depending on the storage volume using equation 4.3.

$$V_s = \frac{\int_{T_{initial}}^{T_M} m_{PCM} C_{p,solid} dT + m_{PCM} \cdot a_{PCM} \Delta h_{PCM} + \int_{T_M}^{T_{final}} m_{PCM} C_{p,liquid} dT}{\rho \Delta h_{PCM}} \quad (4.3)$$

On other hand, the energy density per unit mass in the PCM is given by:

$$(4.4)$$

$$q_{mass} \left(\frac{J}{kg} \right) = \frac{Q_{storage,PCM}}{m} = c_p \Delta T \approx \frac{Q_{storage,PCM}}{V_s \cdot \rho}$$

And the energy density per unit volume is given by

$$q_v \left(\frac{J}{m^3} \right) = \frac{Q_{storage,PCM}}{V_s} = \rho c_p \Delta T \quad (4.5)$$

From equations 4.6 and 4.4, the storage volume can be obtained in terms of total energy storage and energy storage per unit volume m^3 of material as given in equation 4.6.

$$V_s = \frac{Q_{storage,PCM}}{q_v} \quad (4.6)$$

This equation means the energy storage volume is equal to the heat storage over the heat density per unit volume of materials. The equation depends on property of the materials, each material have different energy storage per unit volume. A suitable storage designed for the current model was a large cylindrical shape made from steel with 5 mm depth, 100 cm height and 50 cm radius. The cylinders had 5 m layer acoustic around the inner surface, with a 5 mm iron - box inside the cylinder as shown in Figure 4.7. The internal part of the storage is rectangular in shape with 30 cm by 20 cm by 15 cm dimensions, and Figure 4.7 shows the thermal storage used. The heat capacity of storage system ranges from 2 kW to 100 kW at melting temperatures of 142°C and 222°C. This storage system has phase change materials which have high ability of thermal storage, low volume and low cost.

4.9.2.2-Steps Design:-

There are six main steps in the process of design and fabrication of thermal storage system suitable for current model. These steps give the breakdown of the whole process from the initial design to completion as follows:

- **First step:** Measurement in theory how much Stirling engine can generate power and the efficiency of the engine was calculated using the following formula:

$$\text{Efficiency} = (\text{Work output}) / (\text{Energy input}) \quad (4.7)$$

The power input to the system was estimated by taking the temperature difference between the heated part and the heat sink as follows:

$$\text{Energy input} = \text{Mass of (He)} \times C_p \times \Delta T \quad (4.8)$$

Also the mass of helium can be calculated as shown in equation 4.9.

$$\text{Mass (kg)} = \text{Density}(\rho) \times \text{volume} (V_s) \quad (4.9)$$

where, density (ρ) helium is $\rho = 0.179 \text{ kg/m}^3$, Volume $V_s = 1200 \times 10^{-6} \text{ m}^3$, Mass $= 2.144 \times 10^{-6} \text{ kg}$, specific heat capacity, $C_p = 1005 \text{ J/kg}$, temperature change, $\Delta T \approx (350 - 50) = 300^\circ\text{C}$,

$$\text{Energy input} = 0.179 \times 1200 \times 10^{-6} \times 1005 \times 300 = 64.7$$

Assuming a temperature decrease of 350°C to 50°C (hot to cold) was achieved from equation 4.10, and then the engine work at that temperature is given as equation 4.10.

$$W_o = (1 - (rt)) (rv) \frac{\ln(rv)}{(rt)(\gamma - 1)} \quad (4.10)$$

where,

$$(rt) = \text{temperatureratio} = \frac{(50 + 273.15)}{(350 + 273.15)} = 0.37 \quad (4.11)$$

$$(rv) = \text{compression ratio} = \frac{v_1}{v_2} = \frac{750 \times 10^3 \text{ mm}^3}{125 \times 10^3 \text{ mm}^3} = 6 \quad (4.12)$$

$$W_o = (1 - 0.37) \times 6 \times \frac{\ln(6)}{0.37 \times 0.4} = 45.6 \text{ W} \quad (4.13)$$

Thus with the above assumptions of temperature and compression ratios, the Stirling engine designed can have an estimated output of 45.6 W , and this amount was used in the measurements. It is important to note that the values of the volume are taken from the model parameters, while the values for the temperature are taken from the desired design parameters. Therefore, the efficiency can be calculated as:

$$\text{Actual Efficiency} = 50 / 64.7 \times 100 = 70.5 \% \quad (4.14)$$

Then the actual efficiency of the engine is 70.5%.

Second step; 'Measuring the total amount of energy consumed and duration of working hours'

There are longer nights during the winter period particularly in Oman as shown in Figure 4.6 and this second step considered this period of the year. The PCM-storage is the second source of heat energy to the hybrid Stirling engine and this stored energy as obtained during day as shown in the first step. Figure 4.7 show the process of designing and sizing of thermal energy storage.

There are two seasons in Oman with the summer taking most periods of the year and winter between December to February of every year. Summer period during the year experiences longer days with shorter nights, while the winter period is associated with longer nights, and shorter days. During the winter period in Oman, the night with most hours of darkness was estimated to be between 13 to 11 hours of darkness and that is on or about 21st of January of every year as shown in Figure 4.6. During the winter, the hybrid Stirling engine will use energy stored in PCM storage during night, and during the day, the parabolic dish to deliver thermal energy to the PCM-storage for later use. Figure 4.6 shows methods used to measure the total energy supplied to the hybrid Stirling engine and also the total energy demand for the period of the year with longer nights.

The total energy supply to the Stirling engine at night is equal the energy stored in PCM storage during the day. The energy which transfers from parabolic dish concentrator to the helium gas is given by equation 4.16.

$$Q_{T,He} = Q_{STO,STI} \times t_{CH} \quad (4.16)$$

➤ **Third step:** 'To calculate of the heat stored in the phase change materials (KNO₃-NaNO₃)'.

Assuming that the Stirling engine produces 10W to 50W at night in Oman with longer hours of the night during the winter with shorter daylight hours of ($w_{night} = 13h$, $w_{day} = 11h$) and the reverse happens during the summer. Hence, the total charging processes of PCM-storage during the day is equal ($t_{CH} = 11h$) and total discharging time during the night is equal ($t_{DISCH} = 13h$). Furthermore, the melting temperature of

$\text{KNO}_3\text{-NaNO}_3$ is 222°C this is within the same operating temperature range of helium ($100\text{-}350$) $^\circ\text{C}$ that is shown in Table 4.4 below. Also the heat of fusion of $\text{KNO}_3\text{-NaNO}_3$ is 100 (kJ/kg) and density of $1950(\text{kg}/\text{m}^3)$, for further information on the thermo physical properties of solid – liquid PCM, see Table 4 .4 below.

Thermo-physic properties of $\text{KNO}_3\text{-NaNO}_3$:-

- ❖ Melting temperature is 222°C .
- ❖ Enthalpy of fusion $100(\text{kJ}/\text{kg})$.
- ❖ Low density charge 4.6% (solid – liquid).
- ❖ No or little sub-cooling.
- ❖ Chemically stable.
- ❖ No phase segregation.
- ❖ Low cost.
- ❖ Good physical characterization.
- ❖ Perfectly suits our need.

Table4.4Thermo physical properties of solid – liquid PCM

Salt system	Melting Point ($^\circ\text{C}$)	Latent Heat (kJ/kg)	Heat Capacity in Solid State (J/kg·K)	Heat Capacity in Liquid State (J/kg·K)	Density (kg/m^3)	Heat Conductivity solid (W/mK)	Heat Conductivity Liquid (W/mK)
NaNO_3	306	175	1.66	1.6	1910	0.6	0.51
KNO_3	337	100	1.4	1.3-1.4	1870-1890	n.a.	0.4-0.5
$\text{KNO}_3\text{-NaNO}_3(60\text{-}40)$	222	100	1.4	1.5	1950	0.51	0.5
LiNO_3	250	357	1.5	1.6	2.380	0.51	0.5

From previous data, measurement of the total energy produced by Stirling engine at night with compensation is given in the following equation:

$$Q_{T,S} = \text{POWER (W)} \times t_{\text{DISCH}} \text{ (s)} \quad (4.17)$$

$$Q_{T,S} \text{ (J)} = 50 \text{ (W)} \times 13 \times (3600\text{s}) = 23.4 \text{ kJ} \quad (4.18)$$

On the other hand, all 'Q_{T, S}' (J) are coming from PCMs (KNO₃-NaNO₃) directly by helium. Furthermore, all energy stored equal to energy used by Stirling engine in closed thermal circuit (mean without heat losses).

$$Q_{T,S} (J) = Q_{L,STO} (J) \quad (4.19)$$

The heat stored in the PCMs depends on the mass of materials and the heat of fusion, heat capacity from solid to liquid, and this can be given in equation 4.20.

$$Q_{char}(J) = m(\text{kg})[C_{p,s}(T_M - T_{initial}) + a_{PCM} \Delta h \left(\frac{\text{kJ}}{\text{kg}}\right) + C_{p,s}(T_{final} - T_M)] \quad (4.20)$$

From Figure 4.6 and Table 4.4 is compensation for the values in equation is given equation 4.21.

$$Q_{char}(J) = 312.8 (J/\text{kg}) \times m (\text{kg}) \quad (4.21)$$

$$Q_{char}(J) = m (\text{kg})[1.4(495\text{K} - 373\text{K}) + 100 \left(\frac{\text{kJ}}{\text{kg}}\right) + 1.5(495 - 523)] \quad (4.22)$$

➤ **Forth step:** measurement of the storage volume

From compensation equation 4.6 in equation 4.3 the total mass of PCM used in thermal storage is:

$$m_{PCM} (\text{kg}) = \frac{2340(\text{KJ})}{312.8(\text{KJ}/\text{Kg})} = 74 (\text{kg}) \quad (4.23)$$

From mass measured in the volume size of storage is given by equation 4.25.

$$V_{sto}(\text{m}^3) = \frac{m_{PCM}(\text{kg})}{\text{Density} \left(\frac{\text{kg}}{\text{m}^3}\right)} = \frac{149.6}{1950} = 0.76 (\text{m}^3) \quad (4.24)$$

Also the total volume of PCMs (KNO₃NaNO₃) is 0.76 m³. From the internal storage shape as shown in Figure 4.7 which is the total volume of phase materials is given in equation 4.27. PCM Volume (cylinder) = Total volume of storage – Volume of pipe

$$V_{in,PCM} = V_{in,s} - V_{in,pipe} \quad (4.25)$$

$$V_{in,PCM} = \pi r_p^2 h_s - \pi r_p^2 h_p \quad (4.26)$$

$$= \pi [r^2 h_s - r^2 h_p] = \pi [(0.368)^2 * 1.30 - (0.003)^2 * 15] = 0.366 \text{m}^3 \quad (4.27)$$

➤ **Fifth step;** 'Design of the storage volume using the solid-works software'

After storing the heat in the PCM-storage, then many applications are required for the working fluid to guarantee a steady thermal output. Heat will be stored in the materials of thermal storage to act as a damper for heat transfer. When momentary cloud cover blocks energy input to the system the working fluid can store a large amount of heat energy through the phase change materials. Energy can be stored in any material by increasing its temperature. The amount of energy stored is proportional to the mass, heat capacity and temperature increase in heat of fusion and melting temperature of materials. The storage capacity of a mass can be made more efficient if it undergoes a phase change. This effect increases thermal storage without increasing receiver temperature. The total energy stored in a material that undergoes a phase change can be written in term of PCM storage properties:

$$Q_{storage,PCM} = m_{PCM} [C_{solid}(T_M - T_{initial}) + a_{PCM} \Delta h_{PCM} + C_{liquid}(T_{final} - T_M)] \quad (4.28)$$

The stored heat flux during the charging and discharging phase is given by equation 4.29 and 4.30.

$$Q_{charge,PCM} = \frac{m_{PCM} [C_{solid}(T_M - \bar{T}_{initial,ch,PCM}) + a_{PCM} \Delta h + C_{liquid}(\bar{T}_{final,ch,PCM} - T_M)]}{\Delta t_{charge}} \quad (4.29)$$

$$Q_{discharge,PCM} = \frac{m_{PCM} [C_{liquid}(T_M - \bar{T}_{final,dis,PCM}) + a_{PCM} \Delta h + C_{solid}(\bar{T}_{initial,dis,PCM} - T_M)]}{\Delta t_{discharge}} \quad (4.30)$$

The daily average thermal efficiency of the system is the ratio of the desired energy output of the discharging processes to the total energy input during the charging process given by:

$$\eta\% = \frac{\int Q_{\text{discharge,PCM}}}{\int Q_{\text{charge,PCM}}} \quad (4.31)$$

The energy which transfers from parabolic dish concentrator by helium gas is given by the following equations:

$$Q_{T,He} = \dot{m}C_p\Delta(T) \times t_{CH} \quad (4.32)$$

$$t_{CH} = 1s, C_{p,He} = \frac{5.19kJ}{kg.K}, Q_{T,He} = 1(kW), \Delta(T) = 250 - 100 \quad (4.33)$$

$$\dot{m} = \frac{1(kW)}{\frac{5.19kW.s}{kg.K} (523 - 373)K} = 0.0012 \text{ kg/s} \quad (4.34)$$

Density of helium 0.1664(kg/m³)

$$\dot{m}_{He} = \frac{0.0012 \text{ (kg/s)}}{0.1664 \text{ (kg/m}^3\text{)}} = 0.0072 \left(\frac{\text{m}^3}{\text{s}} \right) = 7.2 \text{ L/s} \quad (4.35)$$

$$\dot{m}_{max} = 0.072 \left(\frac{\text{m}^3}{\text{s}} \right) \quad (4.36)$$

The complete storage system for the current model consist of three layers connected to one another; the first inside the storage tank is a cylindrical hollow sheet (r =30cm, l=130cm) made from 6mm iron. This is the main layer where all transport, conversion and heat storage processes was carried out inside the storage tank.It maintained high pressure and do not allow heat exchange with the outside air. The mid layer: is surrounded by 5cm thermally insulating materials which keep the thermal energy in store, made from acoustic insulation. Outer layer: or external layer is a box that keeps the storage material and other connections and made from 3mm iron. Description Inside the hollow from of storage:

- ❖ Copper pipe (3mm*15m)
- ❖ Phase change materials(KNO₃-NaNO₃)

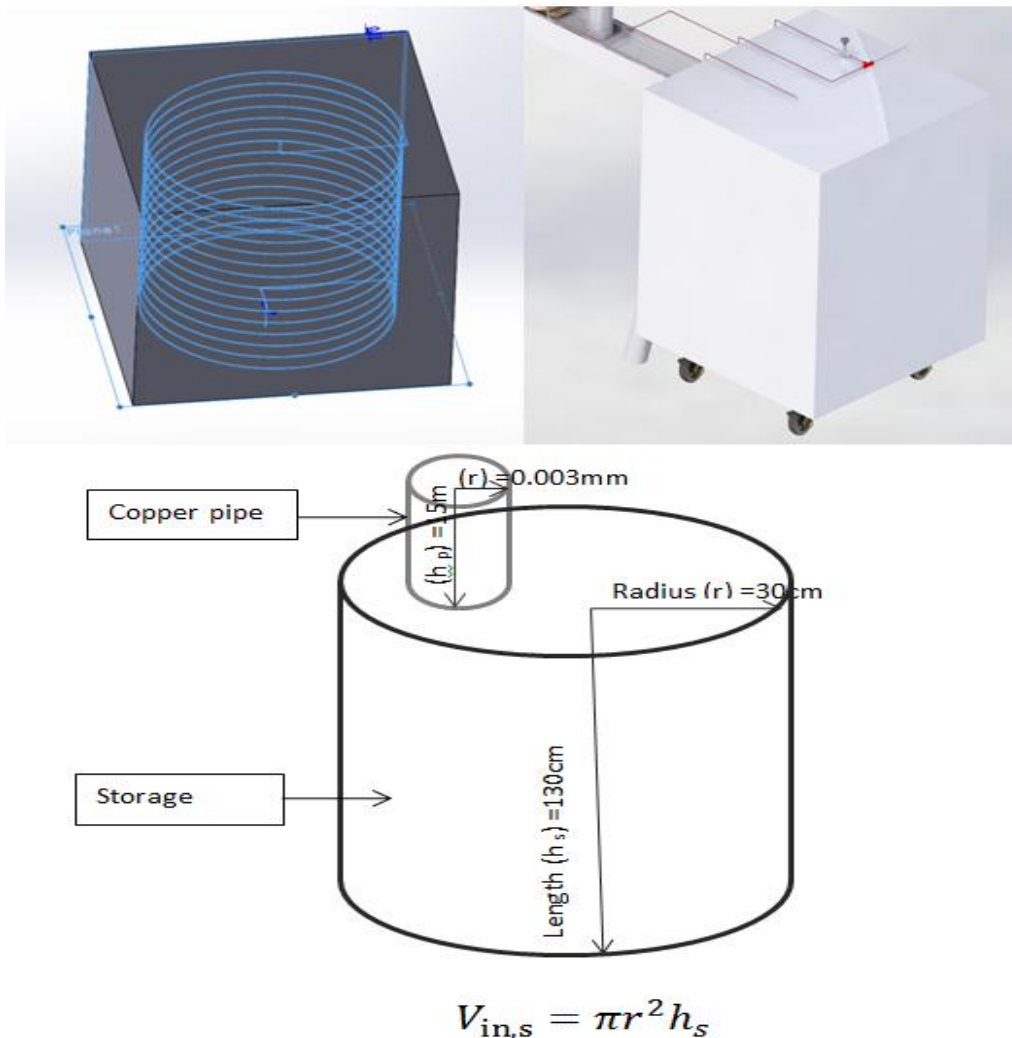


Figure 4.6 Design of thermal storage using Solidworks

Figure 4.6 and appendices (C) shows the thermal storage system with storage heat capacity ranging from 2-50 kW at melting temperatures of 142°C and 222 °C. This storage has phase change materials which have high ability of thermal storage, low volume and cheaper to maintain as mentioned earlier.

➤ **The last step** is fabricating and design of the real model

The final form of storage model is like tank inside the insulation box as shown in Figure 4.7. After installing and assembling three layers covered from the outside storage body, and also covered from the top with copper pipe coming out through the top cover. Inside the thermal storage system is a hollow space which is covered

by (KNO₃-NaNO₃) as phase change material. On the other hand, the copper pipe is fixed within the loop circle inside the hollow spaces of internal storage body.

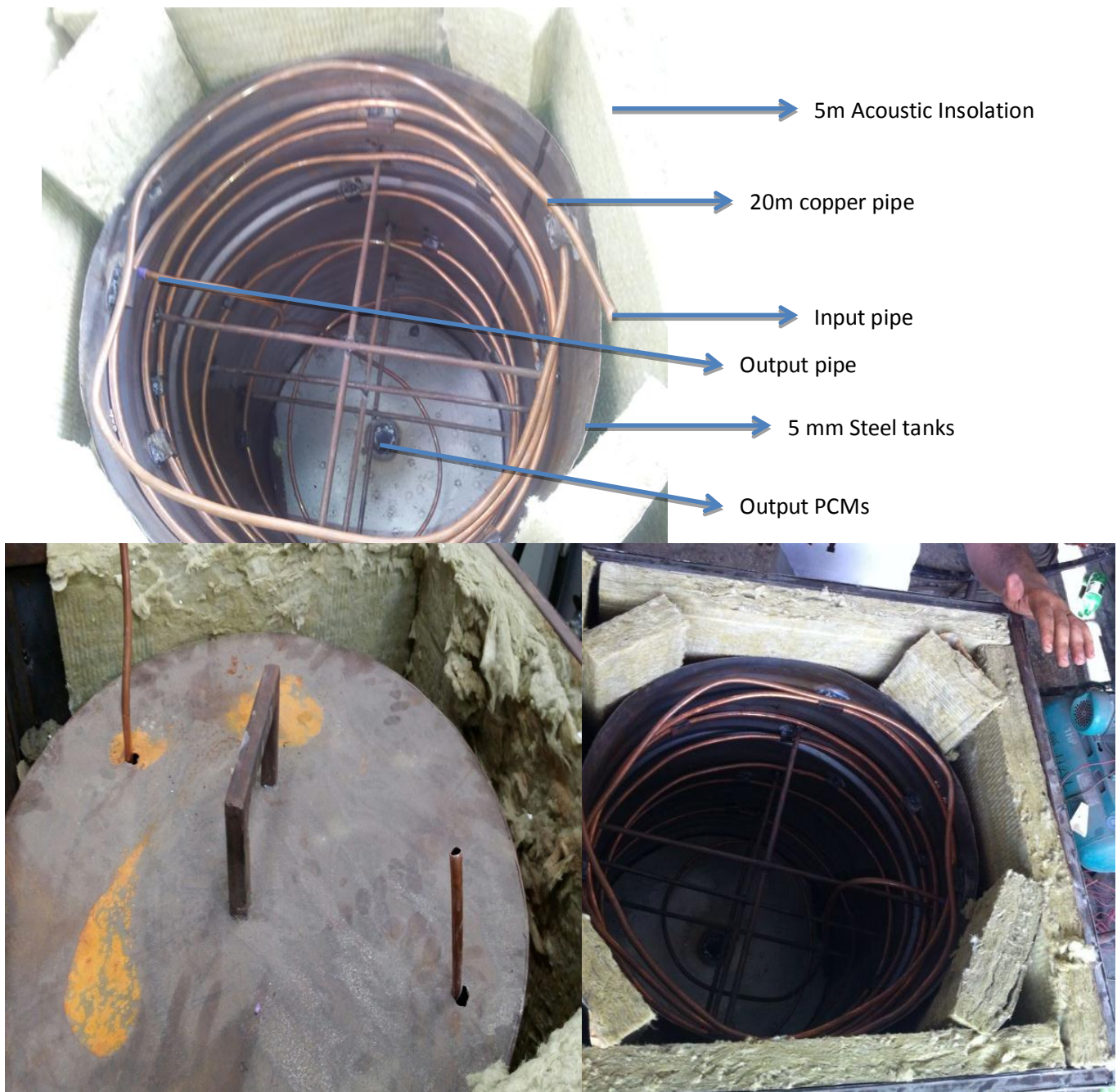


Figure 4.7 The final form of thermal storage which fabrication

When open system (2) while parabolic dish 2m^2 is supplying PCM-storage with the thermal energy. It operates by transferring heat through helium gas, and then the heat is transported to the storage material at the time of the day thereby increasing the capacity of the stored heat.

4.10- Conclusion

This chapter consists of two main sections; the first section studied the background and review of three main types of solar thermal storage and phase change materials for the storage system. The second section discussed the design and fabrication of the PCM-storage, and the use of the thermodynamic equations for the calculation of the storage size, engine capacity, engine working time and total storage capacity. The design of the storage system was based on location and time in Oman. The least amount of daylight hours and maximum night hours in Oman was on about 21 January of each year which is having a total estimated of 11h to 13h of darkness. These times were used to measure the total capacity of storage and this was estimated to be 7.02kWh . The volume of storage 0.73m^3 using $\text{KNO}_3\text{-NaNO}_3$, with melting temperature of about 222°C and this is within the operating temperature of helium ($100\text{-}350^\circ\text{C}$), and also the heat of fusion ($\text{KNO}_3\text{-NaNO}_3$) was 100kJ/kg . Final the fabrication of new phase change materials for the storage suitable for the thermal efficiency of the final model was discussed. More detailed discussion on the manufacturing, installations and assembly of the basic part of the system will be the focus of next chapter.

CHAPTER(5):-Design and Construction of External Devices current apparatus

5.1-Introduction

The previous chapter discussed the design and construction of internal devices in both systems, this is only part of the complete system with the other required parts required before installation and testing. The other components of the system are important as they assist in keeping the dishes firm and safe, tracking the sun and other instrumentation. These components include the base to accommodate two parabolic dishes and all external devices such as thermal flexible pipe, Air pump or compressor, thermal control system and solar tracking system. These components are called external devices and are important in heat conservation and increase heat transportation in the novel model as mentioned in section (3.3). There is the need to discuss the design and construction of these external devices, which is the main focus of this chapter.

This chapter intends to review and describe external devices which were used in the operations of heat charge and discharge of the thermal storage as well as heat space of the engine. All these devices must have certain specifications of high thermal quality for heat transfer at high pressure, high conductivity and high melting temperature.

Also, the choice of other materials including sun reflector, working fluid, and phase change materials storage would be considered at the end of this chapter. However, the priority is the design and fabrication of main body or base which will bear the weight of the main model (about 60kg).

5.2- Base Stand for the Parabolic Dishes

The base stand is required as part of the current method to keep the parabolic dishes firm, and to track the solar radiation during the day. Hence, the base stand is an important part of the external devices in order to have the connection with the internal devices. This section intends to focus on the design and construction of the

base stand for the parabolic dishes. This is bearing in mind the weight and other characteristics of the dishes as shown in Figure 5.1. It is with the aim of creating a suitable support balance for the parabolic dishes, good connections to other parts of the system and safety.

Table 5.1 The characteristics of the two parabolic dish systems in mathematical model.

Concentrator Dish	Dimensions (m)	Area (m ²)	Thickness (mm)	Focal length (m)	Weight (kg)
System(1)	1.25 × 2.4	3	3	1.25	25
System(2)	1.75 × 2.4	4.2	3	1.75	35

The dimensions and weights for both dishes system(1) and system(2) were fabricated previously, the final mathematical method consists of two parabolic concentrator systems (system (1) = 3m² and system (2) = 4.2m²) as mentioned in chapter two. The weight of systems 1 and 2 are 25 kg and 35 kg respectively, this gives a total weight of 60kg. This weight requires a robust physical base stand to be installed. Both dishes are positioned on a directional support considering the two axes to ensure the follow-up on the direction of the sun. For these reasons, a long stand was required to be designed and made from iron to protect the system and keep it at a particular high position.

5.3-Design Base Stand Suitable apparatus

Figure 5.1 and figure 5.2 – C are shows the design of the long base stands to take all internal and external devices. This stand can bear the weight of all designed parts including the parabolic dish concentrators. The dimensions of the stand are length = 8m , width = 5m and height 4.5 m which makes it easy to trace the sun and also take a suitable position in front of the sun. This iron stand as show in Figure 5.2 - A has ability to withstand the weight of more than 150kg and sits on four wheels for ease of movement from one place to another.

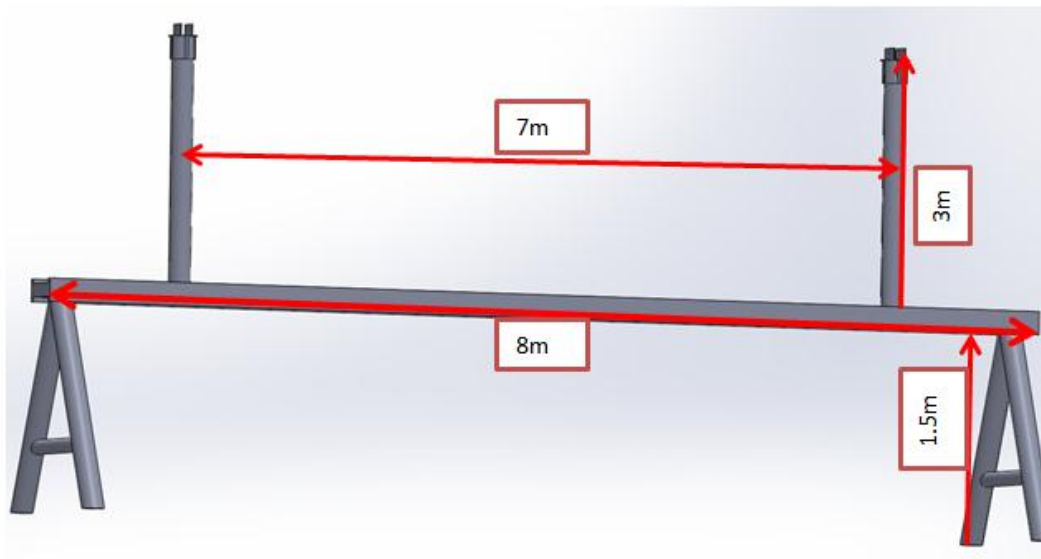


Figure 5.1 The solidworks design of long base stand made from iron

On the other hand, the intra-distance between both dishes on the stand is 8 m. This distance was sufficient to accommodate two parabolic dishes and the installed air compressor was located midway along the stand as shown Figure 5.2. The properties of parabolic dish base stand are given as follows:

- ❖ To be long enough for good balance of both dishes and sufficiently high from the ground for more safety and prevent damage.
- ❖ For easy tracking with sun (working with tracking system).
- ❖ To ease movement to anywhere (it has wheels).
- ❖ To have the ability to bear weight of more than 150kg.
- ❖ To have fixed position from strong wind.
- ❖ To allow for easy maintenance because fixed parts of the model are put in place for easy service.

The figure 5.2 - D shows the final design of novel system uses solidworks software, which it consists of parts as they are mentioned previously. Both parabolic concentrators in system were installed on the long iron stand, to be long enough for good balance of both dishes and sufficiently high from the ground for more safety and prevent damage.

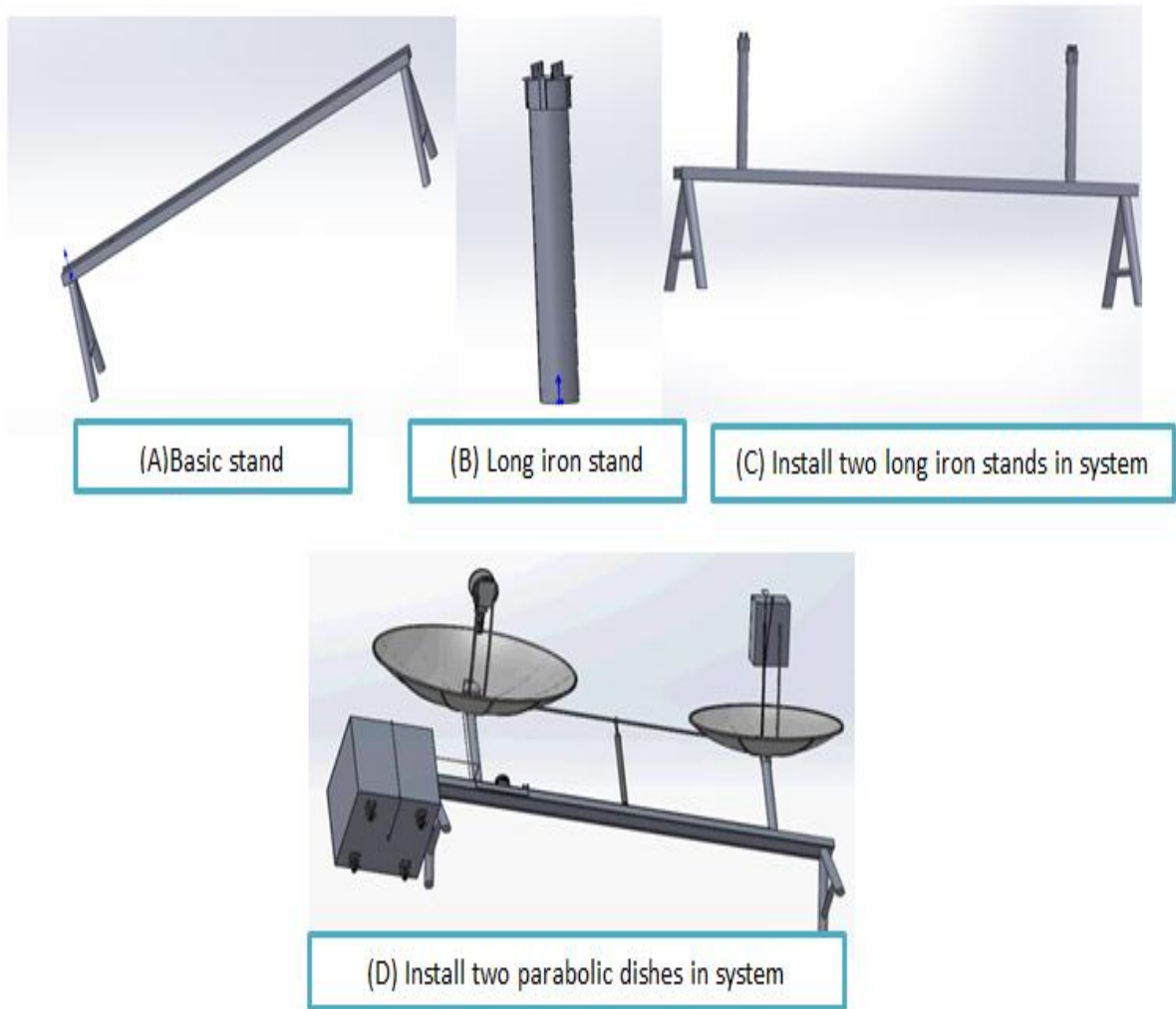


Figure 5.2 The final design of mathematical model by use solidworks software which (A) basic stand, (B) long iron stand, (C) Two long iron stands in system and (D) two parabolic dishes in system with stand

5.4-External Devices

The complete system was intended to operate at medium temperature (50°C – 400°C) and the heat pipe receiver was to transfer this heat to other devices. Hence, the parabolic dish concentrator was developed to accommodate this range of temperature and a feasibility study was performed to get the appropriate external devices. These external devices were thermoplastic flexible pipe (or solar thermal pipe), air compressor, T-thermal valves and thermal control system. All these devices were important for heat transportation from the thermal receiver to storage and from storage to hot space in hybrid engine.

5.4.1- Air Compressor

A gas compressor is a mechanical device that increases the pressure of a gas by reducing gas volume with constant temperature. This air compressor will be connected through a flexible pipe to the thermal receiver in the mathematical model. Helium gas was used as working fluid, it absorbs heat energy and also transport to other part of the system with the help of the compressor. This compressor system depends on pressure, temperature and gas volume inlet and outlet system. The refrigerator compressor was used and some changes were made to be used as air compressor or pump as shown in Figure 5.3. These changes allow the compressor to increase gas temperature and pressure. However, when heat energy was applied to the receiver, the temperature of the gas increases, this allows the compressor to increase the pressure and volume. The average velocity of the gas particles increases resulting in an increase in the rate of collisions and the average force per collision. The velocity of gas without air compressor was not enough to transfer heat receiver to storage or back to the Stirling engine, hence the use of air compressor was necessary.



Figure 5.3 A gas compressor which uses in system

On other hand, the compressor was common in solar application systems which were used in solar trough, solar tower, and solar chemical as well as solar hot water systems [3]. The three basic types of air compressors are reciprocating, rotary screw and rotary centrifugal. These are further specified by; the number of compression

stages, cooling method (air, water, oil), drive method (motor, engine, steam, and others), lubrication (oil, oil-free, where oil free means no lubricating oil contacts the compressed air) and packaged or custom-built. Figure 5.4 shows that air compressor was connected to the thermal control system, helium supply system and mass flow meter. The characteristics of this compressor within the system can be given as follows:

- ❖ It increases gas pressure up to 10 bar.
- ❖ It leads reduction of gas volume 0.162m^3 .
- ❖ It works with constant temperature at 250°C .
- ❖ Increases the gas mass flow rate of the helium 0.03 kg/s .

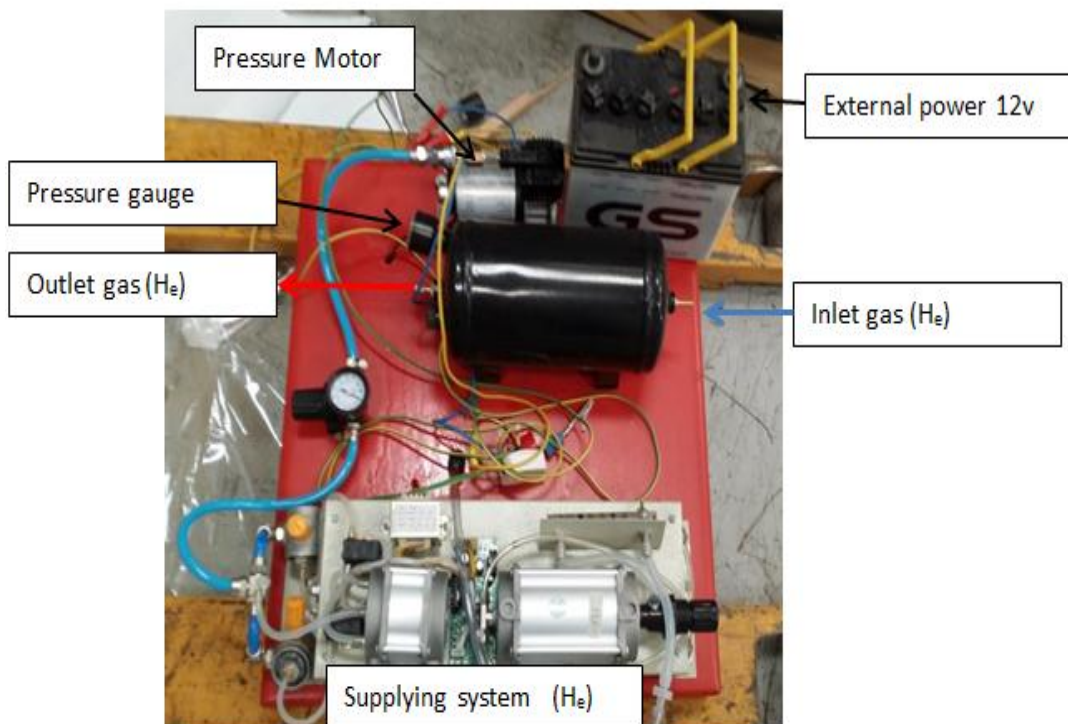


Figure 5.4 The air compressor connecting the thermal control system as well as helium supplying system.

5.4.1.1-Air compressor operation

In order to measure the helium mass flow after the compressor, the inlet volume flow rate and the inlet specific volume were used as given in equation 5.1.

$$\dot{m} = \frac{\dot{V}_{IN}}{v_{in}} = \frac{0.005 \text{ m}^3/\text{s}}{0.162 \text{ m}^3/\text{kg}} = 0.03 \text{ kg/s} \quad (5.1)$$

where ' \dot{m} ' is mass flow rate (kg/s) and \dot{V}_{IN} is inlet volume flow rate (m^3/s) and ' v_{in} ' is specific volume (m^3/kg) and up to 5 bar helium pressure. The work of the compressor can be determined using equation 5.2.

$$\dot{W} = \dot{m} (h_{in} - h_{out}) = \dot{m} C_p (T_{in} - T_{out}) \quad (5.2)$$

Where ' h_{out} ' is outlet enthalpy of helium, ' h_{in} ' is inlet enthalpy of helium, C_p is heat capacity at constant pressure, ' T_{in} ' is inlet gas temperature and ' T_{out} ' is outlet gas temperature in system. To measure out pressure helium of air compressor and temperature:

$$T_{out}(\text{Kelven}) = T_{in} + \frac{\dot{W}}{\dot{m} C_p} \quad (5.3)$$

The isentropic pressure for this outlet temperature and the given inlet conditions were found from equation 5.4 using k is ratio of heat capacity at constant pressure with heat capacity at constant volume which equal $k= 1.4$ which is for helium gas .

$$T_{out} = T_{in} \left[\frac{P_{OUT}}{P_{IN}} \right]^{\frac{k-1}{k}}, P_{out} = P_{in} \left[\frac{T_{OUT}}{T_{IN}} \right]^{\frac{k}{k-1}} \quad (5.4)$$

The properties of helium compressor used in current model are as follows:-

- ❖ It had separation so as bear high temperature.
- ❖ High outlet pressure (8.27 – 34.4 bar).
- ❖ Increase the velocity of gas.
- ❖ Low cost.
- ❖ Easy to install.
- ❖ Available and easy to get.

5.4.2-Stainless Steel Flexible Pipe

The most important technical problem encountered during the installation of the parabolic dishes system was the choice of the thermal pipe to use. This is because most of the existing pipes normally used for thermal technology lack the flexibility required when the tracking system was used.

It requires specific pipes which have this flexibility and can bear the required high temperature. The temperature of the medium used was expected to be approximately 250~350°C, passing through the heat pipe receiver as produced by parabolic dish concentrators. In view of the above, the pipe receiver must be able to bear high temperature and high pressure, be flexible, cheap in price and durable. This pipe was important because it was used to transport heat from copper pipe (in centre of receiver) to copper pipe in the thermal storage at the first stage. The second stage was transporting heat from thermal storage to Stirling engine as uses this engine to produce electricity. There are different types of thermal pipe used in solar thermal technologies as mentioned in the literature review as well as oil piping. But lately solar energy technologist preferred to use stainless steel flexible pipe which will also considered for use in this model. Stainless steel flexible pipe consists of three layers of high quality flexible stainless steel, EPDM- insulation, and thermoplastic polymer as shown in Figure 5.5.

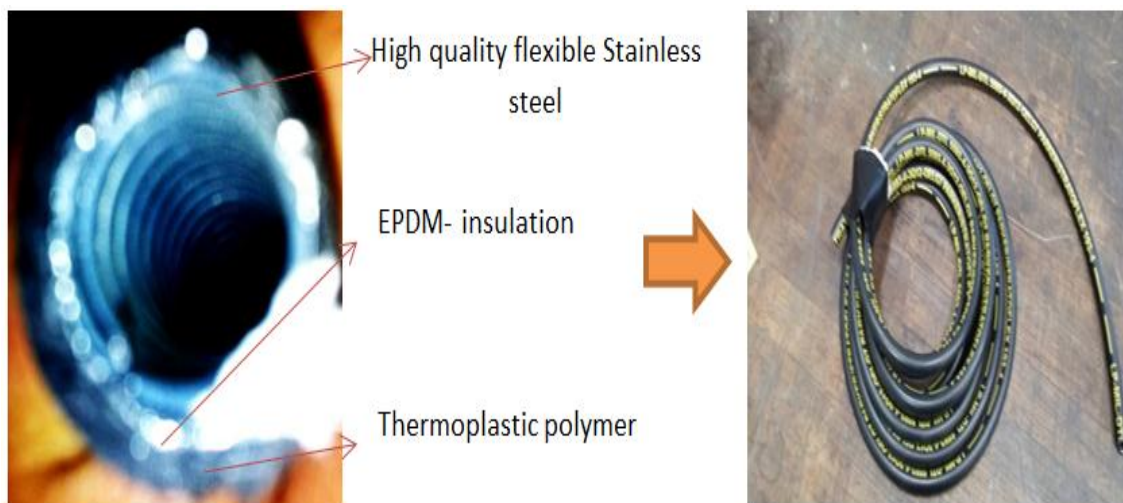


Figure 5.5 The high quality flexible stainless steel-pipes used in the mathematical model.

5.4.3-The Properties of Stainless Steel Flexible Pipe:-

This pipe was a 0.6 cm which easy to connect to the copper receiver pipe as shown in Figure 5.6. The overall flexible pipe length was equal in distance between thermal receiver to storage and distance between storage to engine which was approximately 15m (front / back). The thermodynamic properties of stainless steel flexible pipe include:

- ❖ Temperature rating around 1000°C.
- ❖ Max pressure 827.37 bar in 0.6 cm diameter.
- ❖ For severe hydraulic applications.
- ❖ Flexible.
- ❖ Easy cutting and installation.
- ❖ Available in exotic materials for even higher working pressures.

5.4.4-Thermal Valves (Y- Pattern Gas Ball Valves)

A valve is a mechanical device that controls the flow of fluid and pressure within a system or process. A valve controls the system with fluid flow and pressure by performing any of the following functions:

- ❖ Stopping and starting fluid flow.
- ❖ Varying (throttling) the amount of fluid flow.
- ❖ Controlling the direction of fluid flow.
- ❖ Regulating downstream system or process pressure.
- ❖ Relieving component or piping over pressure.

There are many valve designs and types that satisfy one or more of the functions identified above. A multitude of valve types and designs safely accommodate a wide variety of industrial applications. Regardless of type, all valves have the following basic parts: the body, bonnet, trim (internal elements), actuator, and packing. The basic parts of a valve are illustrated in Figure 5.6.A Y-thermal valve is a type of valve which also controls the flow of fluid and pressure within a system or process but in two directions and the actuator was required to direct the flow to the in any of the directions as shown in Figure 5.6.As mentioned in the design operations, there are two thermodynamic circles; one circle connecting parabolic dish concentrator (system 1) with thermal storage and the second circle connecting parabolic dish concentrator (system 2) also with thermal storage. In view of the above, both circles were linked together by Y- Pattern Gas Ball Valve as shown in Figure 5. 6-B and C.

The properties of Y- Pattern Gas Ball Valve are as follows:

- ❖ Easy to connect to stainless steel flexible pipe as shown in Figure 5.6- C.

- ❖ Bear high temperature up to 300°C.
- ❖ Max pressure up to 34.47 bar .
- ❖ Allows the exit that controls the flow of fluid and does not allow re-entry.

Furthermore, the model had two main closed cycles, the first works during the day (closed loop) which connects thermal receivers to air compressor to PCM-storage. The second works at night (closed loop) which was connected to PCM-storage to air compressor to heat exchanger.

On completion of the design and fabrication of both dish systems, these were fixed to the base stand and connected to the storage through the flexible pipe to the storage system. It is important at this stage to consider the choice of suitable materials for use on the current model and in the experimental section.

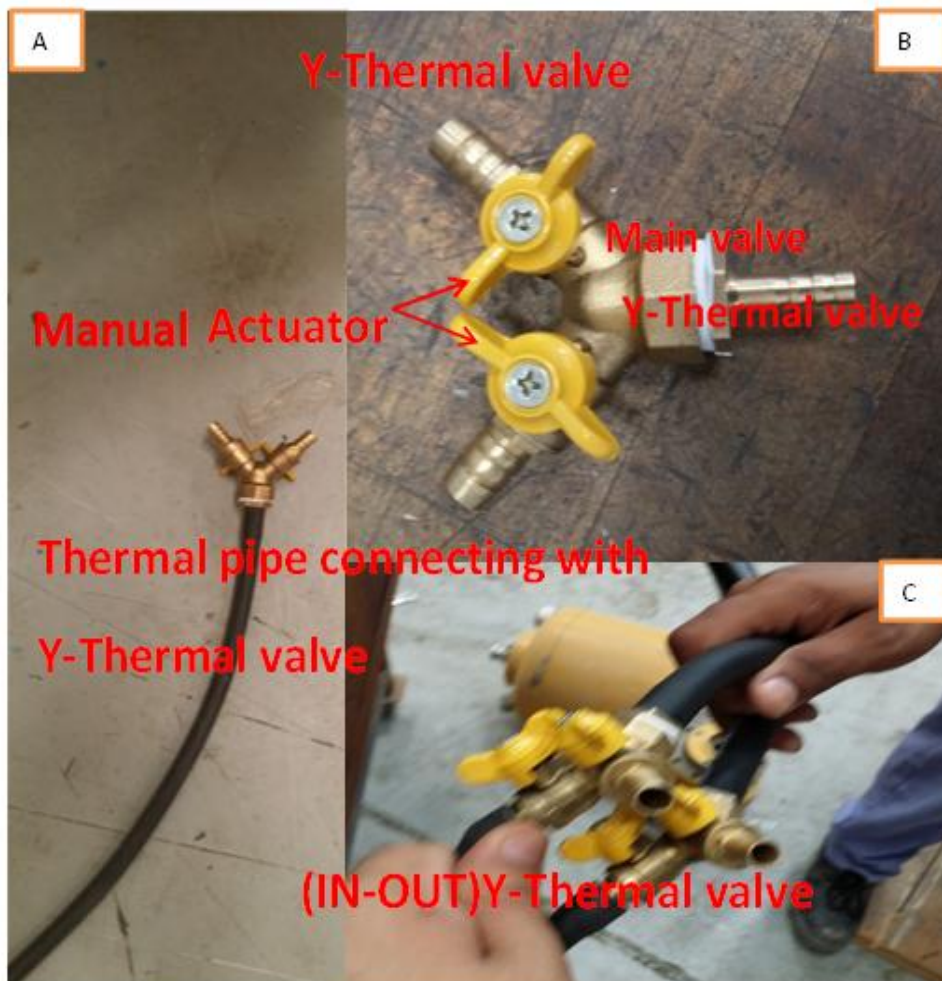


Figure 5.6 Thermal valves (Y- Pattern Gas Ball Valve)

5.5- Choice of other Materials for the mathematical model

This section focuses on the materials required to complete the model such as the sun reflector, working fluid, and phase change materials (PCM) for storage. These materials are so important in processes including reflection of heat, thermal conductivity; absorbing /transfer of heat and heat storage. There are varieties of options to make in obtaining the materials, but the compatibility with other parts of the system is important. In case of reflective materials, the use of highly efficient material with up to 98% efficiency, easy to cut to the required shape and aligned on the parabolic dish. The second material is the phase change materials required for storing heat. The material considered was mixture of $\text{KNO}_3\text{-NaO}_3$ which is a eutectic material in the following weight proportion (60% -40%). Helium gas is the third material with high heat capacity 5.2kJ/kg.K and thermal conductivity $3.9 \times 10^{-4}\text{kW/m.K}$ compared to many gas species. The price of helium is also affordable as it is obtained during natural gas extraction up to 10 bar.

5.5.1- Solar Reflector (98% reflective flexible mirror sheeting)

There are different reflector materials which can be considered in solar thermal technologies such as mirror, reflector silver mirror sheet and reflector colour and aluminium. However, each of these materials have a different reflector ratio. Presently high reflector material with 98% reflective flexible mirror sheeting was used in a California solar station; this was also adopted in the 'Solnova' solar power station in Spain [62, 63]. In addition, this sheet is lightweight, incredibly strong, easy to cut and as reflective as a normal glass mirror.

The Specifications reflective flexible mirror sheeting includes:

- ❖ High reflectance (> 98%).
- ❖ Uniform reflection in visual range.
- ❖ Ultra lightweight, adhesive.
- ❖ Abrasion resistant.
- ❖ Thermally stable.
- ❖ Low shrinkage.
- ❖ Maximum continuous use temperature up to 120°C .

- ❖ Excellent uniformity.
- ❖ Thickness range: 0.05mm to 0.5mm.
- ❖ Width range: 10m to 20m length.

The steps to install the flexible mirror sheet in both parabolic concentrator dishes in previous models are given below.

- ❖ '1st' Step, collect the parabolic dishes and clean surface as much as can.
- ❖ '2nd' Step, paint the parabolic dishes using 'Flash Liquid Paste Wax'.
- ❖ '3rd' Step, laying the flexible mirror sheeting on liquid paste wax.
- ❖ '4th' Step, remove air bubbles as much as possible.
- ❖ '5th' Step, paste the edges of parabolic dishes using extra strong paste as not be influenced by surrounding temperature and wind.
- ❖ '6th' Step, the final shapes both reflector dishes are presented in the photograph as shown in Figure 5.7.



Figure 5.7 Both dishes are covered by 98% reflective flexible sheet

However, the main problems associated with the stages of installing flexible mirror sheet in both parabolic concentrator dishes in the model was air bubbles. These air bubbles deflect sun rays away from the focus point of the system. It is important to remove these bubbles as much as possible and it is obvious this cannot be completely removed. After installation of the flexible mirror sheet in both parabolic concentrators the next phase is to focus on phase change materials.

5.5.2-PCM Molten Salt Composition ($\text{NaNO}_3 + \text{KNO}_3$)

The material considered for the PCM was $\text{KNO}_3\text{-NaNO}_3$. Inorganic – inorganic PCM have thermal properties of salt hydrates including high latent heats of fusion and good in heat transfer properties compared to organic materials and relatively cheap. But there are two setbacks as it suffers from segregation and sub-cooling. This section will consider the choice of $\text{NaNO}_3 - \text{KNO}_3$ as phase change material in the storage system of the prototype model and test the material at different temperature levels. Another common problem with storage system as reported is the issue of corrosion. The present model intends to consider preventing the occurrence of this problem in the current model.

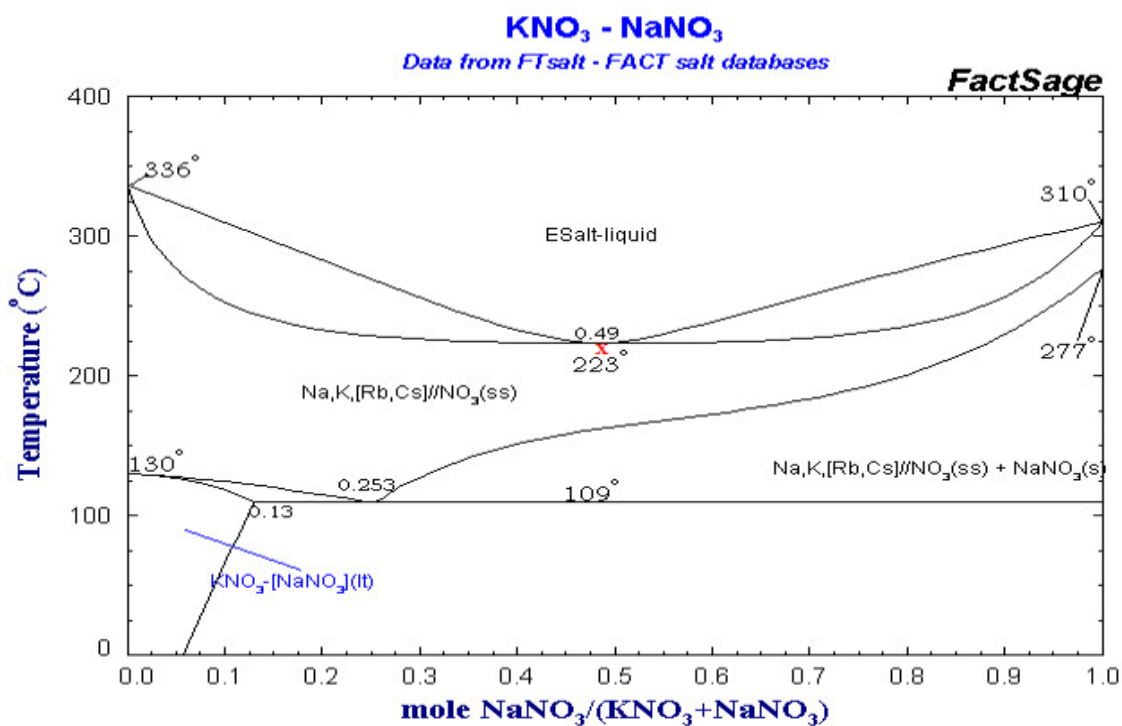


Figure 5.8 The plotting obtained results on phase diagram of $\text{KNO}_3 - \text{NaNO}_3$ [61].

The Figure 5.8 shows phase change diagram for chemical system ideates of KNO_3 - NaNO_3 mixed with the different moles. The weights of the mixture components collected; how many moles of materials \times weight of each mole of same material (g/mol) = weight of monomer gram. If consume, the total mixture KNO_3 and NaNO_3 is 3690 g + 2460 g = 6150 g, and the weight ratio of KNO_3 to total mixture is 3690g/6150g = 60 % and NaNO_3 is 2460 g/6150 g = 40 %.

As mentioned in section 4.8, the Thermo-physic properties were mixed between KNO_3 and NaNO_3 with melting temperature of 222°C as shows in Figure 5.8, enthalpy of fusion 100 kJ/kg, low density change 4.6% (solid – liquid), no or little sub-cooling, chemically stable and no phase segregation. All these properties are good physical characterization which perfectly suits our need in thermal storage produced. The completed storage system expands about 70kg from materials used for storage. However, it is expected when using KNO_3 - NaNO_3 as PCM-storage to have a total storage of 7kW as well as melting temperature with same operating temperature.

One piece of this material 2g weight and 5 mm in radius absorbs heat and changes from solid to liquid phase at moderate pressure. With heat in the system, salt nitrite corrosion occurs within the iron wall of the storage container, this phenomenon affects the process of charging and discharging heat in the system. To solve this problem, a hollow sphere was designed from inside and filled with KNO_3 - NaNO_3 as PCM-storage as shown in Figure 5.9. Figure 5.9 -A and B shows small balls from PCM which were located inside the storage and surrounded by copper pipe as heat exchanger. Also Figure 5.9-D, F and G shows the hollow sphere designed from inside filled with KNO_3 - NaNO_3 as PCM-storage material. On the other hand, the mixed storage materials KNO_3 and NaNO_3 were also tested as described in more details in chapter 7.



Figure 5.9 Phase Change Materials $\text{KNO}_3\text{-NaNO}_3$ (60/40) % suitable storage through (out and in) iron balls

5.5.3-Working Fluid (Helium)

This section discusses helium as working fluid in the hybrid solar thermal model with Stirling-cycle engines and other parts of the system as shown in Figure 5.10. The objective is to provide a new and improved family of thermodynamic working fluids for the hybrid system and Stirling-cycle, reciprocating, thermal machines, other than the usual hydrogen, helium or air.

These hybrid Stirling engine also possess increased dynamic heat transfer coefficients, the novel engine is known as a close cycle regenerative thermal machines, and family of thermodynamic working fluids mentioned above and many others are suitable for application for such machines.

The working fluids of the hybrid solar model are specifically selected considering:

- ❖ High dynamic heat transfer coefficient, as defined by known empirical relations for heat transfer in turbulent flows.
- ❖ Requisite thermo-physical properties such as chemical inertness and thermal stability.

They are known to be improved agents for use in all heat engines which embody a practical approximation to the well-known Stirling thermodynamic cycle and which are employed in the production of both mechanical power ('i.e., prime movers, compressors), fluid pumps' and refrigeration ('i.e., refrigerators, air conditioners, heat pumps, gas liquefiers').

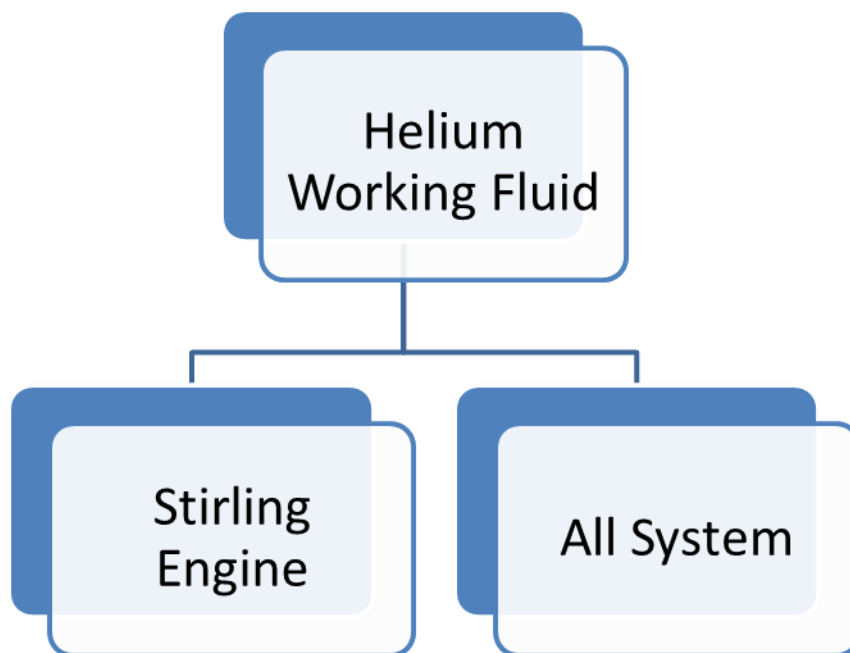


Figure5.10Processes of Helium in Current Model

Helium has many unique properties which includes low boiling point, low density, low solubility, high thermal conductivity, and inertness, so it is ideal for use in any application which intend to exploit these properties. Helium was the first gas used for

filling balloons and dirigibles. This application was used in altitude research and for meteorological balloons. The main use of helium is as an inert protection gas in autogenously welding. Its biggest potential was found in its applications at very low temperatures. Helium is capable of reducing system temperatures, but that is not sufficient to control the gas temperature within the system during expansion and compression. In view of this, water as a cooling fluid was used outside the system in addition to the helium in order to control this temperature.

5.5.3.1-Thermodynamic Properties of Helium

Helium uses as working gas in thermal operations in model; it has a high heat capacity and thermal conductivity compared to many gas species. The price of helium is also affordable as it is obtained during natural gas extraction. During the analysis, the following assumptions were made:

- ❖ It is one of the noble gas families.
- ❖ The helium specific heat is considered constant.
- ❖ The turbine and compressor processes are isentropic.
- ❖ The solar field and air-cooled heat exchanger processes are isobaric.
- ❖ The heat exchanger and heat storage tank flows are fully developed, turbulent flows.
- ❖ No known health hazards resulting from exposure to helium.

Table 5.2 The properties of helium gas with different pressures [62, 60]

	Helium			Air
Operation Temperature (T) [°C]	478	332	293	27
Pressure (P) [MPa]	1	6.9	2.55	1
Density(ρ) [kg/m ³]	0.56	3.75	2.16	1.177
Viscosity (μ) [kg/m.s]	5.017×10 ⁻⁵	4.2×10 ⁻⁵	3.08×10 ⁻⁵	1.845×10 ⁻⁵
Thermal Conductivity (K) [kW/m.K]	3.9×10 ⁻⁴	3.3×10 ⁻⁴	2.4×10 ⁻⁴	2.624×10 ⁻⁴
Specific Heat (C _p) [kJ/kg.K]	5.2	5.2	5.2	1.0049

The table shows the properties of helium at different operating temperature and pressure as well as comparing properties of helium gas with air at low pressure ~ 1 bar and temperature at 27°C.

5.5.3.2- How helium works in the system

Initially, helium gas was supplied in copper pipe (0.95cm,15m length) into the thermal receiver with the valves working to restrict the movement of the He gas in only one direction (in-front).However internal gas will be pressed by initial pressure, as the gas absorbs reflected heat with increase in pressure of the (He) gas and also increases gas velocity.

During the daytime, helium gas works in order to absorb and transport heat from thermal receiver to compressor and to PCM tank. Helium in the storage cycle is heated in the solar field and then charges the PCM tank. The helium gas leaving the heat storage tank was compressed by the low ratio compressor and enters the solar field again to finish the thermal storage cycle. This compressor is only needed to pump the gas through the solar field and storage tank. This cycle can be shut down after the PCM was completely melted, indicating a full heat charge. On the other hand, helium gas in system (1) can directly generate power by expansion and compression in hot Stirling space as discussed in chapter three.

At night, there was no more energy coming from the parabolic dish concentrator but the heat stored in the PCM-tank was used as the second heat source, which was supplied to the engine. Since the sun was not available at night and temperature of 'He' gas was less than the engine operating temperature,hence'He' gas will be supplied from the reservoir PCM-tank not from parabolic dish concentrator.

In all the process above, the exchange gas and heat exchanger plays a vital role in heat transfer in both day and night for both systems. The functions of the gas and heat exchanger are given as follows:

- ❖ Exchange gas: The exchange gas is non-condensable fluid at the operating temperature when introduced, and then pumped away once the operating temperature increases and this also increases the heat transfer process. This eventually increases the amount of heat stored in the PCM.

- ❖ Heat exchanger: is a thermodynamic device which can transfers heat from one working fluid to other. Heat exchangers in general are used to facilitate the movement of generated heat to different part of the system using the exchange helium.

In novel model will uses heat exchanger located in front of hybrid Stirling engine to transfer heat by conduction through the exchanger materials (thermal oil) which separate the mediums a tube heat exchanger passes fluids through and over tubes to hot space of Stirling engine.

5.6-Conclusion

This chapter discussed the design and construction of the PCM-storage, and the process of installation of external devices. It was shown the total weight of both parabolic dishes was 60kg for both dishes; hence the base stand was necessary. This stand was made from iron, designed and fabricated, placed at elevated position to ensure the dishes were firm, secured and have the flexibility of tracking the sun at different directions.

Furthermore, this chapter described the external devices, which were needed to complete the gas cycle inside the model. These devices include air compressor, stainless steel flexible pipe, and thermal valve (Y-pattern gas ball valve). The properties of these devices are important as are required to work with high temperature up to 100°C, for heat charging and discharging of the thermal storage as well as heat space of the engine.

All these devices had specifications of high thermal quality for heat transfer at high pressure, high conductivity and high melting temperature. Flexible pipe was easily connected with copper pipe in thermal receiver and have good thermal specifications such as heat absorption and heat transportation. Air compressor compressed helium gas through the flexible pipe by mass flow up to 0.03kg/s which can be controlled by thermal valves. The Y-valves in the system allows fluid flow and pressure by performing any of the following functions; stopping and starting fluid flow, varying (throttling) the amount of fluid flow, controlling the direction of fluid flow, regulating downstream system or process pressure and relieving component or piping over pressure.

The flexible mirror sheeting was reflective up to 98%, and it was easy to lean on the wall of parabolic dish, but had some disadvantages including presence of air bubbles which was eliminated.

Furthermore, $\text{KNO}_3\text{-NaNO}_3$ was used as phase change materials in the storage models which would be used to test these materials at different temperature level in chapter 7. Thermo-physic properties of the mixed gases between KNO_3 and NaNO_3 had a melting temperature of up to 222°C , enthalpy of fusion 100 kJ/kg , low density change of 4.6% (solid – liquid), no or little sub-cooling, chemically stable and no phase segregation. The storage materials manufactured can expand to around 70kg from materials used for storage. And material was expected to store a total of 7 kW as well as the melting temperature at same operation temperature. Salt nitrites detected corrosion when the PCM was in the process of melting; the mathematical model was designed to compensate for the corrosion during heat operation.

Helium gas has a high heat capacity and thermal conductivity compared to many gas species, the price of helium is also affordable as it is obtained during natural gas extraction. Helium gas works in order to absorb and transport heat from thermal receiver to compressor and to PCM - tank. Helium leaving the heat storage tank was compressed by the low ratio compressor and enters the solar field again to finish the thermal storage cycle.

As mentioned before, both parabolic dishes must have tracking system, which track the solar radiation; this must be considered appropriately in the design and fabrication in the final model.

CHAPTER(6):- Construction of a Solar Tracking System in Research System

6.1- Introduction

The main objective of this chapter is to discuss the solar tracking system, installation of different parts of the system and give a detailed description of how the system works. The design of the tracking system is to compliment the external and internal parts of the final model as discussed in the previous chapter.

Solar tracking system is a mechanical device used to get the orientation of any type of solar system with the sun's position. Solar powered equipment works best when pointed at or near the sun, so a solar tracker can increase the effectiveness of such equipment over any fixed position, at the cost of additional system complexity. There are many types of solar trackers, of varying costs, sophistication, and performance. Some of it moves in one-direction and others move in multiple-directions.

However, a parabolic dish tracker system moves from east to west at day in order to track the sun rays. This tracking device only functions when the sun ray's been available and stops working by reversing to its original position when the sun isun available. Hence, there was need for the design of the tracker system to be compactable with the system.

Assembling the final equipment involved linking all the parts together including the parabolic dish concentrator and dishes with an air compressor, compressor with PCM-Storage and PCM-Storage with dishes by fixable pipes. Finally, a detailed description on how the final system works, with two dynamic gas (helium) cycles within the whole system and a small close circuit through the Stirling engine component are discussed.

6.2-Solar Tracking System

The solar concentrator system depends on sunlight, since the sun moves at different times, the design and fabrication of the best tracker system for the model was necessary. In general, there are two main tracking systems depending on the axis of

movement: single-axis tracking, and two-axis tracking and details are listed in Table 6.1. Hence, more information relating two types of tracking system will be seen most clearly in the context in next section.

Table 6.1 Solar tracking systems used in solar thermal technologies [91]

Motion	Collector	Absorber type	Concentration ratio	Indicative temperature range(°C)
Single –axis tracking	Linear Fresnel reflector	Tubular	10-40	60-250
	Cylindrical trough collector	Tubular	10-50	60-300
	Parabolic trough collector	Tubular	10-85	600-400
Two –axis tracking	Parabolic dish concentrator	Focal point	600-2000	100-1500
	Heliostat concentrator	Focal point	300-1500	150-2000

6.3-Review of solar tracking system

The parabolic dish (concentrator) was used to reflect and concentrate the sun's rays onto the receiver aperture so that the solar heat can be absorbed by the receiver. The heat is then transferred by the working fluid to the thermal storage or direct to the Stirling engine. However, to ensure that the solar radiation stays focused on the receiver throughout a typical day, a tracking system must be used. Different researchers reviewed different types of sun-tracking systems with their advantages and disadvantages [52,50].

The variation of the sun's position moving from east to west with respect to time, season and position is illustrated in Figure 6.1. These variations need a control system to track and variation position of the solar concentrator with respect the position of the sun. Such as system is called a solar tracking system; the device is often used to maximize the amount of solar radiation that reaches the solar converter. However, the Stirling engine, feasibility, usability and effectiveness of solar technology are directly dependent on the amount of solar radiation that can by

focused on thermal receiver. For this reason, an extensive investigation on the different types of solar tracking was conducted and the appropriate tracking system was chosen for the experimental model in this work.

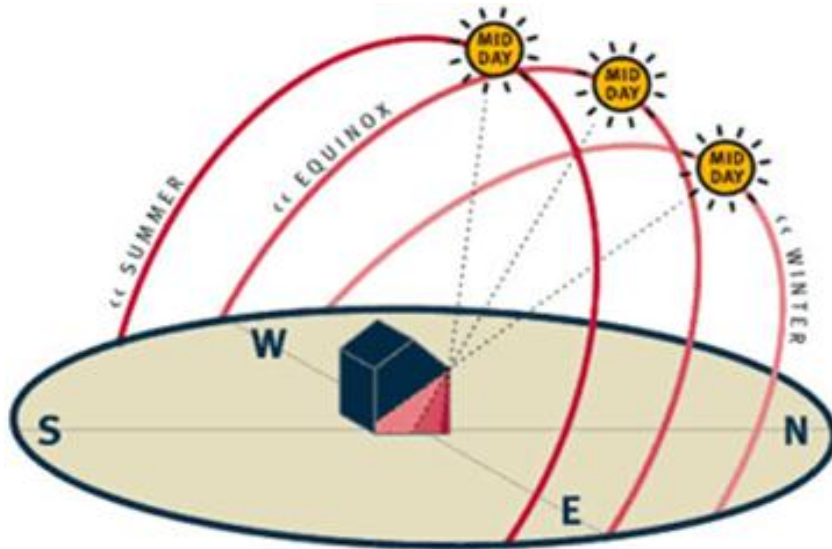


Figure 6.1 The sun's positions during the day and year [91]

6.4-Solar Angles

Normally, the solar position at any time during the day changes and can be described by two angles; altitude angle (α) and azimuth angle (a_s). The solar altitude angle (α) is the angle between the sun's rays and the horizontal plane as shown in Figure 6.2. The azimuth angle (a_s) is defined as the angle between the south axes (s) and the horizontal projection of the line joining the site in consideration and the sun (It is taken to be positive westward). The two main angles are depicted in Figure 6.2. In addition, the solar zenith angle (z) which is given by the angle between the site to sun line and the vertical at the site location can be obtained using equation 6.1.

$$z = 90 - \alpha \quad (6.1)$$

However, the solar angles are not fundamental angle of any project. The information at any point where tracking is required is its location, the time of day and year.

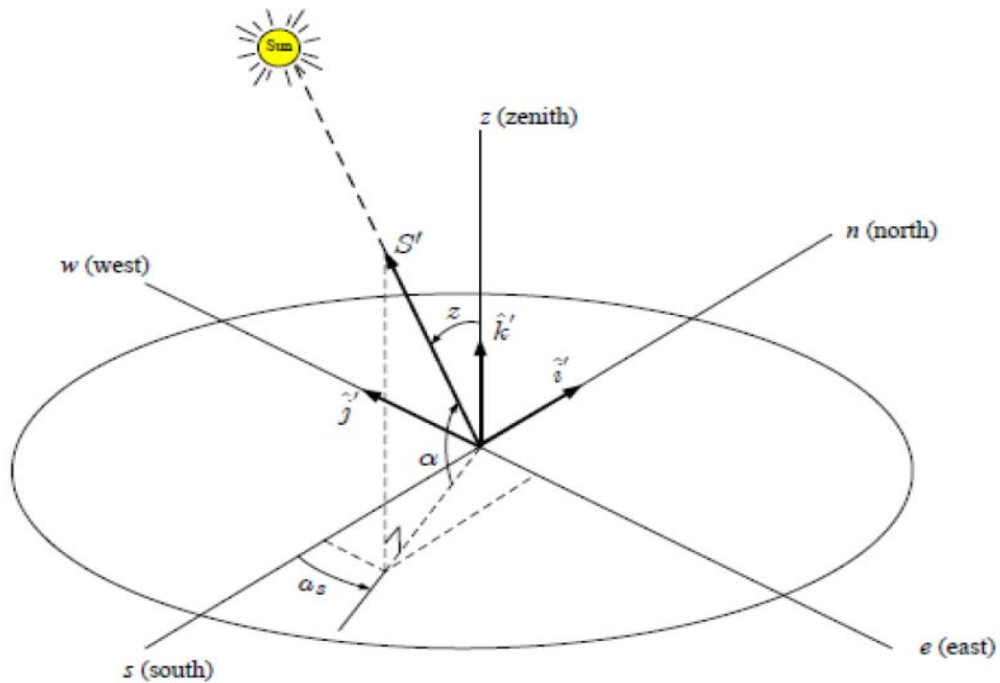


Figure 6.2 Solar angles; altitude angle (α) and azimuth angle (a_s) in solar system [81]

This information can be expressed in the form of three fundamental angles as follows:

6.4.1- The hour angle (h_s)

The hour angle (h_s) is based on the fact that 24 hours correspond in to the sun's rotation of 360° degrees around the earth, which means it moves (15°) in one hour [2]. The hour angle was obtained using equation 6.2.

$$h_s = 15 (t_s - 12) \quad (6.2)$$

where (t_s) is the solar time in hours, which it is related to the local time by the following expression:

$$t_s = t + EOT + (I_{st} - I_{Local})4(\text{min/degree}) \quad (6.3)$$

where (I_{st}) the standard time meridian (I_{Local}) is the local time meridian and EOT is the Equation Of Time which is an empirical expression that accounts for the rotational

speed of the earth. Hence, for more information related the empirical expression will found it in references [].

6.4.2- The latitude

The latitude angle(L) is the angle between the line from the centre of the earth to site and the equatorial plane. It is taken to be positive north of the equator and shown in the Figure 6.3.

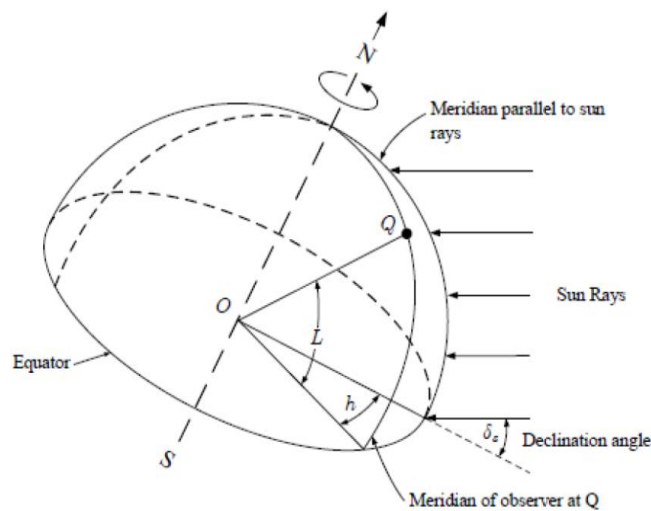


Figure 6.3 The latitude angle (L) [93]

6.4.3- The declination angle

The solar declination angle ' δ_z ' is the angle between the earth-sun line (through their centre's) and the plane through the equator. It varies throughout the year and is given by the following function.

$$\delta_z = 23.45 \sin(360 / 365(284 + N)) \quad (6.4)$$

where 'N' is the number of the day in the year and as shown in the figure below where this angle has the value of (23.45°) in June 21.

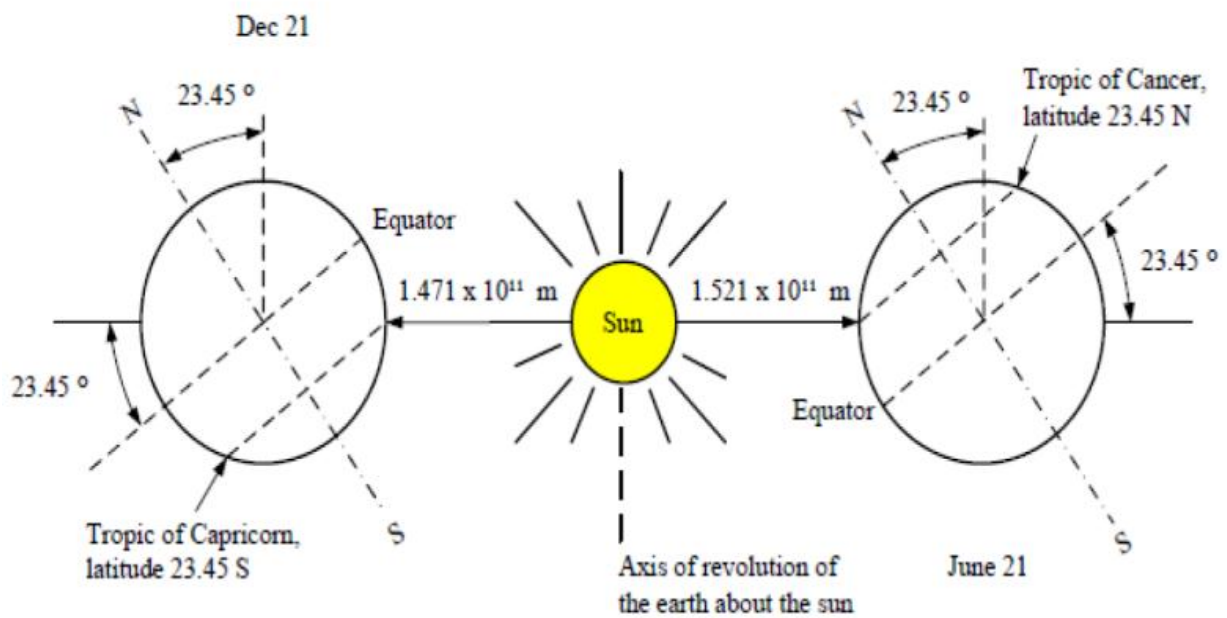


Figure 6.1 Solar declination angle [92]

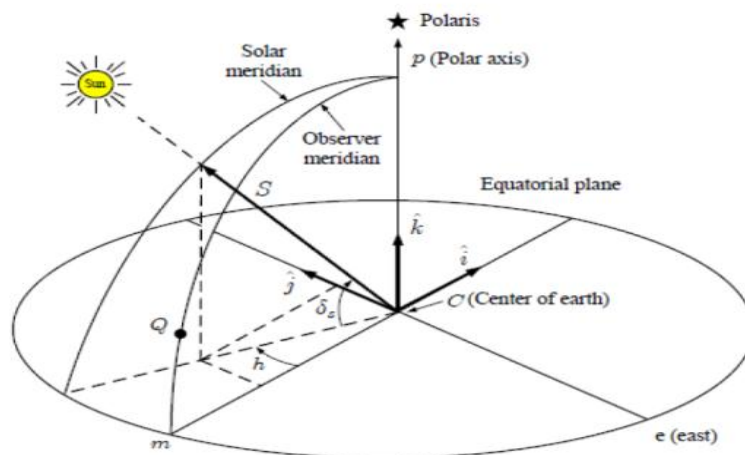


Figure 6.5 The fundamental angles with respect to vector (S) along the solar beam direction [92,93]

6.4.4-Fundamental Angles

It is important to express the solar angles discussed in the previous section, altitude angle (α) and azimuth angle (a_s), and relate to the three fundamental angles including hour angle (h_s), latitude angle (L) and declination angle (δ_z) as shown in Figure 6.5. This fundamental angle in respect to the vector (S) along the sun's direction; and it can be seen that the two coordinate systems are related by the rotation around the East-axis and a conversion along the earth's radius.

Moreover, it is understandable that the solar radiation depends on the 'cosine' of the incident angle in each location. This means, our main task in solar tracking system is to minimize this cosine and increase the system efficiency. In view this, the Oman location was considered based on the fundamental angles, and also principles of trackers. This is to allow for further analysis of how to achieve the best tracking system for application for both dishes and suitable for the final system. Hence, the sultanate of Oman occupies the South – Eastern corner of the Arabian countries and located latitudes $16^\circ 40'$ and $26^\circ 20'$ North and Longitudes $51^\circ 50'$ and $59^\circ 40'$ East [81].

6.5-Solar Tracker Types

The beam radiation on a tracking surface is maximized by orienting the surface, within the constraints of the tracking apparatus, so that the solar radiation incidence angle is minimized. The incidence angle is the angle between a ray from the sun and the normal to the surface. Many researches were provided expressions for the incidence angle in terms of the surface tilt and azimuth angles for fixed-tilt, and for optimally tracking one and two-axis surfaces[86]. Today, there are many solar tracking systems used in different solar thermal technologies. The systems can be divided into two main types depending on the axis of movement. The first type is the single-axis movement such as polar, horizontal and vertical. Second type is the double-axis movement (two-axis) such as altitude–azimuth, horizontal and vertical–axis, any of which may be active and passive trackers as shown in Figure 6.6.

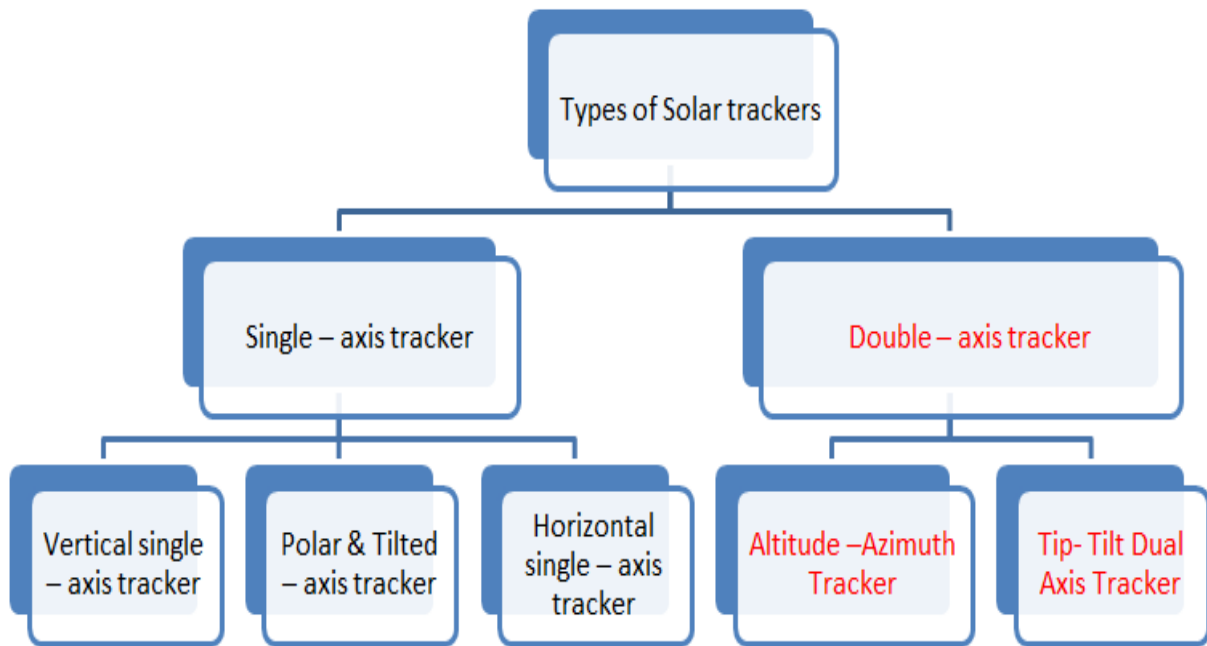


Figure 6.6 Types of Solar trackers which used in solar concentrators [85]

6.5.1-Single Axis Trackers

Single axis tracking is a drive system which rotates the collector body about one axis of rotation until the central beam and the aperture are coplanar. It has one degree of freedom that acts as an axis of rotation. The axis of rotation of single axis trackers is typically aligned along a true north meridian. It is possible to align them in any cardinal direction with advanced tracking algorithms. This kind of tracking system was commonly used in 'PV' and heliostatin solar tower. In 1990, mutation occurred in single axis tracking where designed, developed and introduced the 'Max Tracker PV System' as single-axis tracker with the potential for low cost and high reliability [77]. This simplified design uses a simple mechanical easy to track more than 200 kW of 'PV' with a single motor, driver and controller assembly. This simplified design results in higher energy capture at a similar cost to a fixed array. With the potential for (15% to 35%) improvement in energy production, the introduction of a cost-effective tracking technology facilitated the development of utility-scale PV systems [78].

Today, its introduction to the market and over 110 MW of trackers have been installed worldwide [73]. It is not possible to use single axis tracker in the current model, as it moves in only one direction.

6.5.1.1- Horizontal Single Axis Tracker

First type of single axis tracker is called horizontal single axis tracker, (HSAT) has horizontal axis of rotation with respect to the ground and is illustrated in Figure 6.7.A. The benefit of this design is to support tracking system position at either the end of the axis of rotation of a horizontal single axis tracker or rotates from East to West during a day. Also, this type of tracker when used in a system reduces the overall cost as it is very economical and readily available.

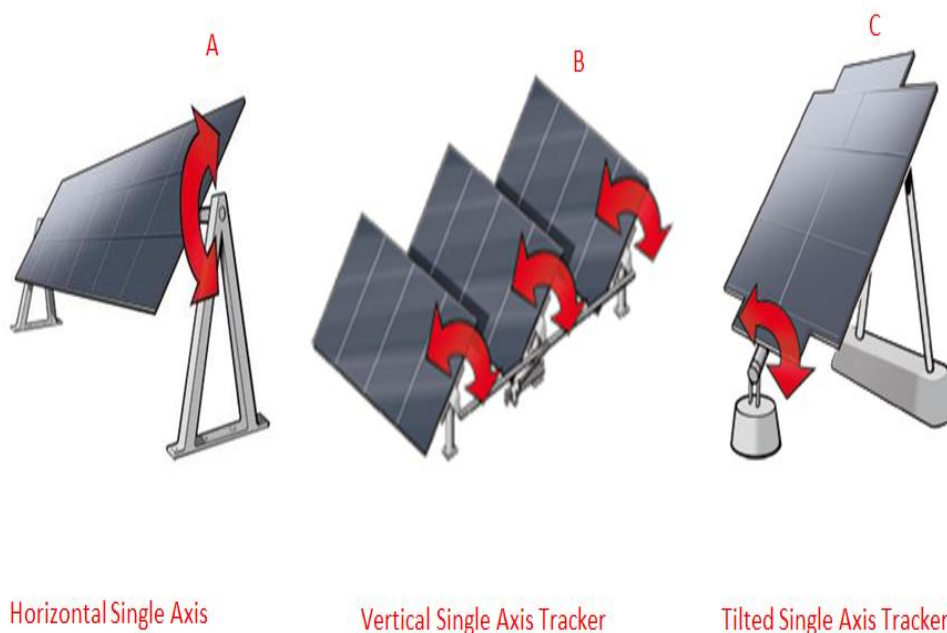


Figure 6.7 Single axis trackers (A) Horizontal single axis, (B) Vertical single axis tracker and (C) Tilted single axis tracker [83]

6.5.1.2- Vertical Single Axis Tracker

Another type of axis rotation is the vertical single axis trackers (VSAT) with respect to the ground as shown in Figure 6.7-B. These trackers rotate from East to West over the course of the day. Such trackers are more effective at high latitudes than the horizontal axis trackers. One of the tracking systems can be used for multiple sheets: hence field layouts must be considered in order to avoid unnecessary energy losses.

6.5.1.3- Tilted Single Axis Tracker (TSAT)

The third type in this class of trackers is the tilted single axis trackers. When compared to previous trackers, its axes of rotation are between horizontal and vertical

and is considered tilted single axis trackers with tilt angle. This angle is between solar radiation and the body of the system sheet, it changes with the season. When this type of tracker was used, the effect of wind speed is often reduced and it is less expensive to acquire. Figures 6.7-C and 6.8 show typical TSAT with 15° change between summer and winter. Hence, this tracking system is not compatible with the current model.

6.5.2-Dual Axis Trackers

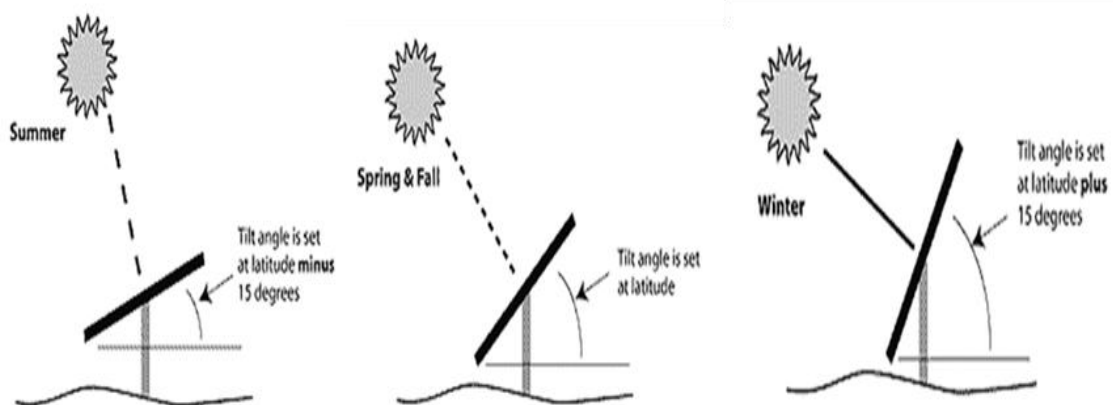


Figure 6.8 Tilted Single Axis Tracker in summer, winter, spring and fall [84]

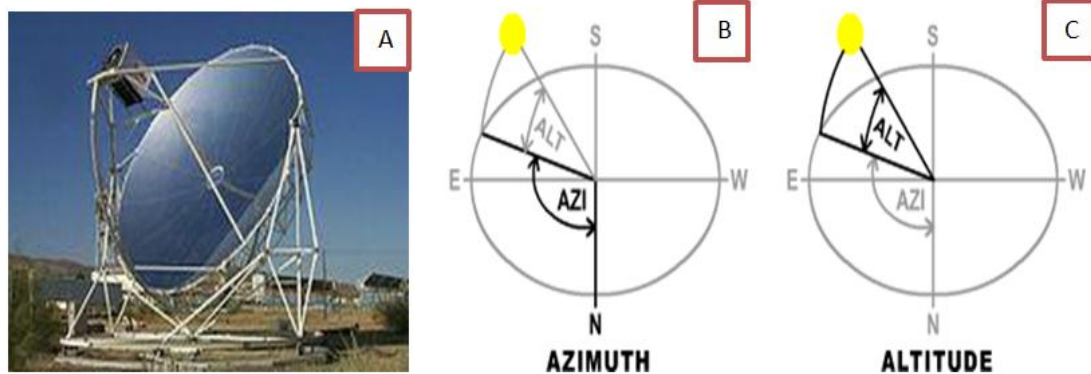
Dual axis trackers have two degrees of freedom that act as axes of rotation. These axes are typically normal to one another. The axis that is fixed with respect to the ground can be considered a primary axis. The axis that is referenced to the primary axis can be considered a secondary axis. There are several common implementations of dual axis trackers and these are classified by the orientation of their primary axes with respect to the ground. There are two common types which are discussed subsequently.

6.5.2.1- Tip – Tilt Dual Axis Tracker (TTDAT)

A Tip–Tilt dual axis tracker has its primary axis horizontal to the ground. The secondary axis is then typically normal to the primary axis. The axes of rotation of (Tip – Tilt) dual axis trackers are typically aligned either along a true north meridian or an east west line of latitude. It is possible to align them in any cardinal direction with advanced tracking algorithms.

6.5.2.2- Azimuth-Altitude Dual Axis Tracker (AADAT)

An Azimuth-Altitude tracker is shown in Figure 6.9-B and C, the dual axis tracker has its primary axis vertical to the ground. The secondary axis is then typically normal to the primary axis. Field layouts must be considered in its application to avoid unnecessary energy losses. By using combinations of the two axes, any location in the upward hemisphere may be adopted. Such systems may be operated under computer control depending on the expected solar orientation, or may use a tracking sensor to control motor drives that orient the panels toward the sun. This type of tracker is also used to orient a parabolic reflector that was mounted on a Stirling engine to produce electricity as shown in Figure 6-A.



Parabolic dish technology with tracking system

Figure 6.9 Solar parabolic dish system, different azimuth angle and altitude angle [83]

6.6- Solar Tracking Dish Systems

Solar dish systems consist of a dish-shaped concentrator (like a satellite dish) that reflects solar radiation onto a receiver mounted on a focal point at the centre, as shown in Figure 6.9. The dish rotates on two axes to track the sun during the day. Dish systems can often achieve higher efficiency than parabolic trough systems partly because of the higher level of solar concentration at the focal point. Dish systems are said to be more suitable for stand-alone small power systems due to their modularity.

The sun position fluctuates due to its movement from east to west with respect to time, season and position. These fluctuations need a control system to track and

move solar concentrator with sun. This system is called solar tracking system, and the device is often used to maximize the amount of solar radiation that reaches the solar converter. However, the Stirling engine feasibility, usability and effectiveness of solar technology are directly dependent on the amount of solar radiation that can be focused on thermal receiver. For this reason, an extensive investigation into different types of solar tracking system was conducted and the appropriate tracking system chosen for the model.

6.7-Design and Construction of Solar Tracking System

6.7.1- Design of Solar Tracking System using Solidworks

Both parabolic dish concentrators' moves with sun during the process of power production, the movement of the dishes are influenced by the tracking system. This system has two axes of movement that can independently track the altitude and azimuth motion of the sun. Figure 6.10 shows the mount system used for both dish systems (1, 2). In the centre of dishes, there is gas struts which moves both dishes up - down and keep it in same position, and this gas strut connects with computer system for control.

As the gas struts moves up and down, the azimuth pivots marked (A_1 , A_2) follows the east-west movement of the sun throughout the day which moves both dishes. These pivots are made from 0.1-0.2 cm thick steel L-brackets that are 0.1 cm wide. The azimuth pivots are controlled by a linear actuator which is mounted to the altitude pivot under the point marked " B_1 , B_2 ".

The altitude pivots (A_1 , A_2) follows the north-south movement of the Sun which was made from 0.2cm square sheet that is 0.1cm wide, with 1.3cm steel plates extending up to the end of the 2.5m tubing. The altitude pivot is mounted on the zenith pivot marked " B_1 , B_2 " which is normally stationary and bolted tight on the dishes. This section has ability to rotate around the zenith axis to align with the south to north celestial during the time of the season.

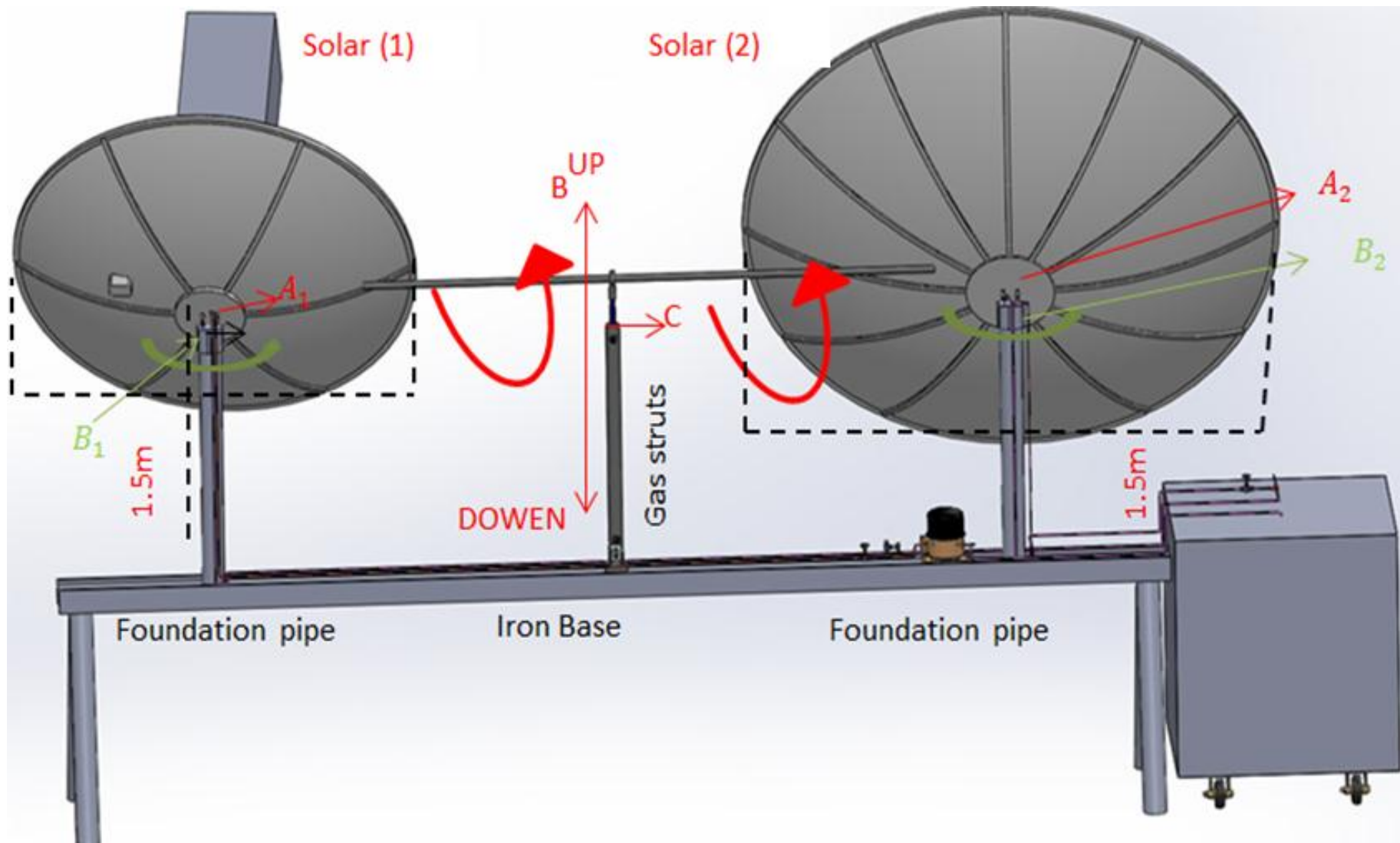


Figure6.10The current prototype showing direction of movement and gas struts.

Both zenith pivots are made from 0.2cm steel plates and welded to a sleeve cap which fits over a 12.7cm nominal steel pipe. This steel pipe is bolted by three 1.6cm bolts to the 15.2cm nominal steel foundation pipes. The foundation pipes are 1.5 m above a 9cm deep concrete which was welded on iron base. The base rail is designed to handle the forces and moments of 1.95m and 2.76m diameter dishes with up to 49 m/s wind speed.

6.7.2- Fabrication of Solar Tracking System for Prototype

The total weight of each of the parabolic dish as mentioned earlier was approximately 35kg. For this reason, a bicycle chain was used and linked with parts of parabolic dish using series of bicycle chain as shown in appendix 6.1.



Figure6.11 Solar hour's sensor

The sun sensor was used which was placed on the parabolic dish and connected to the computer system as well as the machine in the system. The sensor is a two axis device, which measures the sun location relative to its optical axis based upon the relative signal obtained in a quadrant silicon detector. This was based on which a circular spot generated by the sun's irradiance is imaged as shown in Figure 6.11. Sun sensor function as follows:

- It was based upon the angle that the sun line makes with the sensor's optical axis.

- The circular spot applies relative radiant powers in the four detector quadrants, which is proportional to the sun's off-axis angle.
- Although this relationship is relatively linear with sun off axis angle, linearity is not essential, since the sensor transfer function is linearized during the factory calibration in a two dimensional look-up table stored in the spacecraft computer.

This series of bicycle chains have good characteristics that can be used as given below:

- ❖ Bear high tensile (pressure).
- ❖ Easy movement and control.
- ❖ It can be moved manually or by use of machine.
- ❖ Low cost.
- ❖ Needs less maintenance.
- ❖ Easily marketable.

All these characteristics make it easy to use as compared to the previous models.

6.7.3- How the Tracking System operates

A series of iron rods connected both parts of the parabolic side, which passes through the transmission toothed gears and moved by bicycle chain. The system works by pushing the pedals positioned at the back of the rear wheels manually. However, when pushing the pedals positions this connects both parts of the parabolic side with series of the parabolic dish body which moves in altitude angle as shown in appendix A. This section has ability to rotate around the zenith axis to align with the south to north celestial during the time of the season.

6.7.4- Installation of All Parts of the Final Prototype

This section explains how to install all parts of final model that consists of parts mentioned below as shown in Figure 6.10:

- A. Two different parabolic dish concentrators 2m^2 and 4m^2 .
- B. Reflective material 98%.
- C. Two thermal receivers.
- D. Two long iron base stand (1.5m).

- E. Air compressor (more information in section 5.4.1).
- F. Solar tracking system.
- G. Heat exchanger (Thermal oil).
- H. PCM-Storage.
- I. Copper pipe and solar flexible pipe.
- J. Thermal control.
- K. Generator (1-100W).
- L. Hybrid Stirling engine.
- M. Helium gas supply.

The installation of all parts of the final prototype took more than three months of continuous work. The prototype is large with total length 10m, 5m height and 70 weight including PCM-storage. Within the model, the gas was passing through the closed loop from the focus receiver point to compressor, PCM-storage, Stirling engine and back to receiver during period of operation.

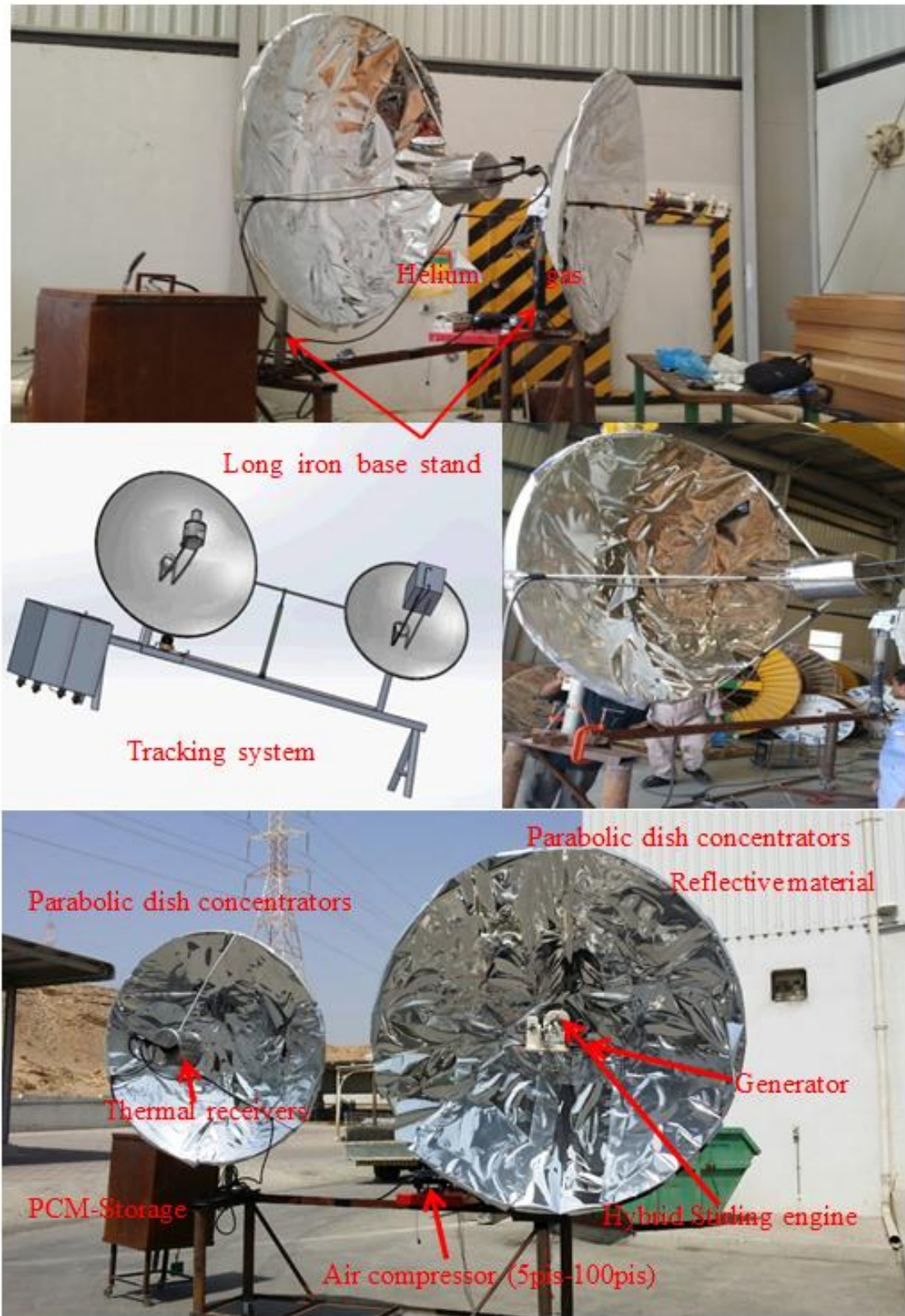


Figure 6.2 The prototype with tracking system

6.7.5 - The Principle Work of the System

After completing the design and fabrication of the appropriate solar tracking system, now the current model was completed construction. The next important step is described how the all system works, to understand in more details how system work, this was given in stages as shown in Figure 6.13.

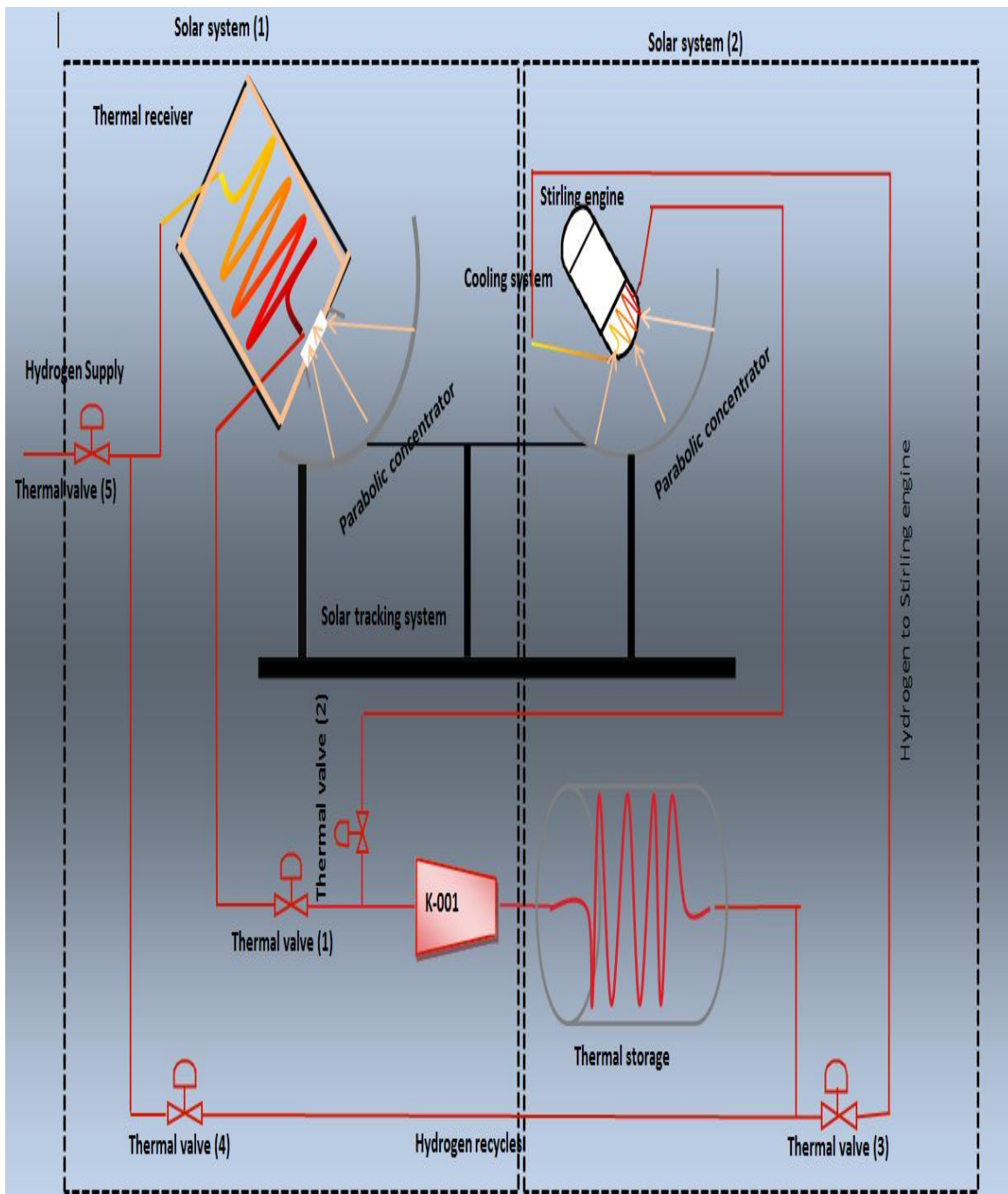


Figure 6.3 The principle and working of the system.

I. System (1) or “Direct Solar Generator System”

❖ Day Time or when Sun is Available:-

- At the beginning of sunrise, move final prototype to any suitable location and ensure that all devices are in good condition as shown in Figure 6.12.
- Open the tracking system in both systems.
- The reflective material worked to collect heat in centre of receiver hot space as discussed in chapter 3.3.
- Close valves (1 and 4) and supply system by helium gas, safety measures to be taken when using the gas.
- Leave gas until the temperature increases, and the pressure to be higher than operating temperature.
- Open valves (1 and 4) and close other valves (5, 2 and 3), and hot gas moved using pressure of compressor.
- The compressor compresses hot gas to move with high pressure and volume to thermal storage. However, the obtained gas will transfer heat energy from focal point to PCM-tank and this process is known as charging operation.
- Leave gas to charge the PCM until it is full charged, the whole charging process observed and final temperature recorded.
- During the experiment, temperatures were measured at each level in the storage tank as discussed in the next chapter.

❖ System (2) or “Indirect Solar Generator System”

- The reflective material worked to collect heat in centre of the Stirling engine hot space as discussed in chapter 3.3.
- The thermal oil in the cylindrical receiver will also absorb heat which needs time even when heated (also this oil work as heat control).
- Move Stirling engine crank shift from time to time, moving of the engine should be done with care considering the heat.
- When engine starts working, this increases the engine sound and increases the focused temperature.
- Allow the engine to work at night, take measurements of the energy produced and take record.

❖ **During the Night or When Sun is Not- Available:**

- At the beginning of sunset, there is not solar source (sun had set).
- Close valves 2 and 3, and open other valves 1, 4 and 5, while hot gas was moved by air compressor. At this point, system1 closes except for the compressor, PCM-storage and system 2 which were open. However, PCM-storage will supply heat to the model rather than sun.
- The compressor compresses hot gas and moves it with high pressure and volume from PCM-storage to supply thermal oil in the cylindrical receiver which was connecting the hot Stirling space.
- Helium gas will transfer heat energy from PCM-storage to engine which is the discharging process.
- Exported temperature at the centre of the engine (main oil and gas fluid) was enough to run the engine. In this case, there are normally two options:
 - Delay opening the valves until engine sound was heard, reduce the sound and open the valve.
 - Open valves and control heat by air compressor.
- Leave engine to work, measure the energy produced and take record.

Table6.2The principle working of the system

System	Day	Night
System (1) parabolic dish with Stirling engine	Work	Work
System (2) parabolic dish with storage	Work	Not Working

Table 6.2 simplify the process of operating the prototype, and the working of both systems. System (1) works 24 hours and system (2) works only during the day and stops working at night. With the exception of storage and system (2), that charges at day and discharges at night.

6.8-Conclusion

The final prototype was lacking a solar tracking system and focus of this chapter is the design and fabrication of suitable solar tracking for the prototype model. The Tracking system was designed considering the fundamental angles of sun. There are two main tracking systems depend on axis's use, the single axis trackers and dual axis trackers. The single axes trackers are moved in only one direction such as horizontal single axis tracker, vertical single axis tracker and tilted single axis tracker. But a single axis tracker is not appropriate for this final prototype. A dual axis tracker moves in two directions such as tip-tilt dual axis tracker and azimuth-altitude dual axis tracker which were considered suitable for this prototype.

Tracking system fabricated will track both parabolic dish concentrators with solar radiation during the day and season. The main characteristics of tracking systems are; bear high tensile (pressure), easy movement control, it can be moved manually or by machine, low cost, ease of maintenance and easily affordable. The tracking system works by pushing the pedals positioned at the back of the rear wheels manually.

However, when pushing the pedal positions this connects both parts of the parabolic side and series of the parabolic dish body moves in altitude angle. This section has ability to rotate around the zenith axis to align from south to north celestial during the time of the season.

The final model consists of 10 devices and assembling all parts was difficult to complete. An approximate period of three months of continuous work was required to complete the model. The total length of model was 10 m, 5m height and 200 kg including PCM-storage weight. The gas goes on the closed loop from focus receiver point to compressor, PCM - storage, Stirling engine and back to receiver during the period of operation.

The simplify final prototype had both systems with system (1) working 24 hours and system (2) working only during the day and stops at night. With exception of the storage, system (2) carries out charging at day and discharging at night.

Finally, this chapter discussed the complete design and fabrication of all parts of model and the model ready to be operated. The results will be explained in the next

two chapters which focus on testing the reflective material, hybrid Stirling engine, and the total system.

CHAPTER(7):-Testing and Comparing Main Parts of equipment with Experiments

7.1- Introduction

After completing the design and fabrication stages of all parts of the hybrid model, it was necessary to consider assembling, instrumentation, and testing of the prototype. In this chapter, the flexible reflective material for the parabolic dish, operation of the hybrid Stirling engine, cylindrical receiver, compressor, and PMC-storage will all be tested. The experimental testing was conducted in Oman (Muscat) during the summer period from 01 July 2013 to 01 August 2013.

Before testing the complete prototype model, the component parts will be tested separately. The flexible reflective material and mirrors with different sizes will be tested. This also includes the hybrid Stirling engine with constant pressure 1-10 bar, air compressor, and cavity receiver during day.

This chapter also intends to discuss the working of the system when the solar radiation was available with parabolic dish reflecting the sun's rays at the centre of the receiver, and transfer of heat to the thermal storage system. The second system uses the heat generated directly to generate energy. The chapter is part of experimental result of the testing and comparison of different parts of the system based on different scenarios.

7.2- Some Basic Information of the Location of Experimental Testing

The sultanate of Oman occupies the South – Eastern corner of the Arabian countries and located latitudes 16°40' and 26°20' North and Longitudes 51°50' and 59°40' East [31]. The following are some information vital to the design and testing of the prototype model based on the geographical nature and the weather of the location (Oman):

- ❖ The total area of Oman is 309,500km² and Oman is one of a solar rich country [1].

- ❖ The average hours of the day in Oman are between 11h and 13h during the year (winter or summer).
- ❖ Most days of the year in Oman have sufficient solar radiation with a total of 320 out of 356 days.
- ❖ Solar radiation in Oman is very high as shown in the experimental results, with the maximum value in the summer of $1200\text{W}/\text{m}^2$ and the minimum during the winter of about $800\text{W}/\text{m}^2$.

7.3- Test Reflective Materials

This section discusses the testing of reflective materials in order to measure the focal temperature in two different reflective materials. Two different materials with 98% flexible reflectivity and normal mirror with different sizes of area (3m^2 and 4.2m^2) were tested and compared.

Figures 7.1-A and 7.1-B shows the two parabolic dish concentrator systems installed on the current model, with system 1 having 3m^2 reflective mirrors and system 2 with 4.2m^2 reflective mirror. The reflective mirrors were made by cutting normal mirrors into small pieces in dimensions of $2\text{cm}\times 2\text{cm}$ and pasted neatly on the surface of the external surface of the parabolic dishes as shown in Figure 7.1 -A, B. These small pieces of mirrors were used to reflect solar radiation on to the face of receiver placed at the focal position with distance 0.75 m.

Also, Figures 7.1-C and D are two parabolic dish concentrators both made from high reflectance (>98% in 300 - 400 nm) mirror film with Figure 7.1-C having 3m^2 and Figure 7.1-D having 4.2m^2 at the focal position with distance 1.05m. The high efficiency flexible sheet was used to reflect solar radiation into the focal point. Unfortunately, it was difficult to get the reflective sheet on the external surface of the dish to be smooth without air bubbles as shown in Figures 7.1-A and B. The air bubbles deflect some of sun's rays in several directions rather than collecting at the focal point, thereby reducing the efficiency. For this reason, effort was made to reduce the bubbles as much as possible. However, better technology is required to completely eliminate the air bubbles and this is not part of the scope of this work, and the technology may be expensive to employ.



Figure 7.1 The parabolic dish concentrators with different reflective materials and different area sizes; A cover by normal mirror with (3 m²), 'B' also normal mirror but (4.2 m²), 'C' cover by flexible reflective sheet (3 m²) and 'D' also cover by flexible reflective sheet

The advantages of using flexible reflective sheet in the model are:

- High reflective efficiency up to 98%.
- Low weight ($1 \text{ m}^2=3.5\text{kg}$) and thickness (300-400) nm.
- Low cost.
- Easy installation.
- Reflective body does not absorb (store) large amount of heat energy.

During the experiments, a Pyranometer (type of actinometer) was used to measure solar radiation on a planar surface and is a sensor that is designed to measure the solar flux density (W/m^2) from a field of view of 180° [33]. Thermocouples are located in different regions of receiver for measuring focal temperature as shown in Figures 7.2 A and B show the cavity thermal receiver used during the experiments, with added thermocouples in specific regions. These installed thermocouples on the walls of the receiver, inside copper pipe and focal point were used to measure helium temperature in these areas. The main aims of this test are measure the gas temperature in centre of receiver and the changes that occur during operations.

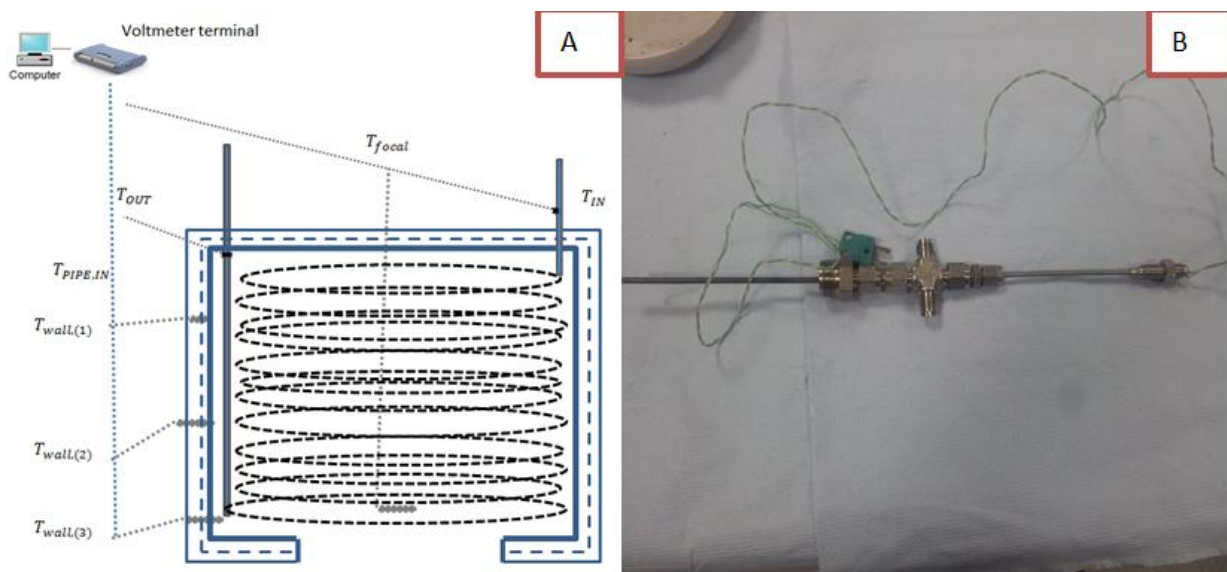


Figure 7.2 Thermal receiver used during the experiment and thermocouples used to measure temperatures

Results of Parabolic Dish 3 m² with Cavity Thermal Receiver

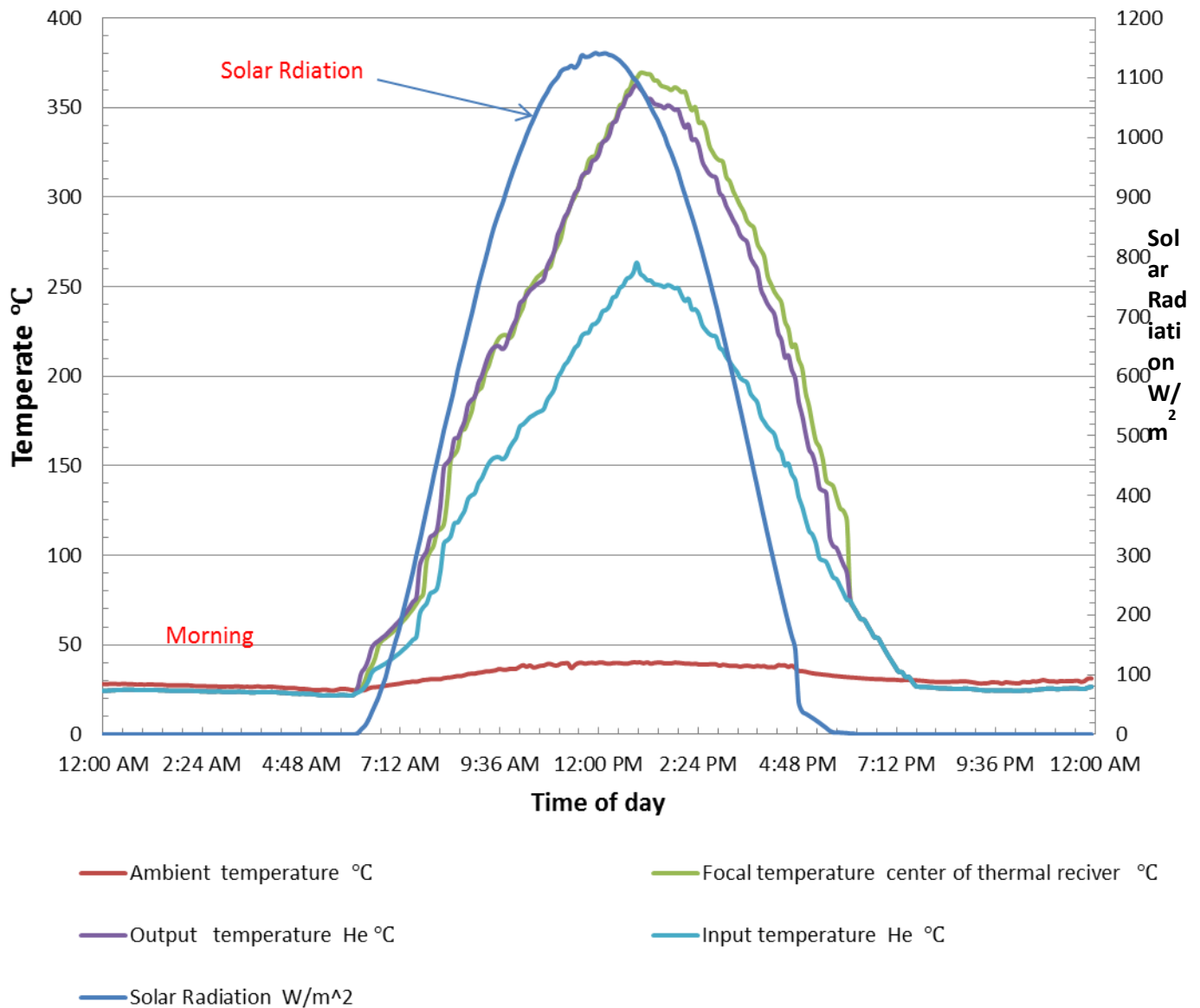


Figure 7.3 Result of Parabolic Dish Concentrators, focal temperature, in solar radiation and ambient temperature

The focal temperature was shown to change by increasing as the time passes, while the heat was collected directly from the commencement of sunrise at 6:05am, so also is solar radiation. Both focal temperature profiles are shown to increase as the solar radiation increases within the first 6hours (6amto 2pm), until it reaches the maximum value and then descends gradually. The maximum measured solar radiation was 1100W/m² at about 1:00pm,and maximum focal temperature was 256°C.The ambient temperature of the experiment alsochanged slight from 20°C to 31°C.The system stops working atsunset at about 6:15pm, but the receiver was

shown to retain some heat, as the thermocouples still measured focal temperature until after sunset at about 8pm. That is because the body of thermal receiver had stored heat during the day and then returned to radiate at beginning of night, so keep the gas temperature hot even lose body heat which stored it. This phenomenon has sparked negative and positive, as is evident in the results of the experiment in Figure 7.3. The negative impact, at the beginning of system work the helium gas temperature increases slowly due to the receiver body stored up a part of the receiving energy. The positive impact, that the receiver body will provide heat to helium gas in the fourth quarter of the day. However there are heat losses (conduction, radiation and convection) in thermal receiver as mentioned in section (3.6.1). The thermal efficiency of receiver related on input and output temperature gas temperature in receiver.

From the first day time experiment or testing of the parabolic dish mirror (3m^2) with flexible reflective, it was concluded that:

- At the beginning of Stirling engine movement, it needs to move or push it crank shaft in order to continue moving.
- Number of working hours within the day time may be more than 13 h.
- The focal or operation temperature was shown to increase with the increase in solar radiation.
- The body of receiver absorb some heat in a beginning of operations and stored in it components so it need time for increase temperature.
- The thermocouple still measured temperature at sunset because body of receiver radiates heat what is stored when sun is available.
- The second half of day showed gradual drop in operation temperature.
- During the day, the operation temperature was shown to produce energy by converting engine irrespective of the solar radiation during the day.
- The maximum measured solar radiation was $1100\text{W}/\text{m}^2$ at about 1:00pm, and maximum focal temperature was 256°C at same time.
- This measured focal temperature is enough to generate power by use Stirling engine.

7.3.2-Comparing between Different Parabolic Dishes Sizes and Materials

This section discusses the experimental result by comparing two different of dish materials including flexible reflective material 98% and normal mirror with different sizes of area (3m^2 , 4.2m^2).

7.3.2.1- Different Dish Sizes

Parabolic Dish Mirror With Different Sizes (3 m^2 & 4.2 m^2)

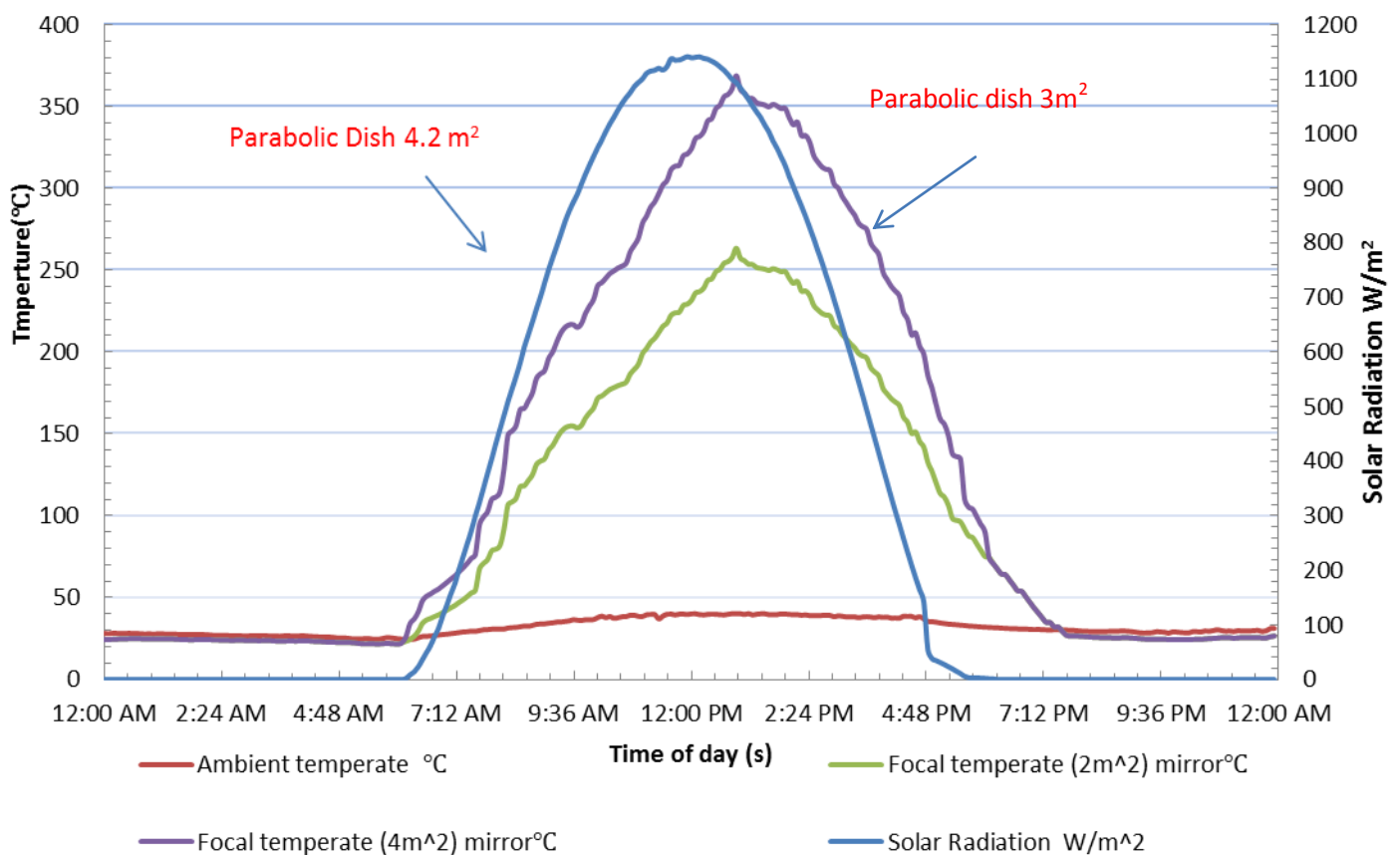


Figure 7.4 Results of parabolic dish Mirror with different sizes (3 m^2 & 4.2 m^2)

Figure 7.4 and appendices (E) shows the results of parabolic dish mirror of sizes 3m^2 and 4.2m^2 . At sunrise at about 6:30 am the temperatures were shown be at the same level but gradually increases until the peak period of solar radiation was reached. There was also a gradual decrease as the sunset approaches, after the

peak period. This was as a result of the decrease in the intensity of solar radio as the day passes.

As the solar radiation increases, the operation temperature increases for both dish sizes. However, the smaller dish size was shown to have lower temperature as compared to larger dish size at any point in time within the day. It was also shown in Figure 7.4 that the 3m² dish sizes had maximum temperature of 256°C as compared to the 4.2 m² dish sizes of 357°C. This is evident that the increase in dish size affects the reflected heat into the thermal receiver. This also increases the energy generated within the working hours of the day (sunrise and sunset).

7.3.2.2- Different Reflective Materials

The experimental testing was carried out on parabolic dishes with different materials including flexible reflective and normal glass mirror. The 4.2 m² reflective sheet and reflective mirror were considered, and the focal temperature and solar radiation in each material were measured and later compared.

Parabolic Dish, Flexible Reflective and Normal Mirror Size (4.2 m²)

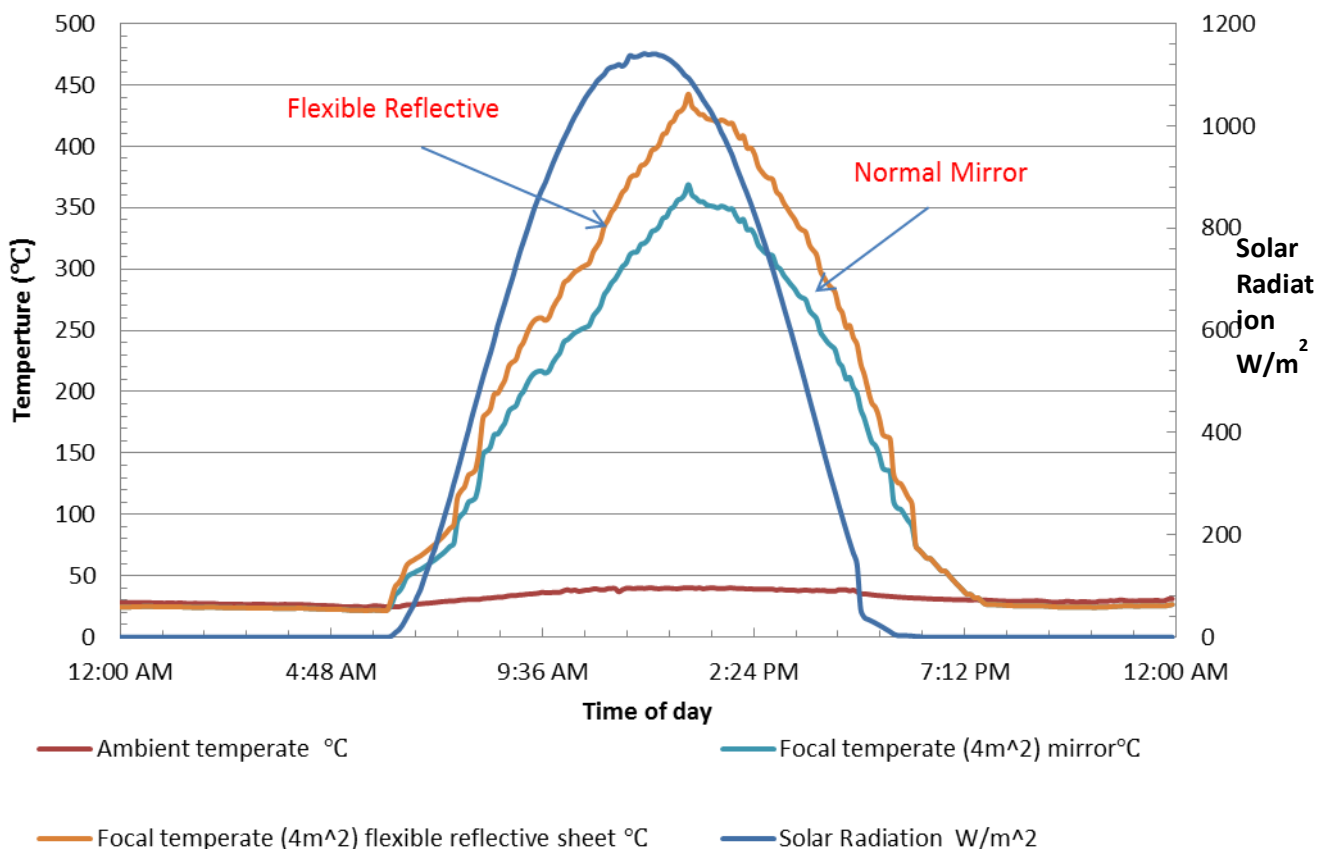


Figure 7.5 The results of parabolic dish with the flexible reflective at size (4 m²)

Figure 7.5 shows the result of the flexible reflective sheet and normal mirror, with the experiments conducted on 21 July 2013 considering the operation temperature against the intensity of solar radiation through the day. The operation temperature for the flexible reflective results was shown to have much higher temperature through first part of the day as compared to the normal mirror. For the second part of the day, the temperatures of both materials showed a decline in temperature from 2 pm until 8:30 pm, with the normal mirror temperature also showing lower temperature than the flexible reflective sheet.

Summary of the comparison between the focal temperatures of the flexible reflective sheets and the normal mirror are given as follows:

- ❖ The focal temperature increases in the first half of the day (6:15 am to 1:30 pm) and decreases during the second half of the day from 1:30 pm to 8:30 pm.
- ❖ The use of different materials also means different efficiency. This work has shown that the increase in the efficiency of the material also means increase in the focal temperature, as the flexible reflective sheet has higher efficiency as compared to the normal mirror.
- ❖ The use of the flexible reflective sheet gives higher operating temperature as well as higher energy generation as compared to the normal mirror. Hence a better choice in solar thermal concentrators technologies.
- ❖ Higher focal temperature shown for the flexible reflective sheet as compared to the normal mirror, this may be as result of difference in thickness of the materials. The increase in the thickness of materials allows more heat absorption on the material there by reducing the amount of reflected heat to the receiver.

7.4-Testing of Hybrid Stirling Engine

Figure 7.6 and Appendices (A) shows the new hybrid Stirling engine with the component parts during the testing after fabrication. During the testing, thermocouples were installed at different locations of the engine in order to measure the focal temperature, hot engine space temperature and cooling engine space temperature.



Figure 7.6 The processes of testing of hybrid Stirling engine

Before installing the hybrid engine at the centre of the parabolic dish, there was the need to know its efficiency before the testing was carried out and also the properties of different parts of the engine. Table 7.1 shows the properties and dimensions of the different components of the Stirling engine and parabolic dish such as hot cylinder, hot (displacer) piston, hot cylinder, and cold (displacer) piston, connecting rod and flywheel.

For the simple design analysis, the Stirling engine operates from two heat sources using solar energy. The shaft rotates when solar energy was focused onto the hot zone of the Stirling engine. The helium gas in the hot engine space expanded by the supplied heat and moved the piston back. For the second process, the expansion forced the hot gas into the cooling space by the regenerator. Finally, the cooled gas leads to compression and putting the piston back to its earlier position. Crank shaft was connected to a generator at the back of the engine to generate the energy.

Table 7.1 The parameters of hybrid Stirling engine

Hybrid Engine Calculations		Parameters	Units
Hot cylinder	Assuming a constant pressure	1.02 - 2	bar
	External diameter of hot cylinder	70	mm
	Thickness of cylinder	1.75	mm
	Internal diameter of hot cylinder	47	mm
	Length of hot cylinder	140	mm
Hot(Displacer) piston	Diameter of hot piston	45	mm
	Thickness of hot piston	≈ 0.5	mm
	Length of hot piston	80	mm
Cold cylinder	Assuming a pressure	1-2	bar
	External diameter of cold cylinder	32	mm
	Thickness of cylinder	1.75	mm
	Internal diameter of cold cylinder	29	mm
	Length of cold cylinder	67	mm
Cold (Displacer) piston	Diameter of hot piston	29	mm
	Thickness of hot piston	0.87	mm
	Length of hot piston	35	mm
Connecting rod	Diameter of connecting rod	6	mm
	Length of connecting rod	11.5	mm
	Radius of gyration of the rod	1.5	mm
Flywheel	Shaft diameter	15	mm
	Diameter of the flywheel(118	mm
	Width of the rim	25	mm
	Thickness of the rim	5	mm
	Hub diameter	30	mm
	Length of the hub	30	mm
	Taking a speed	600	RPM
	Flywheel speed	8	Rev/s
	Weight of the flywheel	0.75	kg

The testing of the engine was carried out to get the optimal functionality of the system. Three different tests were performed, with the first having some challenges and subsequent tests improving on the previous test, with detail description below:

7.4.1.1-Test 1

The first test was carried out by heating the hot space using oxyacetylene flame and cooling using ambient air. Massive air leakages were discovered from the power cylinder assembly. This was because piston rings had not been fitted on the piston during assembly. It was however noted that the piston rings omission was the main

setback to achieve smooth running of the engine with as little friction as possible in the power cylinder.

7.4.1.2-Test 2

For the second test, the piston rings were fitted on the piston and adequate lubrication on the power cylinder and other moving parts to reduce friction. It was noted that after fitting the piston rings, the engine became too stiff and therefore the need to make it as free running as possible. To achieve this, the assembled engine was run on a lathe by clamping the flywheel to the lathe jaw and running at varying speeds.

It was discovered in this test that there was reduced air leak in the power cylinder. Furthermore, due to increased pressure on the power cylinder, air leaks were discovered from the gaskets.

7.4.1.3-Test 3

Before the last test, the engine was disassembled and new gaskets were placed between the flanges and fresh sealant (silicone) used to curb the new found leaks. When the test commenced, the engine developed signs of transmitting power, but due to more air loss during compression stroke in the power cylinder, the engine experienced power loss and could not run. Upon scrutinizing, the engine for the air loss, it was discovered that the engine was losing power due to small air leaks from the power cylinder due to irregularity in the cylinder profile. This irregularity in profile may have been attributed to any of the following stages in fabrication:

- ❖ During welding the cylinder to the flanges.
- ❖ Imperfect machining when the fabrication was outsourced.
- ❖ During the assembly in general.

7.4.2-Calculations Hybrid Stirling Engine Efficiency

All minor challenges with the hybrid Stirling engine were addressed and the engine was shown to function as expected. In view of this, this section intends to use the result obtained from the test above to calculate the efficiency of the engine based on theoretical approach as discussed earlier.

7.5-Parabolic Dish Flexible Reflective (4.2m²) with and Without Hybrid Stirling Engine

The choice of the flexible reflective parabolic dish material as preferred to the reflective mirror was influenced by its high solar heat reflective capacity and efficiency. This section intends to use the flexible reflective sheet with 4 m²dish area, by analysing the process within the receiver and at later stage within the hybrid Stirling engine. This is to look at the different temperature profile required to generate energy during the day or when the solar radiation was available. The hybrid Stirling engine uses the mechanical means to convert heat energy to electrical energy. In view of this, thermocouples were installed at different locations to measure the temperature, Pyranometer to measure the solar radiation and the generated electrical power [42]. The thermocouples were placed in the following locations:

1. The centre of the receiver and Stirling engine to measure the focus temperature and operation temperature respectively.
2. In the hot Stirling engine space to measure input temperature.
3. Thirdly, cooling space of the Stirling engine space to measure output temperature.

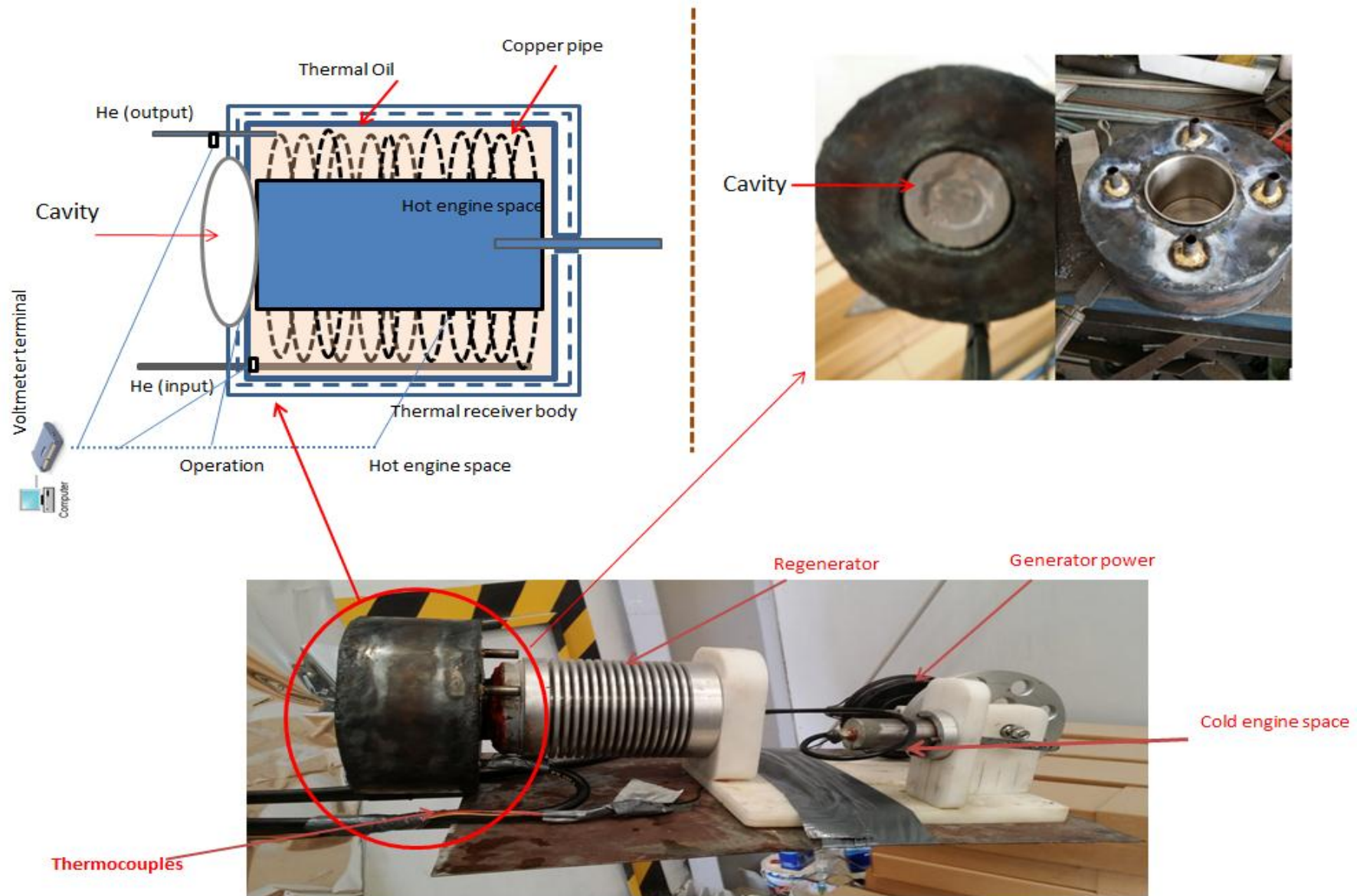


Figure 7.7 The experiment step of hybrid Stirling engine and measurement system

7.5.1- Analysis of Temperature Profiles without Hybrid Stirling Engine

Parabolic Dish (4 m²) without Hybrid Stirling Engine .

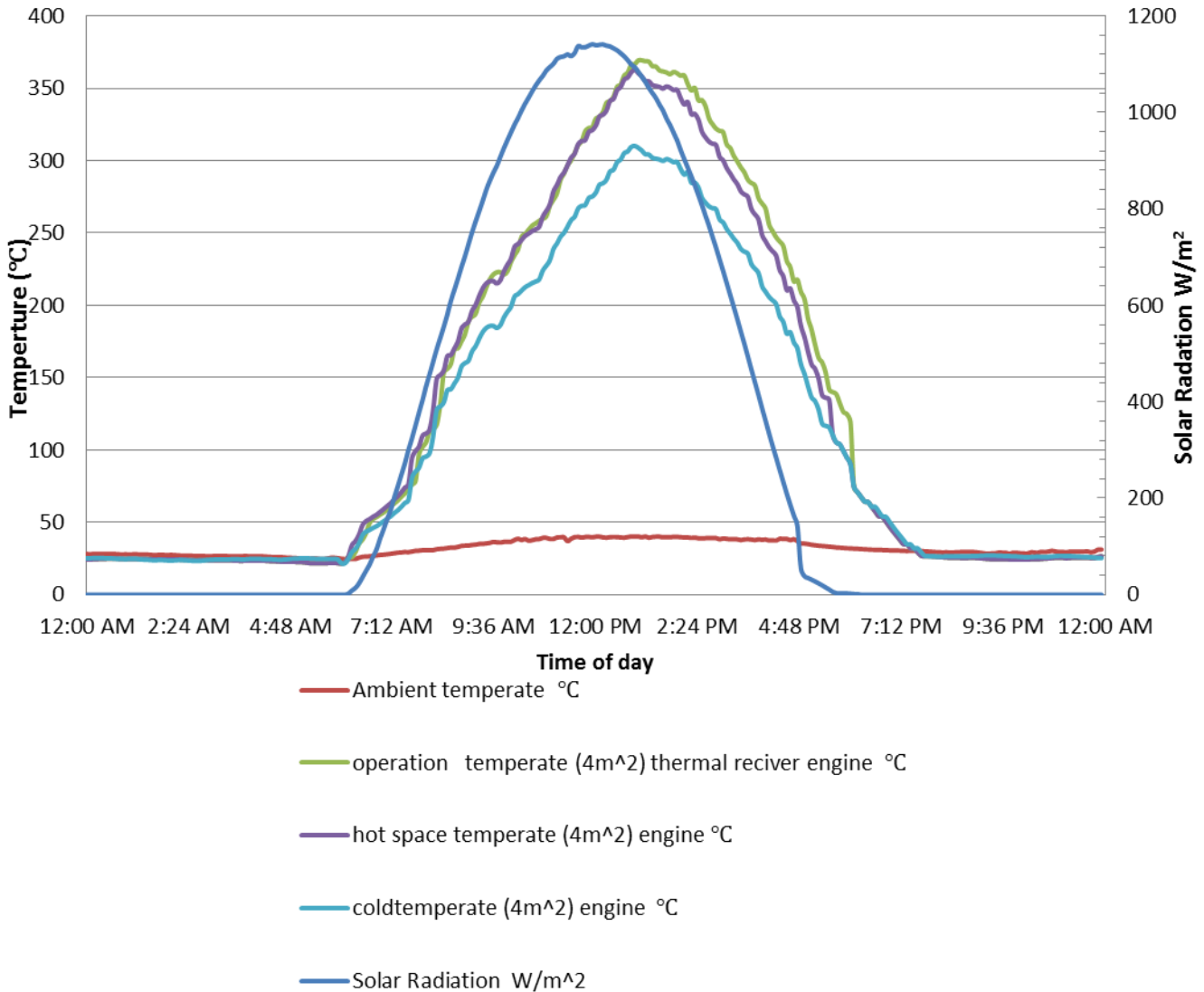


Figure 7.8 Results of testing (4m²) parabolic dish as well as operation temperature, hot engine space temperature, cold engine temperature and solar radiation

Figure 7.8 shows the results of operation temperature, hot engine space temperature, cold engine temperature and solar radiation during the day. Ambient temperature in Oman is usually high with an average of 29°C. However, this ambient temperature differs depending on the time of the year, with winter and summer temperatures of approximately 27°C and 47°C respectively. For this reason, solar radiation in Oman is

usually high, with the average winter value of 800W/m^2 and summer about 1200W/m^2 .

The parabolic dish as shown in Figure 7.8 starts to reflect sun ray at sunrise about 6:15am, and this was also reflected at the centre of the system. As the day goes by, temperatures and solar radiation were shown to increase progressive until 1:30PM, and the solar radiation started from zero (sun was not available). But there was a slight rise in other temperatures as a result of the ambient temperature from surrounding. The maximum solar radiation occurred at 12am with approximately 1200W/m^2 and the minimum at sunset. The maximum operation temperature, hot engine space temperature and cold engine temperature were shown to be 355°C , 352°C and 305°C respectively. Furthermore, when there was an increase in solar radiation as time of day passed, the operation temperature, hot engine space temperature and cold engine temperature also increased. Also, when the operation temperature of system increases during the day, the hot engine space temperature and cold engine temperature also increases, this enriches the design work. The second part of the day after the period of the peak solar radiation, there was gradual decrease in all the temperature until sunset. This trend was similar to other comparison for different dish materials as discussed earlier.

7.5.2- Analysis of Temperature Profiles with Hybrid Stirling Engine

Figure 7.9 show the results of operation temperature and power generation by hybrid Stirling engine during the hours of day. It was shown that the system started to work at sunrise at 6:15am. This increases most of the temperature readings of the thermocouples including operation temperature, hot engine space temperature, and cold engine temperature. Fortunately, hybrid Stirling engine started work at time 6:30am, but only produced a small amount of energy at the beginning of less than 1W. The solar radiation was later shown to increase, this also increases the amount of energy (more and more in first half day) until the maximum power of 50 W was obtained at about 1:10am. In the second half of the day, all temperatures and power produced gradually decreases; this indicates that the relationships between them are a positive.

Parabolic Dish (4 m²) with Hybrid Stirling Engine .

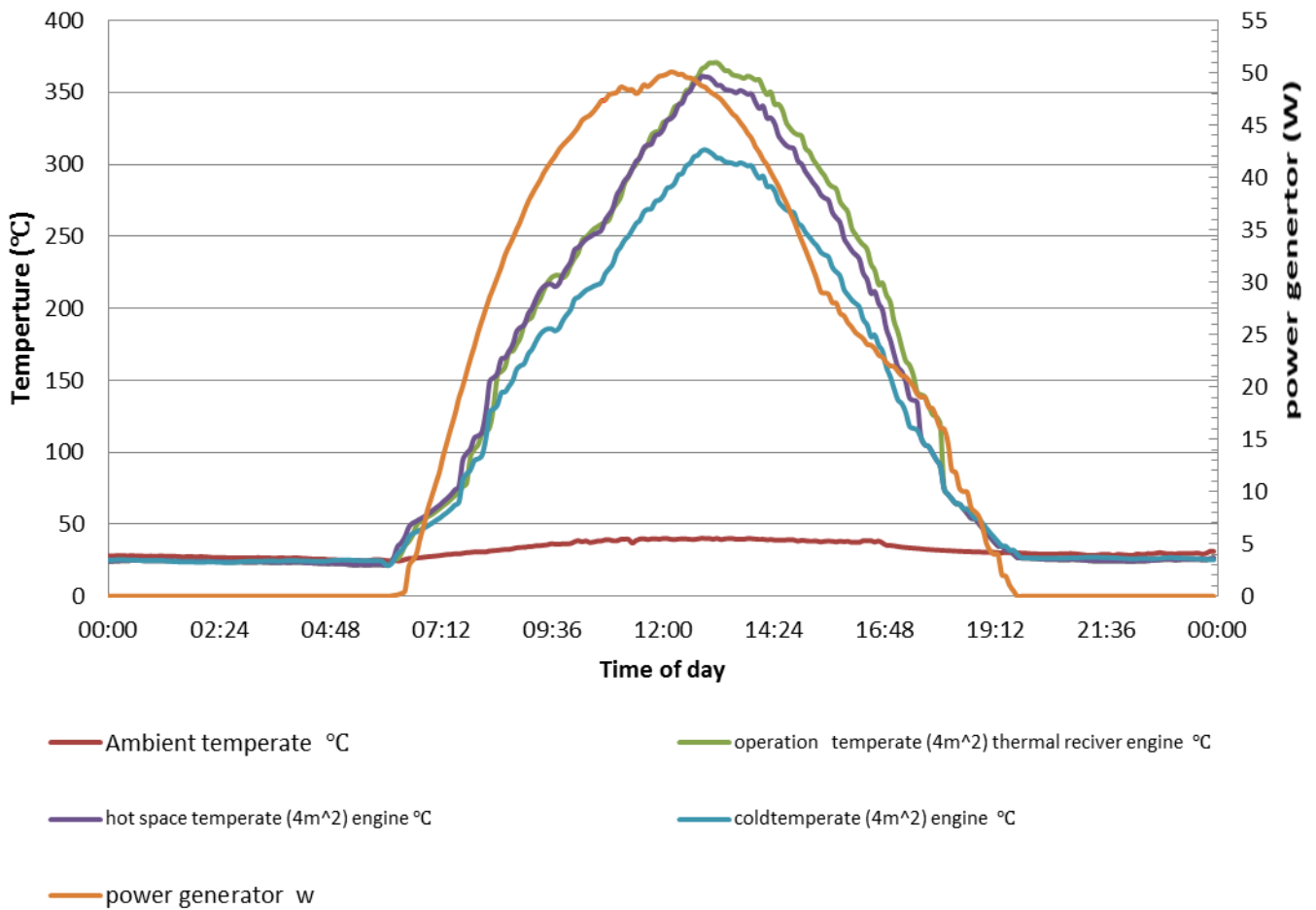


Figure 7.9 Results of testing (4 m²) parabolic dish with hybrid Stirling engine; operation temperature, hot engine space temperature, cold engine temperature, power generator and solar radiation

Furthermore, the gap or difference between hot space temperature and cold space temperature was not sufficient enough to generate energy because hot temperature supplying the engine was not enough to move the piston. The engine stopped working after sunset at about 7:15pm. The total hour of work from this engine was 11.30h that produce 24.420kW.

7.6-Discussion and Summary

Parabolic dish with hybrid Stirling engine tests were carried out with a view of estimating the actual efficiency and calculating power output from the engine. Series of tests were carried out on the engine and the result was not conclusive due to air loss. The intention was to measure the power output which was not feasible. The theoretical efficiency was then used to estimate the net power output using the Baele equation 2.11 as 50W. With this power estimate, the engine efficiency was calculated as 9%. This efficiency was compared to the theoretical Stirling engine efficiency of 60 %, and was found to be more reasonable and practicable.

Some of the losses of power, as reflected from the efficiency, were attributed to friction in the engine. In spite of the thorough lubrication that was done, friction was inevitable. From the assessment carried out, the greatest source of friction was in the flywheel assembly. This was because the flywheel assembly constituted several mating pieces, which rubbed on each other during operation. In addition, there was a lot of friction in contact between the piston and power cylinder arrangement.

Further, the engine experienced power loss due to out-of-balance mass in the assembly. It was noted that the attachment of the crank shaft to the flywheel introduced an out of balance mass that contributed to the power loss. To rectify this, re-examination of the parts in the assembly was recommended, in addition to a kinematic assessment of the engine to ensure all parts were balanced.

The project was undertaken to explore the practicality of power production from a Hybrid Stirling engine. This included research, design, and fabrication. The fabricated model was then tested and it was noted that some air leaks existed in the power cylinder. The power cylinder was an expensive part, and constrained by monetary resources, discussions and recommendations were made and the project was wrapped up.

On the overall, the project was successful on several accounts. Firstly, a successful research led to a design that was simulated on Autodesk Inventor, and showed kinematic synchronization. In addition, the hybrid was fabricated and pointed the project exploration in the right direction. The setbacks encountered were used to give recommendations and pointed out some ways of project improvement. A

theoretical energy assessment showed that with an open flame of sufficient temperature, (about 350°C) the designed Stirling engine would generate 45 watts of power.

7.7- Parabolic dish flexible reflective (3m²) with Hybrid Cavity Receiver and PCM-Storage

It was important to know how much heat could be transferred to the thermal storage system. This is the focus of second part of the model, and this consists of parabolic dish flexible reflective (3m²), cavity Receiver and PCM-Storage. Furthermore, this section to be separated into two parts: the first part to consider the parabolic dish flexible reflective material (3m²) with hybrid cavity receiver in order to measure helium gas temperature. The second parts consider the parabolic dish flexible reflective (3 m²) and PCM-storage, to measure the temperature stored in [KNO₃-NaNO₃] material as shown in Figure 7.10.

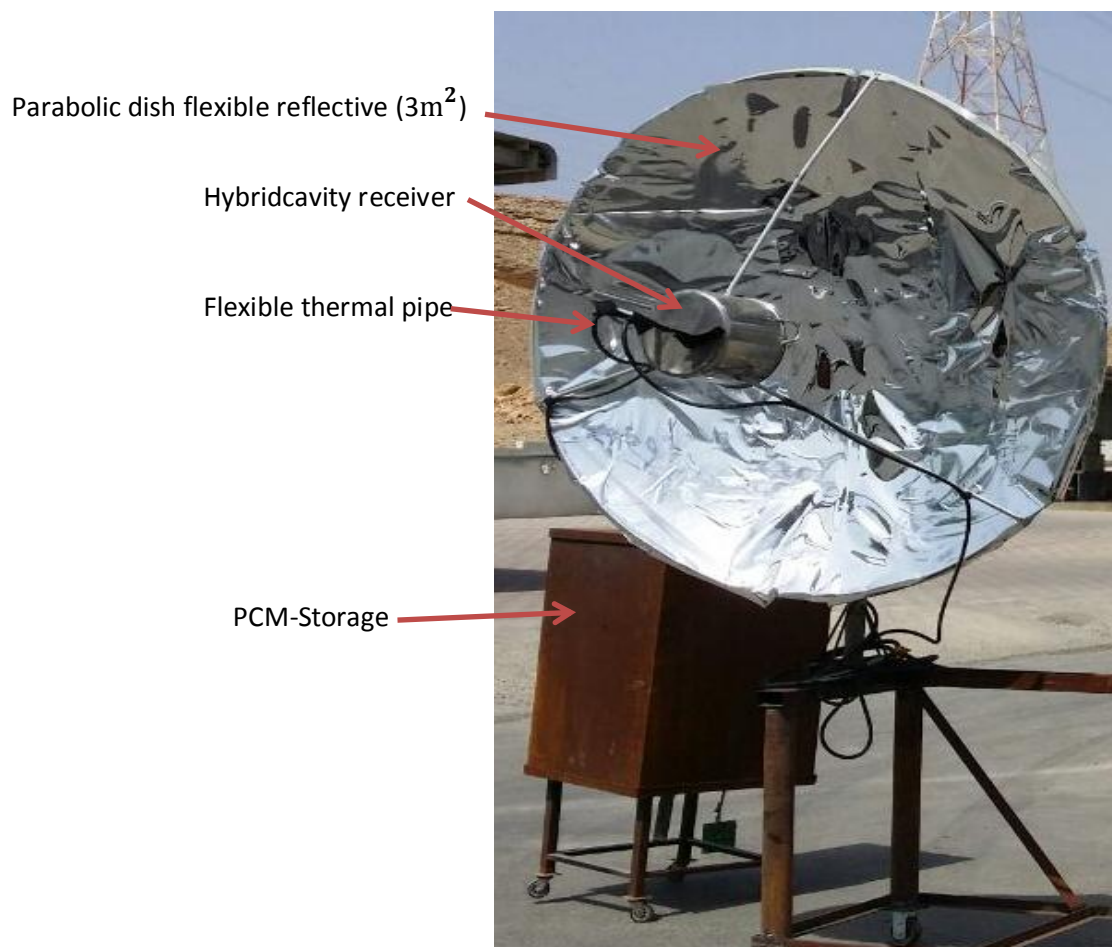


Figure 7.10 Testing parabolic dish (3 m²) flexible reflective sheets with thermal receiver in current system

7.7.1-Parabolic Dish Flexible Reflective (3m²) with Hybrid Cavity Receiver

The main important device in this system is the hybrid cavity receiver as shown in Figure 7.10 and discussed in the previous chapter. Also, five thermocouples were installed at different locations as shown in Figure 7.11. This was to measure the operation temperature of the gas (He), input pipe temperature, output pipe temperature, in and out wall temperatures.

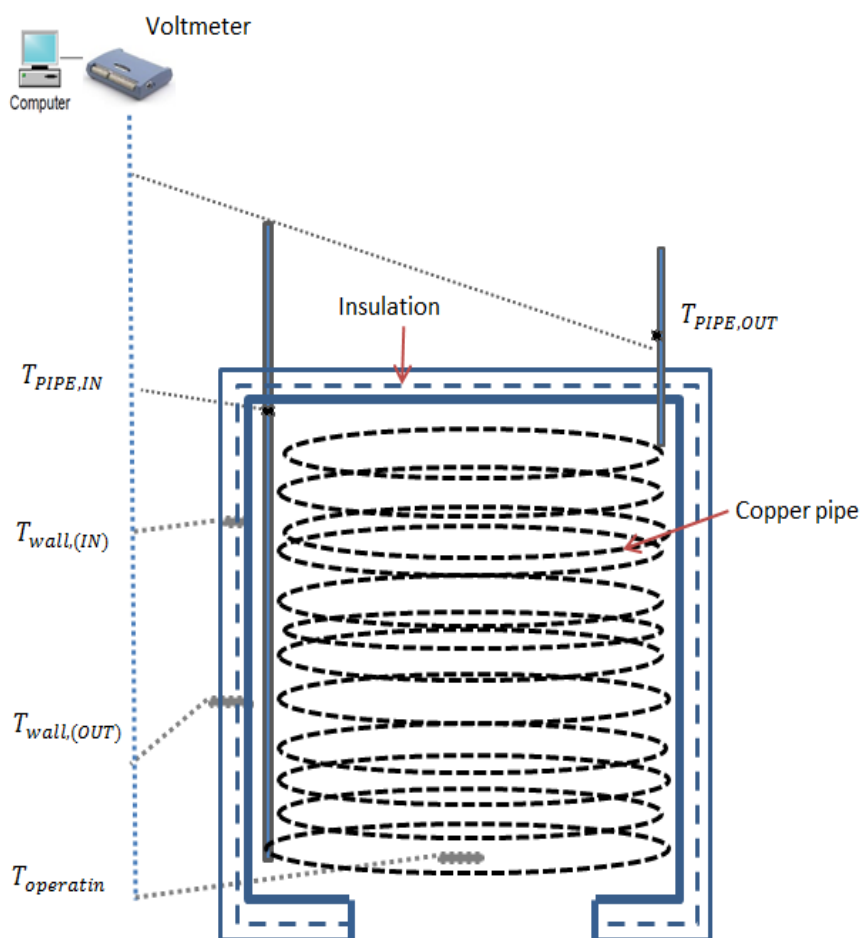


Figure 7.11 The experiment step of cavity receiver and measurement system

Parabolic Dish Flexible Reflective (3 m²) with Hybrid Cavity Receiver

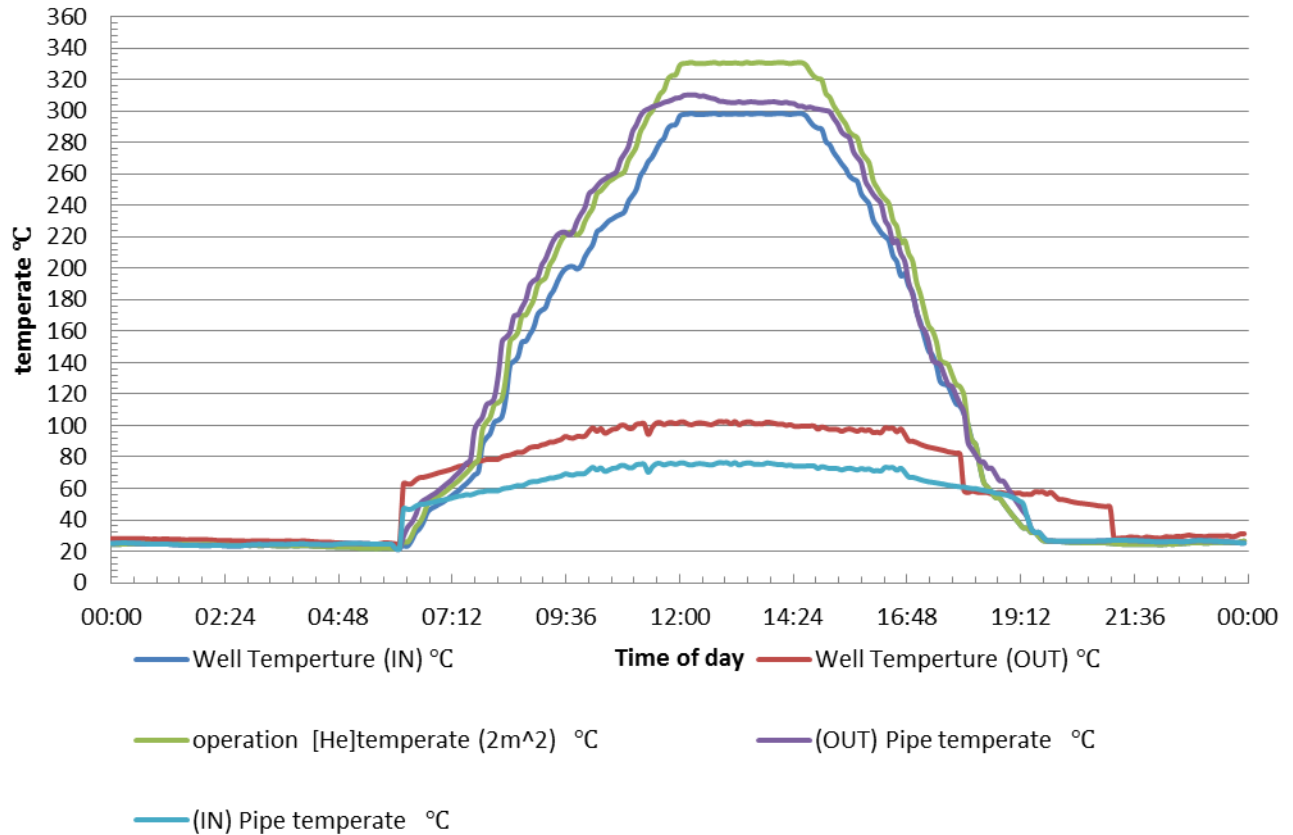


Figure 7.12 Results of parabolic dish flexible reflective (3 m²) and hybrid cavity receiver

Figure 7.12 shows the results in hybrid cavity receiver with parabolic dish flexible reflective material, this was used to measure the operation temperature, in and outside receiver wall, also helium gas temperature in and out of the system. The important parameter is the gas (He) input and output temperatures; based on the reflected solar radiation. After the initial stage during the day, there was an increase in temperature from sunrise at about 6:15am until mid-day. But operation temperature, out gas temperature and internal wall temperature increased more than other temperatures. This continued until the maximum values were reached at midday maximum value (330°C, 320°C and 300°C) at about 1:30PM, and these values were suitable for the working of the system.

On the other hand, input gas temperature, input wall receiver temperature, external wall temperature and input gas temperature were shown to increase as the time of the day passes by, but not sufficient to generate power (less than 100°C). Because receivers had good insulation between internal layer and external layer which does not allow heat transfer. Hence, the internal wall temperature was shown to be more than external temperature.

When comparing the gas input and output temperatures, it was shown that out gas temperature increased more than input temperature as shown in Figure 7.12. This was because hot gas was transferring heat from receiver to PCM-storage throughout the period. There were differences in the temperature profiles from 10:30 am and from this point there was increasing heat transfer through the gas medium.

Some of the important details are given below:

- Output gas temperature was 303.4°C.
- Input gas temperature was 75.6°C.
- Different between both temperatures was 227.8°C.
- Efficiency $(303.4-75.6)/303.4 = 75\%$ (which is a good value).

Temperatures measured within the thermal receiver shows positive progress to accommodate heat energy transportation to the thermal storage. The system was shown to meet the design requirement and prior to its application for transfer of heat to the storage system which is to be discussed subsequently.

7.7.2-Parabolic Dish Flexible Reflective (3m²) with Hybrid Cavity Receiver and PCM-Storage

The histogram in Figure 7.13 shows that the PCM-storage was installed with thermocouples at different locations within the storage system in order to measure the amount of thermal energy stored. The storage system consists of three different layers of length 30cm as mentioned earlier. Each layer had installed thermocouples to enable the measurement of the spread of heat in the storage system as shown in Figure 7.13.

The main objective of this system was to measure the quantity of heat stored in the thermal tank from sunrise until sunset, a total of about 11 hours. For this reason, the results focused on input storage and output storage system heat.

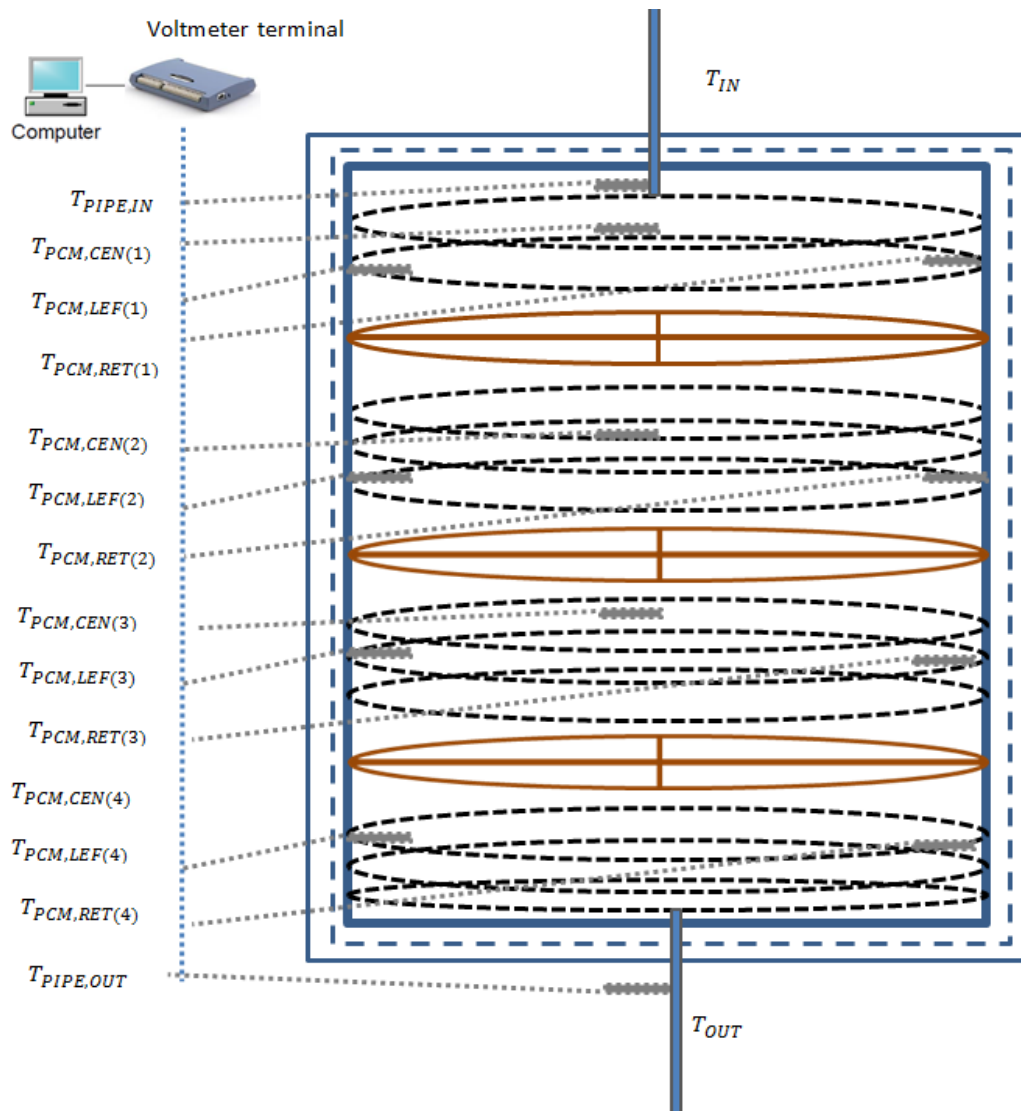


Figure 7.13 The experiment step of PCM - Storage and measurement system

The experimental test measured the gas velocity moving through the pipe, and this was shown to increase as the solar radiation increases. This also shows the increase in the mass flow rate as well as the pressure in the system, but has no

negative effects as it was controlled. The thermal control system was used to regulate the increase in gas temperature as well as the gas flow rate.

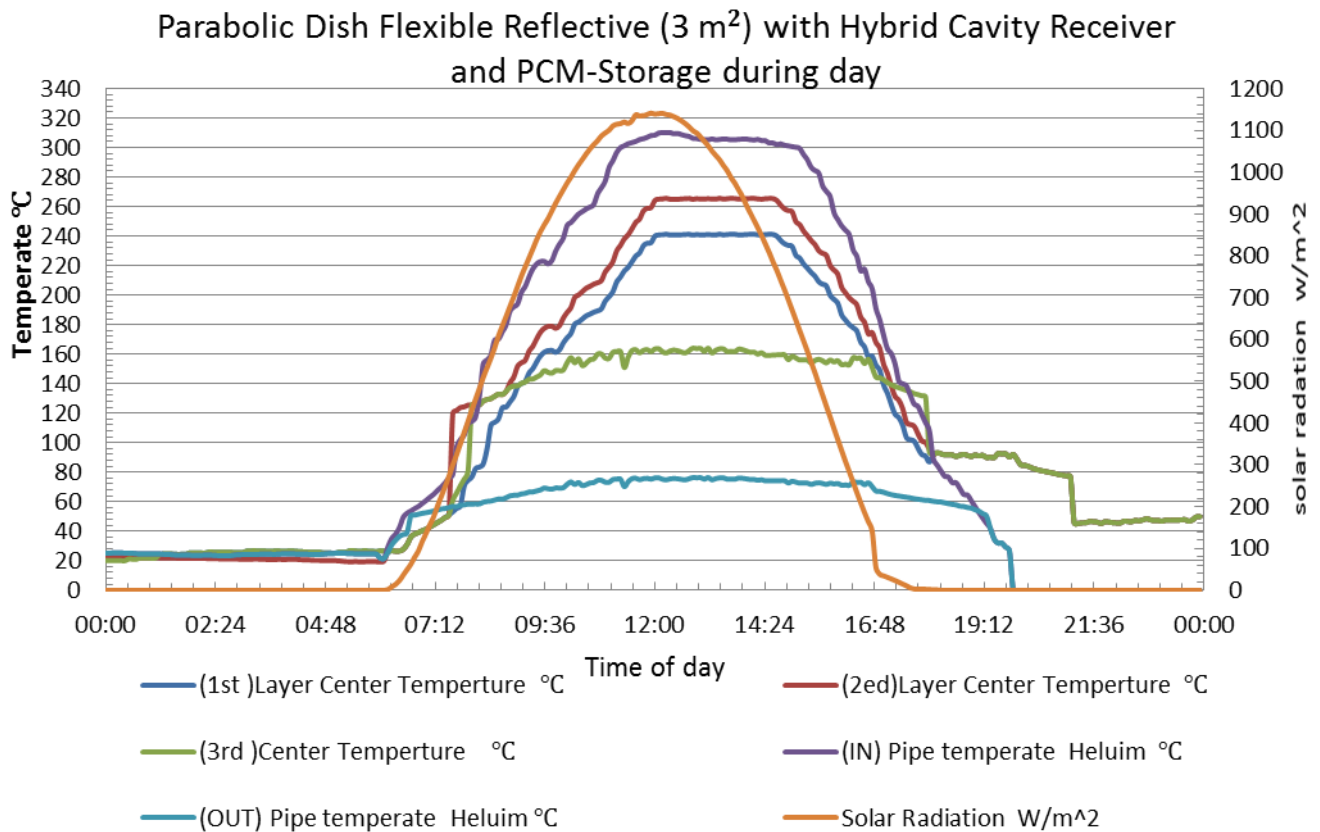


Figure 7.14 Results of heat store in PCM- storage during day

Helium gas transferred heat energy to thermal storage tank during the charging of the PCM-storage. When hot gas enters into the thermal reservoir (storage), temperatures were shown to increase gradually into the storage materials. Heat will be stored in PCM as the time of the day progresses, and later the reverse process was shown to occur. Figure 7.14 shows results of charging thermal storage, which measures the input gas temperature, output gas temperature, centre of 1st layer temperature, centre of 2nd layer temperature, centre of 3rd layer temperature and also solar radiation. All results show the working of the storage, as the charging process of the storage material commenced after one hour from sunrise at about 7:30PM.

The input gas temperature was shown to increase as compared to other measured temperatures. On the other hand, out gas temperature was also increasing as the solar radiation increases, but this happens slowly as evident of the process of storing. Furthermore, the first layer temperature, centre of 2nd layer temperature, and centre of the first layer temperature were shown to increase as the solar radiation increases during day. At 11:30 pm the entering gas temperature in storage system was equal to the melting temperature of the storage material (KNO₃-NaNO₃) at 222°C as show in appendices (D). The maximum input gas temperature was 310°C at 12:00pm, and the value was stable at the point until 2:00pm. After mid-day, the solar radiation start to decrease gradually so also was input gas temperature, but the out gas temperature decreasing regularly. The temperatures of different layers of the storage devise continue to spread through the material. At sunset the solar radiation was at the lowest value, heat source which provides thermal receiver for it input temperature to the system was zero and temperatures of the storage system remain high until morning.

The following are some of the characteristics of PCM-storage:

- Total volume of storage tank chamber was 0.75m³.
- Copper pipe diameter: 3 mm.
- Mean storage pressure: 1-5 Bar.
- Working gas type: helium.
- Heater design temperature: 50-325°C.
- Cooler design temperature: 20-130°C.
- Mass flow= (0.621 to 0.0621) kg/s.

The total energy stored during 6h storage was 5.7kW shown in Figure 7.14.

7.8-Conclusion

The geographical location of Oman was important as days of the year in Oman had high solar radiation (this sunny country), shorter days of year had 11h and minimum of solar radiation during the winter was about at 800W/ m².

As results of the experiment between different parabolic dishes sizes and materials, the following conclusions were made:

1. Solar radiation and focal temperature were shown to increase rapidly in first half of the day and decreasing gradually in the second half of the day.
2. Focal temperature and solar radiation increased when the sizes of the parabolic dish concentrator increases.
3. Power generator by hybrid Stirling engine was shown to increase when the Focal temperature and solar radiation increases.
4. Power generator by hybrid Stirling engine increases but with difference between materials when compared (flexible reflective and normal mirror).
5. Focal temperature and solar radiation were shown to increase when materials flexible reflective and normal mirror were used.
6. Power generator by hybrid Stirling engine also increases when different materials were use but flexible reflective was shown to generate higher energy as compared to normal mirror.
7. Focal temperature and solar radiation were shown to increase as the heat transfer increases.
8. The flexible reflective sheet was shown to be a better choice as compared to the normal mirror in terms of heat reflection and energy generation

CHAPTER(8):- Experiment Results & Discussion

8.1- Introduction

In continuation from the previous chapter, this section will further discuss some other areas of the experiments. Furthermore, more detailed discussions and comparison with results of the previous sections will be highlighted, and also the working of the system during the day and night. The experiments reported in this section were carried out between 20to29-July-2014. The results of the experiments are discussed as follows:

- The working of the system at night (only).
- Working of the system throughout 24h.
- Working of the system for 24h with thermal control system.
- Comparing results of system for 24 h, with and without thermal control.

Thermal control valves were used to control heat in/out of the thermal storage to the hybrid Stirling engine manually. After several tests, it was possible to determine the amount of heat and fixed temperature with specific position of the regulator. This regulates the amount of heat required from the thermal storage to the hybrid Stirling engine at night.

8.2- Working of the Prototype Model During Day and Night

The experimental result of this process during the day was discussed in the previous chapter. While, this section gives more details of on the night process as part the entire 24h process (day and night).

Figure 8.1 is a schematic of shows the three thermal cycles within the model, with the two processes when the solar rays were available and one after sunset in the absence of solar radiation:

1) The first cycle is important as it is a short- term cycle between focal or operating temperature and Stirling engine. This thermal cycle works when the sun was available, the peak temperature was obtained at about 1:30pm with a temperature of 335°C, and this temperature can generate approximately 50W of energy. During this period of the day when the peak temperature was achieved, energy losses were expected at the point of the receiver. Hence the need to put in place measures to reduce these losses. In view of this, a modified thermal receiver for the Stirling engine was used to reduce the heat loss. There was also need to reduce heat when the system operates and a cooling system was used inside the hybrid Stirling engine. However, the existing cooling system (regenerator) was not sufficient to expel the heat outside the engine, but this was modified to accommodate other systems including water. It is important to note that the working fluid used in the system was Helium, and it has high heat transfer coefficient, high thermal conductivity, specific heat, low density and viscosity. These properties are similar to other gases such as hydrogen but helium was considered to be more suitable due to some setbacks associated with hydrogen. This cycle operates with an estimated time period of 11h during the winter and 13 h in the summer.

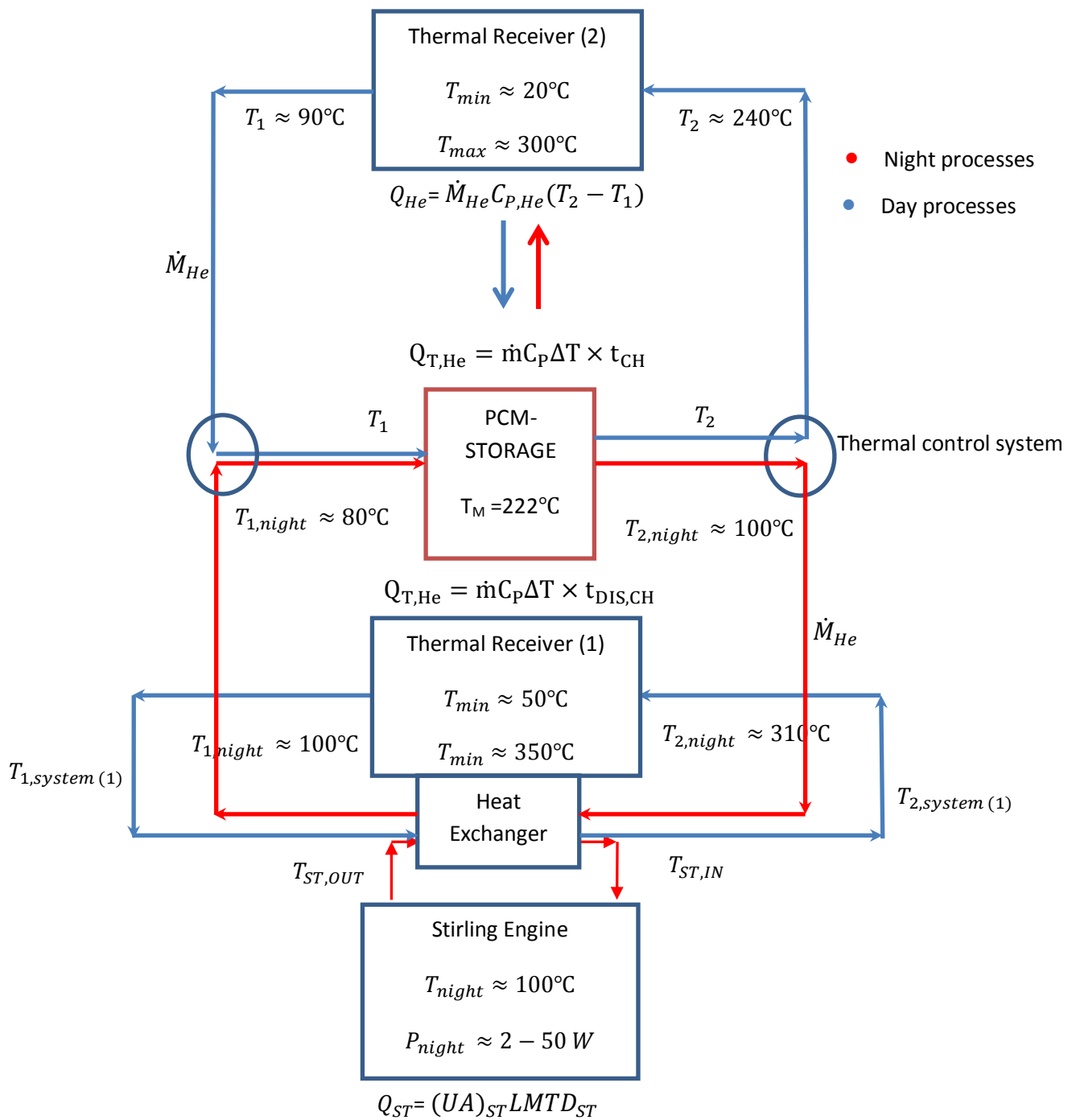


Figure 8.1 The principle work of current model processes during day and night

- 2) In the second cycle, heat was transferred through a longer distance from the receiver to the PCM and back to the receiver, this process is known as charging.

During the day, hot gas was used to charge the PCM-storage until mid-day but the operating temperature was normally higher than the melting material temperature of the PCM (222°C), during the charging process. The charging process of the material continues until the melting temperature of the PCM was reached at about 3:30 pm. After reaching the melting temperature of the PCM, the whole PCM was allowed to completely melt (taking approximately 2h) before the temperature increases as part of the charging process. It was difficult to measure the exact amount of heat stored in the PCM, but rather the amount of energy generated from the heat stored.

- 3) The third cycle transfers heat from the PCM- storage to the Stirling engine. This is a complex process as the process of discharging the storage and charging the hot Stirling engine space (exchange heat between both systems) was carried out simultaneously. This cycle works at night when the sun was not available, and heat energy stored in the PCM was used as heat source instead of the sun. This process was expected to start at sunset and continued to work until the stored heat energy was exhausted in the morning with the process taking about 13 h during the winter. The helium hot gas transfers heat energy from PCM-storage, but temperature of thermal oil (at heat exchanger) receiver of Stirling engine was still hot and was sufficient to move the pistons to produce energy. Results from the previous chapter showed low power generated by hybrid engine using the open hot gas drastically until midnight. This was because the valves on the open pipe connecting the PCM to the engine were opened without controlling the amount of heat transmitted. This shows the importance of having the valve in order to regulate the desired amount of heat to the engine when required.

8.3- Heat Transfer from PCM-Storage System in Current System

The results discussed in the previous chapter showed that the model works for a total of 11h during the day, which also involve the charging process of the PCM-storage system. But at night, the model was tested to work for 13h and the PCM-storage was discharged in this process.



Figure 8.2 The current model under operation in 24h in workshop (Oman).

Figure 8.2 shows the final model as used during the day for direct power generation and as well as the charging process of the PCM-storage system. Furthermore, at sunset the control valves were opened to allow for further testing of the model in the absence of sunrays. In order to have accurate measurement of the experimental data and ensure smooth testing of the novel model, there was the need to ensure proper monitoring of the procedure at night. The following are important points associated with the night procedure:

- The oil in heat exchanger around the hot space of the engine when still hot has ability to produce energy; this implies that the valve must be carefully controlled to regulate the appropriate amount of heat required.
- Ambient temperature around the model gradually decreases with time through the night and the heat transfer from the helium gas to the surrounding increases.
- There are heat losses in the heat exchanger of the Stirling receiver.
- Reduces the amount of heat transfer to the Stirling receiver to control heat supply.
- The model in this case works without control system at night.

8.3.1- Results of System Working at Night (only)

The testing of the final model for the night operation was carried out on 23 June 2014 based on the period of the year as mentioned in chapter 6. Before the experiment, the heat energy was not measured during the charging process but only the total amount of heat stored in the PCM-Storage was measured. Figure 8.3 shows the result obtained during the night experiment including in-out storage temperature, operation–out Stirling temperature and power generator.

After sunset, valves 2 and 3 were opened and hot helium gas allowed into the hybrid Stirling engine at about 6:00 pm. After 30 minutes:

- ❖ Input and output temperatures increased rapidly and maximum values reached were 320°C and 100°C respectively.
- ❖ Operation temperature increased to the highest expected value of 320 °C.
- ❖ Power generation also increased rapidly because it depends on the gas operating temperature and this produced 50W based on the maximum operating temperature.

From Figure 8.3, the result shows that there was gradual increase of the measured temperature from the start time until the maximum expected temperature was reached after about 30 minutes of operation. This maximum temperature was attained within the short period as the control valves were left fully opened and allowed the stored heat energy to be released without been properly regulated. Similarly, this was also responsible for the increase in the operating and Stirling engine operating temperature. Furthermore, the discharging process also indicates low temperature into the storage system, as the charging process which was responsible for increase in storage temperature only occurs during the day. A constant temperature was maintained at the maximum level for 2 h before steady temperature decline was observed. This is also caused by lack of regulation of the valve so control the required heat energy; hence the use of control valve was necessary.

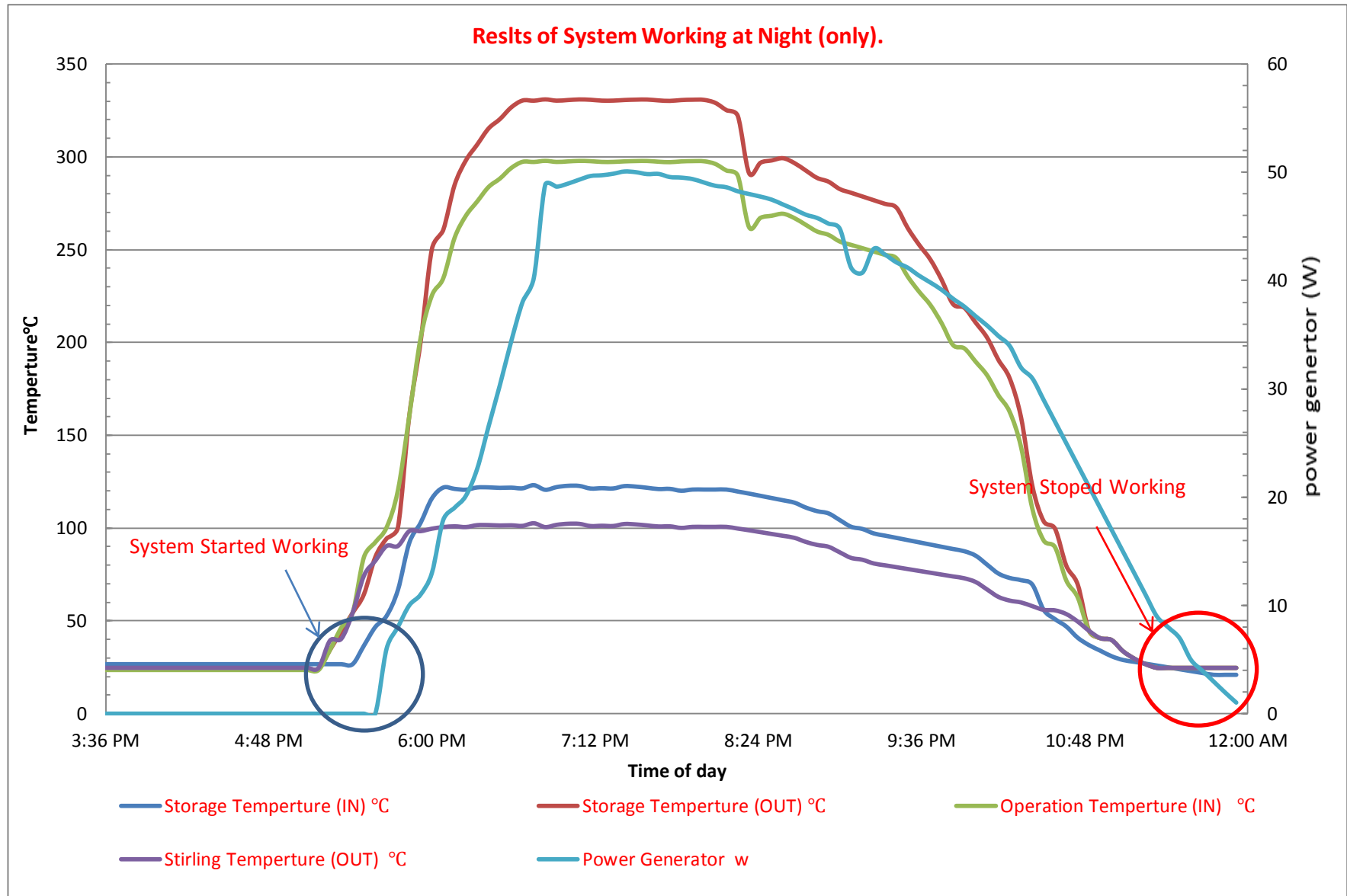


Figure 8.3 the results of system working at night (only)

The temperature coming out of the PCM-storage was known to be approximately 320 °C and this same as the temperature supplying the Stirling engine (operation temperature). However, the out Stirling engine temperature was less than other temperatures with a minimum of 29°C and a maximum of 100°C, the temperature difference of 210°C was shown between the operation temperature of engine and engine out temperature. This indicates that the hybrid Stirling engine suffers from heat losses during operation with a constant value of 2.5bar pressure. At this peak temperature, the engine produced about 50W energy.

At about 10 pm, the energy production begins to drop gradually and this depends on the operation temperature, Stirling engine out temperature as well as the pressure and volume. The system eventually stopped working by midnight as result of fast temperature drop. The total working period for the first test for night procedure was 2 h, generating a total of 360kW of energy for the 6h without the control system. Hence, there was the need to improve the working period of the engine to accommodate the total period of night before the sunrise in order to complement the day time process.

8.3.2- Results of System Working for 24h without Control System

Results from this section show the working of the final prototype through 24 h period. During the day light, the difference between the initial input and output temperature was zero, and no power was generated at this time, this was prior to sunrise. The beginning of sunrise (7:00am) also signifies the increase in temperature in both systems, as well as energy supply. Figure 8.4 shows the increase in temperature and energy generated throughout the day (24h). There was a gradual increase in temperature until the maximum temperature was reached at midday.

At midday, Figure 8.4 shows that the maximum temperatures were reached, including the operating temperature with a maximum of 320°C, and remain constant at this point until 3.00 pm. There was gradual decline of temperature and power generation after 3:00 pm until the sunset was reached at 6:00 PM when the out reached its lowest value. At this stage, the whole charging process of the PCM - storage also stops.

After 6:00pm, there was sudden rise in all temperature profiles from the lowest value of the day time process. This sudden rise in temperatures happened when the valves 3 and 5 were turned fully opened and other valves closed. The hybrid engine at this point relied on the PCM-storage for the supply of heat energy to generate energy as compared to the day time process which uses the heat energy obtained directly from the sun. The result also shows that the highest temperature and energy values were later obtained at about 6:35pm, remained stable at this point and later declined from about 10:00pm. Prior to midnight, the hybrid engine energy generation level dropped to the lowest level, this was a result of the sudden drop in the heat energy level stored in the PCM-storage. The system was allowed to continue working until all the heat energy in the storage used and the engine stopped generating energy.

The whole process discussed above can be summarised as follows:

- The prototype and the PCM - storage where shown to function as expected.
- It was also shown to extend the energy production time from the day light process by approximately 6 h.
- The total energy produced within this for the 24 h was around 0.689kW.
- All stored energy was consumed very fast as the thermal control system was not used.
- The heat transfer through helium gas was very good and encouraging to some extent.
- Decrease in the level of output power at sunset was one of the disadvantages of the prototype and this need to be addressed.

Results of System is Working for 24 h (24-7-2014).

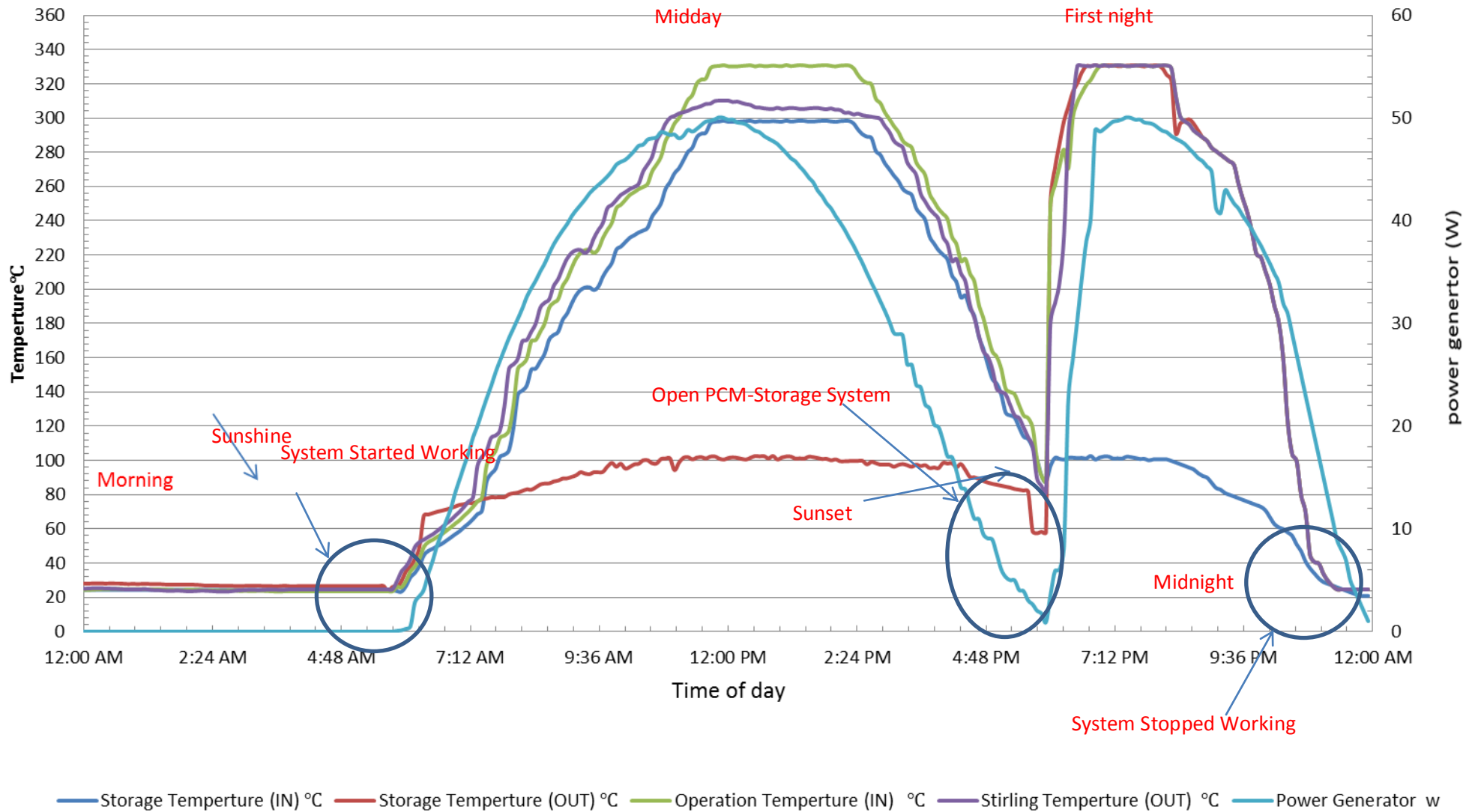


Figure 8.4 Results of system at operation for 24 h (24-7-2014).

The lack of regulating or control of the stored energy from the PCM -storage to the engine was shown to be a key problem in this experiment, which will be addressed in the next section. However, there was also need also need to discussed the thermodynamic aspect of the 24 h process as discussed above.

8.3.3-Thermodynamics of the 24hWorking System

The histogram in Figure 8.6 shows the temperature change and energy produced by hybrid Stirling engine indicating the melting temperature of material used. Furthermore, the histogram is divided into two parts; with the first part showing thermal energy coming from the sun directly to the prototype (both system 1 and 2), while second was the use of the stored heat for the model. Figure 8.6 also shows prototype working until all the stored energy was used through the whole day (day and night) produce energy as discussed earlier.

In the first part, increase in the operation temperature or focal temperatures of the system was shown to increase the power output, and this is similar trend when there was decrease in temperature leading to decline in its output. In Figure 8.4, different temperatures give different powers output, these include the initial temperature, T_1 (this is normally the minimum temperature at different level), maximum temperature, T_2 , and melting temperature, T_m . When there was change in level of heat, this also indicates change in energy production as well as energy storage in system as shown in Figure 8.4.

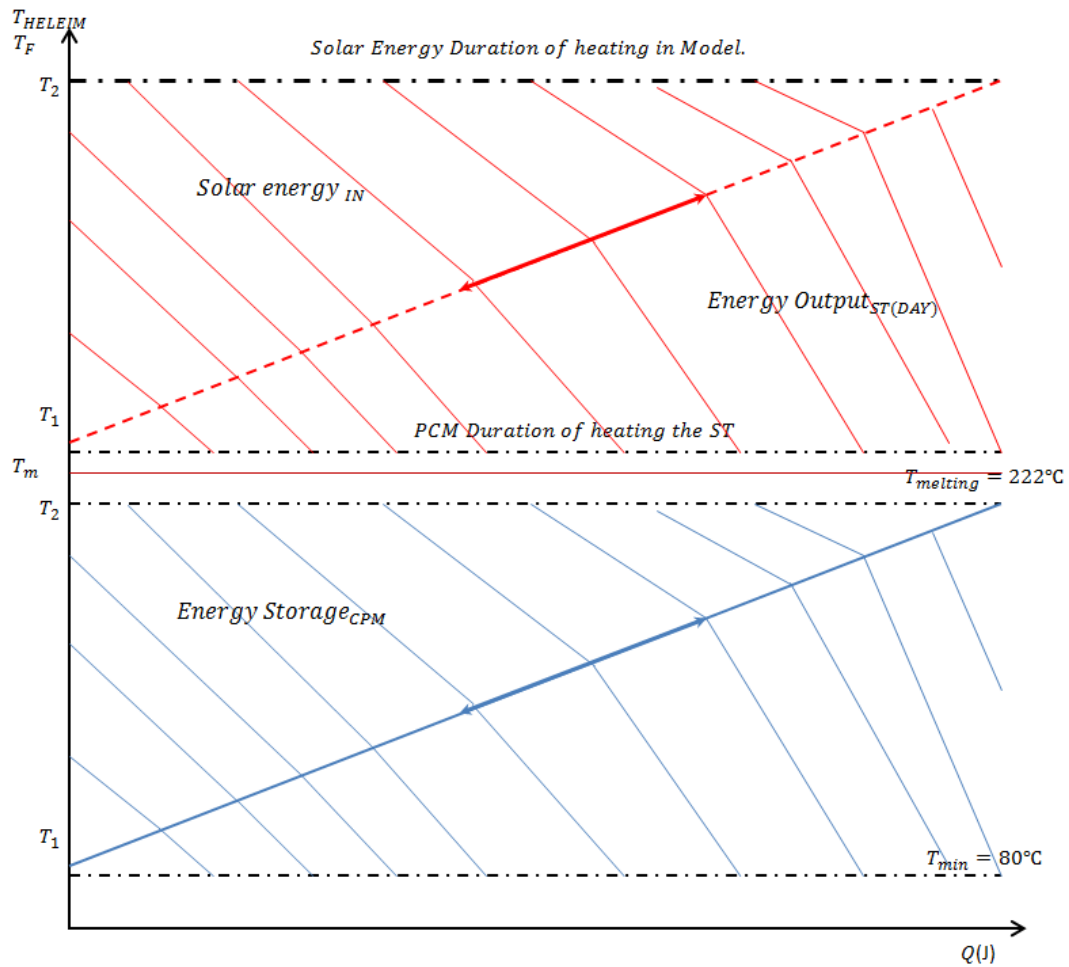


Figure 8.5 The Discussion results how system work in thermodynamic

From Figure 8.5 above, assuming all solar energy reflected on the parabolic dishes were all transferred and converted to energy by hybrid Stirling engine as well as stored in PCM-Storage, there was the need to apply the thermodynamic law. Hence based on this law, heat movement in the system can be obtained based on helium used with mass flow rate ' \dot{M} ', thermal conductivity of material ' c_p ' and different temperature ($T_2 - T_1$).

The helium gas in the close cycle absorbs heat from the solar field, transferred through the pipes to produce power directly during the day. The operation temperature increases through the day and this also increases the velocity of the helium flow within the system. On other hand, when the velocity of the helium increases, this reduces the energy storage as result of less time for heat transfer, thereby reducing the energy transmitted to the hybrid engine. But the result shows

that the system stores energy during heat transfer operation in the daytime as well as during the night. This indicates that the setback as result of high velocity of helium was compensated using air compressor to allow for increase in heat transfer in the storage medium irrespective of the velocity of the gas. The heat generation highly depends on the temperature of the system for both day and night. These temperatures vary depending on the time of the day, with minimum temperature ranging from 29°C to 120°C, maximum temperature between 50°C to 320°C, and a constant melting of the material which is 222°C.

However, the result shows that the operation temperature in the system was higher than the melting temperature after 11am until 3pm for more than 3 h. This period was the period of conversion of the storage material from solid to liquid state known as the charging process as shown in Figure 8.4. Due to the distribution pattern of the heat pipe inside the tank, the process of storing and discharging of heat was uneven.

For the discharging process, helium gas which goes to receiver of Stirling engine had higher temperature than the operation temperature of Stirling engine. This difference in temperature was almost constant during the discharging process, which makes power generation an ongoing process with time that period. Sometimes, this difference in temperature decreases as a result of the sunset, which also reduced the production of energy from 50W to 1W. All the energy generated under red and blue lines in Figure 8.6 are useful energy for the two periods. The first was the direct charging process of the hybrid Stirling engine and the second was the charging of the PCM-storage. In the middle of both stages is melting temperature which is property of the storage material. Furthermore, the material ($\text{KNO}_3\text{-NaNO}_3$) was used to store heat before melting temperature (222°C) was reached during the charging period, even though this temperature was not attained at some point to allow for change of state, there was increase heat energy to the material. During the discharging period, there was also heat supply to the Stirling engine even when the temperature of the material was below the melting temperature, which was a good property as shown in Figure 8.4. In summary, there are differences in energy output during the day and at night by the same hybrid engine and given as follows:

- ❖ Energy output during the day comes directly from sun, while at night PCM - storage supplies the heat energy (indirect).

- ❖ Energy output during the day was higher than the production at night.
- ❖ Energy was produced for longer period during the day as compared to a shorter period at night.
- ❖ There was need for thermal control when using the thermal storage, which was not required during the day.
- ❖ Increases and decreases of energy production depends on the availability of the sun during the day, but at night it dependant on the heat available in the storage.

8.3.4- Result of System is working for 24 h with Thermal Control System

There were different valves attached to the system to assist in controlling the flow of heat from one part of the system to another. Particularly, the heat energy going in and out of the thermal storage was carried out manually during the day and night.

After several tests the control position of the valves and exact amount of heat to be supplied to the engine was achieved as shown in Figure 8.6 and appendices (F). During the early h of morning on the test day (before 6:30am), there was no energy produced because sun is not available as shown from the temperature level, and there also no heat energy from PCM-storage. The remaining 24 h procedure is similar to the process without the thermal control system from sunrise to sunset (about 5:30pm). In summary, the system was shown have good production output in the first 18 h (approximately) of work.

After sunset at about 5:30 pm, the thermal control system was used to regulate the temperatures. The regulated energy output depends on the temperature input and output for storage and Stirling engine. For the below data, the gas flowing in the closed cycle with length of 15 m had a speed of 0.5 cycles per second, and mass flow rate of 0.025 kg/s. The following temperature produces the fixed energy output between 26 W and 29 W:

- | | |
|---------------------------------------------------------------------------------------------------------------------------------------------------------------------------------------------------|--------------------------------------------------------------------------------------------------------------------------------------------------------------------------------------------------------|
| <ul style="list-style-type: none"> ❖ Storage level:- <ul style="list-style-type: none"> ➤ Input temperature 64 °C. ➤ Output temperature 215 °C. | <ul style="list-style-type: none"> ❖ Stirling level:- <ul style="list-style-type: none"> ➤ Operation temperature 209 °C. ❖ Output temperature 70 °C. |
|---------------------------------------------------------------------------------------------------------------------------------------------------------------------------------------------------|--------------------------------------------------------------------------------------------------------------------------------------------------------------------------------------------------------|

Summary of events from the beginning to midnight (6:00 pm to 12:00 am) shown in Figure 8.6 are giving as follows:

- ❖ The output temperature of storage increased.
- ❖ The input temperature of storage decreased.
- ❖ There was energy production continuously from after sunset until nearly midnight.
- ❖ Stored energy level decreases with the passage of time.
- ❖ The total energy produced within the period between 6:00 pm to 12:00am was approximately 561.6kW.

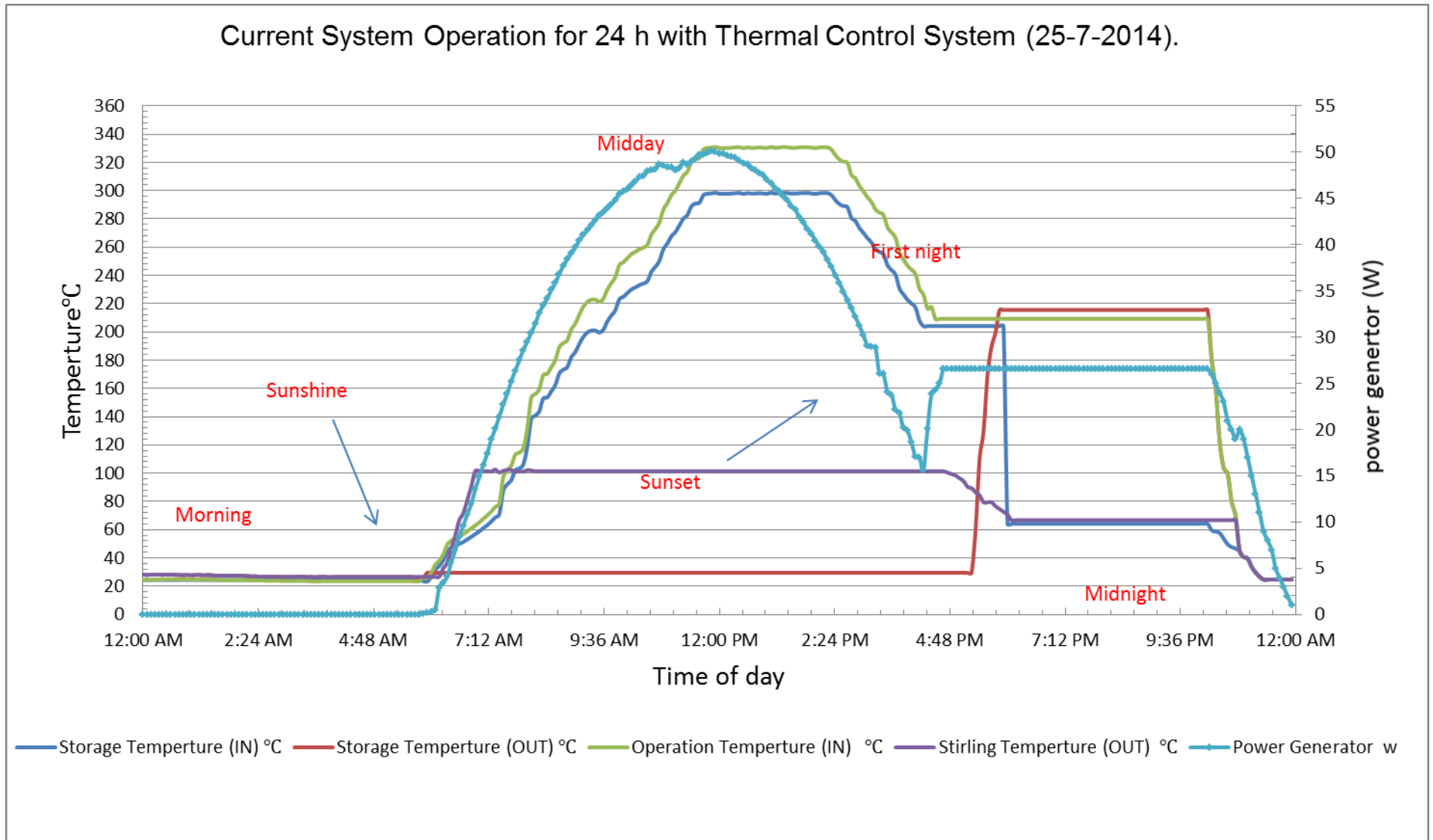


Figure 8.6 The result of system working for 24H with thermal control system (25-7-2014)

At about 11:00 am, sudden decline temperature level was observed, this also resulted in level of energy production, and this signifies that:

- ❖ The use of the control system was necessary to regulate amount of heat to engine.
- ❖ Increases the amount of energy produced.
- ❖ Extends the period of the output power with approximately 6 h.

Unfortunately, prototype with the control system stopped working after midnight, suggesting that all the energy had been consumed. This also indicates even though the manual control was a success, it was not adequate to accommodate the later part of the process particularly later part of the night.

8.4-Comparison for System working for 24 h with and without Thermal Control System

There are similarities and differences between results recorded of the system working with and without thermal control system for 24h. Summary of the Similarities are given as follows:

- ❖ Both results were dependent on the heat coming from sun to produce energy.
- ❖ Two previous cases have the same working pattern and results during the day as shown in Figure 8.6. Both results showed the hybrid engine started to produce power after 30 minutes sunrise. This amount increases as time of day passes until midday. At midday, energy production was constant with the highest value been 50W, which were similar in both results.
- ❖ After midday, the results showed decline in the level of energy produced for both cases.
- ❖ For the first 12h of work, the results were almost similar producing an approximately 0.689 kW.

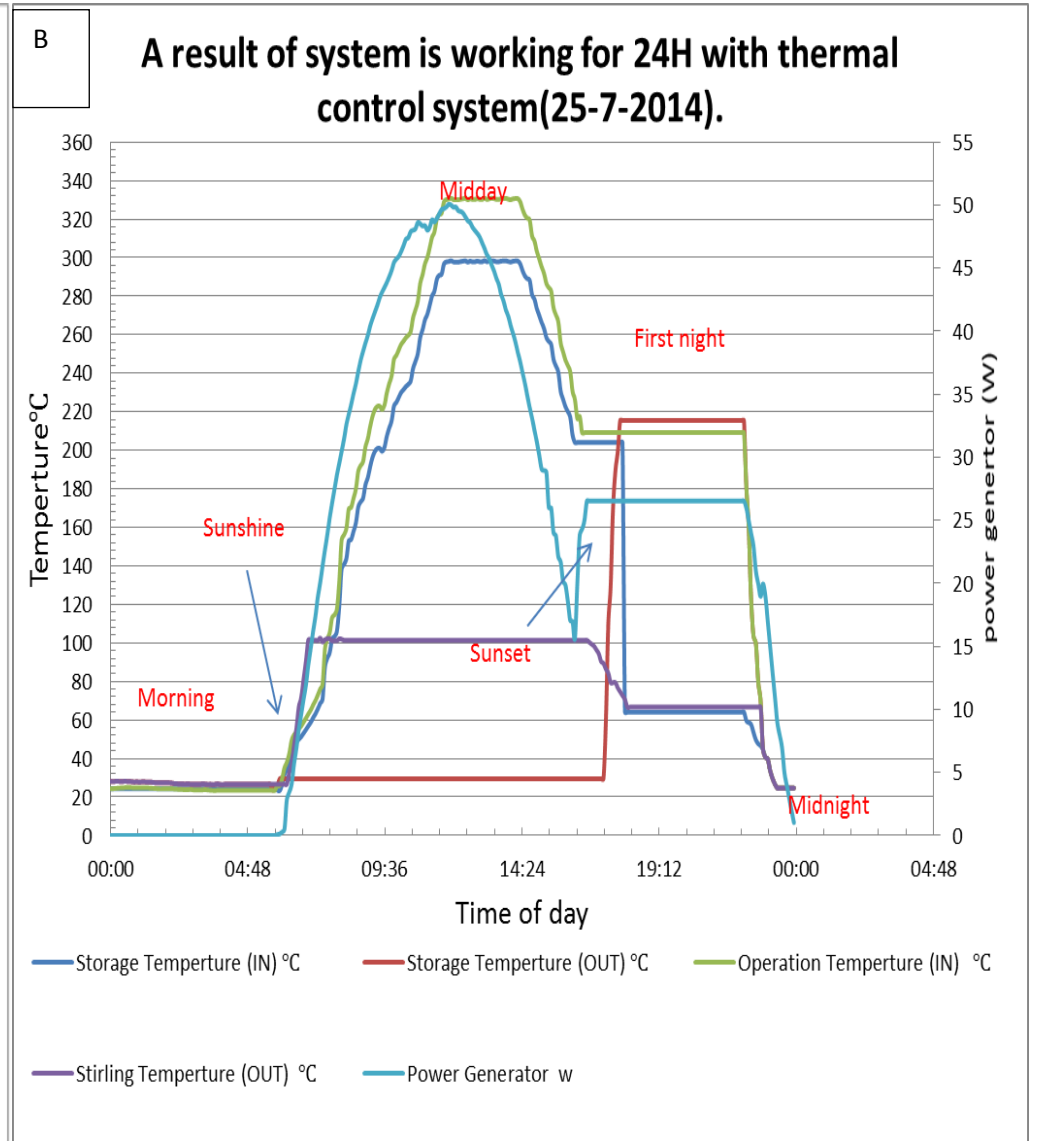
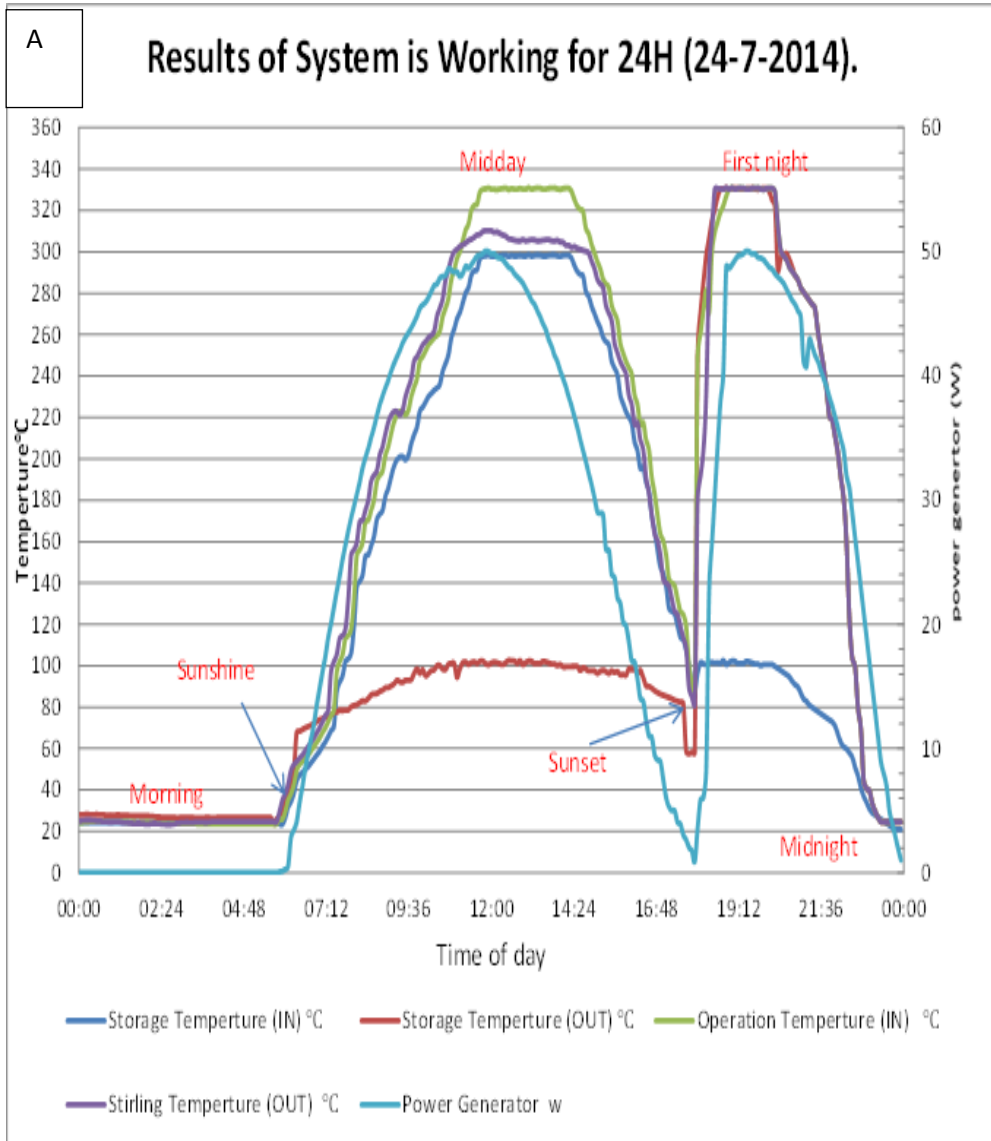


Figure 8.7 Compare between Results of System is working for 24h with and without Thermal Control in current system

The differences between the two results in Figure 8.7-A and 8.7-B are as follows:

- ❖ The major differences were at the point when the thermal control system was manually opened. The heat energy allowed from the storage to the engine was shown to generate between 26W - 29 W for Figure 8.7 - B.
- ❖ Figure 8.7-A without control system showed sudden rises increases in power production to the highest 50W when the valve was fully opened without control.
- ❖ This fluctuation in output power in Figure 8.7- A was not observed in Figure 8.7-B which was steady.
- ❖ This fluctuation in output power in Figure 8.7-A was approximately 2 h, while Figure 8.7-B showed longer period of sustained energy generation.
- ❖ This output power generated without control within 2 h was 0.360kW, while with control system there increase time as well as increase energy produced to 0.626 kW within 6 h.
- ❖ The total energy produced with control system for the 24 h was 1.3158kW higher than without control system of 1.049kW as shown in Table 8.1.
- ❖ It is obvious that the use of the control system has more advantages and generates much energy as compared to leaving the system without control.

Table 8.1 Compare Results of System is working for 24h with and without Thermal Control system

The total capacity produce in system	During day		During night	
	Power (kW)	Time (h)	Power (kW)	Time (h)
System is Working 24 h without thermal control system	0.6894	13	0.360	2
System is Working 24 h with thermal control system	0.6894	13	0.6264	6

8.5-Conclusion

This chapter discusses the results of current prototype unit in order to reveal the working of the system at night, during the 24h period (through day and night) and also how long the system working during 24h of day with / without the thermal control system. Finally, comparisons of the results of the system working for 24h with and without thermal control system are discussed.

The results of system were working through the night without a control system showed that:

- The thermal oil in heat exchanger of Stirling receiver was still hot at sunset, and had the ability to produce some energy. Hence, it was necessary to keep the valve closed until the heat within that system was used.
- There was a gradual decrease in the surrounding temperature or ambient temperature of the system until the early hours of the morning.
- There were heat losses in the heat exchanger of the Stirling receiver, which reduces the amount of heat that is transferred to the Stirling receiver to save energy.
- The maximum temperature reached was 320°C and maximum power generated was 50 W.
- The total working period for the first test for the night procedure was 2h, generating a total of 0.36 kW of energy.

Results of the system working for 24h without a control system demonstrated that:

- There was an extension of the production of energy for nearly 6h, producing a total of 1.04 kW of energy.
- The total working period for the day and night procedure was 15h
- The stored energy was consumed quickly. This could be a major disadvantage of the system.

Results of the system working for 24 h with a thermal control system revealed that:

- Thermal control system was operated based on fixed temperatures in and out of the PCM-storage system.
- Improved system performance work.
- Increased employment of the system for a period of up to 18 h.
- Increased total generated power up to 1.3kW.
- Improved system performance.

Finally, the system worked for 24 h with a thermal control system was better than system without it. The total energy produced with the control system was 1.3kW and this was higher than without control system which was only 1.04 kW.

CHAPTER(9):- Conclusions and Recommendations for Future Work

9.1- Introduction

This thesis focuses on improving the performance of solar thermal technologies. It entails the design and fabrication of a new solar parabolic concentrator connected to a PCM energy storage referred to as the “Electricity Energy Production by Hybrid Stirling Engine”. This prototype differs from the previous designs as it contains two main systems; with each one working independently or complementing each other to generate energy during the day and at night. However, other existing models use only solar concentrator technologies to generate power and store energy, so that energy intercept or solar energy reflected from the parabolic concentrator goes into the two systems at the same time which reduces the efficiency.

The prototype reported in this thesis is the first of its kind, as it combines the solar parabolic concentrator and solar energy storage connected into one system. The design, fabrication and testing of each part as well as the complete system are presented. The experimental results presented in this thesis on the hybrid Stirling engine proved to be very promising, and this is worthy of further investigation by other researchers.

The prototype was designed to work for 24 h, but the Stirling engine was shown to stop working by midnight due to defects within the heat exchanger. This problem was caused by the loss of heat by the storage exchanger, heat transfer system or heat loss in the heat exchanger of the Stirling engine, as these parts were not covered by insulation. However, the engine was shown to work until midnight, which is a positive step during the first test. It was also easy to deal with the technical errors developed in order to improve the efficiency in the future work. Also an economic analysis of prototype is one of the important aspects but was not analysed in this work, this is recommended for future work.

9.2- Conclusions

In this thesis, the concept of this design was to develop new solar parabolic prototype intended to generate energy using the modified hybrid Stirling engine for 24 h. It was achieved by using a new solar parabolic concentrators and PCM energy storage system. A hybrid Stirling engine was hand manufactured and tested in Oman. This hybrid engine was able to convert operational temperature to produce energy during the processes. The results from the experimental tests showed that hybrid engine was working, and that showed the ability to increase energy production from the morning until midday and then decrease as the sunset approaches.

The manufactured PCM-storage used $\text{NaNO}_3 + \text{KNO}_3$ material in the prototype unit, with connection to the solar parabolic concentrator as well as the hybrid Stirling engine. This thermal storage can provide the capacity for higher cycle efficiencies, through the use of molten sodium nitrate and potassium nitrate salt (heat transfer fluid) and used that heat at night.

In summary, chapter 1 revealed the thesis topic, the importance of duplication between solar thermal technologies as well as aims. Chapter 2 is reviews of solar thermal technologies, previous results and applications. Furthermore, Chapters 3, 4, 5 and 6 discussed the theoretical background, design and fabrication of different parts of the prototype model. This also included the assembling of the prototype and the description of the working of the prototype for different times of the day and night. Finally, chapters 7 and 8 discussed the result of the experimental testing of the prototype and comparison based on different scenarios for working of the system during the day, night and through 24 h.

9.2.1- Summary of Design and Fabrication

The design and fabrication of the prototype unit was carried out after a detailed literature review and consideration of different factors in order to arrive at best options to suit the prototype unit. The following are some properties of the prototype:

1. The two parabolic dish systems of prototype unit were elevated in order to guarantee safety, ensure they were firm and secured, and for easy maintenance.

2. The prototype dishes can be moved to any direction and position in spite of the excess weight as it has four wheels.
3. Two parabolic dish systems of the prototype were attached with a tracking system, which allows the dishes to rotate and locate the direction of the sun during the day.
4. The prototype used the flexible thermal pipe work on the parabolic dishes for various connections to allow the flexibility to employ the tracking system.
5. The thermal storage tank system was made to allow for additional tanks depending on the capacity required.
6. The distance between the thermal receiver and PCM-storage was short as well as the distance between PCM-storage and hybrid Stirling engine, in order to reduce heat loss during operations.
7. The prototype was designed to accommodate any change, modification and addition of extra devices in the future.

9.2.2- Summary of Experimental Results

The testing of the complete system was carried out and summary of the conclusions are given as follows:

- I. The prototype was designed to work based three processes, with each working independently or complementing the on. The first process allows the transfer of heat through the copper pipes with helium gas as the medium, collected at the cavity to PCM-storage done during the day. Secondly, the use of the absorbed heat directly to the Stirling engine, also happens during the day. The third process involves helium gas is transferring heat from the PCM-storage to the Stirling engine and this process occurs during the night time.
- II. The choice of Oman as a suitable location for this project because of the high level of solar radiation and clear sky on most days of the year. Some selected days within the summer in this location were used to measure the total capacity of storage and was estimated to be 5.02 kW.
- III. PCM-storage was expected to store total heat about 7 kW, this was after the melting temperature was reached with the operation temperature changing.
- IV. The focal and operation temperatures of both parabolic concentrators were shown to increase after sunshine until midday, and then declined afterwards.

The maximum operation temperatures of both dishes in both systems were 330°C in system 1 and 260°C in system 2.

- V. The efficiency of hybrid Stirling engine was low 17 % when compared with other Stirling engine prototype efficiencies up to 23 %.
- VI. The peak temperature obtained was 330 °C at about noon on a daily basis and at this point the maximum power generated was 45W. Considering the fluctuation of the intensity of the sunrays, this also varies the temperature, and a total day light hours of 17 h was obtained on the average.
- VII. The total energy produced with control system was 1.3 kW, which is higher than without a control system at was 1.04 kW. It was obvious that the use of control was better as more energy was generated.
- VIII. The prototype was designed to work throughout the day, but the experimental results showed that the system could not for 24 h, as the hybrid Stirling engine stopped working after midnight. This may be due to loss of heat within storage exchanger, heat transfer system or heat loss in heat exchanger of Stirling engine as these parts were not insulated.
- IX. The increase in the size of the parabolic dish was shown to increase the energy generated.
- X. When the efficiency of the reflective material increases, it increases the power generation.

9.3-Recommendations for Future Work

The successful implementation prototype power generation prototype is the first step in the development of new solar technology. This prototype will be further improved based challenges observed in the current work. It will afford more opportunity for further research, testing and development of improved thermal power generating system, considering the availability of the new research laboratory established by the author in Oman.

However, after extensive literature survey and testing of the current power generating prototype, there are different areas of further improvement based on the challenges observed. In view of this, the following are recommended for future work:

1. There is the need to develop a fast, robust and effective temperature control system for the receivers and PCM-storage of the current prototype. This will

improve the heat supply to the Stirling engine, thereby improving the power generation.

2. The need to develop an appropriate temperature control strategy in all part of the current prototype.
3. Developing an appropriate temperature control strategy in hybrid Stirling engine to increase its capacity and efficiency.
4. The charging and discharging control strategy in system for PCM-storage in current prototype is required in order to get more controlled heat transfer and improve power generating time.
5. The presence of air bubbles can cause opposite effect. There is the need to employ re-engineering technique of reflective flexible sheet when installed on the parabolic surface in order to reduce air bubbles; this will reduce the dispersion of solar radiation.
6. Developing heat transfer enhancement mechanisms in the current prototype in order to achieve better heat absorption and retention. This can be achieved by the use high thermal heat transfer materials such as petroleum derivatives (gasoline, kerosene).
7. Developing an appropriate system for the PCM-storage in the current prototype to be able to add multiple storages, so as to increase the time of operation, overall capacity and efficiency.
8. A detailed economic analysis of the potential of the prototype in the context of the present day, study the feasibility of manufacturing and marketing in the future.
9. A detailed analysis of the prospects for complementary operation thermal storage material. This may be either combining with the present material or use different materials entirely by comparing with current storage material ($\text{NaNO}_3 + \text{KNO}_3$) to get better efficiency and power generation.
10. An evaluation of the power quality and ancillary power benefits of the overall prototype and develop the power plant from a generation perspective.

9.4-Concluding Remarks for this Thesis

In this work, a theoretical and practical approach of parabolic dish concentrator presented was developed as part of a potential chain of solutions for improving the

performance of power generation and for making clean energy future. In this thesis, by use of design and fabrication of a new solar prototype, the most important parameters that describe the potential operation of the current prototype have been evaluated. From the results, it can be concluded that the prototype is technically feasible, implementable and also a retractable development.

Finally, it can be said that the main objective of this thesis has been achieved. The designed solar prototype will work for a longer time in any high solar radiation location, and also shown to be a significant scope for future work. The current prototype for generating energy from solar system has great potential of meeting the required energy demand as standard renewable source of energy as compared to the previous prototypes. This could be more dependent source of energy in the future in this age of green energy and clamour for the reduction of greenhouse effects.

References

- 1 Kleih, J. Dish-Stifling Test Facility. *Solar Energy Materials*.1991, Vol. 24, pp. 231 – 237.
- 2 Nuwayhid, R.Y. et al. 'The Realization of a Simple Solar Tracking Concentrator for University Research Applications'. *Renewable Energy*. 2001, Vol. 24, N°2, pp. 207 – 222.
- 3 Perez-Rabago, C.A. et al. Heat Transfer in a Conical Cavity Calorimeter for Measuring Thermal Power of a Point Focus Concentrator. *Solar Energy*. 2006, Vol. 80, N°11, pp. 1434 – 1442.
- 4 Kalogirou, S. et al. Low Cost High Accuracy Parabolic Troughs Construction and Evaluation. *Renewable Energy*. 1994, Vol. 5, N°1-4, pp. 384 - 386.
- 5 Palavras, I. and Bakos, G.C. Development of a Low-Cost Dish Solar Concentrator and its Application in Zeolite Desorption. *Renewable Energy*. 2006, vol. 31, N°15, pp. 2422 – 2431.
- 6 Baños, R., et al. Optimization methods applied to renewable and sustainable energy: A review. *Renewable and Sustainable Energy Reviews*, 2011.15(4): p. 1753-1766.
- 7 Sesto, E. and Casale C. Exploitation of wind as an energy source to meet the world's electricity demand. *Journal of Wind Engineering and Industrial Aerodynamics*, 1998.74–76(0): p. 375-387.
- 8 Krewitt, W., et al., Energy [R]evolution 2008—a sustainable world energy perspective. *Energy Policy*, 2009.37(12): p. 5764-5775.
- 9 Karatepe, Y., et al. The levels of awareness about the renewable energy sources of university students in Turkey. *Renewable Energy*, 2012.44(0): p. 174-179.
- 10 Kongtragool, B. and Wongwises S. A four power-piston low-temperature differential Stirling engine using simulated solar energy as a heat source. *Solar Energy*, 2008.82(6): p. 493-500.
- 11 El-Ghonemy, A.M.K. Water desalination systems powered by renewable energy sources: Review. *Renewable and Sustainable Energy Reviews*, 2012.16(3): p. 1537-1556.
- 12 Kongtragool, B. and Wongwises S. A review of solar-powered Stirling engines and low temperature differential Stirling engines. *Renewable and Sustainable Energy Reviews*, 2003.7(2): p. 131-154.
- 13 Kolin, Ivo. *Stirling Motor - History, Theory, Practice*. Dubrovnik: Zagreb University, Publications, Ltd., 1991.
- 14 Dickinson, H. W. *The Steam-Engine to 1830*. Oxford: Oxford University Press, 1958.
- 15 Hargreaves, C.M. *The Philips Stirling Engine*. Amsterdam: Elsevier Science Publishers, 1991.

- 16 Stirling and Hot Air Engine Home Page. *Solar Stirling Engines*. [Online]. 2009. [Accessed 23, July, 2014] Available from: <http://www.stirlingengines.org.uk/gifs/sunpower/mcd.gif>.
- 17 Lovegrove, K. et al. A new paraboloidal dish ,solar concentrator. *Solar Energy*, 2011.85(4): p. 620-626.
- 18 Danielli, A. et al. Improving the optical efficiency of a concentrated solar power field using a concatenated micro-tower configuration. *Solar Energy*, 2011.85(5): p. 931-937
- 19 Xu, E., et al. Modelling and simulation of 1 MW DAHAN solar thermal power tower plant. *Renewable Energy*, 2011.36(2): p. 848-857.
- 20 Segal, A. and Levy M. Modular solar chemical heat pipe for a parabolic dish: conceptual design and model calculations. *Solar Energy*, 1993.51(5): p. 419-422.
- 21 Chong, K.K., et al. Cost-effective solar furnace system using fixed geometry Non-Imaging Focusing Heliostat and secondary parabolic concentrator. *Renewable Energy*, 2011.36(5): p. 1595-1602.
- 22 <http://www.energybulletin.net/stories/2011-07-26/bright-future-solar-powered-factories>
- 23 Wu, S.-Y., et al. A parabolic dish/AMTEC solar thermal power system and its performance evaluation. *Applied Energy*, 2010, 87(2): p. 452-462.
- 24 http://www.energylan.sandia.gov/sunlab/PDFs/solar_overview.pdf, last accessed 23 Sep 2007.
- 25 Journée, M. and Bertrand C. Quality control of solar radiation data within the RMIB solar measurements network. *Solar Energy*, 2011.85(1): p. 72-86.
- 26 Vijayakumar, G., et al. Analysis of short-term solar radiation data. *Solar Energy*, 2005.79(5): p. 495-504.
- 27 Ávila-Marín, A.L. Volumetric receivers in Solar Thermal Power Plants with Central Receiver System technology: A review. *Solar Energy*, 2011.85(5): p. 891-910.
- 28 Xie, G.N. et al. Optimization of compact heat exchangers by a genetic algorithm. *Applied Thermal Engineering*, 2008.28(8–9): p. 895-906.
- 29 García, D. and Prieto J.I., A non-tubular Stirling engine heater for a micro solar power unit. *Renewable Energy*, 2012.46(0): p. 127-136.
- 30 Puech, P. and Tishkova V., Thermodynamic analysis of a Stirling engine including regenerator dead volume. *Renewable Energy*, 2011.36(2): p. 872-878.
- 31 Kongtragool, B. and Wongwises S., A review of solar-powered Stirling engines and low temperature differential Stirling engines. *Renewable and Sustainable Energy Reviews*, 2003.7(2): p. 131-154.
- 32 Pierre G. *Stirling engine*. [Online]. 2003. [Accessed 11, August, 2014] Available from: <http://www.robertstirlingengine.com/other.php>.
- 33 Kongtragool, B. and Wongwises, S. A review of solar-powered Stirling engines and low temperature differential Stirling engines. *Renewable and Sustainable Energy Reviews*, 2003, 7(2): p. 131-154.

- 34 University of Ohio. Chapter 3: First law of thermodynamic.
http://www.ohio.edu/mechanical/thermo/Intro/Chapt.1_6/Chapter3b.html
- 35 Thombare, D.G. and Verma S.K., Technological development in the Stirling
 cycle engines. *Renewable and Sustainable Energy Reviews*, 2008, 12(1): p.
 1-38.
- 36 [http://www.ditii.com/2010/09/29/vdara-hotel-at-citycenter-solar-concentrator-](http://www.ditii.com/2010/09/29/vdara-hotel-at-citycenter-solar-concentrator-in-las-vegas/)
[in-las-vegas/](http://www.pre.ethz.ch/research/projects/?id=solarhydroviaredox)
<http://www.pre.ethz.ch/research/projects/?id=solarhydroviaredox>).
- 37 D.G. Thombarea,_, Vermab S.K., Technological development in the Stirling
 cycle
 engines,<http://www.stirlingengines.org.uk/manufact/manf/usa/new2.htm>.
- 38 Snyman H., et al examination of Design analysis methods for Stirling
 engines. *Journal of energy in South Africa*, 2008, Vol.-19 No.-3, page 4-
 19.South Africa
- 39 Khan K.Y., et al examination of solar dish stirling system and its economic
 prospect in Bangladesh.*Internationaljournal of electrical & computer*
sciences (2001) IJECS-IJENS Vol: 11 No: 04, page 7-Bangladesh.
- 40 Mancini T.R. examination of solar-electric dish stirling system development.
 (year) USA
- 41 Kyei-Manu F. and Obodoako A. examination of solarstirling-engine water
 pump proposal draft. 2005, Page 1-15.
- 42 Heand M. and Sanders S. *examination of design of a 2.5kW low temperature*
stirling engine for distributed solar thermal generation. American institute of
aeronautics and astronautics, (year)page 1-8, USA
- 43 Sukhatme S.P. *Principles of thermal collection and storage*. McGraw Hill,
 New Delhi, 2007.
- 44 Duffie,J.A and Beckman Solar engineering of thermal processes. John willy&
 sons, INC., London, 2006.
- 45 Rai, G.D *solar energy utilisation*. Khanna publishers, India, 2001. Renewable
 Energy focus handbook (2009), ELSEVIER page 335.
- 47 Valentina A. S., et al *Daniele New Trends in Designing Parabolictrough*
Solar Concentrators and Heat Storage Concrete Systems in Solar Power
Plants. Croatia, Italy ,2010.
- 48 FOLARANMI, Joshua (2009) Design, Construction and Testing of a
 Parabolic Solar Steam Generator. *Journal of Practices and Technologies*,
 ISSN 1583-1078. Vol-14, page 115-133, Leonardo
- 49 Xiao G. *A closed parabolic trough solar collector*. 2007. Version 2 Page 1-28
- 50 Brooks, M.J., et al. Performance of a parabolic trough solar collector. *Journal*
of Energy in Southern Africa, 2006, Vol-17, page 71-80 Southern Africa
- 52 Heat storage media; Rainer Tamme (DLR), Thomas Bauer (DLR), Erich
 Hahne (University of Stuttgart).
- 53 State of the art on high temperature thermal energy storage for power
 generation. Part 1- Concepts, materials and modellization; Antoni Gil, Marc

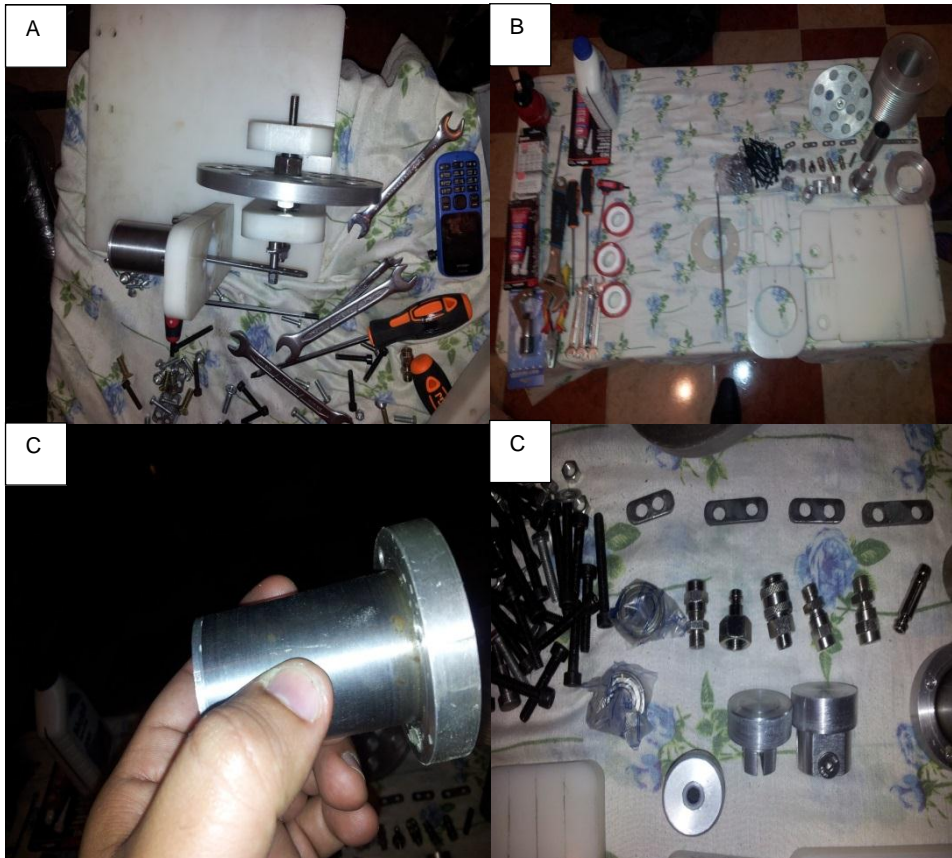
- Medrano, Ingrid Martorell, AnaLázaro, Pablo Dolado, Belen Zalba, Luisa F. Cabeza.
- 54 Technology of latent heat storage for high temperature application: a review, *ISIJ International*, Vol. 50 (2010), No. 9, pp. 1229–1239.
- 55 Mathur, K. N. “Heat storage for solar energy space heating,” *Solar Energy*, vol. 6, no. 3, pp. 110–112, 1962. [View at Scopus](#).
- 56 Kenisarin M., Mahkamov K. Solar energy storage using phase change materials, *Renewable and Sustainable Energy Reviews* 11 (2007) 1913-1965.
- 57 George A. Handbook of thermal design. In: Guyer C, editor. Phase change thermal storage materials. McGraw Hill Book, 1989.
- 58 Farid, M.M. et al. A review on phase change energy storage: materials and applications, *Energy Conversion and Management* 45, 2004 1597-1615.
- 59 Abhat, A. Low temperature latent heat thermal energy storage: heat storage materials, *Solar Energy* 30, 1983, 313-332.
- 60 Mehling, H., Cabeza, L.F. Phase change materials and their basic properties, *Thermal Energy Storage for Sustainable Energy Consumption*. 2007, 257-277.
- 61 T. Wada, R. Yamamoto, Studies on salt hydrate for latent heat storage. Crystal nucleation of sodium acetate trihydrate catalyzed by tetrasodium pyrophosphate decahydrate. *The Chemical Society of Japan*, 55, 1982, 3603-3606.
- 62 J. Li, et al Investigation of a eutectic mixture of sodium acetate trihydrate and urea as latent heat storage. *Solar Energy*. 47, 1991, 443-445.
- 63 Advanced high temperature latent heat storage system-design and test results; D. Laing, T. Bauer, W.-D. Steinmann, D. Lehmann; Institute of Technical Thermodynamics, German Aerospace Center (DLR) Pfaffenwaldring 38-40, 70569 Stuttgart, Germany.
- 64 Cabeza LF, et al A. *Review of Solar Thermal Storage Techniques and Associated Heat Transfer Technologies*. Proceedings of the IEEE 2012; 100(2):525-38.
- 65 Herrmann U, and Kearney DW. Survey of thermal energy storage for parabolic trough power plants. *Journal of Solar Energy Engineering, Transactions of the ASME* 2002;124(2):145-52.
- 66 Mathur A. Latent Heat Storage for Concentrating Solar Power: Terrafore; 2009.
- 67 Mathur A. Heat Transfer and Latent Heat Storage in Inorganic Molten Salts for Concentrating SOLar Plants: Terrafore; 2011.
- 68 Woody, T. Alternative Energy Projects Stumble on a Need for Water. *New York Times*, September 29, 2009.
- 69 U.S. Department of Energy Report to Congress. *Concentrating Solar Power Commercial Application Study: Reducing Water Consumption of Concentrating Solar Power Electricity Generation*, 2007.

- 70 Leonard D. J. A Review of Test Results on Solar Thermal Power Modules With Dish-Mounted Stirling and Brayton Cycle Engines. *Journal of Solar Energy Engineering*, Vol. 110, 1988, pp. 268-274.
- 71 Yuting Wu, et al. Dynamic Simulation of Closed Brayton Cycle Solar Thermal Power System. *3rd International Conference on Sustainable Energy Technologies, 2004, Nottingham, UK, 2004.*
- 72 International Energy Agency. Technology Characterization Solar Parabolic Trough.SolarPaces. [Online]. 2009. [Accessed 20, July, 2014] Available from: http://www.solarpaces.org/CSP_Technology/docs/solar_trough.pdf.
- 73 International Energy Agency. Technology Characterization Solar Power Towers.SolarPaces. [Online]. 2009. [Accessed 20, July, 2014] Available from: http://www.solarpaces.org/CSP_Technology/docs/solar_tower.pdf.
- 74 International Energy Agency. Technology Characterization Solar Dish Systems.SolarPaces. [Online]. 2009. [Accessed 20, July, 2014] Available from: http://www.solarpaces.org/CSP_Technology/docs/solar_dish.pdf.
- 75 Antoni G, et al. State of the art on high temperature thermal energy storage for power generation. *Renewable and Sustainable Energy Reviews*, Vol 14, 2010, pp. 31-55.
- 76 Valmiki,M.M, et al. A Novel Application of a Fresnel Lens for a Solar Stove and Solar Heating, Submitted to *Journal of Renewable Energy* , 2009.
- 77 Incropera, F. P. and DeWitt, D. P. *Introduction to Heat Transfer*. Fourth ed. John Wiley and Sons, Inc. 2002.
- 78 Robert W. S. *Process Heat Transfer, Principles and Applications*.TNQ books and Journal Ltd, 2014.
- 79 Kongtragool, B. and Wongwises, S. A review of solar-powered Stirling engines and low temperature differential Stirling engines. *Renewable and Sustainable Energy Reviews*, 2003. 7(2): p. 131-154.
- 90 Kolin, Ivo. *Stirling Motor - History, Theory, Practice*. Dubrovnik : Zagreb University Publications, Ltd., 1991.
- 91 Dickinson, H. W. *The Steam-Engine to 1830*. Oxford : Oxford University Press, 1958.Hargreaves, C.M. *The Philips Stirling Engine*. Amsterdam : Elsevier Science Publishers,1991.
- 92 Stirling and Hot Air Engine Home Page. Solar Stirling Engines. [Online]. 2009. [Accessed 2, July, 2013] Available from: <http://www.stirlingengines.org.uk/gifs/sunpower/mcd.gif>.
- 93 Lovegrove, K., et al. A new 500m² paraboloidal dish solar concentrator. *Solar Energy*, 2011. 85(4): p. 620-626.
- 94 Danielli, A.,et al. Improving the optical efficiency of a concentrated solar power field using a concatenated micro-tower configuration. *Solar Energy*, 2011, 85(5): p. 931-937.
- 95 Xu, E., et al. Modelling and simulation of 1 MW DAHAN solar thermal power tower plant. *Renewable Energy*, 201. 36(2): p. 848-857.

- 96 Segal, A. and Levy, M. Modular solar chemical heat pipe for a parabolic dish: conceptual design and model calculations. *Solar Energy*, 1993. 51(5): p. 419-422.
- 97 Kongtragool, B. and S. Wong wiset / Renewable and Sustainable Energy Reviews 7 , 2003, 131–154.

Appendices Section

Appendices (A): The processes of fabrication hybrid Stirling engine before install in prototype model.



Appendices (B):The processes of design, fabrication parabolic dish concentrators,before install in prototype model.



Appendices (C):The processes fabrication PCM-Storage in Oman,before install in prototype model.



Appendices (D): Experiment testing of $\text{KNO}_3\text{-NaNO}_3$ as thermal heat storage before install in prototype



t=0 min, temperature 22°C, the thickness of propellant layer is small



At t=17 min, 95°C, sorbitol starts to melt



At 31 min, 140°C, thin layer of liquid appears at the bottom



At 44 min, 175°C, almost all sorbitol melts, liquid layer at the bottom is about 3 mm



5

60 min, 190°C, all sorbitol melts, liquid layer at the bottom is about 3 mm



6

1h 15 min, 190°C, without changes



7

1h 30 min, 190°C, without changes. It is clear that at this temperature propellant will not melt completely. So I start to increase temperature.



8

1h 35 min, 203°C, small bubbles appears at the bottom, sorbitol starts to decompose



9

1h 40 min, 225°C, liquid layer at the bottom starts to grow



10

1h 50 min, 225°C, The thickness of propellant layer is 3cm



11



12

2h, 230 °C, almost half of propellant completely melts, but decomposition of sorbitol starts to accelerate, so I decide to stop further heating.

Appendices (E):The experiment data of prototype modelworking during a day without hybrid Stirling engine (focal temperature, solar radiation and ambient temperature)

Time Stamp	Solar Radiation	Ambient temperature	Focal temperature	Output temperature	Input temperature
hh:mm	W/m ²	°C	centre of thermal receiver °C	He °C	He °C
00:00	0	28.14	24.33	24.33	24.33
00:05	0	28	24.36	24.36	24.36
00:10	0	28.2	24.51	24.51	24.51
00:15	0	28.19	24.62	24.62	24.62
00:20	0	28.12	24.74	24.74	24.74
00:25	0	28.05	24.73	24.73	24.73
00:30	0	28.25	24.91	24.91	24.91
00:35	0	28.11	24.93	24.93	24.93
00:40	0	28.08	24.93	24.93	24.93
00:45	0	27.95	24.85	24.85	24.85
00:50	0	27.78	24.78	24.78	24.78
00:55	0	27.95	24.73	24.73	24.73
01:00	0	27.75	24.73	24.73	24.73
01:05	0	27.89	24.75	24.75	24.75
01:10	0	27.95	24.73	24.73	24.73
01:15	0	27.75	24.69	24.69	24.69
01:20	0	27.78	24.71	24.71	24.71
01:25	0	27.75	24.64	24.64	24.64
01:30	0	27.58	24.53	24.53	24.53
01:35	0	27.42	24.41	24.41	24.41
01:40	0	27.46	24.31	24.31	24.31
01:45	0	27.46	24.23	24.23	24.23
01:50	0	27.43	24.26	24.26	24.26
01:55	0	27.41	24.36	24.36	24.36
02:00	0	27.48	24.34	24.34	24.34
02:05	0	27.36	24.33	24.33	24.33
02:10	0	27.22	24.32	24.32	24.32
02:15	0	26.93	24.1	24.1	24.1
02:20	0	26.91	24.06	24.06	24.06
02:25	0	26.85	24.04	24.04	24.04
02:30	0	26.86	23.97	23.97	23.97
02:35	0	26.74	23.82	23.82	23.82
02:40	0	26.77	23.88	23.88	23.88
02:45	0	26.76	23.93	23.93	23.93
02:50	0	26.61	23.91	23.91	23.91
02:55	0	26.57	23.69	23.69	23.69

03:00	0	26.73	23.77	23.77	23.77
03:05	0	26.68	23.72	23.72	23.72
03:10	0	26.72	23.64	23.64	23.64
03:15	0	26.87	23.81	23.81	23.81
03:20	0	26.66	23.78	23.78	23.78
03:25	0	26.56	23.68	23.68	23.68
03:30	0	26.6	23.51	23.51	23.51
03:35	0	26.43	23.43	23.43	23.43
03:40	0	26.64	23.41	23.41	23.41
03:45	0	26.82	23.53	23.53	23.53
03:50	0	26.54	23.53	23.53	23.53
03:55	0	26.44	23.46	23.46	23.46
04:00	0	26.66	23.59	23.59	23.59
04:05	0	26.67	23.67	23.67	23.67
04:10	0	26.48	23.57	23.57	23.57
04:15	0	26.29	23.35	23.35	23.35
04:20	0	26.16	23.21	23.21	23.21
04:25	0	25.9	23.13	23.13	23.13
04:30	0	25.85	22.96	22.96	22.96
04:35	0	25.94	22.81	22.81	22.81
04:40	0	25.79	22.81	22.81	22.81
04:45	0	25.45	22.65	22.65	22.65
04:50	0	25.44	22.72	22.72	22.72
04:55	0	25.33	22.65	22.65	22.65
05:00	0	25.08	22.59	22.59	22.59
05:05	0	24.76	22.45	22.45	22.45
05:10	0	24.73	22.19	22.19	22.19
05:15	0	24.8	21.87	21.87	21.87
05:20	0	24.95	21.73	21.73	21.73
05:25	0	24.91	21.79	21.79	21.79
05:30	0	24.59	21.79	21.79	21.79
05:35	0	24.48	21.64	21.64	21.64
05:40	0	24.93	21.78	21.78	21.78
05:45	0	25.43	22.04	22.04	22.04
05:50	0	25.48	21.94	21.94	21.94
05:55	0	25.24	21.8	21.8	21.8
06:00	0	24.85	21.58	21.58	21.58
06:05	0	24.65	22.45	22.45	22.45
06:10	2.0055	24.73	26.16	26.32952	23.34
06:15	8.56	24.63	25.896	34.174	24.41
06:20	14.03	24.68	29.481792	36.988	26.42
06:25	23.25	25.56	35.1504	41.342	29.53
06:30	36.2	26.21	38.0448	48.02	34.3
06:35	49.26	26.32	42.5232	50.8256	36.304

06:40	62.17	26.56	49.392	52.2144	37.296
06:45	79.1	26.83	52.27776	53.8496	38.464
06:50	94.36	27.15	53.70624	55.2832	39.488
06:55	116.71	27.48	55.38816	57.232	40.88
07:00	136.1	27.71	56.86272	59.2256	42.304
07:05	157.09	27.97	58.8672	61.3312	43.808
07:10	176.03	28.27	60.91776	63.28	45.2
07:15	201.94	28.66	63.08352	65.8336	47.024
07:20	224.79	29.04	65.088	68.1184	48.656
07:25	248.81	29.19	67.71456	70.896	50.64
07:30	272.55	29.54	70.06464	74.0096	52.864
07:35	300	29.41	72.9216	76.2944	54.496
07:40	324.17	29.86	76.12416	94.3768	67.412
07:45	350.72	30.36	78.47424	99.2712	70.908
07:50	377.86	30.47	97.07328	102.4366	73.169
07:55	403.81	30.77	102.10752	109.956	78.54
08:00	431.71	30.75	105.36336	111.384	79.56
08:05	457.43	30.81	113.0976	114.212	81.58
08:10	483.05	30.81	114.5664	128.0048	91.432
08:15	509.1	31.44	117.4752	149.17	106.55
08:20	532.34	31.7	131.66208	151.76	108.4
08:25	555.34	31.85	153.432	155.05	110.75
08:30	580.53	32.23	156.096	164.8556	117.754
08:35	609.16	32.59	159.48	165.62	118.3
08:40	632.29	32.51	169.56576	170.2792	121.628
08:45	655.39	33.05	170.352	175.0112	125.008
08:50	679.43	33.71	175.14432	183.897	131.355
08:55	702	33.92	180.01152	186.7698	133.407
09:00	727.16	33.96	189.1512	188.7354	134.811
09:05	751.71	34.39	192.10608	196.2352	140.168
09:10	773.58	34.6	194.12784	200.2336	143.024
09:15	794.76	35.06	201.84192	206.4272	147.448
09:20	816.53	35.1	205.95456	211.7976	151.284
09:25	839	35.44	212.32512	215.0904	153.636
09:30	858	35.79	217.84896	216.6192	154.728
09:35	874.52	36.5	221.23584	216.7368	154.812
09:40	889.21	36.21	222.80832	215.0904	153.636
09:45	907.88	36.07	222.92928	217.2856	155.204
09:50	926.02	36.51	221.23584	223.5576	159.684
09:55	942.59	36.49	223.49376	228.1048	162.932
10:00	958.59	36.61	229.94496	232.1424	165.816
10:05	974.38	37.8	234.62208	240.4332	171.738
10:10	988.56	38.64	238.77504	242.382	173.13
10:15	1004.1	37.78	247.30272	245.1834	175.131

10:20	1018.26	38.46	249.3072	247.9848	177.132
10:25	1030.64	37.33	252.18864	249.5682	178.263
10:30	1043.84	37.72	255.07008	251.314	179.51
10:35	1055.97	38.31	256.69872	252.532	180.38
10:40	1066.42	38.45	258.4944	254.352	181.68
10:45	1075.71	39.25	259.7472	261.366	186.69
10:50	1086.79	39.26	261.6192	265.3042	189.503
10:55	1094.05	38.57	268.8336	269.731	192.665
11:00	1100.6	38.53	272.88432	278.7008	199.072
11:05	1110.84	39.53	277.4376	283.0674	202.191
11:10	1114.78	39.66	286.66368	288.5652	206.118
11:15	1116.38	39.67	291.15504	291.753	208.395
11:20	1120.03	37	296.80992	296.786	211.99
11:25	1116.69	38.72	300.0888	302.022	215.73
11:30	1123.02	39.82	305.2656	304.7352	217.668
11:35	1137.43	39.97	310.6512	311.3516	222.394
11:40	1134.79	39.46	313.44192	313.5412	223.958
11:45	1135.21	39.86	320.24736	314.139	224.385
11:50	1138.29	39.97	322.49952	319.8888	228.492
11:55	1141.38	39.67	323.1144	321.048	229.32
12:00	1139.16	40.08	329.02848	324.1644	231.546
12:05	1140.18	40.13	330.2208	330.4784	236.056
12:10	1140.89	39.63	333.42624	331.702	236.93
12:15	1138.26	39.42	339.92064	334.628	239.02
12:20	1136.68	39.77	341.1792	341.25	243.75
12:25	1132.91	39.92	344.1888	342.615	244.725
12:30	1128.72	39.81	351	348.67812	249.0558
12:35	1122.69	39.58	352.404	350.8008	250.572
12:40	1116.44	39.43	358.640352	355.9374	254.241
12:45	1108.33	39.83	360.82368	357.4298	255.307
12:50	1099.29	40.24	366.10704	360.9753	257.8395
12:55	1093.69	40.15	366.64208	362.7936	263.424
13:00	1084.28	40.19	369.28888	360.3572	257.398
13:05	1073.86	39.68	369.33056	358.1298	255.807
13:10	1063.07	40.23	368.65312	355.1198	253.657
13:15	1050.72	39.42	368.36208	354.8188	253.442
13:20	1039.88	39.89	365.26608	352.2302	251.593
13:25	1029.55	40.12	364.95648	351.568	251.12
13:30	1015.75	40.1	362.29392	350.9058	250.647
13:35	1003.54	39.64	361.6128	349.762	249.83
13:40	986.88	39.7	360.93168	351.267	250.905
13:45	973.53	39.65	359.7552	350.3038	250.217
13:50	957.46	40.07	361.3032	348.6784	249.056
13:55	941.55	39.98	360.31248	348.859	249.185

14:00	921.14	39.77	358.64064	343.0798	245.057
14:05	903.29	39.55	358.8264	338.7454	241.961
14:10	885.08	39.58	352.88208	340.431	243.165
14:15	867.39	39.25	348.42384	332.1234	237.231
14:20	848.43	39.46	350.1576	332.304	237.36
14:25	828.34	39.03	341.61264	328.3308	234.522
14:30	807.84	39.03	341.7984	319.9896	228.564
14:35	785.78	39.06	337.71168	316.1088	225.792
14:40	764.97	39.11	329.13216	313.11	223.65
14:45	741.62	39.11	325.14048	311.64	222.6
14:50	719.25	39.12	322.056	310.758	221.97
14:55	695.03	38.32	320.544	302.5554	216.111
15:00	670.93	38.89	319.6368	300.1446	214.389
15:05	646.14	38.59	311.19984	294.8638	210.617
15:10	621.21	38.24	308.72016	291.1328	207.952
15:15	596.81	38.28	303.28848	287.1148	205.082
15:20	571.67	38.25	299.45088	283.7835	202.7025
15:25	545.48	37.78	295.31808	278.768	199.12
15:30	520.02	38.19	291.8916	276.584	197.56
15:35	493.21	38.38	286.7328	274.904	196.36
15:40	466.59	38.12	284.4864	266.5026	190.359
15:45	440.25	37.78	282.7584	262.8444	187.746
15:50	413.81	38.26	274.11696	259.2954	185.211
15:55	386.53	37.93	270.35424	248.71	177.65
16:00	360.36	38.14	266.70384	244.2412	174.458
16:05	334	37.47	255.816	240.0916	171.494
16:10	308.24	37.59	251.21952	237.272	169.48
16:15	283.72	37.46	246.95136	234.2396	167.314
16:20	258.45	38.64	244.0512	224.2422	160.173
16:25	233.63	38.5	240.93216	219.9946	157.139
16:30	209.26	38.58	230.64912	210.4704	150.336
16:35	186.03	37.67	226.28016	211.603	151.145
16:40	163.98	38.38	216.48384	203.364	145.26
16:45	142.05	37	217.6488	198.7272	141.948
16:50	53.91	35.42	209.1744	185.612	132.58
16:55	38.49	35.32	204.40512	178.115	127.225
17:00	34.64	34.99	190.9152	168.028	120.02
17:05	31.17	34.51	183.204	159.159	113.685
17:10	27.43	34.15	172.8288	156.0636	111.474
17:15	23.47	33.85	163.7064	149.184	106.56
17:20	19.48	33.65	160.52256	137.844	98.46
17:25	15	33.43	153.4464	136.122	97.23
17:30	10.75	33.21	141.7824	134.736	96.24
17:35	5.82	32.99	140.0112	110.2116	91.843

17:40	3.25	32.67	138.5856	105.2352	87.696
17:45	3	32.51	132.25392	103.9584	86.632
17:50	2.98	32.32	126.28224	99.3384	82.782
17:55	2.65	32.12	124.75008	94.6608	78.884
18:00	2.2	31.98	119.20608	90.18	75.15
18:05	1.5	31.81	74.475	74.475	74.475
18:10	1.2	31.71	70.848	70.848	70.848
18:15	0	31.57	67.597	67.597	67.597
18:20	0	31.41	64.438	64.438	64.438
18:25	0	31.26	63.998	63.998	63.998
18:30	0	31.1	60.774	60.774	60.774
18:35	0	31.01	57.52	57.52	57.52
18:40	0	30.91	54.207	54.207	54.207
18:45	0	30.84	53.846	53.846	53.846
18:50	0	30.8	50.598	50.598	50.598
18:55	0	30.64	47.175	47.175	47.175
19:00	0	30.52	43.888	43.888	43.888
19:05	0	30.58	40.845	40.845	40.845
19:10	0	30.47	37.786	37.786	37.786
19:15	0	30.33	34.944	34.944	34.944
19:20	0	30.18	34.749	34.749	34.749
19:25	0	30.42	32.076	32.076	32.076
19:30	0	30.37	32.04	32.04	32.04
19:35	0	30.21	29.293	29.293	29.293
19:40	0	30.19	26.8963	26.8963	26.8963
19:45	0	30.03	26.57	26.57	26.57
19:50	0	29.92	26.52	26.52	26.52
19:55	0	29.72	26.43	26.43	26.43
20:00	0	29.5	26.28	26.28	26.28
20:05	0	29.42	26.12	26.12	26.12
20:10	0	29.22	25.88	25.88	25.88
20:15	0	29.29	25.72	25.72	25.72
20:20	0	29.21	25.62	25.62	25.62
20:25	0	29.19	25.61	25.61	25.61
20:30	0	29.33	25.55	25.55	25.55
20:35	0	29.47	25.44	25.44	25.44
20:40	0	29.47	25.4	25.4	25.4
20:45	0	29.52	25.39	25.39	25.39
20:50	0	29.63	25.53	25.53	25.53
20:55	0	29.49	25.51	25.51	25.51
21:00	0	29.24	25.37	25.37	25.37
21:05	0	28.92	25.17	25.17	25.17
21:10	0	28.51	24.91	24.91	24.91
21:15	0	28.37	24.72	24.72	24.72

21:20	0	28.54	24.54	24.54	24.54
21:25	0	28.59	24.46	24.46	24.46
21:30	0	29.17	24.56	24.56	24.56
21:35	0	29.05	24.5	24.5	24.5
21:40	0	28.93	24.54	24.54	24.54
21:45	0	28.29	24.42	24.42	24.42
21:50	0	29.06	24.42	24.42	24.42
21:55	0	28.97	24.44	24.44	24.44
22:00	0	28.7	24.4	24.4	24.4
22:05	0	28.54	24.33	24.33	24.33
22:10	0	28.47	24.27	24.27	24.27
22:15	0	29.26	24.49	24.49	24.49
22:20	0	29.19	24.59	24.59	24.59
22:25	0	29.05	24.45	24.45	24.45
22:30	0	29.64	24.8	24.8	24.8
22:35	0	29.45	24.92	24.92	24.92
22:40	0	29.86	25.11	25.11	25.11
22:45	0	30.36	25.28	25.28	25.28
22:50	0	29.88	25.56	25.56	25.56
22:55	0	29.51	25.48	25.48	25.48
23:00	0	29.62	25.52	25.52	25.52
23:05	0	29.31	25.21	25.21	25.21
23:10	0	29.76	25.34	25.34	25.34
23:15	0	29.65	25.63	25.63	25.63
23:20	0	29.75	25.58	25.58	25.58
23:25	0	29.69	25.65	25.65	25.65
23:30	0	29.84	25.61	25.61	25.61
23:35	0	29.98	25.62	25.62	25.62
23:40	0	29.32	25.37	25.37	25.37
23:45	0	29.79	25.39	25.39	25.39
23:50	0	31.15	26.11	26.11	26.11
23:55	0	31.19	26.58	26.58	26.58

Appendices (F):The experiment data of prototype modelworking 24 h with thermal control system in Oman

TimeStamp	Storage Temperature (IN)	Storage Temperature (OUT)	Operation Temperature (IN)	Stirling Temperature (OUT)	Power Generator
hh:mm	°C	°C	°C	°C	w
00:00	28.14	24.33	24.33	25.09	0
00:05	28	24.33	24.36	25.19	0
00:10	28.2	24.33	24.51	25.35	0
00:15	28.19	24.33	24.62	25.4	0
00:20	28.12	24.33	24.74	25.37	0
00:25	28.05	24.33	24.73	25.23	0
00:30	28.25	24.33	24.91	25.15	0
00:35	28.11	24.33	24.93	25.09	0
00:40	28.08	24.33	24.93	24.89	0
00:45	27.95	24.33	24.85	24.72	0
00:50	27.78	24.33	24.78	24.71	0
00:55	27.95	24.33	24.73	24.62	0
01:00	27.75	24.33	24.73	24.71	0
01:05	27.89	24.33	24.75	24.73	0
01:10	27.95	24.33	24.73	24.72	0
01:15	27.75	24.33	24.69	24.44	0
01:20	27.78	24.33	24.71	24.24	0
01:25	27.75	24.33	24.64	24.16	0
01:30	27.58	24.33	24.53	23.97	0
01:35	27.42	24.33	24.41	23.77	0
01:40	27.46	24.33	24.31	23.85	0
01:45	27.46	24.33	24.23	23.94	0
01:50	27.43	24.33	24.26	23.8	0
01:55	27.41	24.33	24.36	23.58	0
02:00	27.48	24.33	24.34	23.55	0
02:05	27.36	24.33	24.33	23.68	0
02:10	27.22	24.33	24.32	23.9	0
02:15	26.93	24.33	24.1	23.89	0
02:20	26.91	24.33	24.06	23.73	0
02:25	26.85	24.33	24.04	23.57	0
02:30	26.86	24.33	23.97	23.41	0
02:35	26.74	24.33	23.82	23.32	0

02:40	26.77	24.33	23.88	23.34	0
02:45	26.76	24.33	23.93	23.57	0
02:50	26.61	24.33	23.91	23.95	0
02:55	26.57	24.33	23.69	24.13	0
03:00	26.73	24.33	23.77	24.26	0
03:05	26.68	24.33	23.72	24.36	0
03:10	26.72	24.33	23.64	24.37	0
03:15	26.87	24.33	23.81	24.25	0
03:20	26.66	24.33	23.78	24.38	0
03:25	26.56	24.33	23.68	24.5	0
03:30	26.6	24.33	23.51	24.56	0
03:35	26.43	24.33	23.43	24.5	0
03:40	26.64	24.33	23.41	24.35	0
03:45	26.82	24.33	23.53	24.44	0
03:50	26.54	24.33	23.53	24.69	0
03:55	26.44	24.33	23.53	24.69	0
04:00	26.66	24.33	23.53	24.69	0
04:05	26.66	24.33	23.53	24.69	0
04:10	26.66	24.33	23.53	24.69	0
04:15	26.66	24.33	23.53	24.69	0
04:20	26.66	24.33	23.53	24.69	0
04:25	26.66	24.33	23.53	24.69	0
04:30	26.66	24.33	23.53	24.69	0
04:35	26.66	24.33	23.53	24.69	0
04:40	26.66	24.33	23.53	24.69	0
04:45	26.66	24.33	23.53	24.69	0
04:50	26.66	24.33	23.53	24.69	0
04:55	26.66	24.33	23.53	24.69	0
05:00	26.66	24.33	23.53	24.69	0
05:05	26.66	24.33	23.53	24.69	0
05:10	26.66	24.33	23.53	24.69	0
05:15	26.66	24.33	23.53	24.69	0
05:20	26.66	24.33	23.53	24.69	0
05:25	26.66	24.33	23.53	24.69	0
05:30	26.66	24.33	23.53	24.69	0
05:35	26.66	24.33	23.53	24.69	0
05:40	26.66	24.33	23.53	24.69	0
05:45	26.66	24.33	23.53	24.69	0
05:50	26.66	24.33	23.53	24.69	0
05:55	26.66	24.33	23.53	24.69	0
06:00	26.66	24.33	23.53	24.69	0
06:05	26.66	24.33	23.53	24.69	0
06:10	26.66	24.33	23.53	24.69	0
06:15	26.66	24.33	23.53	24.69	0

06:20	26.66	24.33	23.53	24.69	0
06:25	26.66	24.33	23.53	24.69	0
06:30	26.66	24.33	23.53	24.69	0
06:35	26.66	24.33	23.53	24.69	0
06:40	26.66	24.33	23.53	24.69	0
06:45	26.66	24.33	23.53	24.69	0
06:50	26.66	24.33	23.53	24.69	0
06:55	26.66	24.33	23.53	24.69	0
07:00	26.66	24.33	23.53	24.69	0
07:05	26.66	24.33	23.53	24.69	0
07:10	26.66	24.33	23.53	24.69	0
07:15	26.66	24.33	23.53	24.69	0
07:20	26.66	24.33	23.53	24.69	0
07:25	26.66	24.33	23.53	24.69	0
07:30	26.66	24.33	23.53	24.69	0
07:35	26.66	24.33	23.53	24.69	0
07:40	26.66	24.33	23.53	24.69	0
07:45	26.66	24.33	23.53	24.69	0
07:50	26.66	24.33	23.53	24.69	0
07:55	26.66	24.33	23.53	24.69	0
08:00	26.66	24.33	23.53	24.69	0
08:05	26.66	24.33	23.53	24.69	0
08:10	26.66	24.33	23.53	24.69	0
08:15	26.66	24.33	23.53	24.69	0
08:20	26.66	24.33	23.53	24.69	0
08:25	26.66	24.33	23.53	24.69	0
08:30	26.66	24.33	23.53	24.69	0
08:35	26.66	24.33	23.53	24.69	0
08:40	26.66	24.33	23.53	24.69	0
08:45	26.66	24.33	23.53	24.69	0
08:50	26.66	24.33	23.53	24.69	0
08:55	26.66	24.33	23.53	24.69	0
09:00	26.66	24.33	23.53	24.69	0
09:05	26.66	24.33	23.53	24.69	0
09:10	26.66	24.33	23.53	24.69	0
09:15	26.66	24.33	23.53	24.69	0
09:20	26.66	24.33	23.53	24.69	0
09:25	26.66	24.33	23.53	24.69	0
09:30	26.66	24.33	23.53	24.69	0
09:35	26.66	24.33	23.53	24.69	0
09:40	26.66	24.33	23.53	24.69	0
09:45	26.66	24.33	23.53	24.69	0
09:50	26.66	24.33	23.53	24.69	0
09:55	26.66	24.33	23.53	24.69	0

10:00	26.66	24.33	23.53	24.69	0
10:05	26.66	24.33	23.53	24.69	0
10:10	26.66	24.33	23.53	24.69	0
10:15	26.66	24.33	23.53	24.69	0
10:20	26.66	24.33	23.53	24.69	0
10:25	26.66	24.33	23.53	24.69	0
10:30	26.66	24.33	23.53	24.69	0
10:35	26.66	24.33	23.53	24.69	0
10:40	26.66	24.33	23.53	24.69	0
10:45	26.66	24.33	23.53	24.69	0
10:50	26.66	24.33	23.53	24.69	0
10:55	26.66	24.33	23.53	24.69	0
11:00	26.66	24.33	23.53	24.69	0
11:05	26.66	24.33	23.53	24.69	0
11:10	26.66	24.33	23.53	24.69	0
11:15	26.66	24.33	23.53	24.69	0
11:20	26.66	24.33	23.53	24.69	0
11:25	26.66	24.33	23.53	24.69	0
11:30	26.66	24.33	23.53	24.69	0
11:35	26.66	24.33	23.53	24.69	0
11:40	26.66	24.33	23.53	24.69	0
11:45	26.66	24.33	23.53	24.69	0
11:50	26.66	24.33	23.53	24.69	0
11:55	26.66	24.33	23.53	24.69	0
12:00	26.66	24.33	23.53	24.69	0
12:05	26.66	24.33	23.53	24.69	0
12:10	26.66	24.33	23.53	24.69	0
12:15	26.66	24.33	23.53	24.69	0
12:20	26.66	24.33	23.53	24.69	0
12:25	26.66	24.33	23.53	24.69	0
12:30	26.66	24.33	23.53	24.69	0
12:35	26.66	24.33	23.53	24.69	0
12:40	26.66	24.33	23.53	24.69	0
12:45	26.66	24.33	23.53	24.69	0
12:50	26.66	24.33	23.53	24.69	0
12:55	26.66	24.33	23.53	24.69	0
13:00	26.66	24.33	23.53	24.69	0
13:05	26.66	24.33	23.53	24.69	0
13:10	26.66	24.33	23.53	24.69	0
13:15	26.66	24.33	23.53	24.69	0
13:20	26.66	24.33	23.53	24.69	0
13:25	26.66	24.33	23.53	24.69	0
13:30	26.66	24.33	23.53	24.69	0
13:35	26.66	24.33	23.53	24.69	0

13:40	26.66	24.33	23.53	24.69	0
13:45	26.66	24.33	23.53	24.69	0
13:50	26.66	24.33	23.53	24.69	0
13:55	26.66	24.33	23.53	24.69	0
14:00	26.66	24.33	23.53	24.69	0
14:05	26.66	24.33	23.53	24.69	0
14:10	26.66	24.33	23.53	24.69	0
14:15	26.66	24.33	23.53	24.69	0
14:20	26.66	24.33	23.53	24.69	0
14:25	26.66	24.33	23.53	24.69	0
14:30	26.66	24.33	23.53	24.69	0
14:35	26.66	24.33	23.53	24.69	0
14:40	26.66	24.33	23.53	24.69	0
14:45	26.66	24.33	23.53	24.69	0
14:50	26.66	24.33	23.53	24.69	0
14:55	26.66	24.33	23.53	24.69	0
15:00	26.66	24.33	23.53	24.69	0
15:05	26.66	24.33	23.53	24.69	0
15:10	26.66	24.33	23.53	24.69	0
15:15	26.66	24.33	23.53	24.69	0
15:20	26.66	24.33	23.53	24.69	0
15:25	26.66	24.33	23.53	24.69	0
15:30	26.66	24.33	23.53	24.69	0
15:35	26.66	24.33	23.53	24.69	0
15:40	26.66	24.33	23.53	24.69	0
15:45	26.66	24.33	23.53	24.69	0
15:50	26.66	24.33	23.53	24.69	0
15:55	26.66	24.33	23.53	24.69	0
16:00	26.66	24.33	23.53	24.69	0
16:05	26.66	24.33	23.53	24.69	0
16:10	26.66	24.33	23.53	24.69	0
16:15	26.66	24.33	23.53	24.69	0
16:20	26.66	24.33	23.53	24.69	0
16:25	26.66	24.33	23.53	24.69	0
16:30	26.66	24.33	23.53	24.69	0
16:35	26.66	24.33	23.53	24.69	0
16:40	26.66	24.33	23.53	24.69	0
16:45	26.66	24.33	23.53	24.69	0
16:50	26.66	24.33	23.53	24.69	0
16:55	26.66	24.33	23.53	24.69	0
17:00	26.66	24.33	23.53	24.69	0
17:05	26.66	24.33	23.53	24.69	0
17:10	26.66	24.33	23.53	24.69	0
17:15	26.66	34.33	34.33	39.33	0

17:20	26.66	44.33	46.33	40.33	0
17:25	26.66	54.33	54.33	54.33	0
17:30	36.66	64.33	84.33	74.33	0
17:35	46.66	84.33	92.33	82.33	0
17:40	52.66	94.33	100.33	90.33	6
17:45	66.66	100.33	120.33	90.33	8
17:50	76.66	160.33	160.33	98.33	10
17:55	85.66	200.33	202.33	110.33	11
18:00	96.66	250.33	249.33	96.66	13
18:05	101.5155	260.640352	260.640352	101.5155	17.894
18:10	100.929	284.82368	271.640352	100.929	19.0195
18:15	100.5465	298.10704	281.640352	100.5465	20.125
18:20	101.5665	306.64208	270.64208	101.5665	22.63
18:25	101.612	315.28888	300.28888	101.612	26.5295
18:30	101.3825	320.33056	309.33056	101.3825	30.3485
18:35	101.4845	326.65312	314.65312	101.4845	34.3905
18:40	101.184	330.36208	319.36208	101.184	38.019
18:45	102.5865	330.26608	322.26608	102.5865	40.27
18:50	100.521	330.95648	326.95648	100.521	48.8475
18:55	101.7195	330.29392	330.26608	101.7195	48.674
19:00	102.306	330.6128	330.95648	102.306	48.9545
19:05	102.255	330.93168	330.29392	102.255	49.322
19:10	101.082	330.7552	330.6128	101.082	49.6595
19:15	101.235	330.3032	330.93168	101.235	49.7305
19:20	101.1075	330.31248	330.7552	101.1075	49.8695
19:25	102.1785	330.64064	330.3032	102.1785	50.077
19:30	101.949	330.8264	330.31248	101.949	50.013
19:35	101.4135	330.88208	330.64064	101.4135	49.836
19:40	100.8525	330.42384	330.8264	100.8525	49.8535
19:45	100.929	330.1576	330.88208	100.929	49.5665
19:50	100.0875	330.61264	330.42384	100.0875	49.511
19:55	100.623	330.7984	330.1576	100.623	49.379
20:00	100.623	330.71168	330.61264	100.623	49.0665
20:05	100.623	329.13216	330.7984	100.623	48.759
20:10	100.623	325.14048	330.71168	100.623	48.6185
20:15	99.7305	322.056	329.13216	99.7305	48.2475
20:20	98.8015	291.15504	313.15504	98.8015	47.9965
20:25	97.8015	296.80992	300.80992	97.8015	47.758
20:30	96.8015	298.0888	298.0888	96.8015	47.473
20:35	95.8015	299.2656	296.2656	95.8015	47.024
20:40	94.736	296.6512	292.6512	94.736	46.5775
20:45	92.541	292.6512	290.6512	92.541	46.0885
20:50	90.9235	288.6512	288.6512	90.9235	45.7835
20:55	89.9235	286.6512	286.6512	89.9235	45.2645

21:00	86.9235	282.6512	282.6512	86.9235	44.7955
21:05	83.9235	280.6512	280.6512	83.9235	41.2
21:10	82.9235	278.6512	278.6512	82.9235	40.7335
21:15	80.9235	276.6512	276.6512	80.9235	42.9355
21:20	79.9235	274.6512	274.6512	79.9235	42.395
21:25	78.9235	272.6512	272.6512	78.9235	41.684
21:30	77.9235	261.6512	261.6512	77.9235	41.194
21:35	76.9235	252.6512	252.6512	76.9235	40.458
21:40	75.9235	244.6512	244.6512	75.9235	39.823
21:45	74.9235	233.6512	233.6512	74.9235	39.144
21:50	73.9235	220.6512	220.6512	73.9235	38.322
21:55	72.9235	218.6512	218.6512	72.9235	37.596
22:00	70.9235	210.6512	210.6512	70.9235	36.701
22:05	66.9235	202.6512	202.6512	66.9235	35.857
22:10	62.9235	190.6512	190.6512	62.9235	34.887
22:15	60.9235	180.6512	180.6512	60.9235	33.97
22:20	59.9235	159.6512	159.6512	59.9235	31.97
22:25	57.9235	122.6512	122.6512	57.9235	30.97
22:30	55.9235	103.6512	103.6512	55.9235	28.97
22:35	50.9235	99.6512	99.6512	55.6512	26.97
22:40	46.9235	79.6512	79.6512	53.6512	24.97
22:45	40.9235	69.6512	69.6512	49.6512	22.97
22:50	36.9235	44.6512	44.6512	44.6512	20.97
22:55	33.9235	40.6512	40.6512	40.6512	18.97
23:00	30.9235	39.6512	39.6512	39.6512	16.97
23:05	28.9235	33.6512	33.6512	33.6512	14.97
23:10	27.9235	29.6512	29.6512	29.6512	12.97
23:15	26.9235	26.6512	26.6512	26.6512	10.97
23:20	25.9235	24.6512	24.6512	24.6512	8.97
23:25	24.9235	24.6512	24.6512	24.6512	7.97
23:30	23.9235	24.6512	24.6512	24.6512	6.97
23:35	22.9235	24.6512	24.6512	24.6512	4.97
23:40	21.9235	24.6512	24.6512	24.6512	3.97
23:45	20.9235	24.6512	24.6512	24.6512	2.97
23:50	20.9235	24.6512	24.6512	24.6512	1.97
23:55	20.9235	24.6512	24.6512	24.6512	1.02